UNIVERSIDAD NACIONAL AUTÓNOMA DE MÉXICO

PROGRAMA DE MAESTRÍA Y DOCTORADO EN CIENCIAS QUÍMICAS

β-ciclodextrinas pegyladas: estudios de auto-agregación, caracterización biológica y análisis de su contexto tecnológico-farmacéutico por medio de ciencia de datos.

T E S I S
PARA OPTAR POR EL GRADO DE

MAESTRA EN CIENCIAS

P R E S E N T A

Q.I. Juliana Rincón López

Dra. Yareli Rojas Aguirre
Instituto de Investigaciones en Materiales, UNAM

Ciudad de México, Diciembre 2021

Universidad Nacional Autónoma de México
UNAM
Biblioteca Central
Dirección General de Bibliotecas de la UNAM

UNAM – Dirección General de Bibliotecas
Tesis Digitales
Restricciones de uso

DERECHOS RESERVADOS ©
PROHIBIDA SU REPRODUCCIÓN TOTAL O PARCIAL

Todo el material contenido en esta tesis esta protegido por la Ley Federal del Derecho de Autor (LFDA) de los Estados Unidos Mexicanos (México).

El uso de imágenes, fragmentos de videos, y demás material que sea objeto de protección de los derechos de autor, será exclusivamente para fines educativos e informativos y deberá citar la fuente donde la obtuvo mencionando el autor o autores. Cualquier uso distinto como el lucro, reproducción, edición o modificación, será perseguido y sancionado por el respectivo titular de los Derechos de Autor.

UNIVERSIDAD NACIONAL AUTÓNOMA DE MÉXICO

PROGRAMA DE MAESTRÍA Y DOCTORADO EN CIENCIAS QUÍMICAS

β-ciclodextrinas pegyladas: estudios de auto-agregación, caracterización biológica y análisis de su contexto tecnológico-farmacéutico por medio de ciencia de datos.

T E S I S
PARA OPTAR POR EL GRADO DE

MAESTRA EN CIENCIAS

P R E S E N T A

Q.I. Juliana Rincón López

Dra. Yareli Rojas Aguirre
Instituto de Investigaciones en Materiales, UNAM

Ciudad de México, Diciembre 2021

Agradecimientos

A la Universidad Nacional Autónoma de México (UNAM), a las personas que hacen posible su funcionamiento, por ser casa y refugio académico de mexicanos y extranjeros.

Al Consejo Nacional de Ciencia y Tecnología (CONACyT) por la beca otorgada durante mis estudios de Maestría (No. CVU: 1032640).

Al Programa de Maestría y Doctorado en Ciencias Químicas UNAM, a las personas que hacen posible su funcionamiento, por el acompañamiento cada semestre, por la amabilidad y la gestión continua.

A Posgrado UNAM por el Programa de apoyo a los estudios de posgrado (PAEP), el financiamiento para la asistencia al Controlled Release Society Virtual Annual Meeting 2021.

A la Dra. Yareli Rojas Aguirre adscrita al Instituto de Investigaciones en Materiales UNAM, quien dirigió este proyecto de tesis, así como a los Proyectos PAPIIT-UNAM IA200919, PAPIIT-UNAM IA200821 y Proyecto 1306 del IIM por el financiamiento.

Al Dr. Alejandro P. Riascos adscrito al Instituto de Físico UNAM por su colaboración en el análisis por ciencia de datos de tecnologías farmacéuticas a base de ciclodextrinas, por su amabilidad y acompañamiento.

A la Dra. Yara C. Almaza Arjona adscrita al Instituto de Ciencias Aplicadas y Tecnologías UNAM por su colaboración y experticia en el análisis tecnológico de patentes.

A la Dra. Patricia Guadarrama adscrita al Instituto de Investigaciones en Materiales UNAM por su consejo constante en cada etapa de este proyecto.

Al Dr. Alberto S. Luviano y el Dr. Miguel Costas adscritos a la Facultad de Química UNAM por su colaboración en el estudio de fenómenos de auto-agregación a través de mediciones de tensión superficial.

Al Dr. Arturo A. García Figueroa y el Dr. José L. López Cervantes adscritos a la Facultad de Química UNAM por su colaboración en la determinación de la concentración de agregación crítica por densimetría.

Al Dr. Rubén Mendoza Cruz adscrito al Instituto de Investigaciones en Materiales UNAM por su colaboración en las mediciones de TEM.

Al Dr. Héctor Domínguez adscrito al Instituto de Investigaciones en Materiales UNAM por su colaboración en la simulación de las interacciones químicas.

A la Q.F.B. Norma J. Ramírez Rodríguez por su colaboración en las mediciones de DLS.

Al Dr. Salvador López Morales adscrito al Instituto de Investigaciones en Materiales UNAM por su colaboración en las mediciones de DLS.

A la Dra. Karla Juárez Moreno adscrita al Centro de Nanociencias y Nanotecnología UNAM por la colaboración en el estudio biológico *in vitro*.

A la I.B. Miguelina Martínez Aguilera adscrita al Instituto de Investigaciones en Materiales UNAM por su colaboración en el análisis de los resultados en la línea MDCK y RAW264.7.

A mis compañeras de SupraMatLab, Miguelina Martinez, Lorena Meza, Marlene Covarrubias, Ana Laura Coria y Tania.

Dedicatoria

Mi paso por la maestría me ha dejado mucho más que herramientas y conocimientos técnicos (aunque nada de esto sobró). Me enseño, principalmente, a valorar la comunicación. A encontrar la palabra justa, la oración efectiva, el orden de las ideas. Una habilidad que apenas empiezo a cultivar, pero que bien construida, me hará una mejor persona.

Esta tesis, es el proyecto académico más arduo, extenuante y exigente que he enfrentado. Estoy segura de que no lo hubiera logrado sin la disciplina y el amor por las tareas que se deben ejecutar que me ha enseñado mi Mamá con sus actos y palabras.

Por esto, te dedico este trabajo Mami.

Tu voluntad y sentido de servicio inquebrantable hacen del mundo, que son las personas que te rodean, un lugar mejor. Además, tu amor constante y nuestras llamadas nocturnas alimentaron mi alma durante este proceso.

También te agradezco a ti, Mati, por enseñarme que la vida no debe ser exigente y complicada todo el tiempo. Tu espontaneidad, ocurrencias, sonrisas y pensamientos alivianan mi alma y le han dado un nuevo sentido a mi vida.

A mi Papá, por ser deseo, añoranza, motivación. Por ser mi remitente favorito. Por haber cuidado de mi presente y mi futuro, y aún hoy, hacerlo.

A mi Mamita, por amarme, cuidarme y desear conmigo mis sueños. Eres una vela que calienta mi alma. Gracias por regalarme el hogar grande al que cada día, y en especial los domingos, hay una puerta abierta, compañía, fríjoles y amor. Admiro tu fortaleza, resiliencia y determinación.

A mi familia, por la diversidad que alberga, por el amor expresado a través de la comida y el café, por la calidez con que me reciben siempre que vuelvo. Nati, JuanFe, Tía Nana, Mauro (Peter), Pirry, Mauro, Tía Tere, Carlos Arturo, Leo, Cata y Migue.

Mi gratitud eterna.

Para Camilo,

Con quien las palabras se me acaban, escapan y asustan ante la responsabilidad de representar lo que siento.

“Soñé que te tenía
Como quien lo tiene todo
A la mano
Pues tu carne es la plenitud de mi cuerpo
Y tú alma es la plenitud de la mía

Te soñé y me sentí rico
Como quien tiene abundancia de lo necesario
Y me sentí rey de los dominios que son los caminos que se han hecho nuestros

Te soñé y me vi sin hambre
Sin sueño
Sin necesidades humanas que desinteresen los fines del alma

Te soñé
Cómo siempre te he soñado
Libre
Y a mi lado”

Lugar donde se realizó este proyecto

Grupo de investigación en Materiales Supramoleculares y Nanomedicina (SupraMatLab).

Laboratorio C-105, Instituto de Investigaciones en Materiales UNAM.

Publicaciones y presentaciones en congresos derivadas de este proyecto

Publicaciones

J. Rincón-López, Y.C. Almanza-Arjona, A.P. Riascos, Y. Rojas-Aguirre, Technological evolution of cyclodextrins in the pharmaceutical field, J. Drug Deliv. Sci. Technol. (2020) 102156. https://doi.org/10.1016/j.jddst.2020.102156.

J. Rincón-López, Y.C. Almanza-Arjona, A.P. Riascos, Y. Rojas-Aguirre, When Cyclodextrins Met Data Science: Unveiling Their Pharmaceutical Applications through Network Science and Text-Mining, Pharmaceutics. (2021) 1297. https://10.3390/pharmaceutics13081297.

J. Rincón-López, N.J. Ramírez-Rodríguez, A.S. Luviano, M. Costas, J.L. López-Cervantes, A.A. García-Figueroa, H. Dominguez, R. Mendoza-Cruz, P. Guadarrama, S. López-Morales, Y. Rojas-Aguirre, Experimental and theoretical studies of pegylated-β-cyclodextrin: A step forward to understand its tunable self-aggregation abilities, J. Drug Deliv. Sci. Technol. (2021). 102975. https://doi.org/10.1016/j.jddst.2021.102975

J. Rincón-López, M. Martínez-Aguilera, P. Guadarrama, K. Juarez-Moreno, Y. Rojas-Aguirre, Pegylated β-cyclodextrins: the smart combination of PEG and β -cyclodextrin to optimize their *in vitro* biological cellular responses, Pharmaceutics. Submitted (August 2021).

Congresos

J. Rincón-López, Y.C. Almanza-Arjona, A.P. Riascos, Y. Rojas-Aguirre, *When Cyclodextrins met data mining: uncovering their trending and hidden pharmaceutical technologies*. Controlled Release Society 2021 Annual Meeting. Julio 2021. Modalidad: poster.

Índice

Abreviaturas

αCD	α-ciclodextrina
AFM	Microscopía de fuerza atómica
βCD	β-ciclodextrina
γCD	γ-ciclodextrina
cac	Concentración de agregación crítica
CD	Ciclodextrina
CI	Complejo de inclusión
DII	Base de datos Derwent Innovation Index
DIMEB	Di-metil-β-ciclodextrina
DLS	Dispersión dinámica de luz
HPβCD	(2-hidroxi) propil-β-ciclodextrina
HPγCD	(2-hidroxi) propil-γ-ciclodextrina
IV	Intra venoso
IPC	Clasificación internacional de patentes
MβCD	Metil-β-ciclodextrina
MF	Mezcla física
MTT	3-(4,5-dimetiltiazol-2-il)-2,5-difeniltetrazolio
PEG	Polietilenglicol
PM	Peso molecular
RAMEB	β-ciclodextrina metilada al azar
RES	Sistema reticuloendotelial
ROS	Especies reactivas de oxígeno
SBEβCD	Sulfobutil éter-β-ciclodextrina
SEM	Microscopía electrónica de barrido
TEM	Microscopía electrónica de transmisión
USP	Farmacopea de EUA

Resumen

Las ciclodextrinas (CDs) son oligosacáridos cíclicos compuestos por 6, 7 u 8 unidades de glucopiranosa (α-, β-, γ-CD respectivamente). Las CDs nativas y modificadas pueden formar agregados e incluso entidades de mayor orden estructural como micelas o vesículas. La formación de agregados puede afectar la solubilidad y estabilidad de formulaciones farmacéuticas. No obstante, la agregación controlada puede promover la solubilización de cierto tipo de fármacos o aprovecharse para dar lugar a sistemas avanzados de liberación de fármacos basados en CDs. Muchos de estos sistemas son de gran complejidad estructural, y su estudio generalmente se centra en la síntesis y diseño del material, y el estudio de su tamaño, capacidad de carga y liberación del fármaco que contenga. De igual manera, sus estudios biológicos se enfocan únicamente en los modelos celulares en los que el fármaco acarreado tiene que actuar. Por lo tanto, la caracterización fisicoquímica y biológica exhaustiva de los nuevos materiales en la etapa inicial de desarrollo, incluso sin estar cargados de fármacos, es indispensable.

Dentro del grupo de investigación se han sintetizado βCDPEG2 y βCDPEG5 (βCDPEGs), mediante la conjugación de siete cadenas de PEG de 2 y 5 kDa, respectivamente, a la cara primaria de la βCD, por medio de química click. Para determinar su potencial en el campo de la nanomedicina, en este trabajo, primeramente, se investigó su capacidad de auto-agregación de manera experimental por diversas técnicas y también por simulación computacional. A pesar de que las βCDPEGs están formadas por βCD y PEG, ambos biocompatibles, son en realidad nuevas entidades moleculares que podrían inducir respuestas biológicas distintas a las de βCD y PEG por separado. Por ello, se estudió su comportamiento *in vitro* en macrófagos (línea RAW264.7); osteoblastos (línea MC3T3-E1) y células epiteliales (línea MDCK), a manera de conformar un tipo de 'biblioteca biológica'. Por último, se implementaron herramientas de ciencia de datos, basadas en el procesamiento natural del lenguaje y principios de *machine learning*, para conocer las tendencias y áreas emergentes de las tecnologías farmacéuticas basadas en CDs.

Los resultados de este trabajo mostraron que βCDPEG5 se auto-agrega en agua y forma estructuras nanométricas de ~150 nm, y también forman dímeros de ~9 nm de diámetro. La capacidad de auto-agregación se da únicamente cuando se conjugan covalentemente las siete

cadenas de PEG a la cara estrecha de la βCD. Además, se evidenció que la formación de los agregados y su disociación a dímeros es modulable por las condiciones del medio. Los estudios *in vitro* revelaron que la biocompatibilidad de βCD y PEG mejoró cuando se conjugaron como un único sistema, βCDPEGs. Por último, la implementación de las herramientas de ciencia de datos para el análisis de patentes farmacéuticas de CDs indicó que el interés por las CDs sigue aumentando y continuará creciendo en los próximos años por su versatilidad y capacidad para mejorar las formulaciones farmacéuticas en el diseño de terapias innovadoras.

1. Marco teórico

1.1. Las CDs en el área farmacéutica

Las ciclodextrinas (CDs) son oligosacáridos cíclicos unidos por enlaces α-1,4 compuestos por 6, 7 u 8 unidades de glucopiranosa (α-, β-, γ-CD respectivamente). Su estructura tridimensional asemeja a un cono truncado cuya superficie externa es hidrofílica debido a los -OH primarios y secundarios de su cara estrecha y amplia, respectivamente (Figura 1A). La cavidad, por otra parte, tiene un ambiente hidrofóbico (Figura 1B) (Crini, 2014). Esta conformación permite a las CDs albergar entidades poco polares a través de la formación de complejos de inclusión (CIs), a la vez que brinda una gran versatilidad química por la fácil derivatización de sus grupos -OH.

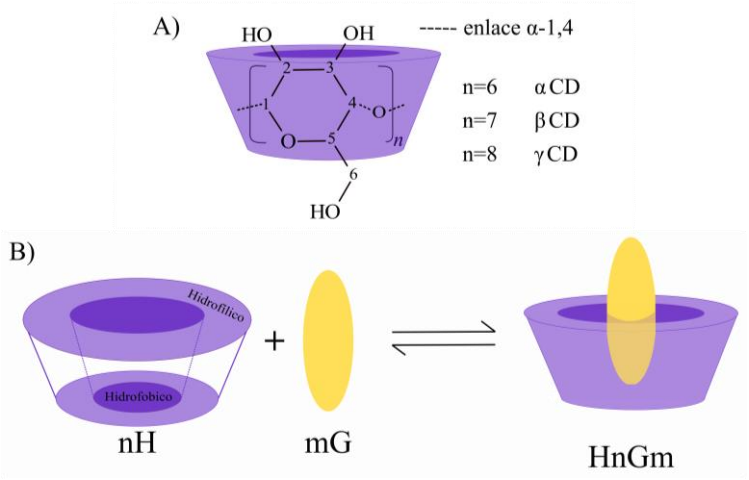

Figura 1. A) Estructura química de las CDs, B) formación de los CIs, H hace referencia al anfitrión, G al huésped, n y m a los coeficientes estequiométricos respectivos.

Los CIs, son sistemas supramoleculares de tipo huésped-anfitrión en los que una molécula (huésped) es 'encapsulada' en la cavidad del anfitrión a través de interacciones no covalentes (Figura 1B). La formación del CI lleva implícito la modificación aparente de las propiedades fisicoquímicas y biológicas de la molécula huésped, ya que las propiedades que percibe el ambiente son las del anfitrión y no las de la molécula encapsulada. El CI está en un equilibrio dinámico con sus componentes, lo que asegura una disponibilidad ininterrumpida del huésped en el medio (Crini *et al*., 2018).

Las CDs se utilizan generalmente en el área farmacéutica para aumentar la solubilidad acuosa de fármacos hidrofóbicos. Actualmente más de 50 formulaciones comercializadas las

contienen. Algunos ejemplos de estas formulaciones aprobadas recientemente por la FDA son: Veklury, sulfobutil éter-β-ciclodextrina (SBEβCD)/remdesivir, para el tratamiento de la COVID-19; Zulresso, SBEβCD/brexanolona, para el tratamiento de la depresión postparto; y Baqsimi, βCD/glucagón, para el tratamiento de hipoglicemia severa (Rincón-López, Almanza-Arjona, *et al*., 2021).

La modificación química de las CDs ha permitido modular sus propiedades fisicoquímicas y biológicas, para aumentar su solubilidad, capacidad de formar CIs y biocompatibilidad (Dhiman & Bhatia, 2020). La funcionalización se lleva a cabo en los -OH primarios y/o secundarios (Figura 2) y puede ser con aminas, esteres o éteres. Por ejemplo, (2-hidroxi) propil-β-ciclodextrina (HPβCD) o SBEβCD, los cuales son ampliamente utilizados debido a su baja toxicidad; estos se expondrán con mayor profundidad en la Sección 6.3.1.

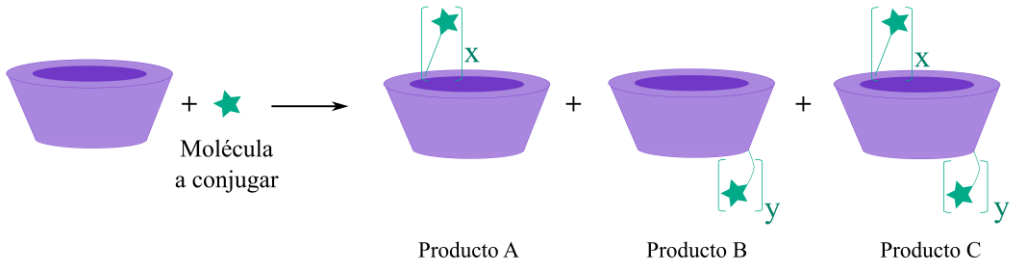

Figura 2. Versatilidad química de las CDs. Obtener el producto A, B, o C dependerá del tipo de reacción. X y Y son determinados por el tipo de CD y la estequiometría de reacción.

Cuando la funcionalización se lleva a cabo con cadenas alquílicas o fragmentos hidrofóbicos se obtienen las CDs anfifílicas (a-CDs). La relevancia de las a-CDs recae, por un lado, en una mayor interacción con los fármacos hidrofóbicos con respecto a las CDs nativas, ya que, además de formar CIs, pueden establecer interacciones no covalentes en las cadenas alifáticas o conjugaciones covalentes al sistema (Bilensoy & Hincal, 2009; Fülöp *et al*., 2012; Jiang *et al*., 2011; Varan *et al*., 2017; Zerkoune *et al*., 2014). Por otro lado, se encuentra la capacidad de formar enlaces no covalentes entre las entidades individuales de a-CDs para auto-agregarse en estructuras irregulares, y ya sea que, posteriormente, adquieran un mayor orden estructural (auto-ensamblados) o no (R. G. Jones *et al*., 2013). Por estas razones, la formación de nanoestructuras a partir de a-CDs ha mostrado un desempeño sobresaliente como sistemas de liberación de fármacos.

Existen dos sistemas de liberación a base de CDs con capacidad de auto-agregarse y formar nanopartículas poliméricas que han llegado a fases clínicas: el CRLX101 y el CALAA-01. El CRLX101, es una nanoestructura de 36 nm que consiste en un sistema de βCD polimérica modificada con polietilenglicol (PEG) con un peso molecular (PM) de 5000 Da, conjugado al fármaco camptotecina (Figura 3). Este sistema logra la liberación sostenida del fármaco con alta concentración en circulación sistémica. Actualmente se encuentra en ensayos clínicos de fase I/II para el cáncer de pulmón de células pequeñas, con una fecha de finalización estimada en 2027 (Cheng *et al*., 2011; *Clinical Trial of CRLX101*, 2016; Weiss *et al*., 2013).

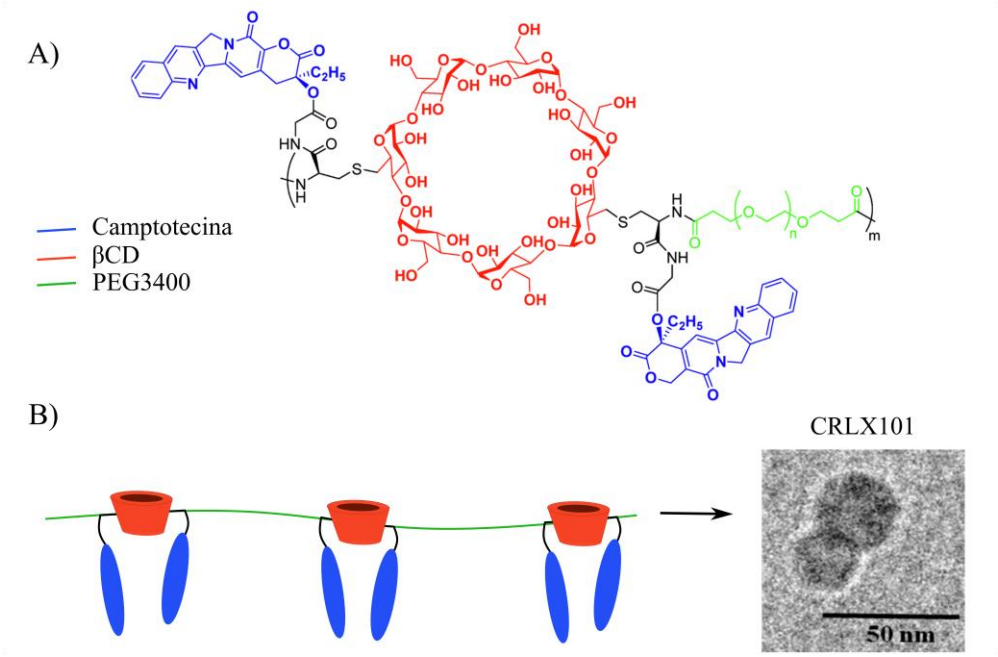

Figura 3. A) Estructura química de la unidad monomérica del CRLX101, B) representación del sistema polimérico CRLX101 y la nanoestructura que conforma; adaptada de Young *et al*., 2011.

El CALAA-01, es un sistema compuesto por un copolímero tipo AB lineal de βCD y dimetil suberimidato (que imparte dos centros de $C=NH_2^+$separados por seis unidades de metileno) (Figura 4A), adamantano-PEG (PEG PM 3400Da) y adamantano-PEG-transferrina, para conformar un sistema entrecruzado que se agrega en nanoestructuras de 79 nm, capaz de transportar y liberar ácido ribonucleico (ARN) (Figura 4b) (Heidel & Schluep, 2012; Oliveri & Vecchio, 2018). Esta nanoestructura culminó fase clínica I en el 2012 para el tratamiento

de tumores sólidos de manera exitosa. Calando Pharmaceuticals, propietario de CALAA-01, no ha continuado con su estudio (ClinicalTrials.gov, 2013).

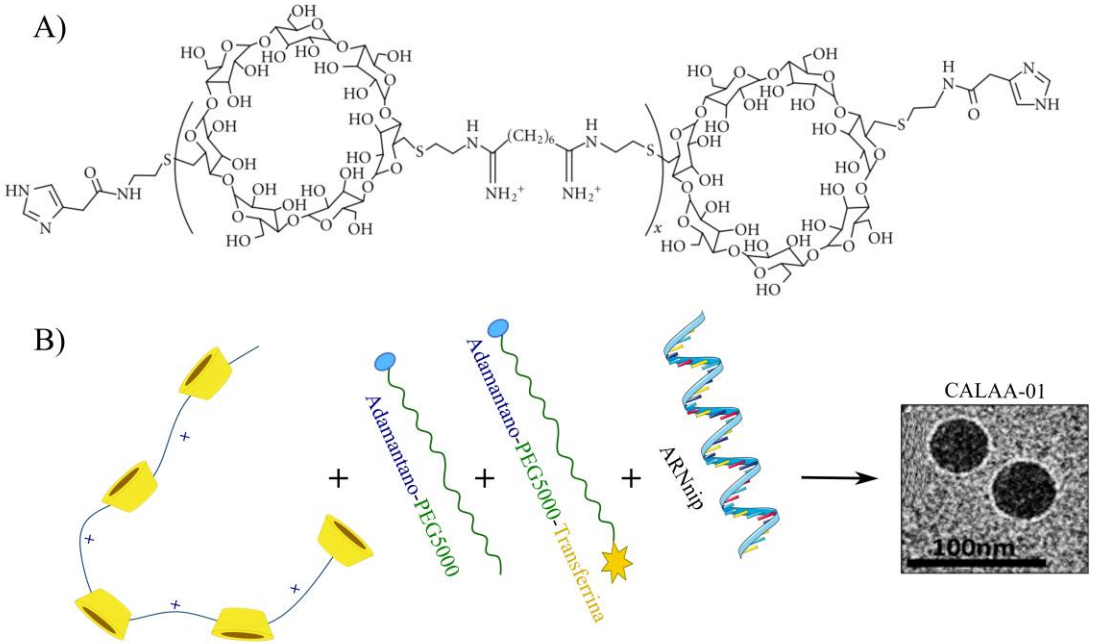

Figura 4. A) Estructura química del copolímero βCD-dimetil suberimidato, B) representación de los componentes de CALAA-01 y la nanoestructura que conforma; adaptada de Zuckerman *et al*., 2014.

1.2. PEG y la pegylación

El PEG (Figura 5) es un polímero que se considera biocompatible. La pegylación es el proceso por el cual se conjuga PEG a otra entidad (polímero, molécula, nanoestructura) para brindar estabilidad fisicoquímica y/o biológica.

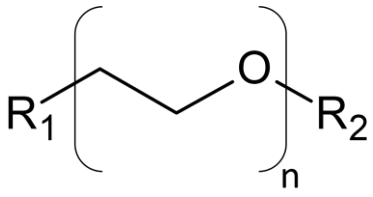

Figura 5. Estructura química del PEG. R1 y R2 pueden ser dos moléculas a las cuales este conjugado, o bien, la molécula a la que este conjugado y un grupo terminal; n indica las unidades monoméricas.

Desde la perspectiva fisicoquímica, la pegylación puede aumentar la solubilidad y estabilidad coloidal del sistema que conforma. Aunque PEG se considere como hidrofílico, al aumentar el PM (por encima de 4700/5000 Da) se comporta más como un polímero anfifílico, debido a la hidrofobicidad conferida por los grupos -CH_2- y al carácter hidrofílico que le da la interacción de -O- con moléculas de agua por enlaces de hidrógeno (Wu *et al*., 2014). Además del PM del PEG, la densidad de injerto ejerce una influencia sobre las características del sistema que conforma; cuando es baja el PEG adopta una conformación de 'hongo', en donde las cadenas establecen interacciones intramoleculares dando lugar a una estructura plegada; cuando aumenta, se transforma en una conformación de 'cepillo', donde predominan las interacciones intermoleculares haciendo que las cadenas se extiendan en el espacio. La conformación de cepillo en la superficie de las nanopartículas le brinda estabilidad coloidal por medio de repulsión estérica. Además, entre más alta sea la densidad de injerto, menos responsivo es el sistema pegylado a cambios en el medio (Brittain & Minko, 2007; D'souza & Shegokar, 2016; Jokerst *et al*., 2011).

Desde la perspectiva biológica, el PEG se utiliza para: conjugar fármacos o ligantes de reconocimiento a nanoestructuras; para eludir el reconocimiento por parte del sistema reticuloendotelial (RES) y, a su vez, para evitar una rápida eliminación del cuerpo (Knop *et al*., 2010; G. Liu *et al*., 2017; Rojas-Aguirre *et al*., 2019).

Por lo tanto, a través de la pegylación se puede modular la respuesta al entorno del material, así que, es una necesidad considerar un diseño racional para la formación de sistemas de liberación pegylados exitosos.

En el caso de las CDs, el PEG también se ha utilizado para modificar o formar plataformas moleculares para acarrear, modificar la liberación o disminuir la toxicidad de fármacos. Tal es el caso de CALAA-01 y CRLX101, o bien de algunos sistemas reportados en la literatura en donde realizan pegylaciones covalentes en la cara primaria y/o secundaria de la CD (Figura 6A), o no covalentes a través de la formación de CIs (Figura 6B) (Abdulrahman, 2018; Godinho *et al*., 2014; Kost *et al*., 2020; O'Mahony *et al*., 2012; Udachin *et al*., 2000), para alcanzar los mismos fines.

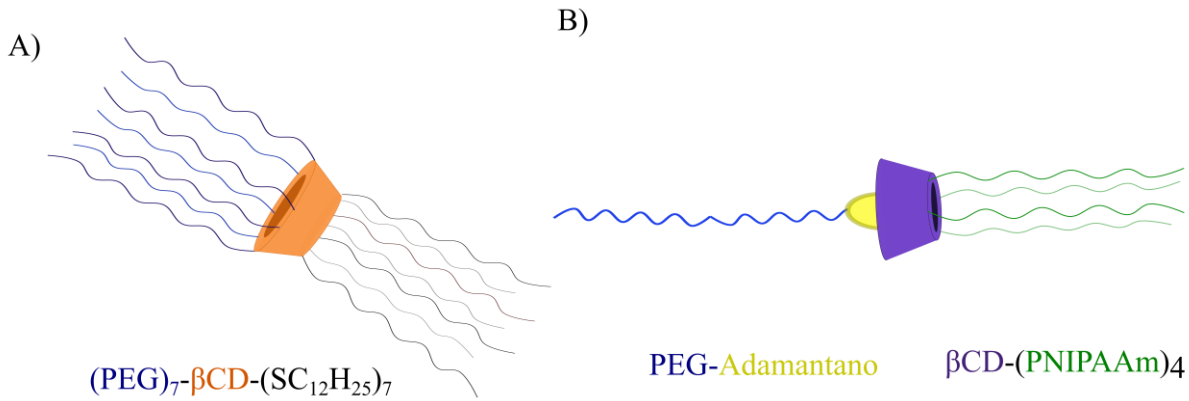

Figura 6. Ejemplos de pegylación reportados en la literatura. A) Pegylación covalente (Godinho *et al*., 2014) , B) pegylación no covalente (Song *et al*., 2017).

1.3. Agregación de CDs nativas y sus derivados

Las CDs nativas tienen la habilidad de formar agregados metaestables y dinámicos en soluciones acuosas. Las modificadas también, aunque en este caso, su agregación dependerá de las características de los derivados, tales como el equilibrio hidrofóbico-hidrofílico en la CD, su concentración, la polaridad del medio y la temperatura. Cuando las CDs se han modificado con sustituyentes hidrofóbicos, la auto-agregación podrá resultar en entidades moleculares de un mayor orden estructural tales como micelas o vesículas (Bonini *et al*., 2006; de Sousa *et al*., 2012; Fülöp *et al*., 2012; González-Gaitano *et al*., 2002; Y. He *et al*., 2008; Jansook *et al*., 2018; Messner *et al*., 2010; Sá Couto *et al*., 2018).

Los agregados de CDs nativas o modificadas se pueden caracterizar por diversas técnicas. Su tamaño se determina generalmente por dispersión dinámica de luz (DLS), al igual que por microscopía de transmisión electrónica (TEM), microscopía electrónica de barrido (SEM) o microscopía de fuerza atómica (AFM), que además proporcionan información sobre su morfología. Los tamaños de los agregados pueden varias según la técnica utilizada, y debido a las diferentes condiciones de la medición, los resultados pueden ser complementarios (Zielińska *et al*., 2020).

El tamaño, la morfología y las fuerzas fisicoquímicas que mantengan a los agregados de CDs determinarán la capacidad de carga y el proceso de liberación de fármaco, y las interacciones con las interfaces biológicas (Anselmo & Mitragotri, 2016). Además, debido a que, como se mencionó, el fenómeno de agregación puede verse influenciado por el medio, es relevante

estudiar la agregación de los sistemas a base de CDs ante cambios de pH, temperatura, fuerza iónica e incluso, tiempo (Pelaz *et al*., 2017).

El estudio de la formación de agregados de CDs y derivados de CDs es sumamente importante; ya que la formación de estos puede afectar la solubilidad y estabilidad de una formulación (Jansook *et al*., 2010). Sin embargo, la formación de agregados de manera controlada podría dar lugar a suspensiones farmacéuticas, e incluso a una mayor solubilización de cierto tipo de fármacos. Tal es el caso de una suspensión acuosa en la que la liberación de un fármaco lipofílico en el segmento posterior del ojo para el tratamiento de enfermedades como la retinopatía diabética y la degeneración macular relacionada con la edad, que comúnmente se tratan con fármacos administrados por inyecciones intravítreas, se logra solamente a partir de la agregación controlada de los CIs de CD/dexametasona (Loftsson & Stefánsson, 2014, 2017).

1.5. Desarrollos farmacéuticos a base de CDs

Como se ha visto a lo largo del marco teórico, las CDs tienen gran potencial en el desarrollo de plataformas de liberación avanzada, pero también como excipientes en formulaciones farmacéuticas. En este último caso, las CDs han permitido el surgimiento de innovaciones cada vez más atractivas que pueden mejorar terapias e incluso vacunas, como el uso de HPβCD en la formulación de la vacuna de Janssen Biontech para la inmunización contra SARS-CoV-2 y el CI SBEβCD/remdesivir, mencionado anteriormente, como único fármaco aprobado para el tratamiento de COVID-19, cuyo desarrollo se llevó a cabo en tiempo récord (Braga *et al*., 2021; Garrido *et al*., 2020). Bajo este contexto, se puede evidenciar la importancia del análisis de la información tecnológica de las CDs en el campo farmacéutico.

Las patentes son una excelente fuente de información tecnológica y su análisis puede proporcionar indicadores para desarrollos novedosos, informar sobre áreas tecnológicas emergentes y apoyar la identificación de oportunidades para la anticipación de tecnologías (Rodriguez-Esteban & Bundschus, 2016). Además, el análisis de los datos de patentes se vuelve más relevante cuando el ciclo de innovación se vuelve más complejo y corto, y cuando el mercado exige respuestas rápidas (Bergeaud *et al*., 2017), como en la situación presentada por la pandemia de COVID-19. A nivel académico, el análisis de patentes permite evaluar la

competitividad de los proyectos y priorizar la investigación, el desarrollo y la inversión de los mismos (Pereira *et al*., 2018).

Prueba de la importancia de las tecnologías que resguardan las patentes, es un trabajo publicado por Liu y colaboradores en el 2020, en el que se analizan patentes relacionadas con los virus SARS y MERS para proporcionar una guía de detección de activos farmacéuticos que pueden ser utilizados contra el SARS-CoV-2 (C. Liu *et al*., 2020).

El análisis de patentes es una tarea desafiante ya que estas tienen un estilo de escritura y una estructura intrincados, caracterizado por oraciones complejas y largas que podrían ocultar información importante (Sarica *et al*., 2020).

La ciencia de redes es una herramienta de la ciencia de datos y estudia los patrones emergentes en un sistema, considerando sus partes e interacciones, a través de la formación de comunidades (Newman, 2010). La ciencia de redes permite la descripción de sistemas complejos, el análisis las redes sociales, análisis bioinformáticos e incluso la descripción de la organización funcional de una célula viva (Barabási & Oltvai, 2004; Newman, 2010; Recanatini & Cabrelle, 2020; Vogt *et al*., 2016).

La ciencia de redes también se ha utilizado para el análisis de patentes (Bergeaud *et al*., 2017; Hu *et al*., 2018; Lee *et al*., 2018; Sarica *et al*., 2020). En este caso, los algoritmos de detección de comunidades en una red, en específico de patentes, sirven como método de agrupación para la clasificación no supervisada de innovaciones con contenido semántico similar (Rincón-López, Almanza-Arjona, *et al*., 2021). El contenido semántico, es un contenido hecho de conceptos que implican premisas con algún sentido, valor o verdad. Las técnicas generales de agrupación constituyen un componente esencial de minería de texto y son fundamentales en las tareas de aprendizaje automático no supervisadas (*machine learning*) (Gan *et al*., 2007; Müller & Guido, 2017). Por lo tanto, la detección de las comunidades en el panorama de las patentes puede revelar áreas tecnológicas poco patentadas, tendencias emergentes e incluso colaboradores académicos o industriales con los que trabajar en investigaciones futuras (Asche, 2017; Boyack *et al*., 2020; Pereira *et al*., 2018).

2. Justificación

En virtud de la versatilidad química y la capacidad de auto-agregación, las CDs se han estudiado ampliamente para desarrollar nanomateriales/nanoplataformas de liberación de fármacos con diversas, e incluso complejas, funcionalizaciones (Cova *et al*., 2018). Sin embargo, la síntesis extensa, la dificultad de escalamiento, la baja reproducibilidad y la gran cantidad de componentes, dificultan el avance de estas plataformas (Lammers, 2013; Metselaar & Lammers, 2020) y es de resaltar, que las que han llegado a la clínica presentan una gran simplicidad estructural. Por lo tanto, el diseño de sistemas simples, la caracterización fisicoquímica y biológica exhaustiva en su etapa inicial de desarrollo, incluso sin estar cargados de fármacos, es indispensable en los nuevos materiales.

Dentro del grupo de investigación se han sintetizado βCDPEG2 y βCDPEG5 (βCDPEGs), dos derivados de βCD obtenidos mediante la conjugación selectiva de siete cadenas de PEG de 2 y 5 kDa respectivamente, a través de un grupo triazol, a la cara primaria de la βCD mediante química click (Figura 7) (Rojas-Aguirre *et al*., 2019), diseñados para transportar moléculas bioactivas, es decir, como sistemas de liberación de fármacos.

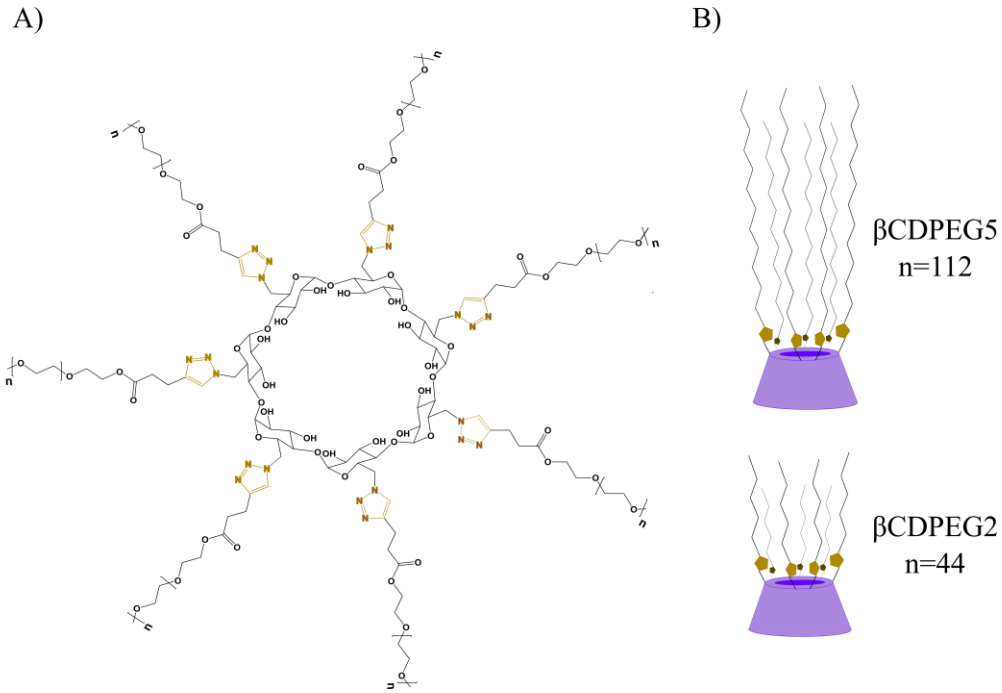

Figura 7. A) Estructura química de los βCDPEGs en donde n representa el número de monómeros del polímero PEG, B) representación esquemática.

Debido al arreglo de las siete cadenas de PEG en la cara estrecha de la βCD y al PM del PEG, se considera que los sistemas βCDPEGs tendrán características anfifílicas, por lo que podrían tener la capacidad de auto-agregarse y dar lugar a nanopartículas poliméricas con la habilidad de acarrear fármacos hidrofóbicos e hidrofílicos.

Al diseñar un nanosistema de liberación basado o no en CDs, la investigación generalmente se centra en determinar el tamaño del sistema, la carga y liberación del fármaco, dejando a un lado, el estudio fisicoquímico el cual es indispensable para entender el desempeño físico, químico y biológico en etapas tempranas de su diseño, aún sin estar cargado con fármaco y que, a su vez, es fundamental para generar conocimiento sólido que dirija al sistema hacia posibles aplicaciones reales.

Así, en este trabajo, se presenta el estudio fisicoquímico de βCDPEG5 para determinar primeramente su capacidad de auto-agregación, la consecuente formación de nanoestructuras y su caracterización.

Como se mencionó, el estudio biológico de plataformas poliméricas para liberación fármacos se enfoca, la mayoría de las veces, en evaluaciones biológicas solamente en células relacionadas con las aplicaciones específicas para las que fueron diseñados. Sin embargo, el nuevo nanomaterial podría interactuar pasiva y activamente con diferentes células bajo diferentes mecanismos. Además, se debe tener en cuenta que las células responden al tamaño, la forma, e incluso a la composición química del nanomaterial (Jesus *et al*., 2019; Villanueva-Flores *et al*., 2020). Por ello, aunque las βCDPEGs están constituidos a partir de bloques biocompatibles, se está formando una nueva entidad, la cual podría inducir respuestas biológicas distintas a las de sus componentes por separado. Bajo este contexto, en este trabajo se investiga el comportamiento biológico *in vitro* de βCDPEG2 y βCDPEG5 en varias líneas celulares para explorar su interacción con interfaces biológicas.

Dada la actual importancia de analizar grandes cantidades de información, en este caso de tipo tecnológico de las CDs en el área farmacéutica, se presenta la implementación de herramientas de ciencia de datos, basadas en el procesamiento natural del lenguaje y principios de *machine learning*, para analizar el panorama tecnológico de las CDs a partir del estudio de patentes farmacéuticas y contextualizar los sistemas de βCDPEGs dentro de dicho panorama.

3. Hipótesis

1. La funcionalización de la cara estrecha de las βCDs con siete cadenas de PEG de PM 5 kDa, le brindará características anfifílicas a βCDPEG5, y, por lo tanto, la capacidad a βCDPEG5 de auto-agregarse en agua y formar estructuras estables de tamaño nanométrico.

2. Las βCDPEGs están constituidos por βCD y PEG, que son dos bloques considerados como biocompatibles. Sin embargo, ya que las βCDPEGs son nuevas entidades moleculares con respecto a sus componentes por separado, podrían inducir respuestas biológicas distintas a βCD y PEG libres.

3. Sí las herramientas de la ciencia de datos son utilizadas para extraer información a partir de conjuntos de datos, su implementación en el análisis de patentes farmacéuticas permitirá conocer el contexto fármaco-tecnológico de las CDs, las tendencias y áreas emergentes.

4. Objetivos

4.1. Objetivo general

Determinar la capacidad de auto-agregación de los βCDPEGs, así como las características de los agregados que generen información sobre su potencial como acarreadores de fármacos; realizar una caracterización biológica sistemática de los βCDPEGs en distintos modelos celulares *in vitro*; e implementar herramientas de la ciencia de datos para develar el panorama fármaco-tecnológico de las CDs.

4.2. Objetivos específicos

4.2.1. Respecto a la caracterización fisicoquímica

- Determinar la capacidad de auto-agregación del sistema βCDPEG5 a través de técnicas como densimetría, DLS, tensión superficial, TEM y simulación computacional.
- Investigar la influencia de la temperatura, el pH, la fuerza iónica y el tiempo en la auto-agregación de βCDPEG5 a través de DLS.

4.2.2. Respecto a la caracterización biológica

- Investigar el efecto de los βCDPEGs, βCD y PEGs en la viabilidad celular, la recuperación posterior al tratamiento, la generación de especias reactivas de oxígeno

(ROS) y de NO_2^- en la línea celular RAW264.7 correspondiente a macrófagos de ratón.

- Evaluar el efecto de los βCDPEGs, βCD y PEGs en la viabilidad celular, la recuperación posterior al tratamiento, la generación de ROS, la evolución del ciclo celular, y la migración celular, en las líneas MC3T3-E1 y MDCK correspondientes a osteoblastos y a células de riñón de perro, como modelo de células epiteliales.

4.2.3. Respecto al análisis fármaco-tecnológico de las CDs

- Implementar las herramientas de ciencia de datos en el análisis de patentes de tecnologías farmacéuticas basadas en CDs.
- Develar y analizar el panorama fármaco-tecnológico de tecnologías farmacéuticas a base de CDs.
- Identificar patrones en las tecnologías farmacéuticas a base de CDs para encontrar tendencias y áreas de oportunidad.

5. Metodología

5.1. Materiales y reactivos

β-ciclodextrina 98% (βCD), polietilenglicol-metil éter PM 2 kDa y 5 kDa (PEG2 y PEG5) se adquirieron de Sigma-Aldrich. Los βCDPEGs se obtuvieron como se reportó anteriormente (Rojas-Aguirre *et al*., 2019).

5.2. Estudio de la auto-agregación de βCDPEG5

5.2.1. Evaluación de la capacidad de auto-agregación de βCDPEG5

5.2.1.1. Determinación de cac por densimetría

Se determinó la concentración de agregación crítica (cac) a través de la medición de densidad de una serie de soluciones de βCDPEG5 en el intervalo de 0.005 a 1.100 mM. Para esto, se utilizó un densímetro Anton Paar DMA 4500 a 25±0.2 °C el cual utiliza el método de tubo en U oscilante. Antes de cada medición, se lavó el tubo de medición con etanol y agua desionizada. Por cada tres evaluaciones de βCDPEG5 a diferentes concentraciones, se hizo una medición con agua desionizada para asegurar la repetibilidad. La incertidumbre de la densidad fue de 0.00003 g/cm^3 a un nivel de confianza del 95%.

Los datos de densidad se suavizaron utilizando la función *UnivariateSpline* de los nodos de grado 4 y 1.1 del paquete *SciPy* en Python. La primera, segunda y tercera derivadas de los valores de densidad en función de la concentración de βCDPEG5 se obtuvieron del cociente de las diferencias discretas de densidad y concentración del paquete *NumPy* en Python. El valor de cac se determinó según el criterio de la tercera derivada (Moroi, 1992; Phillips, 1955). También se medió la densidad del dodecilsulfato sódico (SDS) en el intervalo de 0.849 a 5.278 mM. Los datos de densidad de SDS se trataron de la misma manera que para βCDPEG5 para calcular su cac. Los valores de densidad y de cac del SDS se utilizaron como referencia para el análisis de βCDPEG5.

5.2.1.2. Análisis por DLS

Para determinar la formación de agregados, su tamaño y comportamiento en muestras acuosas se empleó la técnica de DLS. Esta técnica permitió determinar el diámetro hidrodinámico (Dh) y volumen de distribución, el cual se refiere a la proporción de volumen que ocupa una determinada población de agregados en una muestra. La técnica de DLS se

basa en el movimiento browniano de las partículas cuyo Dh se calcula aplicando la ecuación de Stokes-Einstein $D_h = k_B T/3\pi\eta D$, donde k_B es la constante de Boltzman, T es la temperatura absoluta, η es la viscosidad del solvente y *D* es el coeficiente de difusión.

Se utilizó el equipo Nanotrack Wave (Microtrac Inc., Filadelfia, PA, EUA) con un ángulo de dispersión de 180° y una longitud de onda de 780 nm. El tamaño de partícula, mostrado como la función del volumen de distribución, fue proporcionado directamente por el software del instrumento Microtrac 'Flex' ver. 11.0.0.4 (Microtrac, 2021).

Para las mediciones, se prepararon muestras acuosas 0.5 mM de βCDPEG5. También se preparó una mezcla física (MF), a partir de βCD y PEG5 en agua a su concentración equivalente de 0.5 mM con respecto a βCDPEG5. Para el análisis, se incluyeron soluciones acuosas de βCD y PEG5, ambas a 0.5 mM con respecto a βCDPEG5. Todas las muestras se filtraron a través de un filtro de PET de 0.45 µm (Chromafil® Xtra) y se dejaron reposar durante 30 minutos antes del análisis. La muestra de βCD se sonicó durante un minuto (LC ultrasónica 20H) antes de la filtración. Las muestras se midieron una vez con seis corridas por medición y un período de detección de 60 segundos por corrida (n=6). Para el caso de βCDPEG5 0.5 mM, se prepararon y midieron tres muestras independientes en las condiciones mencionadas anteriormente (n=18). Todas estas muestras se analizaron a 25±0.5 °C.

5.2.1.3. Mediciones de tensión superficial

La tensión superficial producida por un intervalo de concentración de 0.0001 a 1.2 mM de βCDPEG5, βCD, PEG5 y la MF en la interfaz aire/agua se midió mediante la técnica de gota colgante utilizando un tensiómetro de perfil de caída de imagen (OCA20, DataPhysics, Alemania). Se utilizó una cámara de alta resolución (máximo 123 cuadros por segundo) para capturar los perfiles de caída y se analizaron por medio de la ecuación de Young-Laplace. Las gotas se mantuvieron a temperatura constante utilizando una celda termostatizada de diseño casero construida con vidrio óptico por Helma, Alemania (Luviano *et al*., 2020). Las mediciones se realizaron a 25±0.1 °C cuya temperatura se controló por un termobaño (Haake K20, Thermo Scientific). Las gotas de solución de βCDPEG5 se dejaron equilibrar durante al menos 6 horas.

5.2.1.4. Estudio por TEM

La morfología y el tamaño de los agregados de βCDPEG5 se determinaron mediante TEM. Las medidas se realizaron en un microscopio electrónico JEOL ARM200F, operado a 200 kV, reduciendo la dosis de electrones y utilizando una apertura de alto contraste. Para obtener las micrografías se dispersó una pequeña cantidad de la muestra seca en agua destilada usando un agitador *vortex*, luego se colocó una gota de la muestra sobre rejillas recubiertas de carbón Cu y se dejó secar completamente antes de la caracterización.

5.2.1.5. Simulación computacional

La molécula de βCDPEG5 se construyó como se muestra en la Figura 7, utilizando un modelo de átomos completos con el campo de fuerza GROMOS 54A7 generado a partir del generador de topología de campo de fuerza automatizado (ATB, http://compbio.biosci.uq.edu.au/atb) (Malde *et al*., 2011). El núcleo de βCD+triazol se modeló explícitamente. Sin embargo, en lugar de las 112 unidades monoméricas de PEG (-CH_2-CH_2-O-)$_{112}$, se simularon solamente 28 para facilitar los métodos computacionales y el análisis. La molécula de βCDPEG5 inicial se minimizó y corrió durante 1 nanosegundo en el conjunto NVT; luego, se construyó el dímero replicando el monómero y colocando ambas moléculas frente a sus grupos -OH. El sistema final se solvató con 50000 moléculas de agua utilizando el modelo SPCE (Berendsen *et al*., 1987). Todas las simulaciones se llevaron a cabo utilizando el software GROMACS-21 (Hess *et al*., 2008) con condiciones de contorno periódicas en todas las direcciones en el conjunto NPT. La temperatura y la presión se ajustaron a $T = 298.15\ K$ y $P = 1\ bar$ utilizando el termostato de escala V, con un tiempo de relajación de $\tau T = 0.2$ picosegundos, y el barostato Parinello-Rahman, con un tiempo de relajación de $\tau P = 2.0$ picosegundos, respectivamente. Las interacciones electrostáticas se manejaron con el método de Ewald de malla de partículas (Essmann *et al*., 1995), y las interacciones de corto alcance se ajustaron a 2.0 nm. Las longitudes de los enlaces se restringieron mediante el algoritmo de Lincs (Hess *et al*., 1997). Luego, se llevaron a cabo simulaciones hasta 80 nanosegundos, con un intervalo de tiempo de $dt = 0.002$ picosegundos, utilizando los últimos 10 nanosegundos para el análisis de datos.

5.2.2. Estudio de los agregados por DLS

5.2.2.1. Influencia de la temperatura, el pH y la fuerza iónica en los agregados de βCDPEG5

Se determinó el efecto de la temperatura, el pH y la fuerza iónica en la auto-agregación de βCDPEG5 por DLS. Los ensayos se realizaron a concentración de βCDPEG5 0.5 mM y todas las muestras se trataron como se describe en la Sección 5.2.1.2.

Para estudiar la influencia de la temperatura se preparó una muestra que posteriormente se introdujo en el equipo de DLS y se calentó a 37 °C (velocidad 1 °C/minuto) antes de las mediciones. Para determinar la influencia del pH, se prepararon varias muestras en solución tampón de acetato de sodio (ACS≥99% p/p Sigma-Aldrich) para obtener un pH 3.8; en una solución tampón salina de fosfatos (PBS en tabletas conteniendo fosfato 0.01 M, KCl 0.0027 M y NaCl 0.137 mM para una solución de 200 mL, ThermoFisher Scientific) para pH 7.4 y en PBS ajustado con NaOH para pH 8.0. Para estudiar la influencia de la fuerza iónica, se prepararon varias muestras en soluciones de NaCl (ACS≥99% p/p Sigma-Aldrich) al 0.9% y 7.5%. Los ensayos de pH y fuerza iónica se realizaron a 25±0.5 °C.

5.2.2.2. Comportamiento de los agregados con respecto al tiempo

Las mediciones de DLS para βCDPEG5 0.5 mM se realizaron en agua, todos los días del día 2 al 5, cada cinco días del día 5 al 35, y el último análisis se realizó el día 55. La muestra se midió una vez con seis corridas por medición como se describió anteriormente (n=6 por día) a temperatura de 25±0.5 °C.

5.2.2.3. Estadística

Para determinar las diferencias estadísticas entre el Dh de los agregados de βCDPEG5 obtenidos en las condiciones experimentales, se calculó un análisis de varianza (ANOVA) unidireccional con una corrección *post hoc* de Dunnett para comparaciones múltiples utilizando el software GraphPad Prism versión 7.0 para Windows (GraphPad Software, San Diego, California, www.graphpad.com). Se estableció el valor alfa en 0.05 y un valor $p<0.05$ se consideró el criterio de significancia. De esta manera, se determinaron los valores promedio de Dh±desviación estándar (DE) con n=6 para todas las mediciones.

5.3. Caracterización biológica de βCDPEGs *in vitro*

5.3.1. Cultivos celulares

Los macrófagos RAW 264.7 (TIB-71), los preosteoblastos MC3T3-E1 subclon 4 (CRL-2593) y las células de riñón MDCK (CCL-34) se adquirieron de la *American Type Culture Collection* (ATCC). Los preosteoblastos MC3T3-E1 se cultivaron en un medio alfa-medio esencial mínimo (MEM), y tanto los macrófagos como las células MDCK se propagaron en un medio de águila modificada de Dulbecco (DMEM). Todos los medios de cultivo se complementaron con suero bovino fetal al 10% (FBS, BenchMark, Gemini Bio Products), estreptomicina de penicilina al 1% (Sigma-Aldrich), L-glutamina al 1% y 1.5 g/L de bicarbonato de sodio, y se incubaron hasta la confluencia a 37 °C y en atmósfera de CO_2 al 5%.

En la Figura 8 se muestran esquemáticamente las pruebas que se realizaron en las tres distintas líneas celulares.

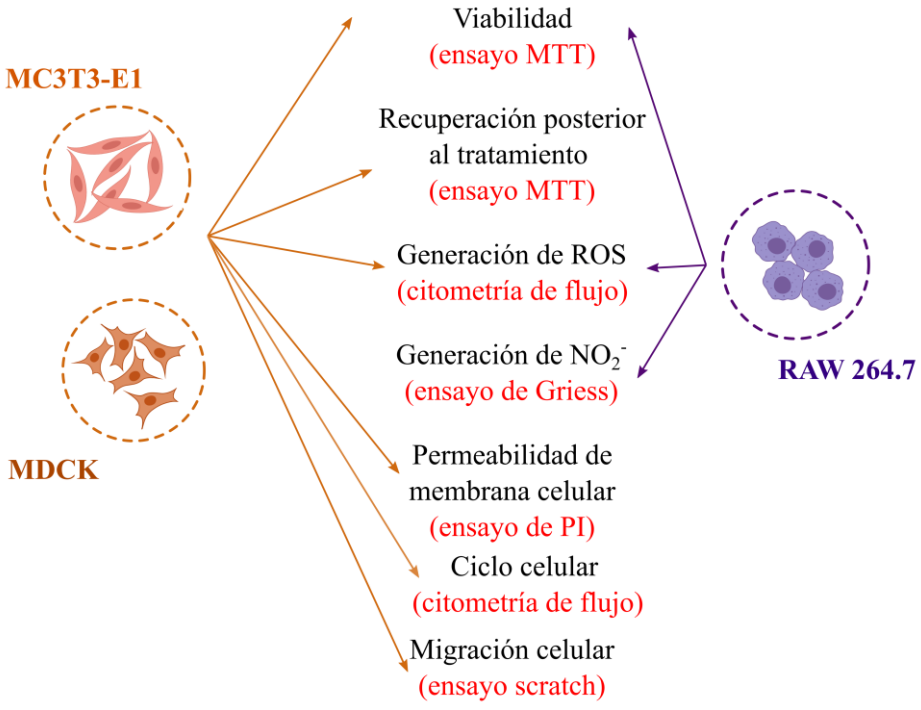

Figura 8. Diagrama de la metodología utilizada para el estudio del efecto βCDPEGs, βCD y PEGs en los modelos MC3T3-E1, MDCK y RAW264.7.

5.3.2. Ensayo de viabilidad celular

La susceptibilidad de las células RAW 264.7, MC3T3-E1 y MDCK a βCDPEGs, βCD y PEGs se llevó a cabo en una placa de 96 pozos con 10000 células por pozo. La viabilidad de las células se midió mediante la reducción del reactivo 3-(4,5-dimetiltiazol-2-il)-2,5-difeniltetrazolio (MTT, Sigma-Aldrich) siguiendo las instrucciones del fabricante. Las células se sembraron durante 24 horas en medio de cultivo celular a 37 °C y en una atmósfera de CO_2 al 5%. Luego, se descartó el medio celular y se agregaron diferentes cantidades de los compuestos (de 25 a 500 µg/mL) en un volumen final de 100 µL de medio celular. Posteriormente, las células se incubaron durante 24 horas a 37 °C y 5% de CO_2. Después de esto, se eliminó el medio de cultivo y las células se enjuagaron tres veces con 200 µl de PBS 1x, para llevar a cabo el ensayo de determinación de actividad citotóxica por medio de MTT. Como control de la viabilidad celular se utilizaron células sin tratar, mientras que el control negativo se evaluó utilizando 100 µl de Triton X-100 al 0.5% en PBS. La medición de la absorbancia de la reducción de MTT se registró con un lector de placas de 96 pozos (GoScan, Thermo Scientific, EUA). La absorbancia de fondo de la viabilidad celular se midió a 690 nm y se sustrajo de los valores de absorbancia de la reducción de MTT debido a que la viabilidad celular se registró a 570 nm. Se realizaron tres experimentos independientes cada uno por triplicado.

5.3.3. Producción de nitrito por macrófagos

Se utilizó el ensayo de Griess para medir la producción de nitritos generados por los macrófagos tras la incubación con los βCDPEGs, βCD y PEGs. Los macrófagos se sembraron en una placa de 96 pozos a una densidad de 10000 células por pozos y se incubaron durante 24 horas a 37 °C y 5% de CO_2. Posteriormente, se agregaron a los pozos diferentes concentraciones, de 25 a 500 µg/mL de βCDPEGs, βCD y PEGs, y se incubaron durante 24 horas a 37 °C y 5% de CO_2. Luego, se mezclaron 20 µL de medio celular de cada pozo en un nuevo pozo con 80 µL de nitroprusiato de sodio 5 mM y se incubaron durante 1 hora en oscuridad a 37 ºC y 5% de CO_2. Después, la reacción se mezcló con 100 µL de solución de reactivo de Griess (sulfanilamida al 0.1% y N-(1-naftil etilendiamina) al 0.1%) y se incubó a 25 °C durante 15 minutos en la oscuridad. La absorbancia de las muestras se leyó a 540 nm, y los valores se compararon con una curva estándar utilizando 1.67 a 100 µM

de nitrito de sodio como reactivo de referencia de producción de nitrito. Se realizaron tres experimentos independientes por triplicado.

5.3.4. Producción de ROS

La producción de ROS se midió por citometría de flujo. Se sembraron 50000 células RAW 264.7, MC3T3-E1 o MDCK en una placa de 24 pozos y se incubaron durante 24 horas con βCDPEGs, βCD y PEGs de 25 a 500 µg/mL a 37 °C y 5% de CO_2. Luego, las células se enjuagaron con PBS 1x y se incubaron con 30 µM de diacetato de 2', 7'-diclorofluoresceína durante 90 minutos a 37 °C y 5% de CO_2. Después de esto, las células se enjuagaron, recolectaron y resuspendieron en PBS 1x para mediciones de citometría de flujo, usando el canal BL-1 para una excitación de 488 nm y láseres de emisión de 525 nm. El nivel endógeno y basal de ROS para cada línea celular se registró a partir de células sin tratamientos con βCDPEGs, βCD o PEGs. La fluorescencia se midió en un citómetro de flujo Attune NxT (Life Technologies, Carlsbad, California, EUA). Los datos consistieron en 10000 eventos (células) calculados por triplicado en tres experimentos independientes para cada muestra. Se utilizó el software de adquisición Attune NxT versión 3.2.1. (ThermoFisher Scientific) para el análisis de los datos.

5.3.5. Ensayo de recuperación posterior al tratamiento (ensayo de re-cultivo)

Para determinar si la exposición de células MC3T3-E1 o MDCK a βCDPEGs, βCD y PEGs inducía algún efecto citostático, se llevó a cabo un ensayo de recuperación posterior al tratamiento, también denominado re-cultivo. Después de incubar las células con βCDPEGs, βCD y PEGs, las células se enjuagaron, recolectaron y colocaron en una nueva placa de cultivo de 96 pozos y se incubaron a 37 °C en una atmósfera de CO_2 al 5% con medio de cultivo celular sin tratamiento durante 24 horas. Después de eso, las células se analizaron mediante el mismo procedimiento que para el ensayo de viabilidad celular MTT.

5.3.6. Ensayo de permeabilidad de la membrana celular

Tras la incubación de células MC3T3-E1 o MDCK con las diferentes concentraciones de βCDPEGs, βCD y PEGs, las células se recolectaron mediante tripsinización, se resuspendieron en 200 µL de PBS 1x y se incubaron durante 30 minutos con yoduro de propidio (PI) a 25 °C, para medir la permeabilidad de la membrana celular. Luego, las células se enjuagaron tres veces con PBS y se analizaron usando el citómetro de flujo Attune NxT

(Life Technologies, Carlsbad, California, EUA). Los datos de la citometría de flujo consistieron en 10000 eventos analizados con BL3 para la detección de PI utilizando el software de adquisición Attune NxT versión 3.2.1. (ThermoFisher Scientific).

5.3.7. Medidas de progresión del ciclo celular por citometría de flujo

Se sembraron células con una densidad de 10000 células por pozo en una placa de cultivo de 96 pozo y se incubaron con diferentes concentraciones de βCDPEGs, βCD y PEGs, durante 24 horas a 37 °C en una atmósfera de CO_2 al 5%. Después de esto, las células se recolectaron mediante tripsinización y se resuspendieron con 1 mL de etanol frio al 70%. Las células se fijaron mediante incubación a 4 °C durante 1 hora. Luego, las células se centrifugaron y resuspendieron en 1 mL de PBS, se agregó 100 μg/mL de RNasa a cada muestra y se incubaron a 37 °C durante 30 minutos. Las células se centrifugaron y resuspendieron en 1 mL de PBS y se tiñeron con 10 μL de PI (50 μg/mL) durante 30 minutos a 4 °C. Los datos se adquirieron en un citómetro de flujo Attune NxT (Life Technologies, Carlsbad, California, EUA) y consistieron en al menos 2000 eventos analizados con el canal BL3 para la detección de PI. Software de adquisición Attune NxT versión 3.2.1. se utilizó para el análisis de datos (ThermoFisher Scientific).

5.3.8. Ensayo de migración celular

La migración celular, evalúa la motilidad de las células a través de su capacidad para migrar y cerrar una herida o brecha hecha en un monocapa celular confluente. Las células se sembraron en una placa de 12 pozos a una densidad de 80000 células por pozo. Una vez que las células fueron confluentes, se hizo un rasguño vertical (herida, brecha) desde el principio hasta el final del pozo. Se colocaron inmediatamente diferentes concentraciones de βCDPEGs, βCD y PEGs en la parte superior de las células en un volumen final de 1 mL. Las células se incubaron durante 24 horas a 37 °C en una atmósfera de CO_2 al 5%. Se tomó como control a las células incubadas solo con medio celular. La migración celular se monitoreo con un microscopio invertido y se tomaron fotografías de las células en cultivo 24 horas después de la adición del tratamiento. Finalmente, se representó gráficamente el tamaño de la brecha para cada tratamiento como el porcentaje de cierre celular en relación con el control.

5.3.9. Estadística

Para todos los ensayos se realizaron tres experimentos independientes con triplicados internos. Los resultados se expresaron como promedio±DE de los tres experimentos independientes. Los datos se evaluaron mediante un ANOVA unidireccional comuna prueba *post hoc* de comparación múltiple Tukey utilizando el software GraphPad Prism versión 6.0c para Windows (GraphPad Software, San Diego, California, www.graphpad.com). Se estableció el valor alfa en 0.05 y un valor $p<0.05$ se consideró el criterio de significancia.

5.4. Panorama fármaco-tecnológico de las CDs

5.4.1. Extracción de patentes farmacéuticas de CDs

Se extrajeron 1998 patentes farmacéuticas de CDs de la base de datos Derwent Innovation Index (DII, Clarivate, 2020; plataforma disponible a través de BiDiUNAM hasta el 2019). Para esto, se utilizó la herramienta de búsqueda avanzada (Web of Science, 2020) y la delimitación de tiempo hasta el año 2019 de DII, los parámetros se establecieron a través de una ecuación búsqueda implementando operadores booleanos (*AND, OR, NOT*) para abarcar o excluir información. La ecuación resultante incluyó a todas aquellas patentes que tuvieran la palabra *'cyclodextrin'* y la clasificación internacional de patentes (IPCs) que se consideraron convenientes:

TS=cyclodextrin AND IP=A61K* AND IP=A61P* AND (IP=A61K-047/40 OR IP=A61K-031/724) NOT IP=A61Q**

A61K* (preparaciones para uso médico, dental o de tocador); A61P* (actividad terapéutica específica de compuestos químicos o preparaciones médica); A61K-047/40 (ciclodextrinas y sus derivados, como preparaciones medicinales caracterizadas por ingredientes inactivos); A61K-031/724 (ciclodextrinas como preparaciones medicinales que contienen ingredientes orgánicos activos) y A61Q*(productos cosméticos o de tocador similares).

5.4.2. Patentamiento con respecto al tiempo

Del conjunto de 1998 datos, y utilizando las herramientas de DII, se clasificaron las patentes por año para identificar el patentamiento con respecto al tiempo y distinguir algunas de las patentes más citadas.

5.4.3. Clasificación en función de solubilidad, estabilidad y enmascaramiento de sabor/olor

Nuevamente, a partir de las 1998 patentes y utilizando las herramientas de DII descritas anteriormente, se buscó identificar el número de innovaciones en las que se utilizaron CDs como solubilizantes, estabilizadores o agentes para enmascarar de sabor u olor. Para ello, se implementaron tres ecuaciones de búsqueda con la combinación de palabras clave truncadas (*) asociadas con solubilidad, estabilidad y enmascaramiento.

TS=(cyclodextrin AND (solubility OR solubilization OR soluble)) AND (IP=A61K* OR IP=A61P*) AND IP=A61K-047/40 NOT IP=A61K-031/724 NOT IP=A61Q**

TS=(cyclodextrin AND (stability OR stabilization)) AND (IP=A61K* OR IP=A61P*) AND IP=A61K-047/40 NOT IP=A61K-031/724 NOT IP=A23* NOT IP=A61Q**

TS=(cyclodextrin AND (mask* OR bitter* OR sweet* OR taste)) AND (IP=A61K* OR IP=A61P*) AND IP=A61K-047/40 NOT IP=A61K-031/724 NOT IP=A23* NOT IP=A61Q**

A23* (formación o elaboración de productos alimenticios) se excluyó debido a que se encontró relación entre estos parámetros y la química o industria de alimentos.

5.4.4. Análisis de patentes con herramientas de ciencia de datos

El análisis de las 1998 patentes se llevó a cabo siguiendo los pasos de la Figura 9. A continuación se describe cada uno de ellos.

5.4.4.1. Pre-procesamiento de datos

El pre-procesamiento se realizó para eliminar ruido, filtrar el texto y preparar el conjunto de datos de las 1998 patentes para su posterior procesamiento. Para esto se utilizaron las librerías de Python: *Natural Lenguage ToolKit* (Bird *et al*., 2009) y Pandas (McKinney, 2010) (Figura 9). El procedimiento en orden cronológico se describe a continuación:

- Se removió la puntuación y los caracteres especiales (números, símbolos matemáticos), y se transformó el texto a caracteres en minúsculas.
- Se removieron las palabras ‘vacías’ (artículos, pronombres, preposiciones) innecesarias para la clasificación de patentes.

- Se hizo una lematización del texto, es decir, familias de palabras derivadas de una raíz única se reemplazaron por una forma de diccionario o base única conocida como el lema.
- Se removieron aquellas palabras que no proveían de un contexto particular al documento, como adjetivos, verbos y adverbios.

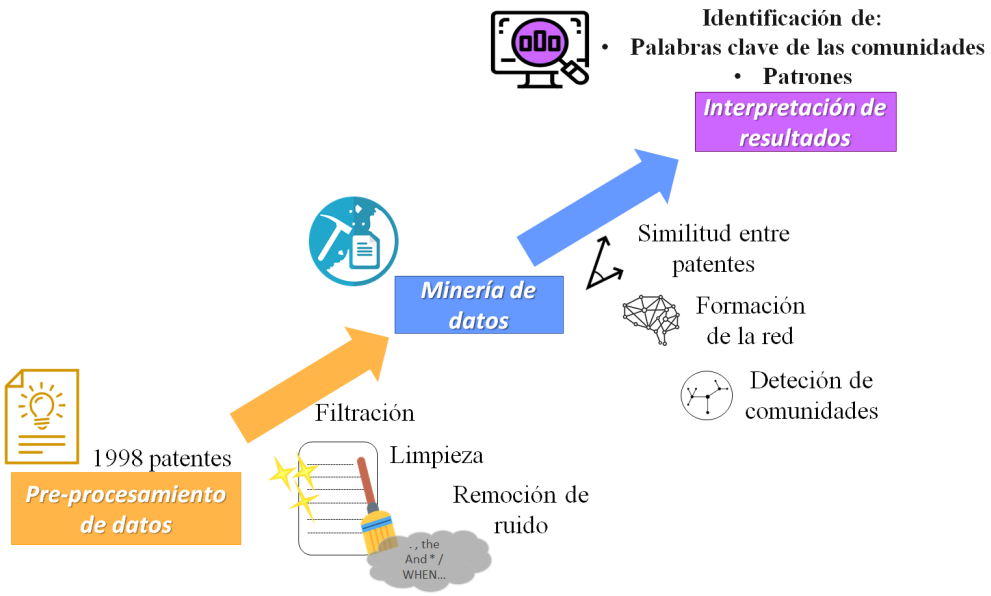

Figura 9. Diagrama de flujo del análisis de patentes por ciencia de datos (Rincón-López *et al.*, 2021).

5.4.4.2. Minería de datos en patentes farmacéuticas de CDs por medio de ciencia de redes

Como resultado del pre-procesamiento se obtuvieron las palabras que proveen de contexto a cada documento, consideradas como representantes del contenido semántico. Estas se utilizaron para definir un espacio euclidiano de d-dimensiones, en el cual, cada patente se representa como un vector, conformado por las 5 palabras más frecuentes en ella.

Una vez representada la información relevante de las patentes como vectores, se definió una medida para cuantificar la similitud entre dos patentes. Se usó la similitud de coseno que da una medida proporcional al ángulo entre patentes i y j, y se define como $c_{ij} = \frac{2}{\pi} cos^{-1}\left(\frac{\vec{v}_i \cdot \vec{v}_j}{|\vec{v}_i||\vec{v}_j|}\right)$, donde $\vec{v}_i$ denota el vector que describe la patente i, $\vec{v}_i \cdot \vec{v}_j$ es el producto punto entre vectores y $|\vec{v}_i| = \sqrt{\vec{v}_i \cdot \vec{v}_i}$ es la norma. Si se comparan dos vectores de patentes diferentes (patentes i y j) y están conformados por las mismas palabras, el cociente de

similitud $c_{ij} = 0$; sí, de lo contrario, están conformadas por palabras diferentes, el cociente de similitud $c_{ij} = 1$.

Luego de comparar todos los pares de patentes, y obtener los valores c_{ij}, se realizó un análisis estadístico para establecer el valor de H que determina cuándo dos patentes se consideran similares o no, es decir, cuándo están conectadas en la red y cuándo no.

Así, utilizando los coeficientes de similitud c_{ij} y los valores de H, se generó una red de patentes en la que se establece un vínculo (conexión) entre dos patentes i y j sí $0 < C_{ij} \leq H$, es decir, una red descrita por una matriz A (denotado como A_{ij}) tendrá el elemento 1 si dos nodos (patentes) están conectados y el elemento 0 en caso contrario; por lo tanto, $A_{ij} = 1$ sí $0 < C_{ij} \leq H$ y $A_{ij} = 0$ para $C_{ij} > H$ para esta red. Por definición, la matriz considera la diagonal $A_{ij} = 0$ para evitar bucles o conexiones de un nodo consigo mismo.

Una vez definida la estructura, se aplicaron diferentes herramientas de la librería Python para su análisis (Hagberg *et al*., 2008). Este se centró en el componente conectado más grande (LCC), que detecta el conjunto más grande de nodos (patentes) conectados dentro de la red; esta subred no incluye grupos pequeños de patentes o patentes individuales. Por otro lado, se estudiaron los grados de red, definidos como $k_i = \sum_{l=1}^{N} A_{il}$ (siendo N el tamaño de la LCC), que proporcionó el número de conexiones de la patente i.

Para detectar comunidades en la red se aplicó el algoritmo de Louvain (Blondel *et al*., 2008), es decir, para encontrar grupos de patentes con contenido semántico similar. La interpretación de estas comunidades se llevó a cabo analizando las palabras clave más frecuentes en cada una de ellas.

5.4.4.3. Evolución temporal de las patentes de acuerdo con las formas farmacéuticas

De acuerdo con los resultados de la primera minería, se hizo una segunda minería en las 1998 patentes guiada por palabras correspondientes a las formas farmacéuticas para determinar el número de patentes relacionadas con cada una de ellas y observar cómo han evolucionado en el periodo de 1980 al 2019.

6. Resultados

6.1. Estudio de la auto-agregación de βCDPEG5

El análisis de la auto-agregación de βCDPEGs se llevó a cabo únicamente para el sistema βCDPEG5. Como se mencionó en los antecedentes, aunque PEG se considere como hidrofílico, al aumentar el PM (por encima de 4700/5000 Da) se comporta más como un polímero anfifílico (Wu *et al*., 2014). Por este motivo, aunque βCDPEG5 no lleva sustituyentes hidrofóbicos en sí, el PM y la densidad de injerto de PEG estaría indicando cierto grado de anfifilicidad (Jokerst *et al*., 2011).

6.1.1. Evaluación de la capacidad de auto-agregación de βCDPEG5

6.1.1.1. Determinación de cac por densimetría

La cac se refiere a la concentración mínima a la que las moléculas se auto-agregan. Existen diversos métodos para determinar la cac, entre ellos se encuentran los análisis densimétricos. Las mediciones de densidad pueden determinar la agregación y la cac, dado que la agregación es un proceso de deshidratación que conduce a un aumento del agua libre con respecto al agua unida por interacciones no covalentes a las moléculas poliméricas no agregadas (Perinelli *et al*., 2020; Z. Zhang *et al*., 2013). Esta es la primera vez que se utiliza un método de densimetría para analizar la agregación de sistemas a base de CDs con aplicación en el área farmaceutica (Rincón-López, Ramírez-Rodríguez, *et al*., 2021).

La Figura 10A muestra el cambio de densidad en función de diferentes concentraciones (de 0.05 a 0.1 mM) de muestras acuosas de βCDPEG5. Se calculó la primera, segunda y tercera derivada, y se identificó la cac cuando la tercera derivada fue igual a cero (Figura 10B): 0.496 mM.

Se incluyó en estos experimentos el análisis del conocido surfactante SDS como punto de referencia para compararlo con βCDPEG5. Inesperadamente, los cambios de densidad inducidos por βCDPEG5 en el medio fueron significativamente mayores que los del SDS. Asimismo, el valor de la cac de βCDPEG5 fue mucho menor que el de SDS, que fue de 2.730 mM (Figura 1 Apéndice A).

Recientemente, Loftsson *et al*. publicó un trabajo que informa los valores de cac, determinados por la permeación a través de membranas de celofán semipermeables, de CDs

nativas y de HPβCD, que van de 7 a 84 mM (Loftsson *et al*., 2019). Un valor bajo de cac se considera como deseable ya que conduce a una mejor estabilidad estructural de los agregados en condiciones diluidas y a una mayor capacidad de solubilización de moléculas lipofílicas por parte de los agregados (Aydin *et al*., 2016; Kulthe *et al*., 2012; Lu *et al*., 2018; Szutkowski *et al*., 2018). Por ello, dentro de este contexto se destaca el valor bajo de cac de βCDPEG5, que parece ser muy prometedor para el desarrollo de sistemas de liberación de fármacos poco solubles.

Se ha señalado que las medidas de densidad no son confiables para obtener valores de cac para tensioactivos no iónicos a bajas concentraciones, ya que la densidad, en esos casos, es prácticamente la misma que la del agua ultra pura (producida por un desionizador de laboratorio) (Perinelli *et al*., 2020). En este estudio, el análisis densimétrico reveló que las moléculas de βCDPEG5 se auto-agregan a concentraciones relativamente bajas y modifican la densidad del medio en un grado más significativo que el SDS.

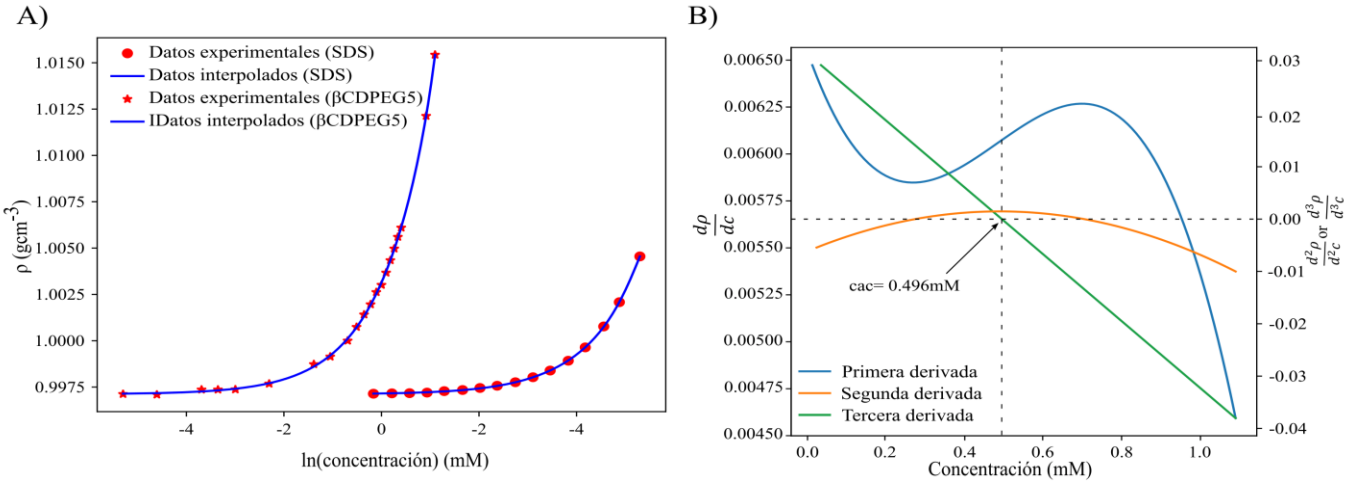

Figura 10. A) Función de densidad para βCDPEG5 y SDS, B) análisis de derivadas de la función de densidad de βCDPEG5 (Rincón-López, Ramírez-Rodríguez, *et al*., 2021).

6.1.1.2. Análisis por DLS

La medición por DLS de una solución de βCDPEG5 0.5 mM reveló la presencia de dos poblaciones con diferente Dh, una con Dh1 de 156.5 nm atribuida a agregados, y otra con Dh2 de 9.0 nm atribuida a dímeros, previamente observados para esta molécula por medio de espectrometría de masas (MS MALDI-TOF) (Rojas-Aguirre *et al*., 2019). La función de volumen de distribución calculada por el equipo mostró que ambas poblaciones coexisten

ocupando volúmenes equiparables de 55.1% y 44.9% respectivamente (Figura 11A, Tabla 1 Apéndice A).

Para corroborar que la formación de agregados es un proceso determinado por la conjugación covalente entre βCD y PEG5, se llevó a cabo el análisis por DLS de una MF y de los componentes por separado.

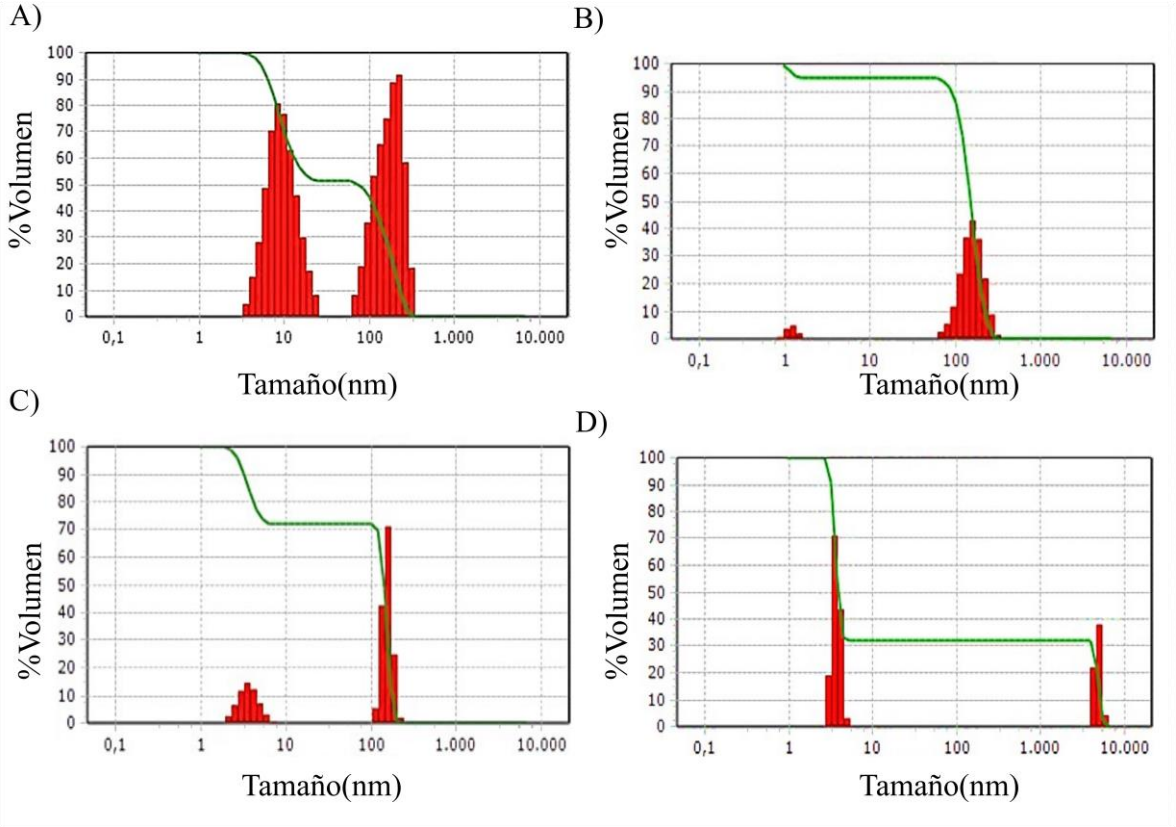

Figura 11. Poblaciones de A) βCDPEG5, B) βCD, C) PEG5, y D) MF por DLS (Rincón-López, Ramírez-Rodríguez, *et al*., 2021).

La medición de βCD mostró una población de Dh de 148.4 nm en simultáneo con otra de 1.2 nm que corresponden a los agregados y monómeros de βCD respectivamente, lo cual coincide con lo ya reportado en la literatura (Figura 11B, Tabla 2 Apéndice A) (Bonini *et al*., 2006; Coleman *et al*., 1992; de Sousa *et al*., 2012; González-Gaitano *et al*., 2002; Sá Couto *et al*., 2018). Para PEG5 se observó la formación de dos poblaciones, una con un Dh1 de 148.8 nm y otra con Dh2 de 3.6 nm (Figura 11C, Tabla 3 Apéndice A), los que, también, coinciden con lo reportado previamente en la literatura (Dey *et al*., 2019; Ho *et al*., 2003;

Linegar *et al*., 2010). Los resultados de la MF presentaron agregados de 3.6 nm, atribuidos al PEG5 libre; también se observaron entre 930-5080 nm que podrían ser agregados o *clusters* grandes débilmente unidos, que resultarían de la interacción de βCD y PEG5 libres, o de CIs βCD/PEG5 (Figura 11D, Tabla 4 Apéndice A).

Los agregados observados en βCDPEG5 de 156 y 9 nm estuvieron ausentes en la MF, lo que indica que la auto-agregación de βCDPEG5 se da únicamente cuando las cadenas de PEG5 están unidas de manera covalente a la βCD. Sin esta conjugación, βCD y PEG5 pueden interactuar de maneras diversas a través de otros mecanismos, incluida la formación de CIs βCD/PEG5 (Abdulrahman, 2018; Udachin *et al*., 2000).

6.1.1.3. Mediciones de tensión superficial

La tensión superficial es una propiedad que depende de las interacciones que se formen entre el medio, las moléculas en él y la presencia de estas en la superficie. Por lo tanto, su medición puede indicar de manera indirecta lo que sucede en el seno de la solución (Sá Couto *et al*., 2018).

En la Figura 12A se muestra el cambio en la tensión superficial que produce βCD, PEG5, la MF y el sistema βCDPEG5 en un periodo de tiempo de 350 minutos. βCD se comportó como el agua, es decir, no modifico la tensión superficial, un comportamiento ya observado para αCD (Hernandez-Pascacio *et al*., 2016; Luviano *et al*., 2020; Sá Couto *et al*., 2018). PEG5 modificó la tensión superficial de manera constante, como ya ha sido reportado para otros PEGs de PM cercano al PEG5 (PM 6 kDa) (Singh *et al*., 2017). Lo anterior también sucedió con la MF, lo que sugiere que cada molécula, de PEG5 y βCD, actuó en la interfaz de manera independiente sin importar si estas interactuaban entre ellas, incluso a través de CIs βCD/PEG5, tal y como se observó por DLS. Para βCDPEG5, se evidenció que por encima de la cac (0.5 mM y 1.2 mM) el sistema se adsorbe lentamente en la interfaz líquido/aire.

Así mismo, se realizó la medición de la tensión superficial al equilibrio entre 0.0002 y 1.2 mM para PEG5, la MF y βCDPEG5 (Figura 12B). Para los primeros dos, la tensión superficial al equilibrio fue constante en todo el intervalo de concentraciones. Las moléculas de PEG han mostrado que se pliegan e interactúan entre ellas en el agua (Alessi *et al*., 2005; Rego *et al*., 2017), por lo que, el cambio en la tensión superficial del agua podría estar dado por el desdoblamiento de las cadenas poliméricas en la interfaz agua/aire. Entonces, está

claro que independientemente de la concentración, e incluso si existen CIs βCD/PEG5, la tensión superficial para la MF está dada por PEG.

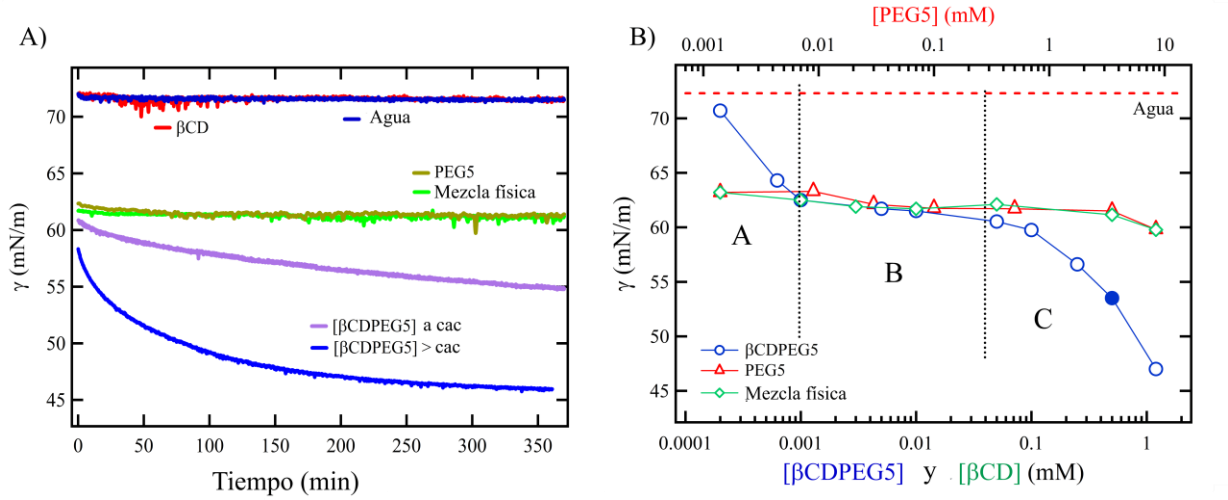

Figura 12. A) Tensión superficial dinámica de soluciones acuosas de βCDPEG5, βCD, PEG5, y la MF; βCDPEG5>cac refiere a 1.2 mM. B) Tensión superficial al equilibrio a diferentes concentraciones de βCD, PEG5, MF; el punto azul relleno simboliza la cac (Rincón-López, Ramírez-Rodríguez, *et al*., 2021).

Por otro lado, se observó que el comportamiento del sistema βCDPEG5 depende de la concentración, identificándose tres regiones (A, B y C) diferentes en la curva de tensión superficial-concentración de βCDPEG5:

- En la región A, a bajas concentraciones (0.0001-0.001 mM), el βCDPEG5 cambió ligeramente la tensión superficial del agua. Por lo tanto, se cree que las moléculas de βCDPEG5 permanecieron principalmente en el seno de la solución como entidades individuales.
- A concentraciones intermedias (región B, entre 0.001-0.05 mM), el comportamiento de βCDPEG5 fue idéntico al observado para PEG5 y la MF. Lo que podría significar que los dímeros observados por MS MALDI-TOF y DLS empiezan a formarse y a migrar a la superficie, el PEG5 del βCDPEG5 entra en la interfaz líquido/aire y reduce la tensión superficial del agua. Este comportamiento indica que la conformación de PEG5 en los dímeros de βCDPEG5 es similar a la conformación plegada del PEG5 libre.

- En el intervalo de 0.05-1.2 mM (región C), en la que se encuentra la cac, empieza la formación de agregados. Por lo cual, los agregados presentes en el seno de la solución migran a la superficie en donde hay una menor área disponible por molécula, empiezan a desenmarañar lentamente las cadenas de PEG5 de su exterior y reducen drásticamente la tensión superficial. Esto, a su vez, sugiere que la conformación de las cadenas de PEG5 de βCDPEG5 en el agregado difiere de la de los dímeros y, por lo tanto, su interacción con las moléculas de agua también es diferente.

En resumen, estos resultados muestran que el cambio en la tensión superficial es una consecuencia indirecta de la formación de dímeros y posterior formación de agregados de βCDPEG5 en el seno de la solución y la migración a la superficie.

6.1.1.4. Estudio por TEM

TEM es una técnica comúnmente utilizada para observar la morfología de agregados (Jansook *et al*., 2018). En la Figura 13 se muestra una micrografía obtenida para una solución de βCDPEG5 en agua, en esta se observa una morfología cuasi esférica con un diámetro promedio de ~120 nm.

La diferencia en el tamaño observado en TEM con respecto a DLS se debe a que este último determina el radio hidrodinámico del agregado en suspensión, es decir incluyendo a la esfera de hidratación; mientras TEM analiza el agregado aislado del medio (Zielińska *et al*., 2020).

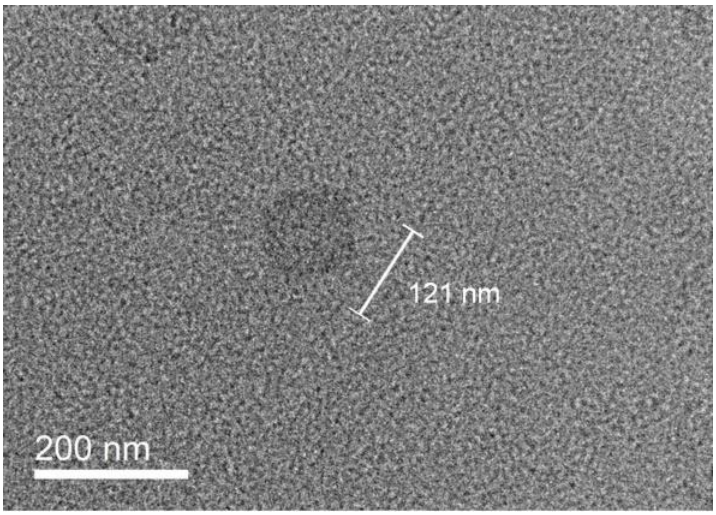

Figura 13. Micrografía TEM de una solución de 0.5 mM de βCDPEG5 en agua (Rincón-López, Ramírez-Rodríguez, *et al*., 2021).

Por lo tanto, las moléculas de βCDPEG5 forman nanoestructuras de ~150 nm, que, junto con el valor bajo de cac (10^{-1} mM), agrupa características que le brindan un gran potencial como sistema de liberación de fármacos.

6.1.1.5. Simulación computacional

Se realizaron estudios computacionales para obtener más información sobre la auto-agregación de βCDPEG5. Debido a la complejidad de simular el agregado de βCDPEG5, se simuló únicamente la interacción entre dos moléculas de βCDPEG5, como una primera etapa en el proceso de formación de agregados de βCDPEG5 ~150 nm, como lo sugiere el análisis de tensión superficial. Los resultados de la simulación se compararon con los experimentos anteriores.

La Figura 14 muestra los perfiles de densidad del agua y del dímero de βCDPEG5, junto con la última configuración del dímero. Se observa que la densidad en moléculas de agua es mínima en la región del dímero de βCDPEG5, lo cual es consistente con las mediciones de densidad (Sección 6.1.1.1.).

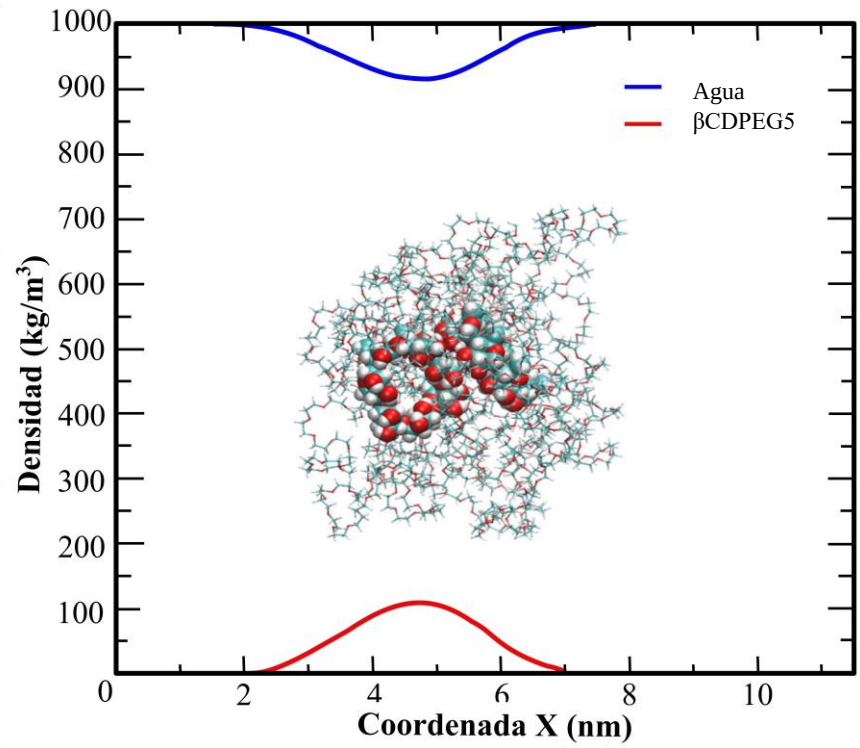

Figura 14. Perfil de densidad en eje X del sistema βCDPEG5-agua. La línea roja inferior es el perfil del dímero βCDPEG5 y la línea azul superior es el perfil del agua. En el medio, se

muestra la última configuración del dímero. Las bolas azules representan los átomos de carbono, las rojas los oxígenos y las blancas los hidrógenos. Las líneas delgadas son las cadenas PEG (Rincón-López, Ramírez-Rodríguez, *et al*., 2021).

En cuanto a la conformación del dímero, las caras anchas de las βCD parecen acomodarse frente a frente y formar un ángulo entre los planos que las contienen. Las cadenas de PEG5 están plegadas, y dispuestas de tal manera que rodean a las βCDs lo cual coincide con lo observado por tensión superficial.

A partir de las simulaciones, se encontró que el núcleo de βCDs ocupa 2.52 nm de diámetro y las cadenas de PEG5 1.84 nm. Con estos valores se pudo calcular el diámetro de la estructura, que correspondió a 4.36 nm. Dado que las simulaciones se realizaron con casi un cuarto del tamaño de las cadenas de PEG5, se estimó el tamaño del dímero multiplicando por cuatro el tamaño de PEG5 calculado y sumándolo al diámetro del núcleo, lo que da como resultado ~9.88 nm, que consistente con los resultados de DLS sobre los dímeros (Sección 6.1.1.2.).

Finalmente, se calculó el número de enlaces de hidrógeno entre las cadenas de PEG5 y el agua, encontrando un número total de 230 enlaces. Si hay 28 unidades monoméricas (-CH_2-CH_2-O-) y 14 cadenas, entonces el número promedio de enlaces por unidad monomérica de PEG es de aproximadamente 0.59, este valor se discutirá a mayor profundidad en la Sección 6.1.2.1.

6.1.1.6. Corolario de la capacidad de auto-agregación de βCDPEG5

Con base en todos los resultados presentados anteriormente, se confirma la hipótesis de βCDPEG5 como una a-CD, además se considera como una estructura dibloque A-B con la capacidad de auto-agregarse para formar nanoestructuras en medio acuoso en función de su concentración (Figura 15A). El bloque A comprende a βCD, con su borde ancho disponible para acercarse a otra molécula de βCDPEG5, que eventualmente podría interactuar a través de enlaces de hidrógeno intermoleculares entre los grupos -OH de su cara secundaria, dando lugar a los dímeros βCDPEG5-βCDPEG5 (Figura 15B).

Las siete cadenas de PEG5 constituyen el bloque B, las cuales dominan la anfifilicidad de βCDPEG5 y promueven la auto-agregación de moléculas de βCDPEG5 en dímeros y

agregados cuando aumenta la concentración de βCDPEG5. Los agregados de βCDPEG5 se mantendrían unidos por fuerzas de atracción entre los bloques de PEG5, y entre los bloques de PEG5 y las moléculas de agua, lo que a su vez induciría un estado más estirado de las cadenas de PEG que envuelven al agregado (Figura 15C).

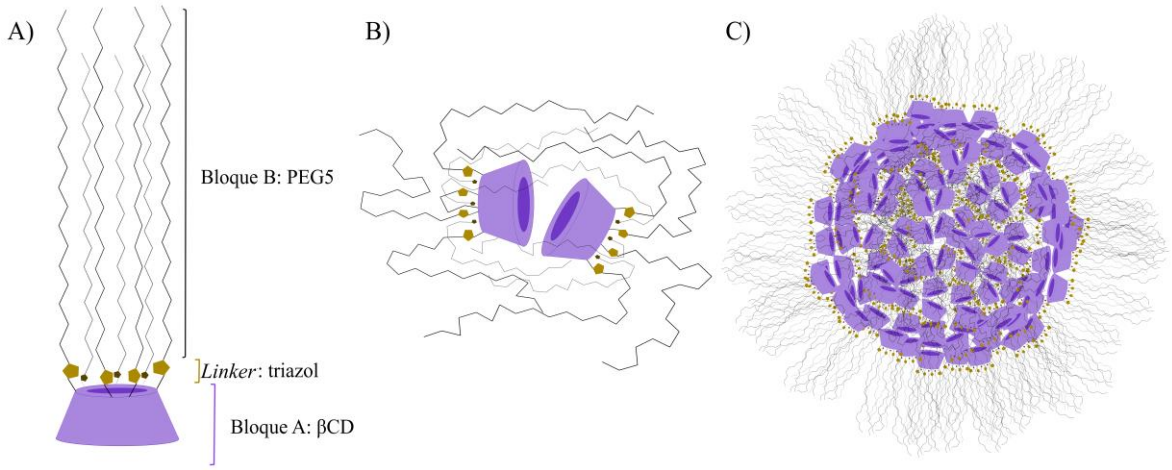

Figura 15. Representación esquemática de A) βCDPEG5, B) dímero de βCDPEG5, y C) agregado de βCDPEG5 (Rincón-López, Ramírez-Rodríguez, *et al*., 2021).

6.1.2. Estudio de los agregados por DLS

6.1.2.1. Efecto de la temperatura

Se estudió el efecto del aumento de la temperatura a 37 °C (temperatura fisiológica) sobre la agregación de βCDPEG5. A esta temperatura se detectó una sola población de agregados con un valor medio de Dh de 152.4±3.3 nm (Figura 16A y C, Tabla 5 Apéndice A), similar al registrado a 25 °C. Por el contrario, los dímeros de βCDPEG5 estuvieron ausentes.

Existe evidencia de que la solvatación del PEG en su forma plegada está dada por la formación de 2 enlaces de hidrógeno con dos átomos de oxígeno PEG vecinos a una sola molécula de H_2O, en forma de puentes de agua (Figura 17A) (Liese *et al*., 2017). Este sería el caso de los dímeros βCDPEG5, en los que las cadenas de PEG5 están plegadas, como lo sugieren los resultados de la tensión superficial (Sección 6.1.1.3.) y los estudios computacionales, que, además, proporcionaron el número promedio de enlaces por unidad de repetición de PEG y H_2O (Sección 6.1.1.5.). Por otro lado, sí las cadenas de PEG se encuentran estiradas, una sola molécula de H_2O forma un enlace de hidrógeno con un átomo de oxígeno de PEG (Figura 17B).

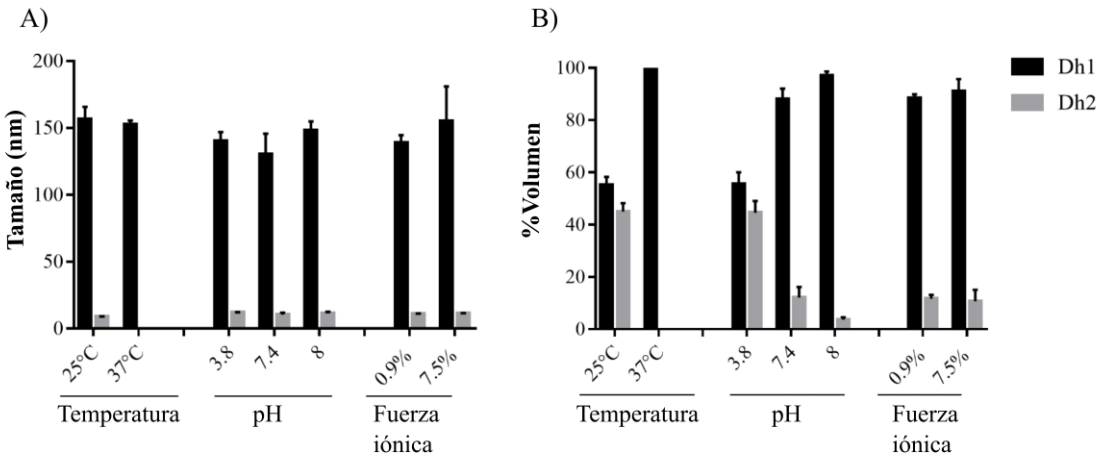

C)

Efecto	Dh1 (nm)	%Vol1	Dh2 (nm)	%Vol2
Temperatura				
37°C	152.4±3.3	--	--	--
pH				
3.8	140.4±6.5	55.5±4.5	11.9±0.3	44.6±4.1
7.4	130.5±15.3	87.9±4.1	10.4±1.5	12.1±4.1
8.0	148.3±6.7	97.0±1.7	11.4±1.1	3.6±0.9
Fuerza iónica				
0.9%	139.0±5.2	88.4±1.5	10.9±0.3	11.7±1.5
7.5%	155.1±25.9	89.3±4.4	11.2±0.3	10.7±4.4

Figura 16. Efecto de la temperatura, el pH y la fuerza iónica de los dímeros y los agregados en A) el Dh y B) el volumen de distribución. Las barras de error corresponden a DE con un n=6. C) Los valores representados en A) y B) se incluyen en formato de tabla para facilitar su lectura (Rincón-López, Ramírez-Rodríguez, *et al*., 2021).

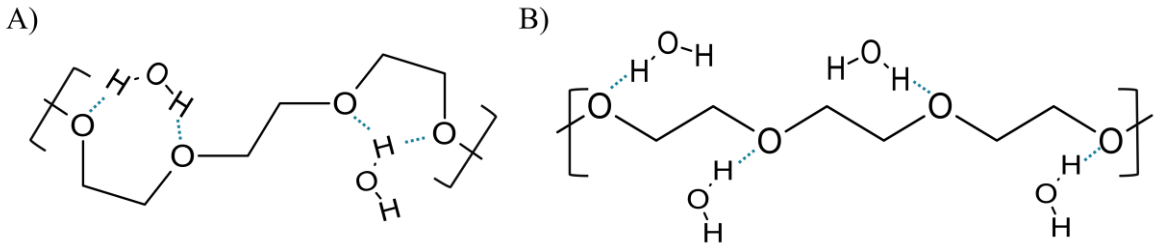

Figura 17. Interacción del PEG con las moléculas de H_2O. A) Cuando este plegado, B) cuando este estirado.

El modo de solvatación para PEG plegado tiene un alto costo entrópico y, por lo tanto, se vuelve desfavorable a altas temperaturas. Por el contrario, para el PEG estirado, la ganancia entrópica del agua liberada compensa la penalización entrópica conformacional del estiramiento del PEG y, en consecuencia, la energía libre de las cadenas de PEG estiradas no depende de la temperatura (Liese *et al*., 2017). Esta afirmación podría explicar por qué la

solvatación de PEG5 en los dímeros de βCDPEG5 se vuelve desfavorable a temperaturas más altas; de modo que su tendencia a formar agregados aumenta, asimismo, el comportamiento inalterado de los agregados de βCDPEG5 a 37 °C.

6.1.2.2. Efecto del pH y la fuerza iónica

Se evaluó el efecto de pH ácido, neutro y básico (3.8, 7.4 y 8.0 respectivamente) y la fuerza iónica provocada por un medio salino isotónico e hipertónico (0.9 y 7.5% respectivamente) sobre el fenómeno de agregación de βCDPEG5. En todo el intervalo de pH y fuerza iónica se detectaron poblaciones bimodales con valores de Dh1 y Dh2 similares a los del agua a 25 °C (Figura 16A y C, Tabla 6 y 7 Apéndice A).

Para determinar sí el cambio en el tamaño de Dh1 y Dh2 bajo estos efectos externos era significativo, se realizó un ANOVA de una vía para comparar todos los resultados de Dh1 con el valor de Dh1 en agua a 25 °C. Debido a la mínima variación entre los datos de Dh2±DE solo se analizaron los valores de Dh1. El análisis estadístico mostró que el pH 7.4 y el medio isotónico indujeron una disminución moderada de 16.6% y 11.2% respectivamente en el valor de Dh1 de los agregados, mientras que, bajo los otros factores evaluados, el Dh1 se mantuvo sin cambios.

A diferencia de los valores de Dh, el volumen de distribución se vio significativamente influenciado por el pH y la fuerza iónica (Figura 16B y C). Al analizar el efecto del pH, se encontró que el volumen de distribución de los dímeros disminuye cuando aumenta el valor del pH. A un pH ácido, el volumen de distribución de ambas poblaciones es comparable. A un pH neutro, el 12.1% de los dímeros estuvieron presentes en la muestra, lo que revela una disminución de 3.7 veces en esta población en comparación con el pH ácido. A pH 8.0, solo el 3.6% del volumen de distribución representó a los dímeros. En este caso, un incremento de 0.6 unidades de pH disminuyo 3.4 veces la población del dímero. Este comportamiento podría explicarse por los grupos triazol formados durante la reacción click que une las cadenas de PEG5 a la cara primaria de βCD. Los grupos triazol son bases fuertes con un pKb de 1.2, que se protonan en condiciones ácidas y, debido a las repulsiones electrostáticas, a pH ácido estarían impulsando a βCDPEG5 hacia un estado dimérico. Aunque estos triazoles se encuentran en una proporción relativamente menor en el dibloque, debido a su respuesta al pH actúan como ‘enlaces inteligentes’, lo que genera un efecto que no se daría por los

bloques βCD y PEG5 sin conjugar. Estos '*linkers* inteligentes' podrían permitir, a través de cambios en el pH, la modulación entre el estado agregado o desensamblado de los βCDPEGs, habilidad útil para controlar la carga y liberación de fármacos.

El volumen de distribución de los dímeros en soluciones isotónicas e hipertónicas fue equivalente entre ellos. El volumen de distribución en estos experimentos asemejó a la de pH 7.4. Cabe mencionar que se preparó la solución de pH 7.4 con tabletas de PBS, que contienen, además de sales de fosfato, NaCl y KCl. Al agregar NaCl y KCl se impuso una fuerza iónica que resultó en un aumento significativo en el volumen de distribución de agregados. Este comportamiento ilustra la delicada competencia de interacciones en el sistema βCDPEG5: a medida que aparecen los iones, compiten con las cadenas de PEG5 por las moléculas de agua. Como era de esperar, se favorece mucho la solvatación de los iones y se inducen las interacciones entre las cadenas de PEG5, lo que se explica los agregados más estrechos y la ligera disminución de Dh1 en presencia de las sales.

6.1.2.3. Comportamiento de los agregados con respecto al tiempo

Se analizó una solución de βCDPEG5 0.5 mM en un periodo de 55 días para explorar el comportamiento de los agregados con el paso del tiempo.

La Figura 18A muestra que el tamaño de los agregados disminuye ligeramente hasta alcanzar una reducción total de tamaño del 27.5% luego de los 55 días. El tamaño del dímero se mantuvo sin cambios.

Por otro lado, el volumen de distribución de los dímeros y de los agregados fluctuó moderadamente durante los primeros cinco días (Figura 18B). Luego, adquirió una tendencia en donde el volumen de distribución de los dímeros disminuyó gradualmente y, consecuentemente, el del agregado aumentó; alcanzando al final del experimento un 6.7% y 97.8% de volumen de distribución respectivamente. La Figura 2 del Apéndice A muestra los histogramas de distribución del tamaño de partícula y la Tabla 8 del Apéndice A los resultados de DLS por día de medición.

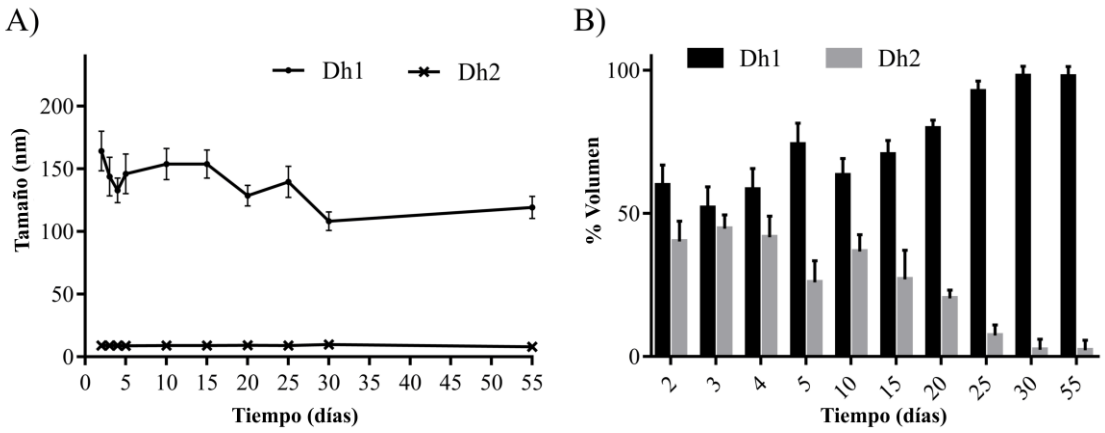

Figura 18. Efecto del tiempo sobre A) tamaño de agregación y B) volumen de distribución de los agregados de βCDPEG5. Las barras de error corresponden a DE con un n=6 (Rincón-López, Ramírez-Rodríguez, *et al*., 2021).

Estos resultados soportan la idea de que βCDPEG5 puede inicialmente formar dímeros que continúan interactuando para formar agregados, esta tendencia de agregación ya ha sido descrita en agregados de CDs (Loftsson *et al*., 2019). Como se mencionó anteriormente, los agregados podrían presentar un arreglo inducido por PEG5 que genera una esfera de hidratación repulsiva de corto alcance, evitando así la interacción con otras entidades, ya sean moléculas de βCDPEG5 o agregados de βCDPEG5. Diferente es el caso de los dímeros βCDPEG5, que tienden a interactuar con otros para formar los agregados estables.

6.1.2.4. Corolario de la influencia de factores sobre la auto-agregación del sistema βCDPEG5

Se encontró como factor común entre el efecto de la temperatura, pH, la fuerza iónica y el paso del tiempo, que ninguna de las condiciones evaluadas afecta el tamaño Dh1 del agregado o del Dh2 de los dímeros. Por el contrario, el volumen de distribución cambia dependiendo perturbación del medio, llevando a los dímeros a conformar agregados o viceversa. Esta habilidad de modular entre dímero y agregado por cambios en el medio, manteniendo un tamaño de agregado constante, es valiosa para el diseño de sistemas de liberación de fármacos, ya que permite realizar de manera controlada la carga y liberación de fármacos a la vez que se mantiene un tamaño de agregado estable.

l

6.2. Caracterización biológica de los βCDPEGs *in vitro*

Como se mencionó en los antecedentes, la composición, estructura, tamaño y forma de los nanosistemas de liberación puede provocar diferentes respuestas dependiendo del tipo de célula en que se evalúe (Jesus *et al*., 2019; Villanueva-Flores *et al*., 2020). Por esto, las evaluaciones biológicas sistemáticas de los acarreadores libres de fármacos y sus componentes son necesarias para precisar cómo los materiales afectan su biocompatibilidad.

A pesar de que PEG se considera como un componente seguro, el entusiasmo abrumador de su uso en el desarrollo de sistemas de liberación de fármacos podría estar ocultando efectos secundarios y conduciendo a una investigación inadecuada de sus limitaciones. Algunos de los inconvenientes conocidos incluyen reacciones de hipersensibilidad, inmunogenicidad y degradación en forma de peróxido (Knop *et al*., 2010; G. Liu *et al*., 2017). En la misma medida, algunas CDs también son consideradas componentes seguros. No obstante, a pesar de la biocompatibilidad de estos dos, una nueva entidad derivada de ellos no necesariamente dará como resultado un material con el mismo comportamiento biológico, ya que el nuevo sistema presentará diferente estructura y propiedades fisicoquímicas que podrían inducir diferentes respuestas celulares (Rojas-Aguirre *et al*., 2019). Por estas razones es crucial realizar una caracterización biológica del nuevo material, en este caso los compuestos βCDPEGs.

En esta sección se exponen los resultados y el análisis del efecto de βCDPEG2, βCDPEG5, βCD, PEG2 y PEG5 en tres modelos de células animales diferentes RAW 264.7, MC3T3-E1 y MDCK.

6.2.1. Macrófagos murinos RAW264.7

La pegylación sigue siendo la estrategia más utilizada para disminuir la captación de células fagocíticas, prolongando así su permanencia en circulación sistémica de los materiales pegylados. Sin embargo, investigaciones recientes han demostrado que la pegylación podría no reducir la fagocitosis (Farace *et al*., 2016). Por el contrario, podría aumentar la internalización por parte de células como los neutrófilos (Kelley *et al*., 2018). Esta variabilidad de PEG se ha atribuido a las variaciones en su de su PM, arquitectura y densidad de injerto (Kelley *et al*., 2018; Knop *et al*., 2010; Sánchez *et al*., 2017; Yang *et al*., 2014). La interacción entre los materiales pegylados y los macrófagos aún no se ha entendido

completamente y la caracterización de las interacciones material-macrófagos, sigue siendo una necesidad para el desarrollo de sistemas de liberación de fármacos que logren evitar el RES y, consecuentemente, aumenten el tiempo en circulación sistémica.

La línea celular RAW 264.7 es un modelo estándar para evaluar procesos inflamatorios generados por biomateriales, así como la respuesta inmune innata *in vitro* (Chamberlain *et al*., 2009; Malachowski & Hassel, 2020). Por lo tanto, se empleó para determinar el efecto los compuestos sobre su viabilidad y sobre la generación de especies radicalarias (ROS y NO).

6.2.1.1. Viabilidad celular

La Figura 19 muestra que ninguno de los compuestos, βCDPEGs, βCD o PEGs, afectaron la viabilidad de RAW264.7. El comportamiento observado para βCD y los PEGs concuerda con otros trabajos en los que las CD (αCD, βCD, Metil βCD(MβCD) y HPβCD) no han alterado la viabilidad de RAW264.7 en concentraciones de 0.001 a 1 mM (Balaraman *et al*., 2015; Davaatseren *et al*., 2017; Giacoppo *et al*., 2017; J. He *et al*., 2020; Ogawa *et al*., 2008; Shibaguchi *et al*., 2019). Lo mismo se reporta para materiales pegylados en concentraciones de 10 a 1000 µg/mL (J. Ye *et al*., 2019).

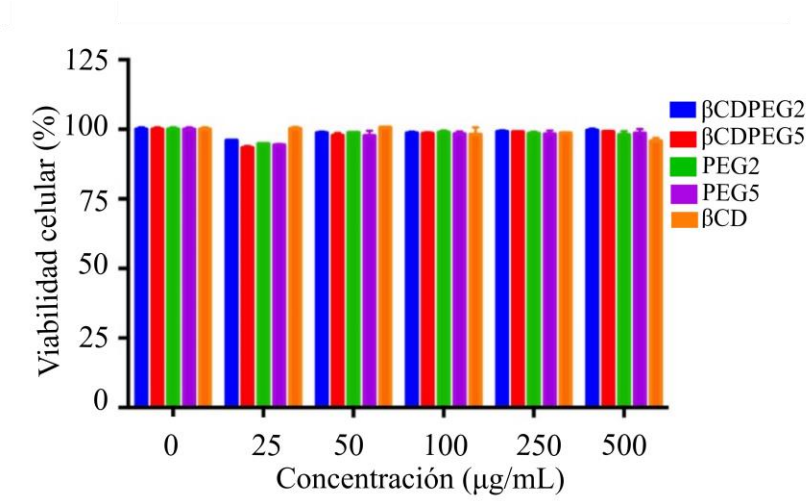

Figura 19. Efecto de los βCDPEGs, βCD y PEGs sobre la viabilidad celular de los macrófagos RAW264.7.

6.2.1.2. Generación de ROS y NO2-

Las ROS son subproductos del metabolismo celular fundamentales en la señalización celular y la homeostasis. La sobreproducción de ROS daña las proteínas celulares, los lípidos y el ADN, activando así una respuesta inflamatoria en los macrófagos (Thannickal & Fanburg, 2021). Por lo tanto, se exploró el efecto de los βCDPEGs, βCD y PEGs sobre la inducción del estrés oxidativo mediante el análisis de los niveles de ROS en las células RAW264.7.

Los nitritos se forman por oxidación del óxido nítrico (NO), uno de los mediadores proinflamatorios secretados por los macrófagos como respuesta inmune a patógenos, y para mediar la inflamación, entre otras respuestas fisiológicas (Wynn *et al*., 2013). Por lo tanto, se cuantificó la cantidad de NO_2^- como un método indirecto para determinar la producción de NO.

La Figura 20A muestra que los βCDPEGs elevaron ligeramente los niveles de ROS intracelulares de una manera dependiente de la concentración. A 200 µg/mL, tanto βCDPEG2 como βCDPEG5 alcanzaron una fluorescencia máxima de 6.1 veces más alta que las células no tratadas. A la misma concentración, los PEGs solo aumentaron 3.3 veces la fluorescencia, mostrando niveles más bajos de producción de ROS en presencia de PEG libre que en presencia de los βCDPEGs. La βCD no afectó la producción de ROS en células RAW 264.7.

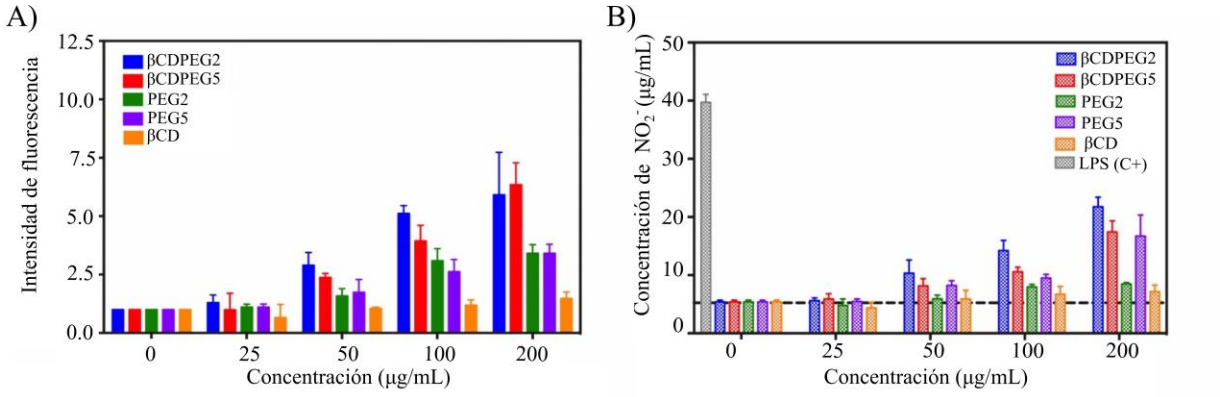

Figura 20. Efecto de los βCDPEGs, βCD y PEGs en la generación de A) ROS y B) NO_2^- en los macrófagos RAW264.7.

Como se observa en la Figura 20B, los βCDPEGs indujeron un pequeño incremento en la producción de NO_2^- de una manera dependiente de la concentración, alcanzando a 200 µg/mL, 2.9 veces más NO_2^- que el control. El efecto de PEG5 fue similar al de los βCDPEGs.

Para PEG2 se observó un escaso aumento de NO_2^-, mientras que βCD no tuvo ningún efecto. La respuesta de RAW264.7 a βCD (Figuras 20A y B) es concordante con Davaatseren 2017, quien reporta que la βCD no afecta la viabilidad de RAW264.7 ni la producción de ROS ni NO (Davaatseren *et al*., 2017).

La diferencia entre βCDPEGs y los PEGs probablemente se deba a la densidad de PEG en los sistemas de βCDPEGs.

En resumen, los βCDPEGs provocaron la generación de pequeñas cantidades de ROS y NO_2^-, lo que sugiere una ligera respuesta inflamatoria sin comprometer la viabilidad de los macrófagos. Aunque se necesitan estudios de internalización para confirmar esta afirmación, los experimentos aquí presentados proporcionan información relevante para el diseño de materiales pegylados y sus implicaciones en la respuesta de los macrófagos en términos de viabilidad y estrés oxidativo.

6.2.2. Osteoblastos MC3T3-E1

En los últimos años, la investigación de biomateriales sintéticos a base de CDs para la regeneración de tejido óseo y la liberación de moléculas que promueven la regeneración ósea ha crecido notablemente (Li *et al*., 2021; Terauchi *et al*., 2021). En este sentido, la línea celular de osteoblastos MC3T3-E1 ha sido un modelo *in vitro* adecuado para estudiar la biocompatibilidad (Quarles *et al*., 1992).

6.2.2.1. Viabilidad celular

La Figura 21A muestra que el βCDPEG2 no redujo la viabilidad de las células MC3T3-E1 de 25 a 50 µg/mL, mientras que entre 100-500 µg/mL la viabilidad celular se mantuvo alrededor de 80%. En comparación, el βCDPEG5 disminuyó la viabilidad celular a un 77% a 25 µg/mL, y de 50 a 500 µg/mL provocó una viabilidad de las células osteoblásticas del 55%.

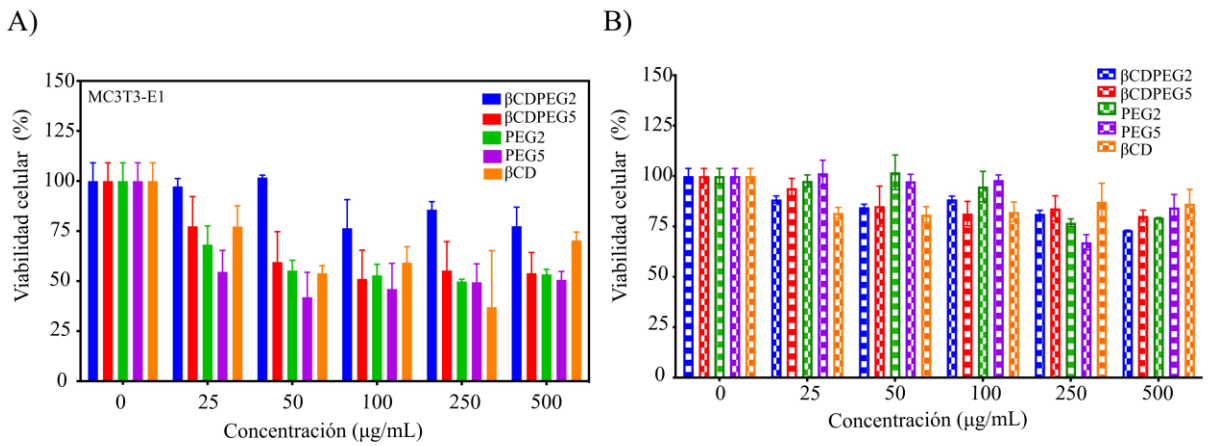

Figura 21. Efecto de los βCDPEGs, βCD y PEGs en A) viabilidad y B) viabilidad en el ensayo de recuperación celular de los osteoblastos MC3T3-E1.

El efecto del PEG2 sobre la viabilidad de los osteoblastos fue mayor que el de βCDPEG2. Por ejemplo, a una concentración de 25 µg/mL, la viabilidad celular fue del 68%, luego disminuyó al 55% a 50 µg/mL y persistió cerca de este valor para el resto de las concentraciones. PEG5 también afectó más la viabilidad de las células MC3T3-E1 que su conjugado βCDPEG5 a 25 y 50 µg/mL. A concentraciones más altas, la toxicidad tanto de PEG5 como de βCDPEG5 fue similar.

Ninguno de los estudios con materiales pegylados (PEG PM 5 y 20 kDa) en la literatura, probados en MC3T3-E1, informan una disminución en la viabilidad celular de los osteoblastos. Tampoco se reporta el efecto del PEG libre ni la concentración efectiva de PEG en estos materiales (Scaffaro *et al*., 2017; Schoonraad *et al*., 2021; Y. Zhang *et al*., 2021). Los sistemas a base de βCD tampoco parecen afectar la viabilidad. Al igual que PEG, el efecto de las βCDs por sí solas, no se ha estudiado a detalle (Terauchi *et al*., 2021). En este trabajo, se ha demostrado que la βCD y los PEGs afectan la viabilidad de las células MC3T3-E1, sin embargo, cuando se conjugan covalentemente, este efecto disminuye.

6.2.2.2. Recuperación posterior al tratamiento

Se realizó un ensayo de recuperación para evaluar si los βCDPEGs, βCD y PEGs podrían inducir un efecto citostático. Para ello, las células cultivadas en presencia de los compuestos se lavaron para eliminarlos y luego se cultivaron nuevamente para determinar su capacidad de proliferación después de 24 horas, como se muestra en la Figura 21B. Sorprendentemente,

la viabilidad de las células MC3T3-E1 fue superior al 80% para todos los compuestos en todo el intervalo de concentración.

6.2.2.3. Generación de ROS

El estrés oxidativo derivado de niveles excesivos de ROS es una de las principales causas de enfermedades óseas, incluida la osteoporosis (Fatokun *et al*., 2008). Por lo tanto, se consideró necesario evaluar la generación de ROS en MC3T3-E1 como una posible causa de la disminución de viabilidad observada en la Figura 21A por parte de todos los compuestos evaluados

La Figura 22A muestra que los βCDPEGs, βCD y PEG2 no indujeron la sobreproducción de ROS. Sin embargo, PEG5 aumentó ligeramente los niveles de ROS y se comportó de manera similar en todas las concentraciones. Este hallazgo particular coincide con trabajos previos que informan sobre la sobreproducción de ROS como mecanismo de citotoxicidad de los derivados de PEG (PM que van desde 400 a 4000 Da) en células L929 (G. Liu *et al*., 2017).

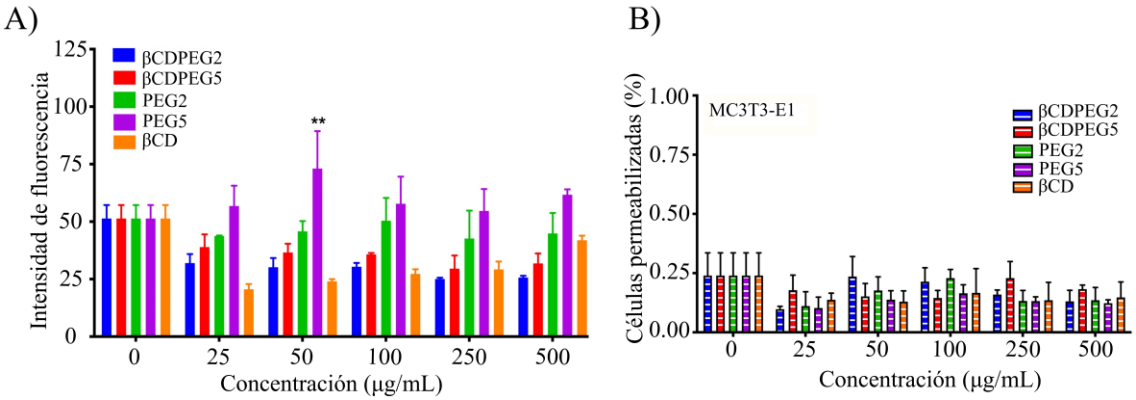

Figura 22. Efecto de los βCDPEGs, βCD y PEGs en A) la generación de ROS y B) la permeabilización de la membrana celular de los osteoblastos MC3T3-E1.

6.2.2.4. Permeabilidad de membrana

Dependiendo del grado hidrofobicidad y del tamaño de la cavidad, los derivados de βCD pueden alterar la permeabilidad de la membrana (Hammoud *et al*., 2019). La Figura 22B muestra que ninguno de los compuestos indujo cambios en la permeabilidad de la membrana de las células MC3T3-E1.

6.2.2.5. Ciclo celular

El ciclo celular es la secuencia de eventos a través de los cuales una célula duplica su genoma, crece y se divide. La progresión de las células por cada una de las fases que comprende el ciclo es un proceso altamente regulado que busca garantizar una adecuada proliferación celular (Golias *et al*., 2004; Poon, 2016). Estudiar la diferencia entre los porcentajes de permanencia en las fases del ciclo entre un grupo celular control y uno de tratamiento, puede informar acerca del efecto de los compuestos en las células (Ashwaq *et al*., 2016; Hippler *et al*., 2019; X. Liu *et al*., 2010). El efecto de PEG y βCD ha sido poco explorado en la progresión del ciclo celular. Con respecto a PEG, solamente se encontró información de un PEG de PM 8 kDa (7.5-10 mM) que arresta ciclo celular en la fase G0/G1 de las células HT29 (Parnaud *et al*., 2001). Por parte de βCD, se observó un efecto similar para el derivado MβCD en el ciclo celular de macrófagos RAW264.7 (Choi *et al*., 2004). Por lo tanto, es valioso investigar el papel de PEG y βCD libres, así como a los βCDPEGs, en la progresión del ciclo celular.

La Figura 23 presenta las poblaciones celulares relativas en cada fase del ciclo celular provocadas por los compuestos βCDPEGs, βCD y PEGs a diferentes concentraciones.

La presencia de βCDPEG2 no generó cambios en la progresión del ciclo celular de los osteoblastos. PEG2, en el intervalo de 25-500 µg/mL, provocó un leve aumento en el número de células en la fase S y la fase G0/G1, con la subsecuente disminución en el G2/M. Asimismo, βCDPEG5 en concentraciones de 50 a 500 µg/mL y, PEG5 y βCD de 25 a 500 µg/mL, presentaron un patrón similar. Lo anterior indica que PEG2, βCDPEG5, PEG5 y βCD pueden estar impidiendo el alcance de la etapa mitótica, y, por tanto, estar generando algún efecto en la replicación del ADN (Poon, 2016).

Ninguno de los compuestos modificó la fase Sub G0/G1, lo que sugiere que la disminución de la viabilidad de los osteoblastos MC3T3-E1 no es el resultado de la muerte celular programada (Mohammad *et al*., 2014; Thangaraj *et al*., 2019).

Estos resultados concuerdan con los valores de viabilidad celular (Sección 6.2.2.1), en el sentido en que, entre menor afectación del ciclo celular, se observa un mayor porcentaje de viabilidad celular.

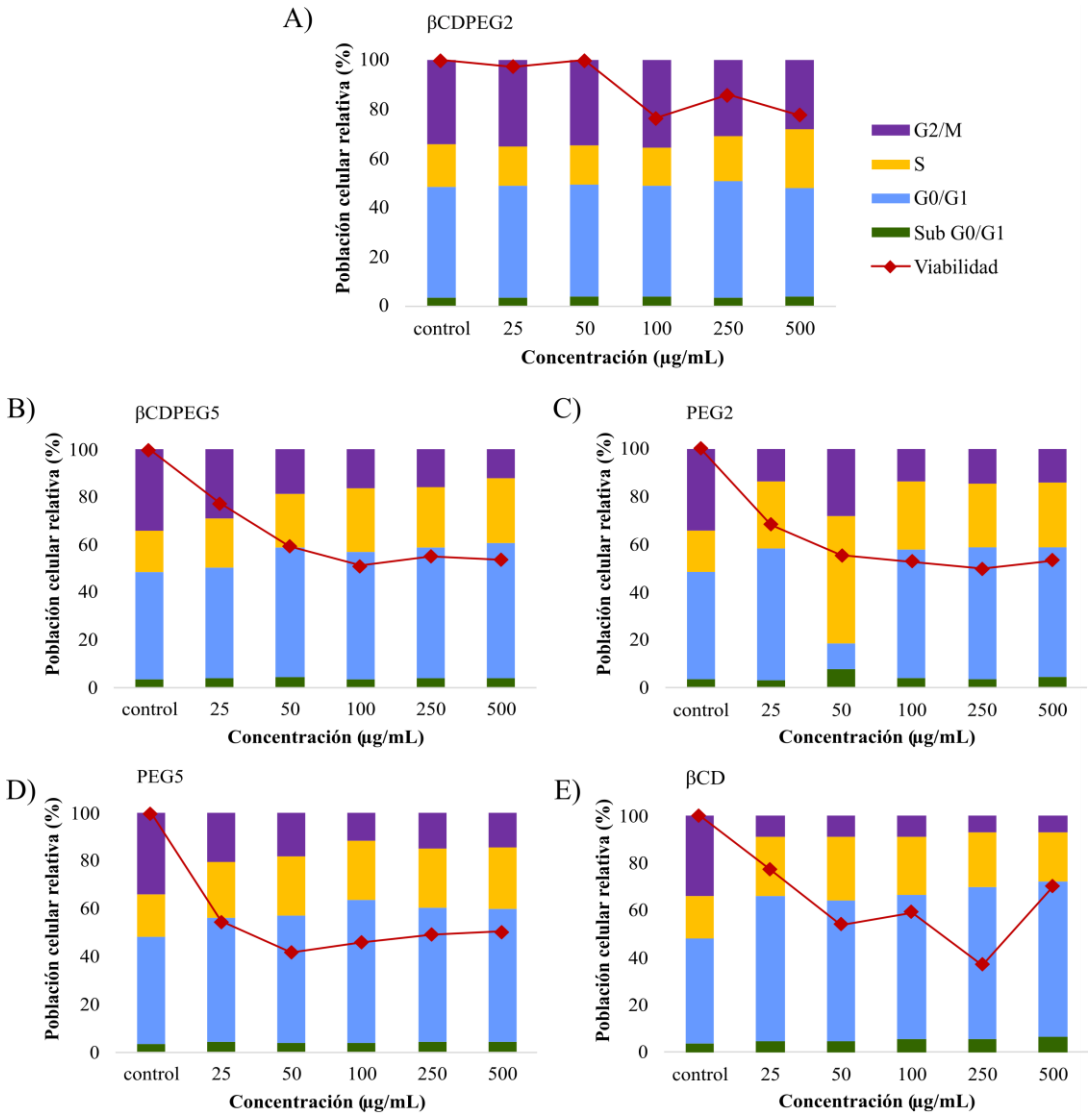

Figura 23. Efecto de A) βCDPEG2, B) βCDPEG5, C) PEG2, D) PEG5, y E) βCD en la progresión del ciclo celular de los osteoblastos MC3T3-E1. Los resultados se representan como el promedio de tres experimentos, en la Tabla 9 Apéndice A se muestra el promedio±DE. Se han incluido los valores de viabilidad celular obtenidos del ensayo informado en la Sección 6.2.2.1 para facilitar su comparación con el % de población celular relativa.

6.2.2.6. Migración celular

La Figura 24 muestra que la migración celular se mantuvo sin cambios de 25 a 100 µg/mL de βCDPEG2. Sin embargo, de 250 a 500 µg/mL, la migración celular se inhibió

significativamente de una manera dependiente a la concentración, con un cierre de brecha del 26% a la concentración más alta. Por el contrario, su contraparte PEG2 obstaculizó la migración celular en todas las concentraciones, manteniendo el cierre de la brecha alrededor del 50% en todos los casos. Por encima de 25 µg/mL de βCDPEG5, prevalecieron los cierres de las brechas alrededor del 50%. PEG5 se comportó de manera similar a βCDPEG2; sin embargo, los valores de cierre de brechas fueron más bajos para los primeros. El comportamiento anterior también lo presentó βCD, que interfirió en la migración de osteoblastos MC3T3-E1, a 25-100 µg/mL, en donde el cierre de brecha fue cercano al 50%, mientras que, a 250-500 µg/mL, permaneció alrededor del 25%. Vale la pena señalar que la βCD y sus derivados pueden perturbar la migración celular, como lo muestran Maki *et al*. 2020 con βCD en células Caco-2 o Guerra *et al*. 2016 con MβCD en células MDA-MB 231 (Guerra *et al*., 2016; Maki *et al*., 2020).

Estos efectos podrían atribuirse a la conocida capacidad de las CDs para formar CIs con el colesterol de las membranas celulares; sin embargo, se requieren estudios en profundidad para confirmar esta afirmación.

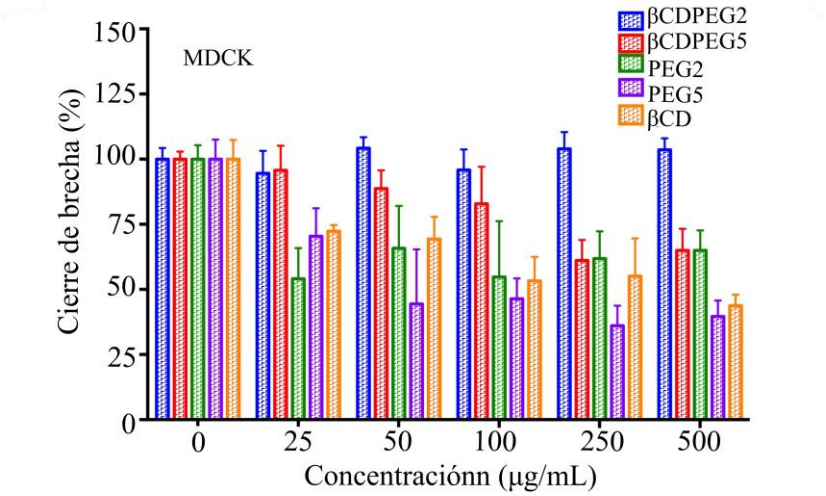

Figura 24. Migración de los osteoblastos MC3T3-E1 en presencia de βCDPEGs, βCD y PEGs.

Los βCDPEGs, βCD y PEGs disminuyeron la viabilidad de las células MC3T3-E1 e impidieron el crecimiento celular en diferentes grados. Sin embargo, dado que ningún compuesto mostró alterar la integridad la membrana ni generar ROS, los efectos podrían deberse a la inhibición de la motilidad celular más que a una actividad citotóxica. Este

postulado está respaldado por las observaciones de la migración celular y la viabilidad posterior al tratamiento.

En resumen, se demostró que la biocompatibilidad de βCD y PEG se ve mejorada cuando se conjugan en forma de βCDPEGs. En particular, el sistema βCDPEG2, a concentraciones entre 25-100 µg/mL, podría usarse para desarrollar biomateriales novedosos para aplicaciones en regeneración ósea e ingeniería de tejidos. En concentraciones superiores a 250 µg/mL, podría ejercer un efecto sinérgico con fármacos citotóxicos para el tratamiento de neoplasias óseas.

6.2.3. Células MDCK

6.2.3.1. Viabilidad celular

En la Figura 25A se muestra el efecto de los βCDPEGs, βCD y PEGs en la viabilidad de las células MDCK.

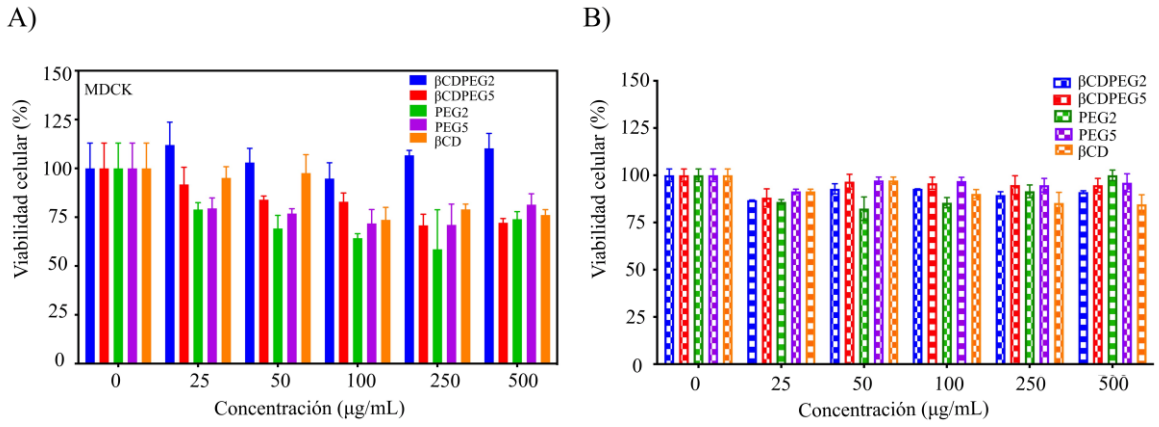

Figura 25. Efecto de los βCDPEGs, βCD y PEGs en A) viabilidad y B) viabilidad en el ensayo de recuperación celular de la línea MDCK.

βCDPEG2 no alteró la viabilidad de las células, βCDPEG5 y βCD mantuvieron la viabilidad celular en valores cercanos al 80% para todo el intervalo de concentraciones.

El efecto de algunos derivados de la βCD sobre la viabilidad de la línea MDCK ya han sido reportados: Francis *et al* evaluaron el efecto de la MβCD sobre la viabilidad de las células MDCK y encontraron que a 10 mM se obtuvo un 95% de viabilidad celular; Hailstones *et al*. obtuvieron un resultado similar con trimetil-βCD a 1 mg/mL (Francis *et al*., 1999; Hailstones *et al*., 1998). Incluso las CDs modificadas, como las reportadas por Chen *et al*. que son βCD

funcionalizadas con triterpeno pentacíclico, diseñadas para inhibir la actividad del virus de la influenza, no mostraron citotoxicidad contra las células MDCK (Chen *et al*., 2020).

Como se mencionó anteriormente, el PEG se considera un polímero biocompatible, no obstante, podría provocar una respuesta biológica en función de su PM, grupos terminales, concentración y arquitectura (G. Liu *et al*., 2017; Verhoef & Anchordoquy, 2013; Wang *et al*., 2020). En este caso, el efecto de PEG2 y PEG5 fue moderado, ya que se observa una reducción máxima del 25% en todas las concentraciones.

Esta es la primera vez que se reporta el efecto de PEG2 y PEG5 libres sobre la viabilidad de las células MDCK.

6.2.3.2. Recuperación posterior al tratamiento

Una vez que se eliminaron βCDPEG5, PEG y βCD del medio celular, las células MDCK proliferaron como se observa en la Figura 25B, mostrando que la viabilidad celular se recuperó hasta en un 90%, y que los compuestos evaluados no ejercieron un efecto citostático sobre las células MDCK.

6.2.3.3. Generación de ROS

Como se muestra en la Figura 26A, ninguno de los compuestos indujo la producción de ROS, incluso βCDPEG2, que permeabilizó la membrana celular (ver más abajo). Nuevamente, esta es la primera vez que se investiga la generación de ROS en células MDCK en respuesta a βCD.

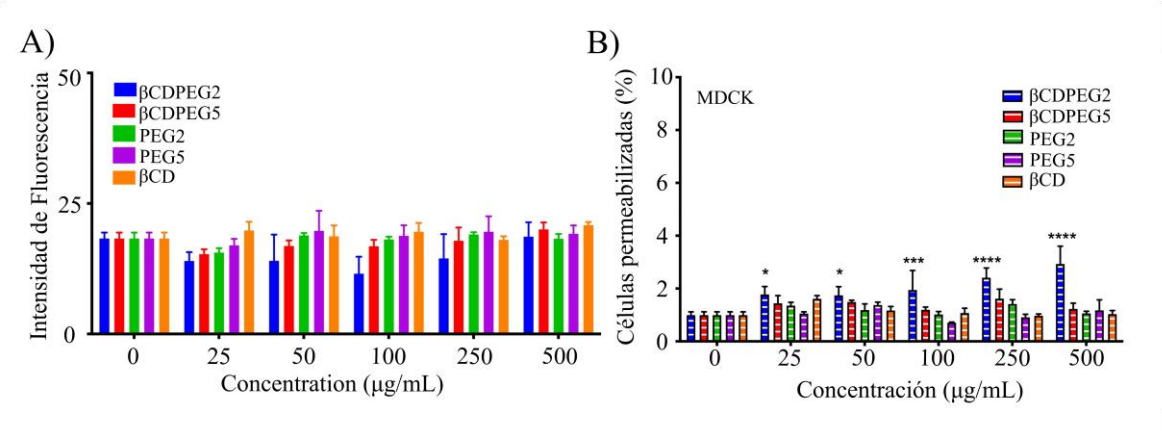

Figura 26. Efecto de los βCDPEGs, βCD y PEGs en A) la generación de ROS y B) la permeabilización de la membrana de las células MDCK.

6.2.3.4. Permeabilidad de membrana

La Figura 26B muestra que de 25-50 µg/mL βCDPEG2 tuvo un efecto leve sobre la permeabilidad de la membrana, el cual aumentó ligeramente en el intervalo de 100-500 µg/mL. Este ensayo informa sobre la capacidad de modificar la permeabilidad de la membrana, más no acerca de la internalización; sin embargo, Wang *et al*. recientemente reportaron que el PEG libre de bajo peso molecular (~2 kDa) es internalizado por las células MDCK por difusión pasiva, mientras que los PEG de entre 5 y 20 kDa se internalizan mediante una combinación de difusión pasiva y endocitosis mediada por caveolinas (Wang *et al*., 2020). Dado que βCDPEG2 (PM_{teo} 15973.95 g/mol) tiene siete cadenas de PEG2 conjugadas a la cara primaria de βCD, la densidad de injerto de PEG es significativa (Rojas-Aguirre *et al*., 2019). Por lo tanto, βCDPEG2 podría comportarse como un PEG de alto PM, siendo internalizado por transporte pasivo y activo. Se necesitan estudios adicionales para saber si el cambio en la permeabilidad promueve la internalización de βCDPEG2.

Por otro lado, los compuestos βCDPEG5, βCD y PEGs no interfirieron con la integridad de la membrana a ninguna concentración.

6.2.3.5. Ciclo celular

En la Figura 27 se muestran los resultados del efecto de los βCDPEGs, βCD y PEGs en el ciclo celular de MDCK.

El βCDPEG2 disminuyó la población celular en la fase S a 250 y 500 µg/mL. Por su parte, el βCDPEG5 aumentó la población celular en la fase S con la consecuente disminución de población en la fase G2/M, en igual medida para todas las concentraciones. Se observó un patrón similar al de βCDPEG5 para los PEGs libres. El arresto del ciclo celular en la fase S podría afectar la replicación del ADN y, en consecuencia, el crecimiento celular (Poon, 2016).

La βCD aumentó la población de células en la fase S de 50 a 500 µg/mL en igual magnitud, con una disminución en la fase G2/M; sin embargo, en este último, parece un efecto dependiente de la concentración.

Estos resultados sugieren que, a excepción de βCDPEG2, todos los compuestos interfirieron con la progresión del ciclo celular de las células MDCK, lo que podría correlacionarse con

la disminución moderada de la viabilidad celular. En concentraciones de 250-500 µg/mL, la βCD causó el deterioro más significativo en las células MDCK, seguida de βCDPEG5 y luego, en la misma medida, PEG2 y PEG5. Por último, como ocurrió con los osteoblastos, el βCDPEG2 fue el compuesto con menos efectos sobre la progresión del ciclo celular.

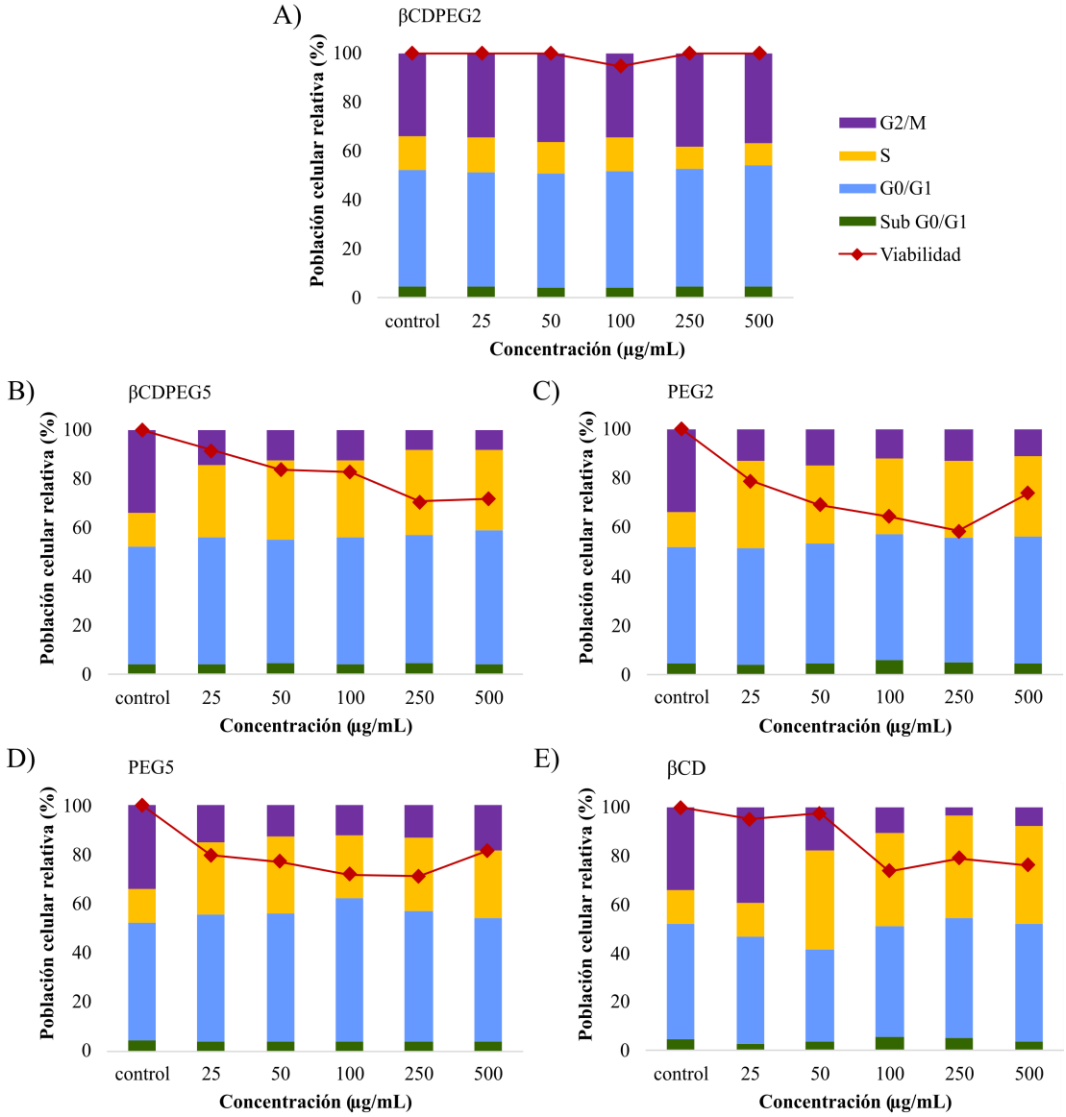

Figura 27. Efecto de A) βCDPEG2, B) βCDPEG5, C) PEG2, D) PEG5, y E) βCD en la progresión del ciclo celular de los osteoblastos MC3T3-E1. Los resultados se representan como el promedio de tres experimentos, en la Tabla 10 Apéndice A se muestra el promedio±DE. Se han incluido los valores de viabilidad celular obtenidos del ensayo informado en la Sección 6.2.3.1 para facilitar su comparación con el % de población celular relativa.

6.2.3.6. Migración celular

La Figura 28 muestra que el cierre de la brecha para las células MDCK expuestas a βCDPEG2 fue del 100% para todas las concentraciones evaluadas. El βCDPEG5 no interfirió con la migración celular a 25-100 µg/mL, pero a concentraciones más altas el cierre de brecha fue de aproximadamente 60%. Para PEG2 y PEG5, la migración celular representó el 44-68%. De forma interesante, la βCD mostró una relación decreciente entre el cierre de la brecha y la concentración, pasando de 72% a 25 µg/mL a 44% a 500 µg/mL. Como se mencionó en la Sección 6.2.2.6., estudios previos han demostrado que βCD interfiere con la migración de diferentes células. Por lo tanto, a través de este trabajo, se proporciona evidencia sobre el efecto de la βCD en la motilidad celular, lo que alienta a realizar más estudios para dilucidar los mecanismos celulares y moleculares involucrados.

Dados que βCDPEG2 promueve la migración celular, esta molécula podría tener potencial en el área de la ingeniería de tejidos; aunque se requieren estudios extensos de proliferación celular y adhesión, este trabajo presenta una perspectiva para los posibles usos que el conjugado pegylado puede tener en todo el campo de la nanomedicina.

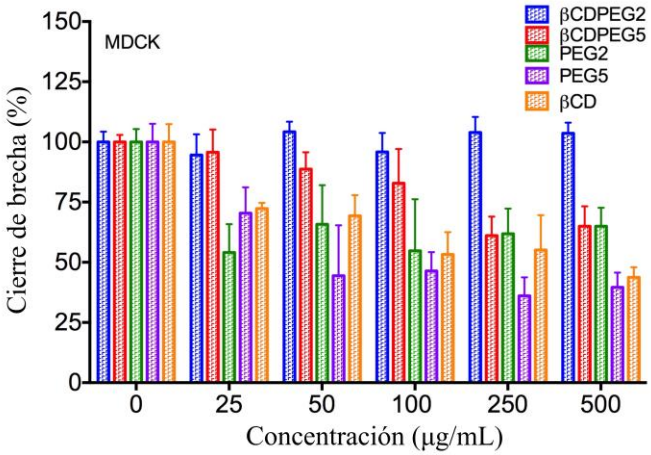

Figura 28. Migración de las células MDCK en presencia de βCDPEGs, βCD y PEGs.

6.2.4. Comparación en los efectos globales sobre la línea MC3T3-E1 y MDCK

Aunque las células MDCK y MC3T3-E1 comprenden modelos celulares distintos, se identificaron algunos patrones en términos de su respuesta biológica a los compuestos.

A concentraciones bajas (25 µg/mL), el efecto de los compuestos en la viabilidad de las células MC3T3-E1 y MDCK fue PEGs>βCD≈βCDPEG5>βCDPEG2. Cuando la

concentración aumenta (50-500 µg/mL), se observa el mismo patrón para las células MDCK. Sin embargo, para los osteoblastos MC3T3-E1, el efecto fue βCDPEG5≈PEGs≈βCD.

Excepto por βCDPEG2 en las células MDCK, ninguno de los compuestos modificó la permeabilidad de la membrana celular en ambos modelos celulares. De igual forma, los compuestos no indujeron una sobreproducción significativa de ROS.

βCDPEG2 no detuvo el ciclo de las células MC3T3-E1 ni de MDCK. Además, βCDPEG2 no interfirió con la migración de las células MDCK, aunque perturbó la migración de las células MCT3-E1. A bajas concentraciones (25-50 µg/mL), el efecto de βCDPEG5 en el ciclo y la viabilidad celulares fue similar al βCDPEG2 en ambos modelos celulares. En cuanto a la migración celular, βCDPEG5 tuvo un menor efecto que βCDPEG2 en los osteoblastos, mientras que para las células MDCK se comportó como PEG libres.

Los ensayos biológicos realizados aquí revelan que las células MC3T3-E1 son más sensibles que las células MDCK a los compuestos evaluados, demostrando que el efecto de todos los compuestos varía dependiendo de la línea celular.

6.3. Panorama fármaco-tecnológico de las CDs

6.3.1. Patentamiento con respecto al tiempo de las tecnologías farmacéuticas de CDs

Se realizó un análisis de las 1998 patentes para observar su comportamiento con respecto al tiempo. En la Figura 29 se muestra el número de patentes registradas por año y el total acumulado. En esta se pueden identificar dos tendencias. La primera, entre 1983-2000, con un total de 125 registros; la segunda entre 2000-2019, con 1873 nuevas patentes registradas, que representan el 93% del total de documentos, lo cual refleja un gran interés sobre las CDs en las últimas dos décadas.

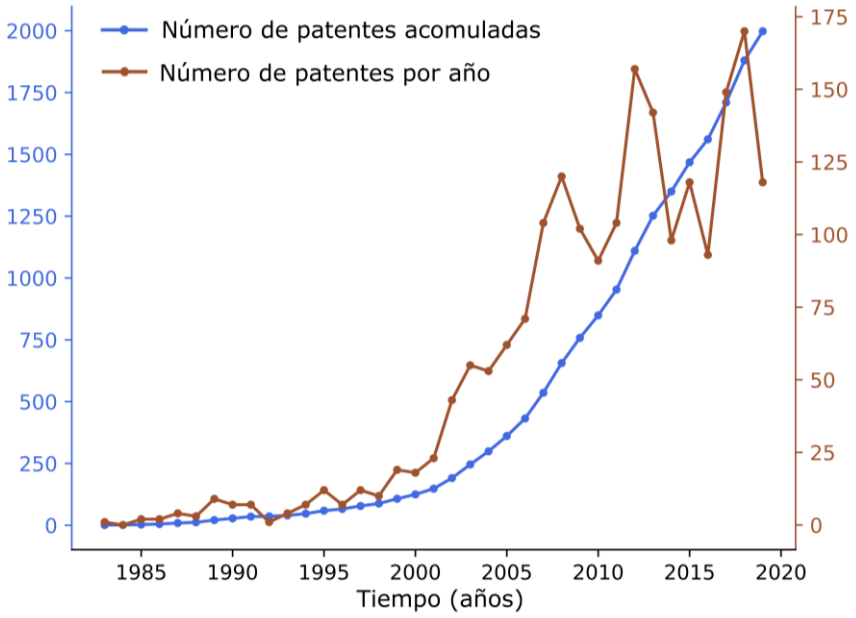

Figura 29. Registro por año de patentes de tecnologías farmacéuticas basadas en CDs. Los datos representados en esta gráfica se obtuvieron a través de herramientas de búsqueda de DII (Web of Science, 2020); como se describe en la metodología (Sección 5.4.1.).

La línea de tiempo de la Figura 30 muestra algunos hitos en el patentamiento de CDs en el área farmacéutica. La primera innovación del grupo de patentes analizado se ubica en el año de 1983, registrada por el cesionario Teijin limited (Makino & Suzuki, 1983, 1988). Este documento trata del uso de las CDs como adyuvantes en la estabilización de la vitamina D_3 y la metodología de preparación (Makino & Suzuki, 1983, 1988). Todos sus antecedentes están relacionados a otras patentes o artículos científicos que demostraron la capacidad de las CDs de modificar de manera aparente la solubilidad y estabilidad de una molécula huésped a través de la formación de CIs (Bavley *et al*., 1954; H. P. Jones, 1982; Solms, 1969).

En el periodo de 1983-2000, se encuentran una patente registrada por Stella & Rajewsky y otra por Pitha (Pitha *et al*., 1994; Stella & Rajewski, 1994) que resaltan por ser las más citadas del periodo con 413y 385 citas respectivamente. Ambas tratan sobre la funcionalización exitosa de las CD α, β y γ, la primera con sustituyentes sulfoalquilo, y la segunda con alquilo, para mejorar las características fisicoquímicas de las CDs nativas, su capacidad de formar CIs con diversos fármacos y la disminución de su toxicidad. Esto, sin duda, marca un parteaguas en el uso de las CDs, ya que estas patentes presentan a la SBEβCD y la HPβCD,

dos CDs que se pueden administrar por vía parenteral y enteral con un buen perfil de biocompatibilidad; y que aceleraron el uso y patentamiento observado a partir del año 2000. Justamente en ese año, una patente registrada por CyDex Inc (193 citas) describe formulaciones farmacéuticas de liberación controlada a base de sulfoalquil éter CDs, en las que se utilizaron derivados de CDs, en combinación con otros componentes, para modificar la biodisponibilidad y/o la tasa de bioabsorción de agentes terapéuticos (Stella *et al*., 2000). Así, en las últimas dos décadas, el auge en el uso de CDs, ha sido paralelo al desarrollo de sistemas de liberación funcionales en las cuales las CDs han jugado un papel importante.

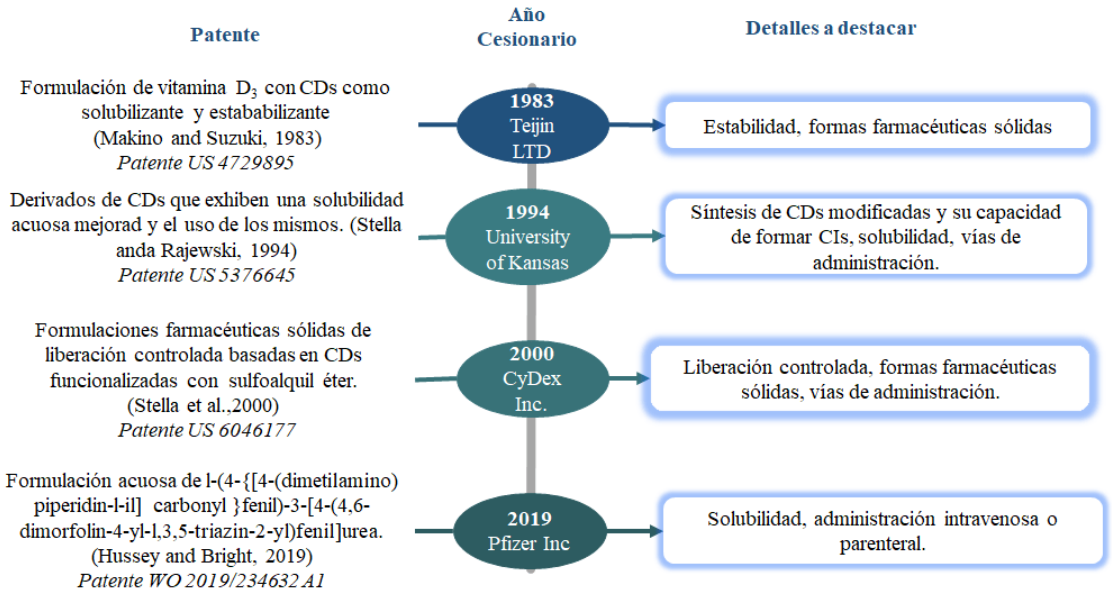

Figura 30. Innovaciones farmacéuticas de CDs en el período de 1980-2019 (Rincón-López *et al*., 2020).

6.3.2. Clasificación en función de solubilidad, estabilidad y enmascaramiento de sabor/olor

Como se mencionó en la metodología, también se analizó el grupo de 1998 patentes para clasificarlas según la función que desempeñan las CDs: solubilizar, estabilizar, enmascarar sabor. En la Figura 31 se observa que la habilidad de las CDs de modificar de manera aparente la solubilidad acuosa a los fármacos ha sido el atributo por el que más se han utilizado en tecnologías farmacéuticas a lo largo del tiempo. Sin embargo, partir del 2002, se refleja un aumento en el interés por el uso de las CDs como agentes estabilizantes. Cabe mencionar que, debido a que la modificación de la solubilidad aparente de un compuesto puede influir en la estabilidad, muchas patentes pueden estar registrando tanto la mejora de la solubilidad

como la de la estabilidad de un mismo fármaco. El uso de las CDs para enmascarar el sabor/olor comenzó a ser visible hasta la década de los 90s. Y, en general, el número global de patentes que hacen referencia a esta aplicación es considerablemente menor en comparación con las dos anteriores.

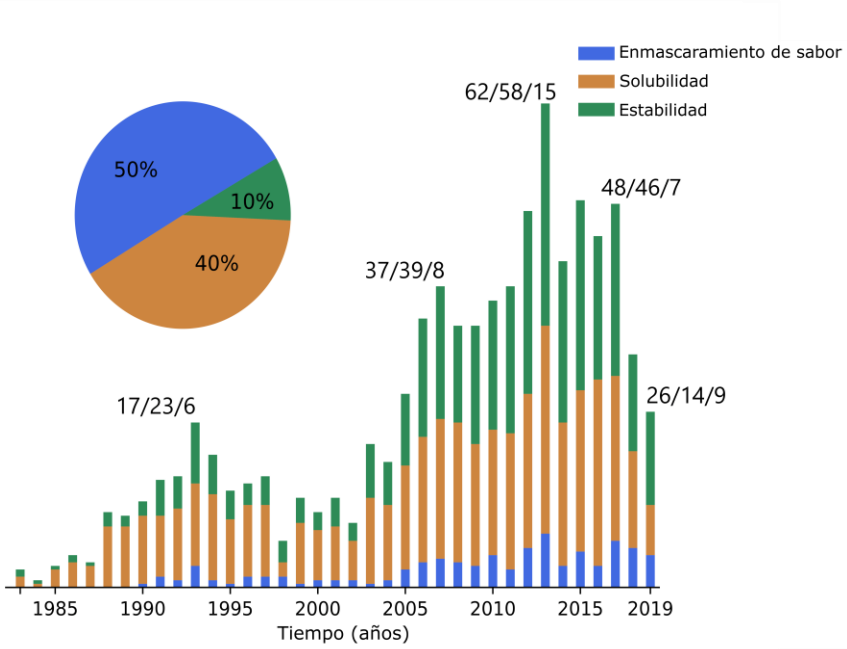

Figura 31. Patentes que registran la aplicación de las CDs para mejorar la solubilidad, la estabilidad y las propiedades organolépticas a través de los años. Los valores indican las patentes en estabilidad/solubilidad/enmascaramiento en el año señalado. Los datos representados en esta gráfica se obtuvieron a través de herramientas de búsqueda de DII (Web of Science, 2020); como se describe en la metodología (Sección 5.4.3.).

6.3.3. Minería de datos en patentes farmacéuticas de CDs por medio de ciencia de redes

Las 1998 patentes se representaron en dos redes, una de ellas clasificó los documentos según su Novedad y otra de acuerdo con el Uso o aplicación de las CDs en dicha patente. Para la formación de estas redes, fue indispensable definir un valor H a través del análisis de los índices de similitud (C_{ij},Figura 3 Apéndice A), este valor H establece la conectividad en las redes y, a su vez, el componente conectado más grande (LCC) o subred a estudiar (Tabla 1).

Por otro lado, como se mencionó en la metodología, el valor de k representa el número de conexiones de cada uno de los nodos (patentes). Este valor también es sumamente relevante, ya que el análisis estadístico de la densidad de probabilidad de k ($\rho(k)$, Figura 3 Apéndice

A) define el tipo de red que se conforma. En este caso, las dos redes (la LCC de cada una) formadas a partir del contenido semántico de las patentes farmacéuticas de CDs muestran ser redes complejas. Este tipo de redes se caracterizan por tener una organización jerárquica no aleatoria, en donde los nodos se juntan en pequeños grupos, los cuales se relacionan para formas otros más grandes a través de conexiones que unen a toda la subred o LCC.

Posteriormente, se detectaron las comunidades en ambas redes aplicando el algoritmo Louvain. La detección de comunidades modela y guía la comprensión de la interacción de las comunidades en una estructura compleja. En este trabajo, las comunidades representan grupos de patentes con contenido semántico similar (Figura 32), las cuales surgen de considerar toda la información contenida en la red, algo que no es visible si se comparan los textos de las patentes en una tabla o gráfico estándar.

Tabla 1. valor de los parámetros que definen la red de novedad y la red uso.

Parámetro	**Red de Novedad**	**Red de Uso**
Dimensión del espacio de la red (palabras que contiene)	2807	2223
Valor *H*	0.75	0.8
Número de patentes involucradas en la LCC(nodos)	1623	1779
Número de comunidades	9	11

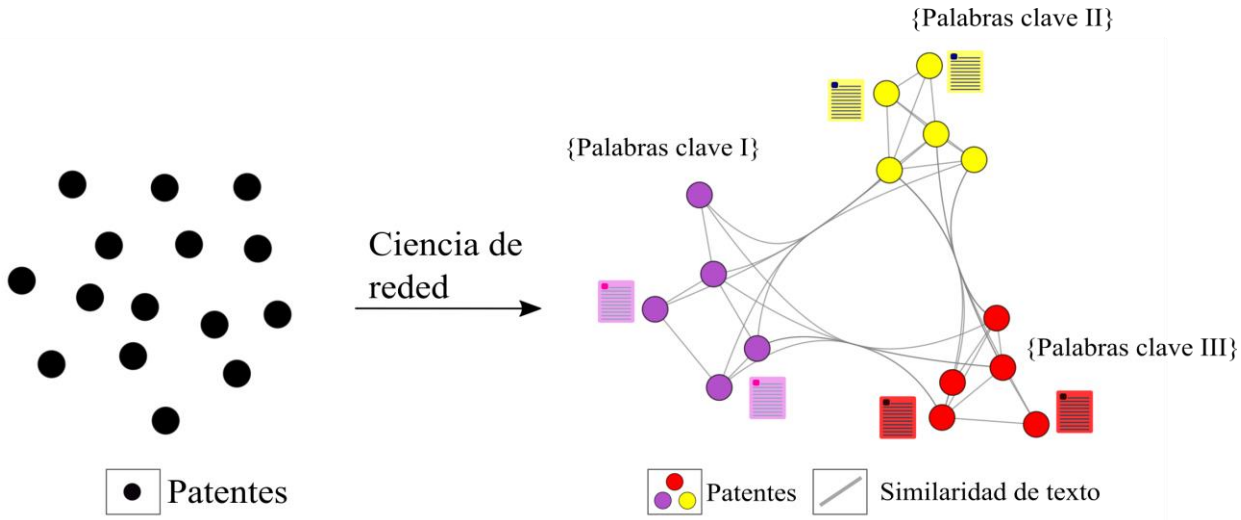

Figura 32. Conformación de una red a partir de comunidades de patentes con contenido semántico similar (Rincón-López, Almanza-Arjona, *et al*., 2021).

Para interpretar las comunidades, se identificaron las palabras más frecuentes en cada una de ellas, es decir, las palabras clave que definen el contenido semántico de las patentes en cada comunidad.

- Red de Novedad

La Figura 33A muestran la red de Novedad y las Comunidades que hay en ella, la Tabla 2a presenta las palabras clave de cada Comunidad. Para este caso, las patentes se basan principalmente en el incremento de la solubilidad acuosa de un fármaco para su formulación en solución como forma farmacéutica. Esto se evidencia en la Comunidad 7, que es la más grande y está ubicada en el centro de la red, uniendo las otras ocho Comunidades, siendo un punto de convergencia para el resto de la red.

Dentro de las palabras más frecuentes que componen a la Comunidad 7 se encuentran *complejo*, *agua* y *solución*. Esto se refiere a la formación de CIs de CD/fármaco para la mejora de la solubilidad acuosa de los fármacos, con el fin de formularlo como una solución. Esta comunidad y el papel que juega en la red confirma lo observado en el estudio de las propiedades clásicas de las CDs (Sección 6.3.2.) en donde la aplicación de las CDs para el aumento de solubilidad es predominante. De igual manera, la Comunidad 3 y la Comunidad 4 se suman a esta descripción ya que contienen la palabra *solución*.

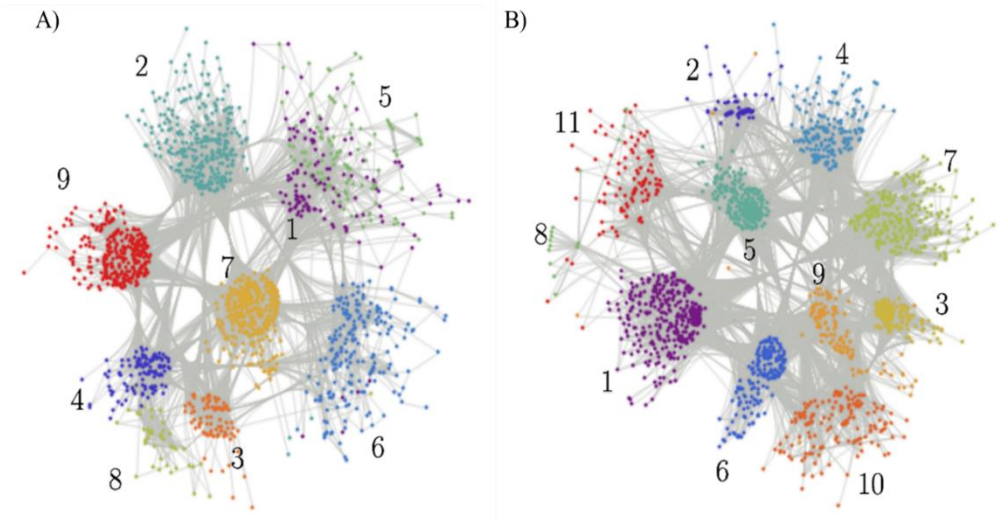

Figura 33. LCC de A) Novedad y B) Uso; la herramienta de visualización utilizada para generar estas redes fue Wolfram Mathematica 12.0 (Rincón-López, Almanza-Arjona, *et al*., 2021).

La Comunidad 1 con la palabra *tableta*, que a su vez contiene la palabra *soluble*, y la Comunidad 6 con la palabra *polvo*, resaltan la importancia de estas formas farmacéuticas en las innovaciones tecnológicas. La Comunidad 8, que, aunque más pequeña, muestra las palabras *aceite* y *volátil*, lo que revela cómo las CDs, a través de la formación de CIs, permiten la incorporación de este tipo de componentes en formulaciones estables; ya sea como polvos amorfos o superando su baja solubilidad e inestabilidad en agua (Rincón-López *et al*., 2020). En resumen, se observa que la Novedad de las patentes farmacéuticas de CDs consiste en la mejora de la solubilidad acuosa de los fármacos para su adecuada formulación como soluciones acuosas. Además, se reveló la importancia de las tabletas y los polvos.

Tabla 2. Las 5 palabras más comunes que se encuentran en cada comunidad de la red (LCC) para a) Novedad y b) Uso.

	C	Size	W I	F	W II	F	W III	F	W IV	F	W V	F
(a) Novelty	1	129	water	0.35	cyclodextrin	0.2	soluble	0.17	tablet	0.15	beta-cyclodextrin	0.13
	2	294	cyclodextrin	0.28	salt	0.25	pharmaceutical	0.21	component	0.14	active	0.11
	3	88	acid	0.63	cyclodextrin	0.14	beta-cyclodextrin	0.08	salt	0.08	solution	0.07
	4	112	solution	0.53	water	0.12	beta-cyclodextrin	0.12	aqueous	0.12	cyclodextrin	0.11
	5	102	sodium	0.33	cellulose	0.21	hydroxypropyl	0.16	beta-cyclodextrin	0.16	starch	0.15
	6	197	material	0.3	powder	0.28	beta-cyclodextrin	0.15	cyclodextrin	0.14	radix	0.14
	7	357	cyclodextrin	0.66	complex	0.17	water	0.08	solution	0.04	salt	0.04
	8	42	oil	0.41	mixture	0.18	volatile	0.17	beta-cyclodextrin	0.15	water	0.09
	9	302	beta-cyclodextrin	0.53	hydroxypropyl	0.23	acid	0.1	hydrochloride	0.07	cyclodextrin	0.07
	C	**Size**	**W I**	**F**	**W II**	**F**	**W III**	**F**	**W IV**	**F**	**W V**	**F**
(b) Use	1	342	tablet	0.41	medicine	0.2	capsule	0.16	granule	0.13	medicinal	0.1
	2	59	sustained	0.58	hydrochloride	0.25	antibacterial	0.06	patient	0.05	drug	0.05
	3	136	cancer	0.64	cell	0.13	disease	0.08	breast	0.08	lung	0.07
	4	175	drug	0.62	tumor	0.11	anti-inflammatory	0.11	carrier	0.09	treat	0.08
	5	238	disease	0.55	disorder	0.23	syndrome	0.11	inflammatory	0.06	chronic	0.05
	6	183	pharmaceutical	0.57	drink	0.14	animal	0.11	cosmetic	0.09	drug	0.09
	7	256	pain	0.39	complex	0.22	bone	0.14	cyclodextrin	0.13	oral	0.12
	8	16	particle	0.58	peptide	0.19	active	0.08	ingredient	0.08	heat	0.08
	9	124	injection	0.42	powder	0.24	freeze	0.14	dried	0.14	soluble	0.05
	10	151	treatment	0.32	infection	0.31	virus	0.18	disease	0.13	medicament	0.07
	11	99	eye	0.28	nasal	0.28	allergic	0.18	drop	0.14	macular	0.12

*C hace referencia a comunidad, **n al número de patentes y ***F a frecuencia

- Red de Uso

En esta red (Figura 33B y Tabla 2b), las patentes se agrupan según las formas farmacéuticas, no obstante, algunas enfermedades y las familias de fármacos también hicieron que las patentes formaran Comunidades.

Con respecto a la agrupación por formas farmacéuticas, está la Comunidad 1, la más grande de toda la red, con palabras como *tableta, capsula, granulo* confirma la relevancia de las CDs o los CIs CD/fármaco en estas formas físicas. La Comunidad 9 agrupa la preparación de polvos liofilizados para administración parenteral. La Comunidad 11 con las palabras *ocular* y *nasal*, sugiere el uso de CDs en formulaciones dirigidas a estas vías de administración.

Por otro lado, las comunidades relacionadas con familias de fármacos o enfermedades a tratar incluyen a la Comunidad 2 hace referencia al uso de CDs con fármacos con antimicrobianos, mientras que las Comunidades 3 y 4 a anticancerígenos. La Comunidad 5 se relaciona con antiinflamatorios, y la Comunidad 10, aunque pequeña, hace referencia a tratamientos antivirales. Estas Comunidades reflejan la relevancia de las CDs en el desarrollo de terapias dirigidas a enfermedades como cáncer, trastornos inflamatorios e infecciones bacterianas y virales.

6.3.4. Evolución temporal de las patentes de acuerdo con formas farmacéuticas

Las redes resultantes indicaron que la mayoría de las patentes se agrupan de acuerdo con las formas farmacéuticas en las que se encuentran. Por ello, se realizó una segunda minería de datos en las 1998 patentes; esta vez, la minería fue supervisada y guiada por palabras clave relacionadas a formas farmacéuticas para identificar, contar y clasificar por año el número de patentes relacionadas con cada una de ellas.

En la Figura 34 se observa que las soluciones acuosas son la forma farmacéutica en la que más han utilizado las CDs. Este resultado muestra que, aunque la modificación de la solubilidad aparente a través de las CDs no es una novedad, sigue siendo una estrategia valiosa en el área farmacéutica.

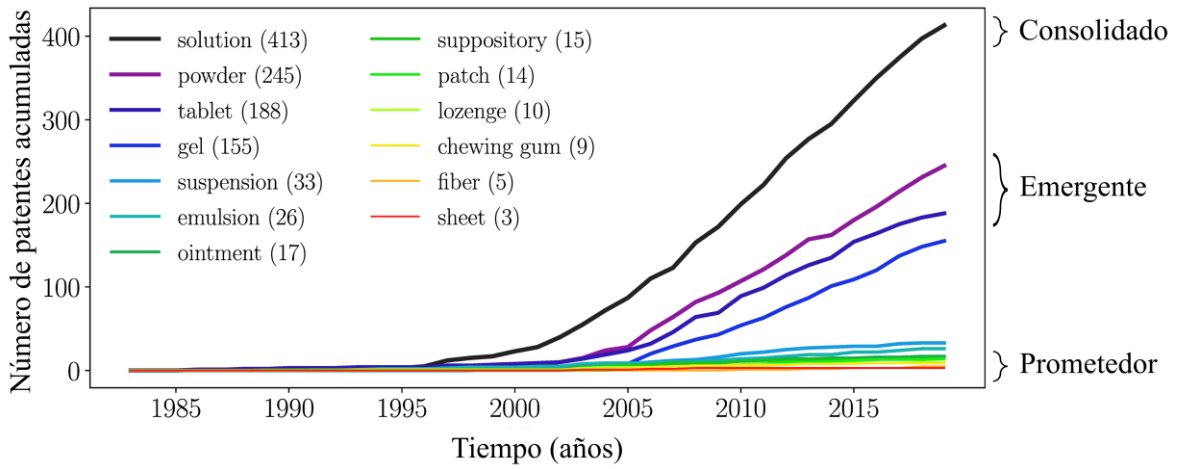

Figura 34. Evolución tecnológica del uso de las CDs en la innovación en formas farmacéuticas (Rincón-López, Almanza-Arjona, *et al*., 2021).

Esta tendencia respalda las observaciones que surgen de la Sección 6.3.3., que muestra que la Comunidad más grande de la red de Novedad, y el puente entre todas las otras Comunidades, está formada por patentes relacionadas con soluciones acuosas, que sin duda resultan de los CIs CD/fármaco.

Siguiendo en número de registros a las soluciones acuosas, se encuentran los polvos, las tabletas y los geles. Los polvos y las tabletas surgieron de forma conjunta a principios de 2000, y desde 2005 se ha observado un crecimiento significativo en ambos. Otra vez, estas tendencias correlacionan con el análisis de la red de Novedad, en donde alrededor de la palabra *tableta* y *polvo* se forman Comunidades de patentes. De hecho, la investigación sobre las CDs como excipientes multifuncionales para tabletas orales, bucales y sublinguales (Abouhussein *et al*., 2021; Rincón-López *et al*., 2020) reforzará el patentamiento de estas tecnologías a corto plazo.

A pesar de que la palabra gel no se encontró como una de las palabras clave en las redes, tuvo 155 registros y su incremento en patentamiento surge partir de 2005. En los hidrogeles, las CDs se pueden unir covalentemente para dar lugar a arquitecturas supramoleculares con perfiles de liberación modulables. Si las cavidades de las CDs están disponibles, pueden albergar moléculas de fármaco y, al mismo tiempo, evitar su liberación tras la dilución en el medio. Además, se ha observado la posibilidad de administrar fármacos de manera secuencial o en respuesta a un estímulo (Concheiro & Alvarez-Lorenzo, 2013).

La convergencia de la nanotecnología, las ciencias farmacéuticas y la ciencia e ingeniería de materiales ha intensificado el uso de CDs para el desarrollo de geles funcionales, con características atractivas para el campo de la biomedicina. Algunas innovaciones tecnológicas incluyen, sistemas que funcionan como adhesivos y promueven la regeneración de tejidos (Park *et al*., 2017) y sistemas termo-responsivos para liberación sostenida de fármacos (Q. Ye *et al*., 2018). De la misma manera, en la literatura científica se encuentran reportes como hidrogeles inyectables de αCD para la liberación de plásmidos (Lin *et al*., 2017) e hidrogeles de quitosano-βCD para vendajes de heridas (Flores *et al*., 2017). Por ello, se evidencia que la investigación reciente está ampliando el alcance de las tecnologías de hidrogeles basados en CDs. En consecuencia, el uso de las CDs en esta forma farmacéutica es una tecnología emergente y se espera un aumento significativo de la investigación, las patentes y las innovaciones en esta dirección en los próximos años.

Las formas farmacéuticas como suspensiones, emulsiones, ungüentos, supositorios, parches, fibras, hojas y gomas de mascar han sido las menos exploradas a través de la aplicación tecnológica de las CDs. La tasa de patentamiento se ha mantenido sin cambios a lo largo del tiempo; no obstante, el desempeño de las CDs demuestra su versatilidad y potencial como excipientes funcionales para esas formulaciones.

En el caso de las suspensiones, las CDs pueden utilizarse como agentes estabilizantes (Jansook *et al*., 2020; Muankaew *et al*., 2016).

Por otro lado, las CDs pueden brindar estabilidad a las emulsiones. Este atributo ha sido poco explorado y constituye una gran área de oportunidad, ya que se pueden desarrollar formulaciones de fármacos lipofílicos libres de solventes orgánicos, surfactantes, co-surfactantes u otros aditivos (Duchêne *et al*., 2003; Laza-Knoerr *et al*., 2012).

El desarrollo de las gomas de mascar medicadas, útiles para la liberación local o sistémica, representan una alternativa para la administración de fármacos para pacientes pediátricos, geriátricos y pacientes con dolor de garganta severo. Las CDs se han utilizado en estas como solubilizantes y como enmascaradores de sabor (al Hagbani *et al*., 2018; Romer Rassing, 1994). Investigaciones detalladas a este respecto se requieren para develar el potencial de las CDs en estas formas farmacéuticas.

En cuanto a las formulaciones transdérmicas, la capacidad solubilizante y estabilizadora de las CDs, combinada con sus propiedades mucoadhesivas, evidencia el gran potencial de las CDs para este fin (Jug *et al*., 2012). El uso de las CDs en la obtención de fibras cargadas con fármaco (Tonglairoum *et al*., 2015), implantes transdérmicos (M. Zhang *et al*., 2019) e incluso como biosensores epidérmicos portátiles (Kim *et al*., 2019), son un indicativo de que este tipo de tecnologías que contienen CDs sean las que vayan a crecer a mayor velocidad en un futuro no muy lejano, y constituyen una atractiva área de oportunidad.

Con este análisis se expone la importancia de las CDs en el desarrollo de diversas formas farmacéuticas, las cuales se pueden agrupar según su evolución temporal de registros de patentes en consolidado, emergente y prometedor (Figura 34).

Cómo se mencionó, el aumento de solubilidad no es una novedad, pero sigue siendo una herramienta valiosa. Sin embargo, la combinación de este atributo con los avances en la química supramolecular y la ciencia e ingeniería de materiales podrán detonar desarrollos de tecnologías farmacéuticas novedosas en las que las CDs jueguen un papel fundamental. Dentro de este contexto, el desarrollo de nuevos materiales basados en CDs, como βCDPEGs pueden posicionarse adecuadamente dentro del panorama tecnológico de las CDs en el área farmacéutica. Su biocompatibilidad, capacidad de auto-agregarse y desensamblarse según las condiciones del medio, resaltan su potencial como sistema de liberación y motiva para estudios posteriores con fármacos.

7. Conclusiones

Se determinó la capacidad de auto-agregación de βCDPEG5. Los resultados obtenidos por densimetría, DLS, tensión superficial, TEM y la simulación computacional muestran que a una cac de 0.5 mM βCDPEG5 forma nanoestructuras de ~150 nm. A la misma concentración, βCDPEG5, también forma dímeros de ~9 nm de diámetro, los cuales son probablemente la primera etapa en la formación del agregado. La capacidad de auto-agregación del βCDPEG5 se da únicamente cuando se conjugan covalentemente las siete cadenas de PEG a la cara estrecha de la βCD. Además, se evidenció que la concentración, temperatura, pH y fuerza iónica pueden modular la formación y disociación de agregados a dímeros; siendo esta una habilidad que le confiere gran potencial a los como sistemas de liberación.

Los modelos celulares empleados en este trabajo informaron el diferente comportamiento de los βCDPEGs en macrófagos, osteoblastos y células epiteliales, conformando así un tipo de 'biblioteca biológica' que puede proporcionar información clave para orientar el desarrollo y las posibles aplicaciones de los βCDPEGs, βCD y PEGs, siendo este último ampliamente utilizado en la investigación farmacéutica y sistemas de liberación de fármacos avanzados.

La caracterización biológica *in vitro* a través del estudio del efecto los βCDPEGs, βCD y PEGs en las líneas RAW264.7 de macrófagos, MC3T3-E1 de osteoblastos y MDCK reveló que la biocompatibilidad de βCD y PEG mejoró cuando se conjugaron como un único sistema los βCDPEGs. Además, mostró que βCDPEG2 fue el mejor candidato, en términos de biocompatibilidad para todas las líneas celulares evaluadas, con especial potencial para su uso en ingeniería de tejidos.

El análisis del patentamiento a través del tiempo de tecnologías farmacéuticas de CDs permitió reconocer que su progreso tecnológico se ha dado por la capacidad de mejorar la solubilidad y estabilidad de fármacos. No obstante, su capacidad para modificar propiedades organolépticas está emergiendo y representa una gran área de oportunidad.

De la misma manera, el uso de herramientas de ciencia de datos para minar las patentes farmacéuticas de CDs exhibió que el análisis de estas a través de la similitud de su contenido semántico da lugar a redes complejas. La detección de las comunidades en estas evidenció que la mayoría de las innovaciones se asocian a la capacidad de las CDs de aumentar de manera aparente la solubilidad acuosa. Se observó un progreso tecnológico significativo para las tabletas y polvos, mientras que los geles parecen ser un área prometedora de innovación. La utilización de las CDs en parches y fibras transdérmicas están emergiendo. El potencial de las CDs en suspensiones y emulsiones aún no se ha reconocido, y una mejor comprensión de las CDs en estas formas farmacéuticas hará que estas tecnologías sean una gran área de oportunidad.

El interés por las CDs sigue aumentando y, de acuerdo con nuestro análisis, esta tendencia continuará en los próximos años por su versatilidad y fascinante capacidad para mejorar las formulaciones farmacéuticas en el diseño de terapias innovadoras.

Referencias

Abdulrahman, A. (2018). A new perspective for possible formulation and characterization of beta-cyclodextrin/poly (ethylene glycol) crystalline inclusion complexes. *Journal of Clinical Trials*, *8*, 83–84. https://doi.org/10.4172/2167-0870-C3-029

Abouhussein, D. M. N., el Nabarawi, M. A., Shalaby, S. H., & El-Bary, A. A. (2021). Sertraline-Cyclodextrin Complex Orodispersible Sublingual Tablet: Optimization, Stability, and Pharmacokinetics. *Journal of Pharmaceutical Innovation*, *16*, 53–66. https://doi.org/10.1007/s12247-019-09416-1

al Hagbani, T., Altomare, C., Kamal, M. M., & Nazzal, S. (2018). Mechanical Characterization and Dissolution of Chewing Gum Tablets (CGTs) Containing Co-compressed Health in Gum® and Curcumin/Cyclodextrin Inclusion Complex. *AAPS PharmSciTech*, *19*, 3742–3750. https://doi.org/10.1208/s12249-018-1174-1

Alessi, M. L., Norman, A. I., Knowlton, S. E., Ho, D. L., & Greer, S. C. (2005). Helical and coil conformations of poly(ethylene glycol) in isobutyric acid and water. *Macromolecules*, *38*(22), 9333–9340. https://doi.org/10.1021/ma051339e

Anselmo, A. C., & Mitragotri, S. (2016). Nanoparticles in the clinic. *Bioengineering & Translational Medicine*, *1*(1), 10–29. https://doi.org/10.1002/btm2.10003

Asche, G. (2017). "80% of technical information found only in patents" – Is there proof of this? *World Patent Information*, *48*, 16–28. https://doi.org/10.1016/j.wpi.2016.11.004

Ashwaq, A.-A., Al-Qubaisi, M., Rasedee, A., Abdul, A., Taufiq-Yap, Y., & Yeap, S. (2016). Inducing G2/M Cell Cycle Arrest and Apoptosis through Generation Reactive Oxygen Species (ROS)-Mediated Mitochondria Pathway in HT-29 Cells by Dentatin (DEN) and Dentatin Incorporated in Hydroxypropyl-β-Cyclodextrin (DEN-HPβCD). *International Journal of Molecular Sciences*, *17*(10), 1653. https://doi.org/10.3390/ijms17101653

Aydin, F., Chu, X., Uppaladadium, G., Devore, D., Goyal, R., Murthy, N. S., Zhang, Z., Kohn, J., & Dutt, M. (2016). Self-Assembly and Critical Aggregation Concentration Measurements of ABA Triblock Copolymers with Varying B Block Types: Model Development, Prediction, and Validation. *Journal of Physical Chemistry B*, *120*(15), 3666–3676. https://doi.org/10.1021/acs.jpcb.5b12594

Balaraman, K., Vieira, N. C., Moussa, F., Vacus, J., Cojean, S., Pomel, S., Bories, C., Figadère, B., Kesavan, V., & Loiseau, P. M. (2015). In vitro and in vivo antileishmanial properties of a 2-n-propylquinoline hydroxypropyl β-cyclodextrin formulation and pharmacokinetics via intravenous route. *Biomedicine and Pharmacotherapy*, *76*, 127–133. https://doi.org/10.1016/j.biopha.2015.10.028

Barabási, A., & Oltvai, Z. N. (2004). Network biology: Understanding the cell's functional organization. *Nature Reviews Genetics*, *5*, 101–113. https://doi.org/10.1038/nrg1272

Bavley, A., Lazier, W. A., & Timreck, A. E. (1954). *Fat-soluble vitamin-containing products and process thereof* (Patent US 2691619).

Berendsen, H. J. C., Grigera, J. R., & Straatsma, T. P. (1987). The missing term in effective pair potentials. *The Journal of Physical Chemistry*, *91*(24), 6269–6271. https://doi.org/10.1021/j100308a038

Bergeaud, A., Potiron, Y., & Raimbault, J. (2017). Classifying patents based on their semantic content. *PLoS ONE*, *12*(4), 0176310. https://doi.org/10.1371/journal.pone.0176310

Bilensoy, E., & Hincal, A. A. (2009). Recent advances and future directions in amphiphilic cyclodextrin nanoparticles. *Expert Opinion on Drug Delivery*, *6*(11), 1161–1173. https://doi.org/10.1517/17425240903222218

Bird, S., Klein, E., & Loper, E. (2009). *Natural Language Processing with Python* (First Edit). O´REILLY.

Blondel, V. D., Guillaume, J.-L., Lambiotte, R., & Lefebvre, E. (2008). Fast unfolding of communities in large networks. *Journal of Statistical Mechanics: Theory and Experiment*, *2008*(10), P10008. https://doi.org/10.1088/1742-5468/2008/10/P10008

Bonini, M., Rossi, S., Karlsson, G., Almgren, M., lo Nostro, P., & Baglioni, P. (2006). Self-assembly of beta-cyclodextrin in water. Part 1: Cryo-TEM and dynamic and static light scattering. *Langmuir*, *22*(4), 1478–1484. https://doi.org/10.1021/la052878f

Boyack, K. W., Smith, C., & Klavans, R. (2020). A detailed open access model of the PubMed literature. *Scientific Data*, *7*, 408. https://doi.org/10.1038/s41597-020-00749-y

Braga, S. S., Barbosa, J. S., Santos, N. E., El-Saleh, F., & Paz, F. A. A. (2021). Cyclodextrins in antiviral therapeutics and vaccines. *Pharmaceutics*, *13*, 409–433. https://doi.org/10.3390/pharmaceutics13030409

Brittain, W. J., & Minko, S. (2007). A structural definition of polymer brushes. *Journal of Polymer Science Part A: Polymer Chemistry*, *45*(16), 3505–3512. https://doi.org/10.1002/pola.22180

Chamberlain, L. M., Godek, M. L., Gonzalez-Juarrero, M., & Grainger, D. W. (2009). Phenotypic non-equivalence of murine (monocyte-) macrophage cells in biomaterial and inflammatory models. *Journal of Biomedical Materials Research Part A*, *88*(4), 858–871. https://doi.org/10.1002/jbm.a.31930

Chen, Y., Wang, X., Zhu, Y., Si, L., Zhang, B., Zhang, Y., Zhang, L., Zhou, D., & Xiao, S. (2020). Synthesis of a Hexavalent Betulinic Acid Derivative as a Hemagglutinin-Targeted Influenza Virus Entry Inhibitor. *Molecular Pharmaceutics*, *17*(7), 2546–2554. https://doi.org/10.1021/acs.molpharmaceut.0c00244

Cheng, J., Davis, M. E., & Khin, K. T. (2011). *Cyclodextrin-based polymers for delivering the therapeutic agents covalently bound thereto* (Patent EP 1534340).

Choi, Y.-A., Rho Chin, B., Hoon Rhee, D., Choi, H.-G., Chang, H.-W., Kim, J.-H., & Baek, S.-H. (2004). Methyl-β-cyclodextrin inhibits cell growth and cell cycle arrest via a prostaglandin E2 independent pathway. *Experimental and Molecular Medicine*, *36*(1), 78–84. https://doi.org/10.1038/emm.2004.11

Clinical Trial of CRLX101. (2016). https://clinicaltrials.gov/ct2/show/study/NCT02769962

ClinicalTrials.gov. (2013). *Safety Study of CALAA-01 to Treat Solid Tumor Cancers*. https://clinicaltrials.gov/ct2/show/NCT00689065?term=CALAA&draw=2&rank=1

Coleman, A. W., Nicolis, I., Keller, N., & Dalbiez, J. P. (1992). Aggregation of cyclodextrins: An explanation of the abnormal solubility of β-cyclodextrin. *Journal of Inclusion Phenomena and Molecular Recognition in Chemistry*, *13*(2), 139–143. https://doi.org/10.1007/BF01053637

Concheiro, A., & Alvarez-Lorenzo, C. (2013). Chemically cross-linked and grafted cyclodextrin hydrogels: From nanostructures to drug-eluting medical devices. *Advanced Drug Delivery Reviews*, *65*(9), 1188–1203. https://doi.org/10.1016/j.addr.2013.04.015

Cova, T. F. G. G., Cruz, S. M. A., Valente, A. J. M., Abreu, P. E., Marques, J. M. C., & Pais, A. A. C. C. (2018). Aggregation of Cyclodextrins: Fundamental Issues and Applications. In *Cyclodextrin - A Versatile Ingredient*. InTechOpen. https://doi.org/10.5772/intechopen.73532

Crini, G. (2014). Review: A History of Cyclodextrins. *Chemical Reviews*, *114*(21), 10940–10975. https://doi.org/10.1021/cr500081p

Crini, G., Fourmentin, S., Fenyvesi, É., Torri, G., Fourmentin, M., & Morin-Crini, N. (2018). Fundamentals and Applications of Cyclodextrins. In *Cyclodextrin Fundamentals, Reactivity and Analysis. Environmental Chemistry for a Sustainable World* (Vol. 16, pp. 1–55). Springer, Cham. https://doi.org/10.1007/978-3-319-76159-6_1

Davaatseren, M., Jo, Y.-J., Hong, G.-P., Hur, H., Park, S., & Choi, M.-J. (2017). Studies on the Anti-Oxidative Function of trans-Cinnamaldehyde-Included β-Cyclodextrin Complex. *Molecules*, *22*(12), 1868. https://doi.org/10.3390/molecules22121868

De Sousa, F. B., Lima, A. C., Denadai, Â. M. L., Anconi, C. P. A., de Almeida, W. B., Novato, W. T. G., dos Santos, H. F., Drum, C. L., Langer, R., & Sinisterra, R. D. (2012). Superstructure based on β-CD self-assembly induced by a small guest molecule. *Physical Chemistry Chemical Physics*, *14*(6), 1934–1944. https://doi.org/10.1039/c2cp22768a

Dey, J., Ghosh, R., & das Mahapatra, R. (2019). Self-Assembly of Unconventional Low-Molecular-Mass Amphiphiles Containing a PEG Chain. *Langmuir*, *35*(4), 848–861. https://doi.org/10.1021/acs.langmuir.8b00779

Dhiman, P., & Bhatia, M. (2020). Pharmaceutical applications of cyclodextrins and their derivatives. *Journal of Inclusion Phenomena and Macrocyclic Chemistry*, *98*, 171–186. https://doi.org/10.1007/s10847-020-01029-3

D'souza, A. A., & Shegokar, R. (2016). Polyethylene glycol (PEG): a versatile polymer for pharmaceutical applications. *Expert Opinion on Drug Delivery*, *13*(9), 1257–1275. https://doi.org/10.1080/17425247.2016.1182485

Duchêne, D., Bochot, A., Yu, S.-C., Pépin, C., & Seiller, M. (2003). Cyclodextrins and emulsions. *International Journal of Pharmaceutics*, *266*(2), 85–90. https://doi.org/10.1016/S0378-5173(03)00384-3

Essmann, U., Perera, L., Berkowitz, M. L., Darden, T., Lee, H., & Pedersen, L. G. (1995). A smooth particle mesh Ewald method. *The Journal of Chemical Physics*, *103*(19), 8577–8593. https://doi.org/10.1063/1.470117

Farace, C., Sánchez-Moreno, P., Orecchioni, M., Manetti, R., Sgarrella, F., Asara, Y., Peula-García, J. M., Marchal, J. A., Madeddu, R., & Delogu, L. G. (2016). Immune cell impact of three differently coated lipid nanocapsules: pluronic, chitosan and polyethylene glycol. *Scientific Reports*, *6*, 18423. https://doi.org/10.1038/srep18423

Fatokun, A. A., Stone, T. W., & Smith, R. A. (2008). Responses of differentiated MC3T3-E1 osteoblast-like cells to reactive oxygen species. *European Journal of Pharmacology*, *587*(3), 35–41. https://doi.org/10.1016/j.ejphar.2008.03.024

Flores, C., Lopez, M., Tabary, N., Neut, C., Chai, F., Betbeder, D., Herkt, C., Cazaux, F., Gaucher, V., Martel, B., & Blanchemain, N. (2017). Preparation and characterization of novel chitosan and β-cyclodextrin polymer sponges for wound dressing applications. *Carbohydrate Polymers*, *173*, 535–546. https://doi.org/10.1016/j.carbpol.2017.06.026

Francis, S. A., Kelly, J. M., McCormack, J., Rogers, R. A., Jean, L., Schneeberger, E. E., & Lynch, R. D. (1999). Rapid reduction of MDCK cell cholesterol by methyl-β-cyclodextrin alters steady state transepithelial electrical resistance. *European Journal of Cell Biology*, *78*(7), 473–484. https://doi.org/10.1016/S0171-9335(99)80074-0

Fülöp, Z., Kurkov, S. v., Nielsen, T. T., Larsen, K. L., & Loftsson, T. (2012). Self-assembly of cyclodextrins: Formation of cyclodextrin polymer based nanoparticles. *Journal of Drug Delivery Science and Technology*, *22*(3), 215–221. https://doi.org/10.1016/S1773-2247(12)50032-8

Gan, G., Ma, C., & Wu, J. (2007). *Data Clustering: Theory, Algorithms, and Applications* (Second Edi). ASA-SIAM. https://doi.org/10.1137/1.9781611976335

Garrido, P. F., Calvelo, M., Blanco-González, A., Veleiro, U., Suárez, F., Conde, D., Cabezón, A., Piñeiro, Á., & Garcia-Fandino, R. (2020). The Lord of the NanoRings: Cyclodextrins and the battle against SARS-CoV-2. *International Journal of Pharmaceutics*, *588*, 119689. https://doi.org/10.1016/j.ijpharm.2020.119689

Giacoppo, S., Rajan, T. S., Iori, R., Rollin, P., Bramanti, P., & Mazzon, E. (2017). The α-cyclodextrin complex of the Moringa isothiocyanate suppresses lipopolysaccharide-induced inflammation in RAW 264.7 macrophage cells through Akt and p38 inhibition. *Inflammation Research*, *66*(6), 487–503. https://doi.org/10.1007/s00011-017-1033-7

Godinho, B. M. D. C., Ogier, J. R., Quinlan, A., Darcy, R., Griffin, B. T., Cryan, J. F., & Caitriona, M. O. D. (2014). PEGylated cyclodextrins as novel siRNA nanosystems: Correlations between polyethylene glycol length and nanoparticle stability. *International Journal of Pharmaceutics*, *473*(2), 105–112. https://doi.org/10.1016/j.ijpharm.2014.06.054

Golias, C. H., Charalabopoulos, A., & Charalabopoulos, K. (2004). Cell proliferation and cell cycle control: a mini review. *International Journal of Clinical Practice*, *58*, 1134–1141.

González-Gaitano, G., Rodríguez, P., Isasi, J. R., Fuentes, M., & Tardajos, G. (2002). The aggregation of cyclodextrins as studied by photon correlation spectroscopy. *Journal of Inclusion Phenomena and Macrocyclic Chemistry*, *44*, 101–105. https://doi.org/https://doi.org/10.1023/A:1023065823358

Guerra, F. S., Sampaio, L. da S., Konig, S., Bonamino, M., Rossi, M. I. D., Costa, M. L., Fernandes, P., & Mermelstein, C. (2016). Membrane cholesterol depletion reduces breast tumor cell migration by a mechanism that involves non-canonical Wnt signaling and IL-10 secretion. *Translational Medicine Communications*, *1*, 3. https://doi.org/10.1186/s41231-016-0002-4

Hagberg, Aric. A., Schult, D. A., & Swart, P. J. (2008). Exploring Network Structure, Dynamics, and Function using NetworkX. *Proceedings of the 97h Python in Science Conference, SciPy*, 11–15. http://conference.scipy.org/proceedings/SciPy2008/paper_2

Hailstones, D., Sleer, L. S., Parton, R. G., & Stanley, K. K. (1998). Regulation of caveolin and caveolae by cholesterol in MDCK cells. *Journal of Lipid Research*, *39*(2), 369–379. https://doi.org/10.1016/S0022-2275(20)33898-0

Hammoud, Z., Khreich, N., Auezova, L., Fourmentin, S., Elaissari, A., & Greige-Gerges, H. (2019). Cyclodextrin-membrane interaction in drug delivery and membrane structure maintenance. *International Journal of Pharmaceutics*, *564*, 59–76. https://doi.org/10.1016/j.ijpharm.2019.03.063

He, J., Yang, Y., Zhou, X., Zhang, W., & Liu, J. (2020). Shuttle/sink model composed of -cyclodextrin and simvastatin-loaded discoidal reconstituted high-density lipoprotein

for enhanced cholesterol efflux and drug uptake in macrophage/foam cells. *Journal of Materials Chemistry B*, *8*(7), 1496–1506. https://doi.org/10.1039/c9tb02101a

He, Y., Fu, P., Shen, X., & Gao, H. (2008). Cyclodextrin-based aggregates and characterization by microscopy. *Micron*, *39*(5), 495–516. https://doi.org/10.1016/j.micron.2007.06.017

Heidel, J. D., & Schluep, T. (2012). Cyclodextrin-Containing Polymers: Versatile Platforms of Drug Delivery Materials. *Journal of Drug Delivery*, *2012*, 262731. https://doi.org/10.1155/2012/262731

Hernandez-Pascacio, J., Piñeiro, Á., Ruso, J. M., Hassan, N., Campbell, R. A., Campos-Terán, J., & Costas, M. (2016). Complex Behavior of Aqueous α-Cyclodextrin Solutions. Interfacial Morphologies Resulting from Bulk Aggregation. *Langmuir*, *32*(26), 6682–6690. https://doi.org/10.1021/acs.langmuir.6b01646

Hess, B., Bekker, H., Berendsen, H. J. C., & Fraaije, J. G. E. M. (1997). LINCS: A linear constraint solver for molecular simulations. *Journal of Computational Chemistry*, *18*(12), 1463–1472. https://doi.org/10.1002/(SICI)1096-987X(199709)18:12<1463::AID-JCC4>3.0.CO;2-H

Hess, B., Kutzner, C., van der Spoel, D., & Lindahl, E. (2008). GROMACS 4: Algorithms for Highly Efficient, Load-Balanced, and Scalable Molecular Simulation. *Journal of Chemical Theory and Computation*, *4*(3), 435–447. https://doi.org/10.1021/ct700301q

Hippler, M., Lemma, E. D., Bertels, S., Blasco, E., Barner-Kowollik, C., Wegener, M., & Bastmeyer, M. (2019). 3D Scaffolds to Study Basic Cell Biology. *Advanced Materials*, *31*(26). https://doi.org/10.1002/adma.201808110

Ho, D. L., Hammouda, B., & Kline, S. R. (2003). Clustering of poly(ethylene oxide) in water revisited. *Journal of Polymer Science Part B: Polymer Physics*, *41*, 135–138. https://doi.org/10.1002/polb.10340

Hu, J., Li, S., Yao, Y., Yu, L., Yang, G., & Hu, J. (2018). Patent keyword extraction algorithm based on distributed representation for patent classification. *Entropy*, *20*(2), 104. https://doi.org/10.3390/e20020104

Jansook, P., Maw, P. D., Soe, H. M. S. H., Chuangchunsong, R., Saiborisuth, K., Payonitikarn, N., Autthateinchai, R., & Pruksakorn, P. (2020). Development of amphotericin B nanosuspensions for fungal keratitis therapy: effect of self-assembled γ-cyclodextrin. *Journal of Pharmaceutical Investigation*, *50*(5), 513–525. https://doi.org/10.1007/s40005-020-00474-z

Jansook, P., Moya-Ortega, M. D., & Loftsson, T. (2010). Effect of self-aggregation of γ-cyclodextrin on drug solubilization. *Journal of Inclusion Phenomena and Macrocyclic Chemistry*, *68*, 229–236. https://doi.org/10.1007/s10847-010-9779-3

Jansook, P., Ogawa, N., & Loftsson, T. (2018). Cyclodextrins: structure, physicochemical properties and pharmaceutical applications. *International Journal of Pharmaceutics*, *535*(2), 272–284. https://doi.org/10.1016/j.ijpharm.2017.11.018

Jesus, S., Schmutz, M., Som, C., Borchard, G., Wick, P., & Borges, O. (2019). Hazard Assessment of Polymeric Nanobiomaterials for Drug Delivery: What Can We Learn From Literature So Far. *Frontiers in Bioengineering and Biotechnology*, *7*, 261. https://doi.org/10.3389/fbioe.2019.00261

Jiang, L., Yan, Y., & Huang, J. (2011). Versatility of cyclodextrins in self-assembly systems of amphiphiles. *Advances in Colloid and Interface Science*, *169*, 13–25. https://doi.org/10.1016/j.cis.2011.07.002

Jokerst, J. v, Lobovkina, T., Zare, R. N., & Gambhir, S. S. (2011). Nanoparticle PEGylation for imaging and therapy. *Nanomedicine*, *6*(4), 715–728. https://doi.org/10.2217/nnm.11.19

Jones, H. P. (1982). *Inclusion complex of β-cyclodextrin and digoxin* (Patent US 4555504).

Jones, R. G., Ober, C. K., Hodge, P., Kratochvíl, P., Moad, G., & Vert, M. (2013). Terminology for aggregation and self-assembly in polymer science (IUPAC recommendations 2013). *Pure and Applied Chemistry*, *85*(2), 463–492. https://doi.org/10.1351/PAC-REC-12-03-12

Jug, M., Kosalec, I., Maestrelli, F., & Mura, P. (2012). Development of low methoxy amidated pectin-based mucoadhesive patches for buccal delivery of triclosan: Effect of cyclodextrin complexation. *Carbohydrate Polymers*, *90*(4), 1794–1803. https://doi.org/10.1016/j.carbpol.2012.07.074

Kelley, W. J., Fromen, C. A., Lopez-Cazares, G., & Eniola-Adefeso, O. (2018). PEGylation of model drug carriers enhances phagocytosis by primary human neutrophils. *Acta Biomaterialia*, *79*, 283–293. https://doi.org/10.1016/j.actbio.2018.09.001

Kim, K. O., Kim, G. J., & Kim, J. H. (2019). A cellulose/β-cyclodextrin nanofiber patch as a wearable epidermal glucose sensor. *RSC Advances*, *9*(40), 22790–22794. https://doi.org/10.1039/c9ra03887f

Knop, K., Hoogenboom, R., Fischer, D., & Schubert, U. S. (2010). Poly(ethylene glycol) in drug delivery: Pros and cons as well as potential alternatives. *Angewandte Chemie*, *49*(36), 6288–6308. https://doi.org/10.1002/anie.200902672

Kost, B., Brzezinski, M., Socka, M., Basko, M., & Biela, T. (2020). Biocompatible polymers combined with cyclodextrins: Fascinating materials for drug delivery applications. *Molecules*, *25*(15), 3404. https://doi.org/10.3390/molecules25153404

Kulthe, S. S., Choudhari, Y. M., Inamdar, N. N., & Mourya, V. (2012). Polymeric micelles: Authoritative aspects for drug delivery. *Designed Monomers and Polymers*, *15*(5), 465–521. https://doi.org/10.1080/1385772X.2012.688328

Lammers, T. (2013). SMART drug delivery systems: Back to the future vs. clinical reality. *International Journal of Pharmaceutics*, *454*(1), 527–529. https://doi.org/10.1016/j.ijpharm.2013.02.046

Laza-Knoerr, A.-L., Gref, R., Amiel, C., & Couvreur, P. (2012). *Method for forming cyclodextrin polymer and lipophilic compound emulsions, resulting emulsions, and compositions including said emulsions* (Patent US 2012/0304577A1).

Lee, C., Kwon, O., Kim, M., & Kwon, D. (2018). Early identification of emerging technologies: A machine learning approach using multiple patent indicators. *Technological Forecasting and Social Change*, *127*, 291–303. https://doi.org/10.1016/j.techfore.2017.10.002

Li, X., Xu, L., Nie, H., & Lei, L. (2021). Dexamethasone-loaded β-cyclodextrin for osteogenic induction of mesenchymal stem/progenitor cells and bone regeneration. *Journal of Biomedical Materials Research - Part A*, *109*(7), 1125–1135. https://doi.org/10.1002/jbm.a.37104

Liese, S., Gensler, M., Krysiak, S., Schwarzl, R., Achazi, A., Paulus, B., Hugel, T., Rabe, J. P., & Netz, R. R. (2017). Hydration Effects Turn a Highly Stretched Polymer from an Entropic into an Energetic Spring. *ACS Nano*, *11*(1), 702–712. https://doi.org/10.1021/acsnano.6b07071

Lin, Q., Yang, Y., Hu, Q., Guo, Z., Liu, T., Xu, J., Wu, J., Kirk, T. B., Ma, D., & Xue, W. (2017). Injectable supramolecular hydrogel formed from α-cyclodextrin and PEGylated arginine-functionalized poly(l-lysine) dendron for sustained MMP-9 shRNA plasmid delivery. *Acta Biomaterialia*, *49*, 456–471. https://doi.org/10.1016/j.actbio.2016.11.062

Linegar, K. L., Adeniran, A. E., Kostko, A. F., & Anisimov, M. A. (2010). Hydrodynamic radius of polyethylene glycol in solution obtained by dynamic light scattering. *Colloid Journal*, *72*(2), 279–281. https://doi.org/10.1134/S1061933X10020195

Liu, C., Zhou, Q., Li, Y., Garner, L. v., Watkins, S. P., Carter, L. J., Smoot, J., Gregg, A. C., Daniels, A. D., Jervey, S., & Albaiu, D. (2020). Research and Development on Therapeutic Agents and Vaccines for COVID-19 and Related Human Coronavirus Diseases. *ACS Central Science*, *6*(3), 315–331. https://doi.org/10.1021/acscentsci.0c00272

Liu, G., Li, Y., Yang, L., Wei, Y., Wang, X., Wang, Z., & Tao, L. (2017). Cytotoxicity study of polyethylene glycol derivatives. *RSC Advances*, *7*(30), 18252–18259. https://doi.org/10.1039/C7RA00861A

Liu, X., Yang, J.-M., Zhang, S. S., Liu, X.-Y., & Liu, D. X. (2010). Induction of cell cycle arrest at G1 and S phases and cAMP-dependent differentiation in C6 glioma by low concentration of cycloheximide. *BMC Cancer*, *10*, 684. https://doi.org/10.1186/1471-2407-10-684

Loftsson, T., Saokham, P., & Sá Couto, A. R. (2019). Self-association of cyclodextrins and cyclodextrin complexes in aqueous solutions. *International Journal of Pharmaceutics*, *560*, 228–234. https://doi.org/10.1016/j.ijpharm.2019.02.004

Loftsson, T., & Stefánsson, E. (2014). *Cyclodextrin nanotechnology for ophthalmic drug delivery* (US patent 8633172B2).

Loftsson, T., & Stefánsson, E. (2017). Cyclodextrins and topical drug delivery to the anterior and posterior segments of the eye. *International Journal of Pharmaceutics*, *531*(2), 413–423. https://doi.org/10.1016/j.ijpharm.2017.04.010

Lu, Y., Zhang, E., Yang, J., & Cao, Z. (2018). Strategies to improve micelle stability for drug delivery. *Nano Research*, *11*(10), 4985–4998. https://doi.org/10.1007/s12274-018-2152-3

Luviano, A. S., Hernández-Pascacio, J., Ondo, D., Campbell, R. A., Piñeiro, Á., Campos-Terán, J., & Costas, M. (2020). Highly viscoelastic films at the water/air interface: α-Cyclodextrin with anionic surfactants. *Journal of Colloid and Interface Science*, *565*, 601–613. https://doi.org/10.1016/j.jcis.2019.12.012

Maki, M. A. A., Cheah, S.-C., Bayazeid, O., & Kumar, P. V. (2020). Cyclodextrin inclusion complex inhibits circulating galectin-3 and FGF-7 and affects the reproductive integrity and mobility of Caco-2 cells. *Scientific Reports*, *10*, 17468. https://doi.org/10.1038/s41598-020-74467-1

Makino, Y., & Suzuki, Y. (1983). *Composition for solid pharmaceutical preparations of active vitamins D3* (Patent EP 0116755B1).

Makino, Y., & Suzuki, Y. (1988). *Composition for solid pharmaceutical preparations of active vitamins D3 and process for preparation thereof* (Patent US 4729895).

Malachowski, T., & Hassel, A. (2020). Engineering nanoparticles to overcome immunological barriers for enhanced drug delivery. *Engineered Regeneration*, *1*, 35–50. https://doi.org/10.1016/j.engreg.2020.06.001

Malde, A. K., Zuo, L., Breeze, M., Stroet, M., Poger, D., Nair, P. C., Oostenbrink, C., & Mark, A. E. (2011). An Automated Force Field Topology Builder (ATB) and Repository: Version 1.0. *Journal of Chemical Theory and Computation*, *7*(12), 4026–4037. https://doi.org/10.1021/ct200196m

McKinney, W. (2010). Data Structures for Statistical Computing in Python. *Proceedings of the 9th Python in Science Conference*, *1697900*(Scipy), 51–56. http://conference.scipy.org/proceedings/scipy2010/mckinney.html

Messner, M., Kurkov, S. v., Jansook, P., & Loftsson, T. (2010). Self-assembled cyclodextrin aggregates and nanoparticles. *International Journal of Pharmaceutics*, *387*(1–2), 199–208. https://doi.org/10.1016/j.ijpharm.2009.11.035

Metselaar, J. M., & Lammers, T. (2020). Challenges in nanomedicine clinical translation. *Drug Delivery and Translational Research*, *10*(3), 721–725. https://doi.org/10.1007/s13346-020-00740-5

Microtrac. (2021). *Dynamic Light Scattering: DLS Particle Analyzer*. https://www.microtrac.com/products/particle-size-shape-analysis/dynamic-light-scattering/

Mohammad, N., Malvi, P., Meena, A. S., Singh, S. v., Chaube, B., Vannuruswamy, G., Kulkarni, M. J., & Bhat, M. K. (2014). Cholesterol depletion by methyl-β-cyclodextrin augments tamoxifen induced cell death by enhancing its uptake in melanoma. *Molecular Cancer*, *13*, 204. https://doi.org/10.1186/1476-4598-13-204

Moroi, Y. (1992). Critical Micelle Concentration. In *Micelles: theorical and applied aspects* (First edit, pp. 47–55). Springer US.

Muankaew, C., Jansook, P., Sigurđsson, H. H., & Loftsson, T. (2016). Cyclodextrin-based telmisartan ophthalmic suspension: Formulation development for water-insoluble drugs. *International Journal of Pharmaceutics*, *507*(2), 21–31. https://doi.org/10.1016/j.ijpharm.2016.04.071

Müller, A. C., & Guido, S. (2017). Introduction to with Python Learning Machine. In *Proceedings of the Speciality Conference on Infrastructure Condition Assessmenr: Art, Science, Practice* (First Edit). O´REILLY.

Newman, M. (2010). Networks: An introduction. In *Oxford University Press* (First Edit). https://doi.org/10.1093/acprof:oso/9780199206650.003.0001

Ogawa, Y., Goda, S., & Morita, S. (2008). The Effect of Methyl-β-cyclodextrin on the Differentiation of RAW264 Cells into Osteoclasts. *Oral Science International*, *5*(1), 15–23. https://doi.org/10.1016/s1348-8643(08)80002-x

Oliveri, V., & Vecchio, G. (2018). Cyclodextrin-based nanoparticles. In *Organic Materials as Smart Nanocarriers for Drug Delivery* (pp. 619–658). Elsevier. https://doi.org/10.1016/B978-0-12-813663-8.00015-4

O'Mahony, A. M., Ogier, J., Desgranges, S., Cryan, J. F., Darcy, R., & O'Driscoll, C. M. (2012). A click chemistry route to 2-functionalised PEGylated and cationic β-cyclodextrins: Co-formulation opportunities for siRNA delivery. *Organic and Biomolecular Chemistry*, *10*(25), 4954–4960. https://doi.org/10.1039/c2ob25490e

Park, K. D., Park, K. M., Lee, Y. K., Hoang, T. T. T., & Le, T. P. (2017). *Injectable tissue adhesive hydrogel including gamma-cyclodextrin and biomedical use thereof* (US 2017/0281781A1).

Parnaud, G., Corpet, D. E., & Gamet-Payrastre, L. (2001). Cytostatic effect of polyethylene glycol on human colonic adenocarcinoma cells. *International Journal of Cancer*, *92*,

63–69. https://doi.org/10.1002/1097-0215(200102)9999:9999<::AID-IJC1158>3.0.CO;2-8

Pelaz, B., Alexiou, C., Alvarez-Puebla, R. A., Alves, F., Andrews, A. M., Ashraf, S., Balogh, L. P., Ballerini, L., Bestetti, A., Brendel, C., Bosi, S., Carril, M., Chan, W. C. W., Chen, C., Chen, X., Chen, X., Cheng, Z., Cui, D., Du, J., … Parak, W. J. (2017). Diverse Applications of Nanomedicine. *ACS Nano*, *11*(3), 2313–2381. https://doi.org/10.1021/acsnano.6b06040

Pereira, C. G., Picanco-Castro, V., Covas, D. T., & Porto, G. S. (2018). Patent mining and landscaping of emerging recombinant factor VIII through network analysis. *Nature Biotechnology*, *36*(7), 585–590. https://doi.org/10.1038/nbt.4178

Perinelli, D. R., Cespi, M., Lorusso, N., Palmieri, G. F., Bonacucina, G., & Blasi, P. (2020). Surfactant Self-Assembling and Critical Micelle Concentration: One Approach Fits All? *Langmuir*, *36*(21), 5745–5753. https://doi.org/10.1021/acs.langmuir.0c00420

Phillips, J. N. (1955). The energetics of micelle formation. *Transactions of the Faraday Society*, *51*(i), 561. https://doi.org/10.1039/tf9555100561

Pitha, J., Gerloczy, A., & Olivi, A. (1994). Parenteral hydroxypropyl cyclodextrins: Intravenous and intracerebral administration of lipophiles. *Journal of Pharmaceutical Sciences*, *83*(6), 833–837. https://doi.org/10.1002/jps.2600830615

Poon, R. Y. C. (2016). Cell Cycle Control: A System of Interlinking Oscillators. In *Cell Cycle Oscillators. Methods in Molecular Biology*. Humana Press. https://doi.org/https://doi.org/10.1016/B978-0-12-801238-3.98748-8G

Quarles, L. D., Yohay, D. A., Lever, L. W., Caton, R., & Wenstrup, R. J. (1992). Distinct proliferative and differentiated stages of murine MC3T3-E1 cells in culture: An in vitro model of osteoblast development. *Journal of Bone and Mineral Research*, *7*(6), 683–692. https://doi.org/10.1002/jbmr.5650070613

Recanatini, M., & Cabrelle, C. (2020). Drug Research Meets Network Science: Where Are We? *Journal of Medicinal Chemistry*, *63*(16), 8653–8666. https://doi.org/10.1021/acs.jmedchem.9b01989

Rego, A. C. B., de Melo, J. F., Neto, A. O. W., & Fonseca, J. L. C. (2017). Coil Interpenetration, Segment Aggregation and Adsorption of PEG at Water/Air Interface. *Journal of Surfactants and Detergents*, *20*(4), 977–983. https://doi.org/10.1007/s11743-017-1959-3

Rincón-López, J., Almanza-Arjona, Y. C., Riascos, A. P., & Rojas-Aguirre, Y. (2020). Technological evolution of cyclodextrins in the pharmaceutical field. *Journal of Drug Delivery Science and Technology*, *61*, 102156. https://doi.org/10.1016/j.jddst.2020.102156

Rincón-López, J., Almanza-Arjona, Y. C., Riascos, A. P., & Rojas-Aguirre, Y. (2021). When Cyclodextrins Met Data Science: Unveiling Their Pharmaceutical Applications through Network Science and Text-Mining. *Pharmaceutics*, *13*(8), 1297. https://doi.org/10.3390/pharmaceutics13081297

Rincón-López, J., Ramírez-Rodríguez, N. J., Luviano, A. S., Costas, M., López-Cervantes, J. L., García-Figueroa, A. A., Domínguez, H., Mendoza-Cruz, R., Guadarrama, P., López-Morales, S., & Rojas-Aguirre, Y. (2021). Experimental and theoretical studies of pegylated-β-cyclodextrin: A step forward to understand its tunable self-aggregation abilities. *Journal of Drug Delivery Science and Technology*, 102975. https://doi.org/10.1016/j.jddst.2021.102975

Rodriguez-Esteban, R., & Bundschus, M. (2016). Text mining patents for biomedical knowledge. *Drug Discovery Today*, *21*(6), 997–1002. https://doi.org/10.1016/j.drudis.2016.05.002

Rojas-Aguirre, Y., Torres-Mena, M. A., López-Méndez, L. J., Alcaraz-Estrada, S. L., Guadarrama, P., & Urucha-Ortíz, J. M. (2019). PEGylated β-cyclodextrins: Click synthesis and in vitro biological insights. *Carbohydrate Polymers*, *223*, 115113. https://doi.org/10.1016/j.carbpol.2019.115113

Romer Rassing, M. (1994). Chewing gum as a drug delivery system. *Advanced Drug Delivery Reviews*. https://doi.org/10.1016/0169-409X(94)90028-0

Sá Couto, A. R., Ryzhakov, A., & Loftsson, T. (2018). Self-Assembly of α-Cyclodextrin and β-Cyclodextrin: Identification and Development of Analytical Techniques. *Journal of Pharmaceutical Sciences*, *107*(8), 2208–2215. https://doi.org/10.1016/j.xphs.2018.03.028

Sánchez, L., Yi, Y., & Yu, Y. (2017). Effect of partial PEGylation on particle uptake by macrophages. *Nanoscale*, *9*, 288–297. https://doi.org/10.1039/C6NR07353K

Sarica, S., Luo, J., & Wood, K. L. (2020). TechNet: Technology semantic network based on patent data. *Expert Systems with Applications*, *142*, 112995. https://doi.org/10.1016/j.eswa.2019.112995

Scaffaro, R., Lopresti, F., Maio, A., Botta, L., Rigogliuso, S., & Ghersi, G. (2017). Electrospun PCL/GO-g-PEG structures: Processing-morphology-properties relationships. *Composites Part A: Applied Science and Manufacturing*, *92*, 97–107. https://doi.org/10.1016/j.compositesa.2016.11.005

Schoonraad, S. A., Trombold, M. L., & Bryant, S. J. (2021). The Effects of Stably Tethered BMP-2 on MC3T3-E1 Preosteoblasts Encapsulated in a PEG Hydrogel. *Biomacromolecules*, *22*(3), 1065–1079. https://doi.org/10.1021/acs.biomac.0c01085

Shibaguchi, K., Tamura, A., Terauchi, M., Matsumura, M., Miura, H., & Yui, N. (2019). Mannosylated polyrotaxanes for increasing cellular uptake efficiency in macrophages

through receptor-mediated endocytosis. *Molecules*, *24*(3), 439. https://doi.org/10.3390/molecules24030439

Singh, R., Chauhan, S., & Sharma, K. (2017). Surface Tension, Viscosity, and Refractive Index of Sodium Dodecyl Sulfate (SDS) in Aqueous Solution Containing Poly(ethylene glycol) (PEG), Poly(vinyl pyrrolidone) (PVP), and Their Blends. *Journal of Chemical and Engineering Data*, *62*(7), 1955–1964. https://doi.org/10.1021/acs.jced.6b00978

Solms, J. (1969). *Inclusion resins of cyclodextrin and methods of use* (Patent US 3420788).

Song, X., Zhu, J. ling, Wen, Y., Zhao, F., Zhang, Z. X., & Li, J. (2017). Thermoresponsive supramolecular micellar drug delivery system based on star-linear pseudo-block polymer consisting of β-cyclodextrin-poly(N-isopropylacrylamide) and adamantyl-poly(ethylene glycol). *Journal of Colloid and Interface Science*, *490*, 372–379. https://doi.org/10.1016/j.jcis.2016.11.056

Stella, V. J., & Rajewski, R. (1994). *Derivatives of cyclodextrins exhibiting enhanced aqueous solubility and the use thereof* (Patent US 5376645).

Stella, V. J., Rajewski, R. A., Rao, V. M., Mcginity, J. W., & Mosher, G. L. (2000). *Sulfoalkyl ether cyclodextrin based controlled release solid pharmaceutical formulations* (Patent US 6046177).

Szutkowski, K., Kołodziejska, Z., Pietralik, Z., Zhukov, I., Skrzypczak, A., Materna, K., & Kozak, M. (2018). Clear distinction between CAC and CMC revealed by high-resolution NMR diffusometry for a series of bis-imidazolium gemini surfactants in aqueous solutions. *RSC Advances*, *8*(67), 38470–38482. https://doi.org/10.1039/c8ra07081d

Terauchi, M., Tamura, A., Arisaka, Y., Masuda, H., Yoda, T., & Yui, N. (2021). Cyclodextrin-based supramolecular complexes of osteoinductive agents for dental tissue regeneration. *Pharmaceutics*, *13*(2), 136. https://doi.org/10.3390/pharmaceutics13020136

Thangaraj, Balasubramanian, Park, Natesan, Liu, & Manju. (2019). Orientin Induces G0/G1 Cell Cycle Arrest and Mitochondria Mediated Intrinsic Apoptosis in Human Colorectal Carcinoma HT29 Cells. *Biomolecules*, *9*(9), 418. https://doi.org/10.3390/biom9090418

Thannickal, V. J., & Fanburg, B. L. (2021). Reactive oxygen species in cell signaling. *American Journal of Physiology - Lung Cellular and Molecular Physiology*, *279*(78), L1005–L1028. https://doi.org/10.1152/ajplung.2000.279.6.L1005

Tonglairoum, P., Ngawhirunpat, T., Rojanarata, T., Panomsuk, S., Kaomongkolgit, R., & Opanasopit, P. (2015). Fabrication of mucoadhesive chitosan coated polyvinylpyrrolidone/cyclodextrin/clotrimazole sandwich patches for oral candidiasis. *Carbohydrate Polymers*, *132*, 173–179. https://doi.org/10.1016/j.carbpol.2015.06.032

Udachin, K. A., Wilson, L. D., & Ripmeester, J. A. (2000). Solid polyrotaxanes of polyethylene glycol and cyclodextrins: The single crystal x-ray structure of PEG-β-cyclodextrin. *Journal of the American Chemical Society*, *122*(49), 12375–12376. https://doi.org/10.1021/ja002189k

Varan, G., Varan, C., Erdoğar, N., Hıncal, A. A., & Bilensoy, E. (2017). Amphiphilic cyclodextrin nanoparticles. *International Journal of Pharmaceutics*, *531*(2), 457–469. https://doi.org/10.1016/j.ijpharm.2017.06.010

Verhoef, J. J. F., & Anchordoquy, T. J. (2013). Questioning the use of PEGylation for drug delivery. *Drug Delivery and Translational Research*, *3*(6), 499–503. https://doi.org/10.1007/s13346-013-0176-5

Villanueva-Flores, F., Castro-Lugo, A., Ramírez, O. T., & Palomares, L. A. (2020). Understanding cellular interactions with nanomaterials: towards a rational design of medical nanodevices. *Nanotechnology*, *31*(13), 132002. https://doi.org/10.1088/1361-6528/ab5bc8

Vogt, M., Stumpfe, D., Maggiora, G. M., & Bajorath, J. (2016). Lessons learned from the design of chemical space networks and opportunities for new applications. *Journal of Computer-Aided Molecular Design*, *30*(3), 191–208. https://doi.org/10.1007/s10822-016-9906-3

Wang, T., Guo, Y., He, Y., Ren, T., Yin, L., Fawcett, J. P., Gu, J., & Sun, H. (2020). Impact of molecular weight on the mechanism of cellular uptake of polyethylene glycols (PEGs) with particular reference to P-glycoprotein. *Acta Pharmaceutica Sinica B*, *10*(10), 2002–2009. https://doi.org/10.1016/j.apsb.2020.02.001

Web of Science. (2020). *Advanced Search - Derwent Innovations Index*. https://www-webofscience-com.pbidi.unam.mx:2443/wos/diidw/advanced-search

Weiss, G. J., Chao, J., Neidhart, J. D., Ramanathan, R. K., Bassett, D., Neidhart, J. A., Choi, C. H. J., Chow, W., Chung, V., Forman, S. J., Garmey, E., Hwang, J., Kalinoski, D. L., Koczywas, M., Longmate, J., Melton, R. J., Morgan, R., Oliver, J., Peterkin, J. J., … Yen, Y. (2013). First-in-human phase 1/2a trial of CRLX101, a cyclodextrin-containing polymer-camptothecin nanopharmaceutical in patients with advanced solid tumor malignancies. *Investigational New Drugs*, *31*(4), 986–1000. https://doi.org/10.1007/s10637-012-9921-8

Wu, J., Zhao, C., Lin, W., Hu, R., Wang, Q., Chen, H., Li, L., Chen, S., & Zheng, J. (2014). Binding characteristics between polyethylene glycol (PEG) and proteins in aqueous solution. *Journal of Materials Chemistry B*, *2*(20), 2983–2992. https://doi.org/10.1039/c4tb00253a

Wynn, T. A., Chawla, A., & Pollard, J. W. (2013). Macrophage biology in development, homeostasis and disease. *Nature*, *496*, 445–455. https://doi.org/10.1038/nature12034

Yang, Q., Jones, S. W., Parker, C. L., Zamboni, W. C., Bear, J. E., & Lai, S. K. (2014). Evading immune cell uptake and clearance requires PEG grafting at densities substantially exceeding the minimum for brush conformation. *Molecular Pharmaceutics*, *11*(4), 1250–1258. https://doi.org/10.1021/mp400703d

Ye, J., Yang, Y., Dong, W., Gao, Y., Meng, Y., Wang, H., Li, L., Jin, J., Ji, M., Xia, X., Chen, X., Jin, Y., & Liu, Y. (2019). Drug-free mannosylated liposomes inhibit tumor growth by promoting the polarization of tumor-associated macrophages. *International Journal of Nanomedicine*, *14*, 3203–3220. https://doi.org/10.2147/IJN.S207589

Ye, Q., Dellamary, L. A., & Piu, F. (2018). *Modulation of gel temperature of poloxamer-containing formulations* (Patent US 2018/0125781A1).

Young, C., Schluep, T., Hwang, J., & Eliasof, S. (2011). CRLX101 (formerly IT-101) – A Novel Nanopharmaceutical of Camptothecin in Clinical Development. *Current Bioactive Compounds*, *7*(1), 8–14. https://doi.org/10.2174/157340711795163866

Zerkoune, L., Angelova, A., & Lesieur, S. (2014). Nano-Assemblies of Modified Cyclodextrins and Their Complexes with Guest Molecules: Incorporation in Nanostructured Membranes and Amphiphile Nanoarchitectonics Design. *Nanomaterials*, *4*(3), 741–765. https://doi.org/10.3390/nano4030741

Zhang, M., Zhang, J., Chen, J., Zeng, Y., Zhu, Z., & Wan, Y. (2019). Fabrication of Curcumin-Modified TiO2 Nanoarrays via Cyclodextrin Based Polymer Functional Coatings for Osteosarcoma Therapy. *Advanced Healthcare Materials*, *8*(23), 1901031. https://doi.org/10.1002/adhm.201901031

Zhang, Y., Wang, P., Mao, H., Zhang, Y., Zheng, L., Yu, P., Guo, Z., Li, L., & Jiang, Q. (2021). PEGylated gold nanoparticles promote osteogenic differentiation in in vitro and in vivo systems. *Materials and Design*, *197*(321), 109231. https://doi.org/10.1016/j.matdes.2020.109231

Zhang, Z., Wang, H., & Shen, W. (2013). Densities, conductivities, and aggregation numbers of aqueous solutions of quaternary ammonium surfactants with hydroxyethyl substituents in the headgroups. *Journal of Chemical and Engineering Data*, *58*(8), 2326–2338. https://doi.org/10.1021/je400463n

Zielińska, A., Carreiró, F., Oliveira, A. M., Neves, A., Pires, B., Venkatesh, D. N., Durazzo, A., Lucarini, M., Eder, P., Silva, A. M., Santini, A., & Souto, E. B. (2020). Polymeric Nanoparticles: Production, Characterization, Toxicology and Ecotoxicology. *Molecules*, *25*(16), 3731. https://doi.org/10.3390/molecules25163731

Zuckerman, J. E., Gritli, I., Tolcher, A., Heidel, J. D., Lim, D., Morgan, R., Chmielowski, B., Ribas, A., Davis, M. E., & Yen, Y. (2014). Correlating animal and human phase Ia/Ib clinical data with CALAA-01, a targeted, polymer-based nanoparticle containing siRNA. *Proceedings of the National Academy of Sciences of the United States of America*, *111*(31), 11449–11454. https://doi.org/10.1073/pnas.1411393111

Apéndices

Apéndice A

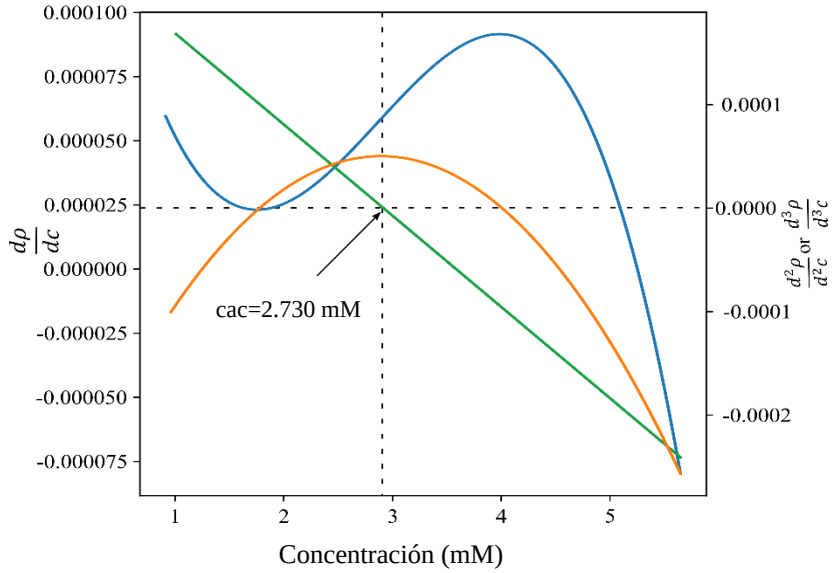

Figura 1. Primera, segunda y tercera derivadas de la densidad en función de la concentración para SDS (Rincón-López, Ramírez-Rodríguez, *et al*., 2021).

Tabla 1. Datos de DLS de βCDPEG5 0.5 mM.

Muestra	Dh1 (nm)	%Vol1	Dh2 (nm)	%Vol2
1	173.0	50.8	9.02	49.2
	163.5	51.7	8.9	48.3
	201.2	69.8	8.9	30.2
	150.6	55.9	8.7	44.1
	208.3	58.9	8.9	41.1
	150.5	46.7	9.1	53.3
2	161.7	52.1	9.1	47.9
	144.9	49.7	9	50.3
	132.9	43.3	8.9	56.7
	141.9	58.7	9.1	41.3
	145.6	55.5	9.2	44.5
	143.3	57.9	9.1	42.1
3	150.5	52.5	9.13	47.5
	138.9	52.5	9.1	47.5
	156.2	61.0	9.1	39.0

	164.1	61.9	9.0	38.1
	150.1	56.5	9.0	43.5
	140.1	55.9	9.17	44.1
Promedio	156.5	55.1	9.0	44.9
DE	20.3	6.1	0.1	6.1

Tabla 2. Datos de DLS de βCD.

Repetición	Dh1 (nm)	%Vol1	Dh2 (nm)	%Vol2
1	154.6	94.1	1.2	5.9
2	114.9	25.6	1.2	74.4
3	221.2	97.9	1.3	2.1
4	179.6	74.6	1.2	25.4
5	112.1	25.6	1.2	74.4
6	107.9	10.7	1.1	89.3
Promedio	148.4	54.8	1.2	45.3
DE	45.6	38.6	0.1	38.6

Tabla 3. Datos de DLS de PEG5.

Repetición	Dh1 (nm)	%Vol1	Dh2 (nm)	%Vol2
1	153.7	71.0	3.6	29.0
2	157.2	65.6	3.6	34.4
3	123.0	68.6	3.6	31.4
4	153.3	54.5	3.5	45.5
5	183.7	87.3	3.7	12.7
6	122.1	55.7	3.5	44.3
Promedio	148.8	67.1	3.6	32.9
DE	23.3	12.0	0.1	12.0

Tabla 4. Datos de DLS de la mezcla física.

Repetición	Dh1 (nm)	%Vol1	Dh2 (nm)	%Vol2
1	--	--	3.6	100
2	4850	46.5	3.6	53.5
3	5080	51.2	3.7	48.8
4	4910	24.8	3.7	75.2
5	--	--	3.5	100
6	930	15.1	3.5	84.9
Promedio	3942.5	34.4	3.6	77.1
DE	2010.7	17.3	0.1	22.2

Tabla 5. Efecto de la temperatura sobre la estabilidad de los agregados βCDPEG5.

Repetición	T=37 °C
1	155.0
2	151.1
3	152.3
4	151.2
5	157.0
6	147.7
Promedio	152.4
DE	3.3

Tabla 6. Efecto del pH sobre la estabilidad de los agregados de βCDPEG5.

	pH=3.8				pH=7.4				pH=8			
Repetición	Dh1 (nm)	%Vol1	Dh2 (nm)	%Vol2	Dh1 (nm)	%Vol1	Dh2 (nm)	%Vol2	Dh1 (nm)	%Vol1	Dh2 (nm)	%Vol2
1	136.5	47.1	12.1	52.9	137.4	90.1	10.94	9.9	150.1	96.8	10.4	3.2
2	131.1	56	11.92	44.0	130.8	89.5	10.69	10.5	160.2	97.7	12.27	2.3
3	145.5	59.1	12.44	40.9	145.5	91.3	10.85	8.7	145.9	96.2	11.21	3.8
4	138.8	56.9	11.65	43.1	142.6	88.9	10.76	11.1	148.8	95.4	10.29	4.6
5	149.5	54.2	11.63	45.8	104.5	79.9	7.52	20.1	143.2	95.7	12.8	4.3
6	140.7	59.5	11.68	40.8	121.9	87.9	11.72	12.1	141.3	100	--	--
Promedio	140.4	55.5	11.9	44.6	130.5	87.9	10.4	12.1	148.3	97.0	11.4	3.6
DE	6.5	4.5	0.3	4.5	15.3	4.1	1.5	4.1	6.7	1.7	1.1	0.9

Tabla 7. Efecto de la fuerza iónica sobre la estabilidad de los agregados de βCDPEG5.

	Isotónico=0.9% NaCl				Hipertónico=7.5% NaCl			
Repetición	Dh1 (nm)	%Vol1	Dh2 (nm)	%Vol2	Dh1 (nm)	%Vol1	Dh2 (nm)	%Vol2
1	148.0	91.3	11.2	8.7	142.6	85.9	10.8	14.1
2	142.5	87.2	10.8	12.8	138.9	85.2	11.6	14.8
3	136.1	88.1	11.4	11.9	156.6	91.8	11.4	8.2
4	136.9	88.1	11.0	11.9	135.4	86.0	11.1	14
5	131.6	88.2	10.8	11.8	151.7	90.7	11.5	9.3
6	138.7	87.2	10.4	12.8	205.5	96.2	10.9	3..8
Promedio	139.0	88.4	10.9	11.7	155.1	89.3	11.2	10.7
DE	5.2	1.5	0.3	1.5	25.9	4.4	0.3	4.4

Tabla 8. Efecto del tiempo sobre la estabilidad de los agregados de βCDPEG5.

Tiempo (días)	Dh1 (nm)	%Vol1	Dh2 (nm)	%Vol2
2	164.4±15.8	59.8±7.1	9.1±0.1	40.2±7.1
3	143.8±15.3	52.0±7.3	9.0±0.1	48.0±7.3
4	132.9±9.7	58.3±7.3	9.0±0.1	41.7±7.3
5	146.0±16.0	74.1±7.5	9.0±0.1	26.0±7.5
10	153.9±12.3	63.3±5.9	9.1±0.1	36.7±5.9
15	153.8±11.3	70.6±4.9	9.2±0.1	27.0±10.1
20	128.8±8.4	79.6±2.9	9.3±0.3	20.4±2.9
25	139.8±12.5	92.6±3.6	9.1±0.8	7.4±3.6
30	108.3±7.4	98.0±3.4	9.8±0.6	6.1±3.0
55	119.2±8.9	97.8±3.5	8.2±1.0	6.7±0.8

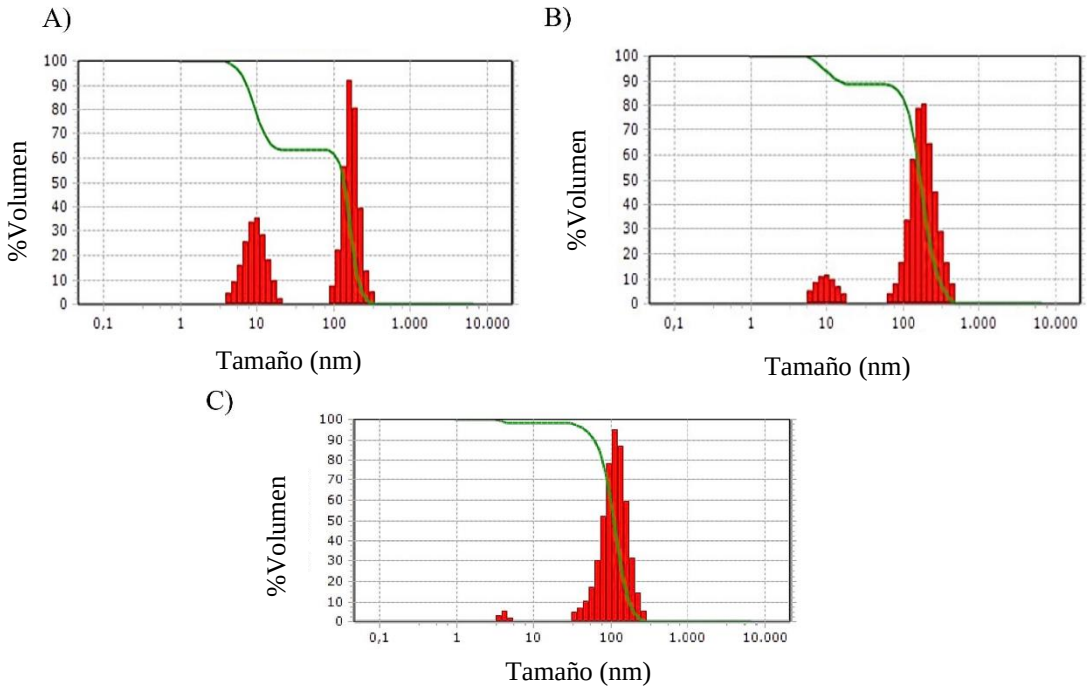

Figura 2. Distribución del tamaño de partícula de agregados de βCDPEG5 0.5 mM a lo largo del tiempo. A) después de 5 días, B) después de 20 días, C) después de 55 días (Rincón-López, Ramírez-Rodríguez, *et al*., 2021).

Tabla 9. Comparación del efecto de βCDPEGs, βCD y PEGs sobre el ciclo celular y la viabilidad de los osteoblastos MC3T3-E1. Los resultados se presentan como valores promedio± DE de experimentos por triplicado.

Compuesto	**Parametro**	**Población celular relativa (%)**					
		control	**25 µg/mL**	**50 µg/mL**	**100 µg/mL**	**250 µg/mL**	**500 µg/mL**
βCDPEG2	Sub G0/G1	3.7±0.1	3.7±0.4	3.7±0.2	3.8±0.4	3.4±0.3	3.8±0.3
	G0/G1	47.4±2.1	47.1±2.3	44.9±4.2	47.4±2.2	47.1±2.6	43.8±2.2
	S	18.4±0.6	16.5±4.0	15.5±3.8	15.9±0.8	18.0±5.7	23.6±3.7
	G2/M	36.1±2.3	36.4±1.4	34.0±3.5	37.4±0.8	30.6±1.6	27.9±1.3
	*Viabilidad	100.0±9.1	97.3±3.9	100.0±1.2	76.4±14.2	85.7±4.0	77.5±9.5
βCDPEG5	Sub G0/G1	3.7±0.1	3.6±1.5	4.2±0.4	3.7±0.7	4.2±1.4	4.0±0.2
	G0/G1	47.4±2.1	45.5±2.9	54.7±4.9	56.5±2.4	57.7±1.8	56.4±1.6
	S	18.6±0.8	19.8±1.9	22.5±1.2	28.1±1.3	26.5±2.8	27.0±2.6
	G2/M	36.1±2.3	28.2±0.8	18.6±0.8	17.2±5.4	16.6±4.0	12.0±1.2
	*Viabilidad	100.0±9.1	77.4±14.9	59.5±15.2	51.1±14.4	55.3±14.4	53.9±10.4
PEG2	Sub G0/G1	3.7±0.1	2.8±.4	3.7±0.3	4.1±0.1	3.4±0.5	3.9±0.2
	G0/G1	47.4±2.1	46.4±3.4	5.2±1.0	50.2±1.5	49.7±3.5	47.7±6.9
	S	18.6±0.8	23.5±3.0	25.5±3.0	26.9±2.4	24.0±3.3	24.0±1.8
	G2/M	36.1±2.3	11.6±0.8	13.5±1.1	12.9±1.1	13.1±1.5	12.5±2.1
	*Viabilidad	100.0±9.1	68.3±9.3	55.3±5.1	52.8±5.6	49.8±1.2	53.4±2.5
PEG5	Sub G0/G1	3.7±0.1	3.9±0.4	3.8±0.6	3.4±1.2	3.9±0.6	4.1±0.5
	G0/G1	47.4±2.1	46.8±3.4	50.5±1.4	54.9±4.0	52.4±2.7	53.7±3.2
	S	18.6±0.8	21.1±0.8	23.4±3.2	22.8±5.3	23.3±3.7	24.9±4.0
	G2/M	36.1±2.3	18.2±5.5	17.2±5.2	10.4±0.8	13.7±2.3	13.7±5.3
	*Viabilidad	100.0±9.1	54.6±10.8	41.9±12.5	46.1±12.8	49.4±9.2	50.6±4.2
βCD	Sub G0/G1	3.7±0.1	3.9±0.1	4.0±0.1	5.5±2.1	5.2±3.2	5.9±1.6
	G0/G1	47.4±2.1	53.8±2.2	53.9±10.3	60.6±2.5	59.5±7.2	59.9±9.2
	S	18.6±0.8	21.6±8.3	24.3±3.8	24.6±3.8	21.8±2.9	18.9±5.7
	G2/M	36.1±2.3	7.8±4.0	7.8±2.4	8.8±4.8	6.4±3.5	6.3±3.5
	*Viabilidad	100.0±9.1	77.3±10.4	54.0±3.7	59.2±8.0	37.0±28.2	70.3±4.2

*% Valores de viabilidad celular obtenidos del ensayo informado en la Sección 6.2.2.1. se han incluido para facilitar su comparación con el % de población celular relativa.

Tabla 10. Correlación entre el efecto de βCDPEGs, βCD y PEG en el perfil de distribución del ciclo celular y la viabilidad en MDCK. Los resultados se presentan como promedio± DE de experimentos por triplicado.

Compuesto	Parametro	Población celular relativa (%)					
		control	25µg/mL	50µg/mL	control	250µg/mL	500µg/mL
βCDPEG2	Sub G0/G1	4.1±0.5	3.7±0.3	3.6±0.5	3.6±1.0	3.7±0.1	3.8±0.3
	G0/G1	44.6±6.4	39.6±1.0	39.5±5.6	38.4±0.7	36.5±2.2	40.9±2.3
	S	13.0±5.4	11.9±4.3	10.7±1.1	10.9±1.7	7.2±3.3	7.4±2.5
	G2/M	31.7±0.2	28.9±1.8	30.8±1.8	27.7±1.0	29.1±5.2	30.5±3.2
	*Viabilidad	100.0±13.0	100.0±11.7	100.0±7.2	94.8±8.1	100.0±2.5	100.0±7.7
βCDPEG5	Sub G0/G1	4.1±0.5	3.6±1.5	4.2±0.4	3.7±0.7	4.2±1.4	4.0±0.2
	G0/G1	44.6±6.4	43.1±2.5	42.8±2.8	45.8±5.9	46.5±2.2	50.2±8.0
	S	13.0±5.4	24.5±3.4	27.8±4.3	27.9±0.9	31.1±1.0	30.2±2.7
	G2/M	31.7±0.2	11.9±4.3	10.7±1.1	10.9±1.7	7.2±3.3	7.4±2.5
	*Viabilidad	100.0±13.0	91.8±8.8	83.9±1.9	82.9±4.5	70.8±5.7	72.1±2.2
PEG2	Sub G0/G1	4.1±0.5	3.5±1.0	4.0±0.9	5.5±1.2	4.6±0.3	4.2±0.1
	G0/G1	44.6±6.4	43.6±4.1	45.2±5.5	46.8±1.1	45.0±1.9	45.3±4.3
	S	13.0±5.4	32.4±3.3	29.1±2.2	28.1±5.3	27.5±3.4	29.1±4.2
	G2/M	31.7±0.2	11.6±0.8	13.5±1.1	11.2±0.8	11.6±1.1	9.7±1.0
	*Viabilidad	100.0±13.0	78.9±3.5	69.2±6.8	64.3±2.3	58.6±20.3	74.0±3.9
PEG5	Sub G0/G1	4.1±0.5	3.3±0.4	3.5±0.3	3.6±0.5	3.3±0.2	3.5±0.6
	G0/G1	44.6±6.4	45.4±3.1	47.9±10.4	56.3±1.2	47.3±7.4	46.4±7.6
	S	13.0±5.4	26.0±3.4	28.9±1.4	25.0±0.9	26.8±2.9	25.4±2.8
	G2/M	31.7±0.2	13.1±2.3	11.5±1.7	11.7±0.6	11.6±1.1	16.7±3.4
	*Viabilidad	100.0±13.0	79.5±5.4	76.9±2.5	71.8±7.1	71.1±10.7	81.4±5.6
βCD	Sub G0/G1	4.1±0.5	2.8±0.9	3.7±0.3	4.9±1.1	4.1±1.1	3.5±0.7
	G0/G1	44.6±6.4	42.0±8.9	36.0±7.4	41.8±3.7	41.8±3.2	45.1±5.0
	S	13.0±5.4	13.3±2.2	38.6±2.4	35.2±1.2	35.6±3.1	37.8±4.0
	G2/M	31.7±0.2	37.8±12.4	17.1±4.1	9.4±1.3	2.7±0.5	7.2±2.6
	*Viabilidad	100.0±13.0	95.1±5.8	97.6±9.4	73.7±6.4	79.0±2.7	76.1±2.8

*% Valores de viabilidad celular obtenidos del ensayo informado en la Sección 6.2.3.1. se han incluido para facilitar su comparación con el % de población celular relativa

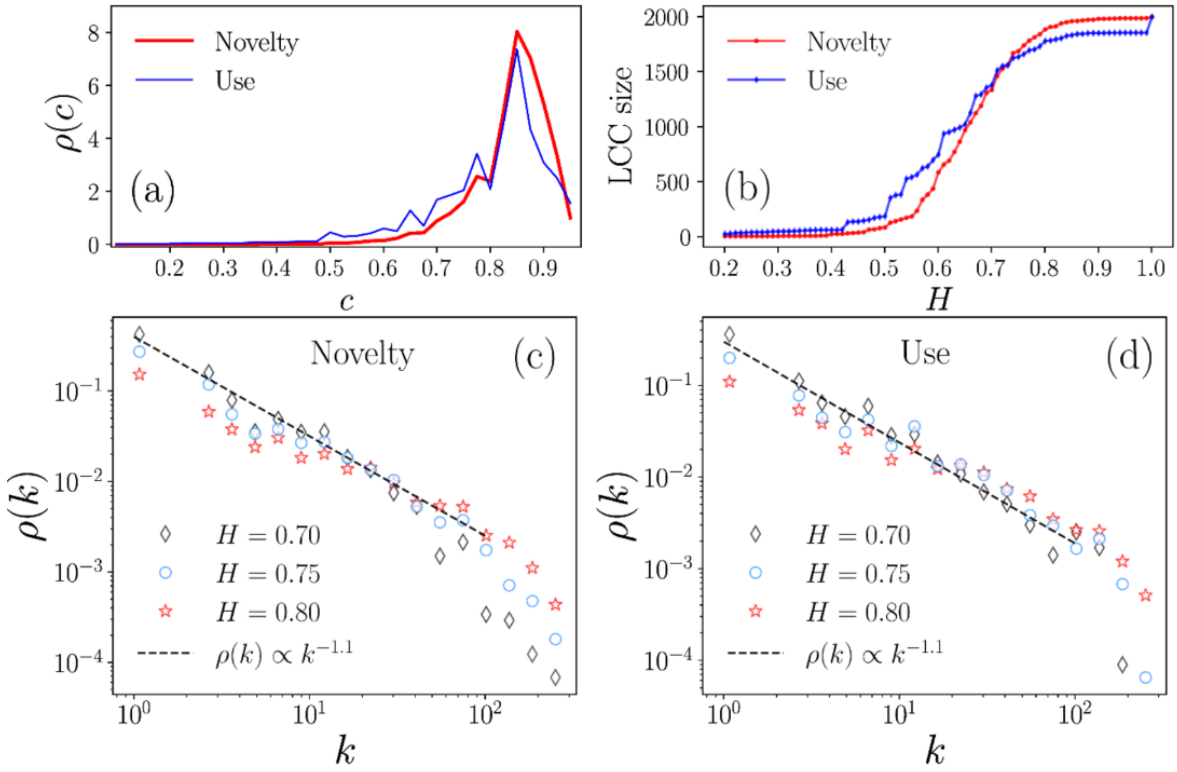

Figura 3. Caracterización de las redes que surgen de la similitud del contenido semántico de las patentes farmacéuticas de CDs en el área de Novedad y Uso. A) Análisis estadístico de los valores de *c* en el intervalo $0.1 \leq C \leq 0.95$, B) Tamaño del LCC formado según el valor umbral de *H*. Densidad de probabilidad de los grados *k* de la red generada para H=0.7, 0.75, 0.8 en la red de C) Novedad y D) Uso (Rincón-López, Almanza-Arjona, *et al*., 2021).

Apéndice B

Journal of Drug Delivery Science and Technology 61 (2021) 102156

Contents lists available at ScienceDirect

Journal of Drug Delivery Science and Technology

journal homepage: www.elsevier.com/locate/jddst

Review article

Technological evolution of cyclodextrins in the pharmaceutical field

Juliana Rincón-López [a], Yara C. Almanza-Arjona [b], Alejandro P. Riascos [c,**], Yareli Rojas-Aguirre [a,*]

[a] Instituto de Investigaciones en Materiales, Universidad Nacional Autónoma de México, Circuito Exterior S/N, Ciudad Universitaria, 04510, Mexico City, Mexico
[b] Instituto de Ciencias Aplicadas y Tecnología, Universidad Nacional Autónoma de México, Circuito Exterior S/N, Ciudad Universitaria, 04510, Mexico City, Mexico
[c] Instituto de Física, Universidad Nacional Autónoma de México, Apartado Postal 20-364, 01000, Ciudad de México, Mexico

ARTICLE INFO

Keywords:
Cyclodextrin
Supramolecular
Patents
Text mining
Administration route

ABSTRACT

We herein disclose how global cyclodextrin-based pharmaceutical technologies have evolved since the early 80s through a 1998 patents dataset retrieved from Derwent Innovation Index. We used text-mining techniques based on the patents semantic content to extract the knowledge contained therein, to analyze technologies related to the principal attributes of CDs: solubility, stability, and taste-masking enhancement. The majority of CDs pharmaceutical technologies are directed toward parenteral aqueous solutions. The development of oral and ocular formulations is rapidly growing, while technologies for nasal and pulmonary routes are emerging and seem to be promising. Formulations for topical, transdermal, vaginal, and rectal routes do not account for a high number of patents, but they may be hiding a great potential, representing opportunity research areas. Certainly, the progress in materials sciences, supramolecular chemistry, and nanotechnology, will influence the trend of that, apparently neglected, research. The bottom line, CDs pharmaceutical technologies are still increasing, and this trend is expected to continue in the coming years.

Patent monitoring allows the identification of relevant technologies and trends to prioritize research, development, and investment in both, academia and industry. We expect the scope of this approach to be applied in the pharmaceutical field beyond CDs technological applications.

1. Introduction

Cyclodextrins, cyclic oligomers linked by α-1,4 glycosidic bonds, are well known for their truncated cone structure, comprising a hydrophilic surface and a cavity bearing a hydrophobic microenvironment. CDs have been considered "all-purpose molecular containers" because their cavity can selectively accommodate a diversity of molecules through supramolecular host-guest interactions, giving rise to an IC (Fig. 1). CDs are chemically versatile and can be modified to get mono- or poly-substituted derivatives, which can improve their properties (i.e., solubility and stability), and tune their complexation abilities. The complexation process leads to significant changes in guest spectral properties, reactivity, volatility, solubility, and stability; thus, giving the CDs a great potential to be applied in a diversity of technological fields [1].

CDs have been of particular importance on drug delivery and pharmaceutical technologies. Undoubtedly, the most acknowledged application is the enhancement of aqueous solubility of poorly soluble drugs through the formation of CD/drug ICs. However, the complexation can also protect drugs from heat, light, hydrolysis, and oxidation, thereby improving the formulations stability. In other cases, it allows the manipulation of volatile compounds, reduces unpleasant tastes and odors, and decreases the effect of irritating compounds. Moreover, CDs can modify the release rate of drugs working as excipients for immediate or sustained release. Native CDs and several CD-derivatives are FDA-approved for pharmaceutical use and their success is evident with more than 50 medications containing CDs currently marketed [2–5]. The growth in the number of approved formulations over time suggests CDs are still a useful tool in the pharmaceutical field and that their applications could be expanding into a promising future.

Comprehensive reviews describing the CDs' abilities to enhance the solubility and stability of drugs, and the mechanisms of CD/drug complexation, have previously been reported [4,6–10]. However, an overview to understand the technological evolution of CDs in the pharmaceutical field is missing.

* Corresponding author. Universidad Nacional Autónoma de México, Instituto de Investigaciones en Materiales, Circuito Exterior S/N, 04510, Mexico City, Mexico
** Corresponding author. Instituto de Física, Universidad Nacional Autónoma de México, Apartado Postal 20-364, 01000, Mexico City, Mexico.
E-mail address: yareli.rojas@materiales.unam.mx (Y. Rojas-Aguirre).

https://doi.org/10.1016/j.jddst.2020.102156
Received 21 July 2020; Received in revised form 21 September 2020; Accepted 5 October 2020
Available online 14 October 2020
1773-2247/© 2020 Elsevier B.V. All rights reserved.

Abbreviations

BCS	Biopharmaceutics Classification System
CDs	Cyclodextrins
DII	Derwent Innovation Index
EMA	European Medicines Agency
EPO	European Patent Office
FDA	U.S. Food and Drug Administration
FDI	Foreign direct investment
HIV	Human immunodeficiency virus
HPβCD	Hydroxypropyl-β-cyclodextrin
HPγCD	Hydroxypropyl-γ-cyclodextrin
IC	Inclusion Complex
IM	Intramuscular
IPC	International Patent Classification
IV	Intravenous
MAGL	Monoacylglycerol lipase
MERS	Middle East Respiratory Syndrome
MβCD	Methyl-β-cyclodextrin
NSAIDs	Nonsteroidal anti-inflammatory drugs
PGE2	Prostaglandin E2
RMβCD	Random methyl-β-cyclodextrin
SARS	Severe Acute Respiratory Syndrome
SARS-CoV-2	Severe acute respiratory syndrome coronavirus 2
SBEβCD	Sulfobutylether-β-cyclodextrin
GI	Gastrointestinal
VP	Vantage Point Software
WIPO	World Intellectual Property Organization

Patents are a significant source of technical and commercial knowledge, as well as a good indicator of innovation. Thus, their analysis is a useful approach for researchers interested in studying the evolution of technological trends and changing demands for technological forecasting. At the academic level, patent analysis has great potential for identifying relevant technologies, evaluating the competitiveness of projects, and prioritizing research, development, and investment. Moreover, the analysis of patent data becomes highly relevant when the innovation cycle becomes more complex and shorter and when the market demands rapid responses [11,12]. For instance, Liu et al. analyzed data from patents related to the SARS and MERS viruses, thereby providing a substantial background for the ongoing development of therapies to treat or prevent SARS-CoV-2 infection [13].

Some outstanding publications have included some technological breakthroughs of CDs in their discussion. For instance, the first patent for CDs pharmaceutical applications in the '50s, the first formulation launched on the market in the '70s, and some relevant patents registered by the early '80s [3,4,8,14]. In 2011, Deorsola et al. briefly presented the global industrial applications of CDs through the analysis of scientific literature and patents [15]. Also, some reports examine the current patenting of the use of CDs as applied to specific families of drugs [16–18]. Nonetheless, an extensive analysis of CDs patents to inform how the CD-based pharmaceutical technologies have evolved over time has not been published so far.

In the pharmaceutical field, CDs patents fall into four categories: 1) methods for the synthesis/production of CDs and their derivatives; 2) methods to improve the performance of CDs, for instance, formulation techniques to improve the solubilizing ability of CDs; 3) ICs of CDs with a specific type of drug to render a particular result; and 4) pharmaceutical applications of CDs and their derivatives [8]. Hereafter, the analysis presented in this paper is based on pharmaceutical applications.

Thus, we herein present the global technological landscape of CDs for pharmaceutical applications and the evolution of those technologies over time, through text-mining techniques, using patents as the technical source. We based our analysis on the patent's semantic content [11]. Patent text-mining systems are generally focused on the analysis of title and abstract of the patent documents. In our approach, we analyzed keywords in terms of the "novelty" and "use" of each document to extract crucial information that might be hidden in the claims and description sections, thus allowing us to correlate the CDs properties and their pharmaceutical technologies intended for specific administration routes. Bottom line, from the knowledge mined from patents, we aim to inform the progress of such technologies, the current trends, and opportunity areas in the pharmaceutical applications of CDs.

2. Methodology

2.1. CD pharmaceutical patents dataset

Patents were retrieved from the database DII (Clarivate, 2020; access through the National Autonomous University of Mexico). To obtain the initial patent dataset, the search considered all documents filed until

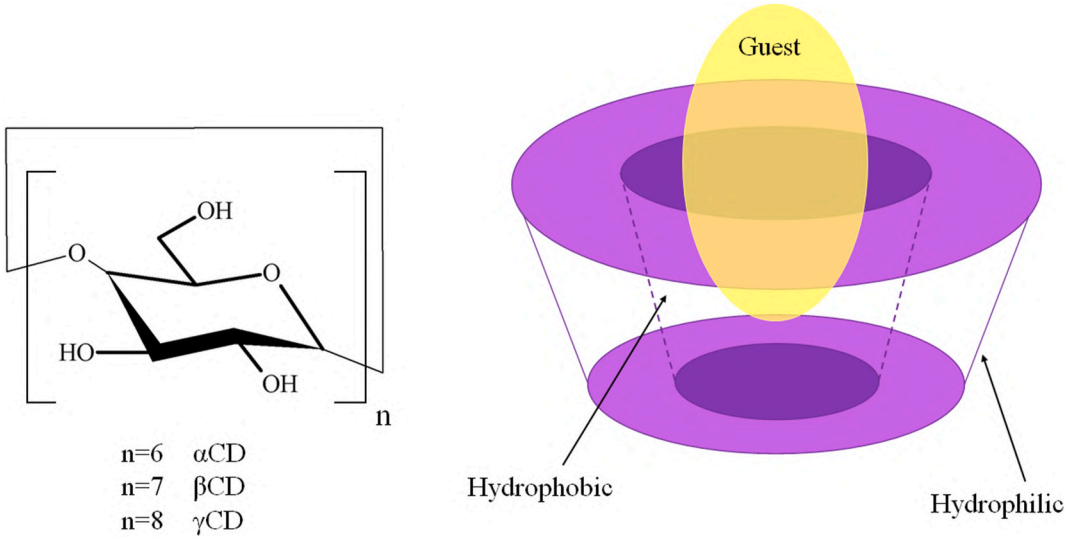

Fig. 1. Structural representation of α-, β-, and γ-CDs and the formation of an IC.

2019, the specific CDs' IPC codes [19,20], and the keyword *cyclodextrin* (Fig. 2a). Our query excluded the IPC A61Q, that refers to "Specific use of cosmetics or similar toilet preparations".

2.2. Solubility, stability, and taste-masking

A second search was performed, from the initial dataset, to identify the number of patents in which CD molecules were used as solubilizers, stabilizers, or taste-masking agents. For this end, the combination of truncated keywords (by using the wildcard asterisk, *) associated with solubility, stability, and taste-masking were entered, in addition to Boolean operators used as conjunctions to include or exclude keywords (Fig. 2b).

2.3. Technological development of CDs as functional excipients

To identify and count the number of patents related to a particular CD use as an excipient concerning administration routes, we conducted a text mining analysis. Furthermore, we analyzed the evolution of a particular technology by determining the change in the number of patents over time. For this aim, we used different tools for text and data processing implemented in Python's library pandas [21]. We first pre-processed the text (word lowering, removal of special symbols and punctuation) and then applied algorithms to identify specific words and logical Boolean operators like OR and AND, for the analysis of combinations of words in each patent (Fig. 2c). The text mining was performed in the fields of "novelty" and "use" for the documents retrieved from DII CDs patents dataset.

2.4. CD patents: Where and who?

VP [22] software was used to process, filter, classify, and analyze the dataset, for purposes of identifying assignees and geographical regions, as well as for ranking them and detecting the trends and behaviors with regard to CD patenting for pharmaceutical applications.

The matching rule was set as "General" for identifying priority year and countries. For this analysis, the top 10 countries were chosen because they encompass more than 99 registered patents each. It must be considered that each patent (e.g., the same technology) may be registered in more than one country, so the sum of patents in this section does not necessarily correspond to the total number of patents in the initial search. To retrieve the assignees, the matching rule was "Organization name (dept ignore)". In this case, our criteria were based on the selection of the top 20 assignees which are the ones having more than 10 patents each (Fig. 2d).

3. Results

3.1. Evolution of CD patents

Through our search, we retrieve an initial dataset of 1998 patents from DII. When analyzing the data, we identified two trends in patenting behavior over time. The first one, between 1983 and 2000, with a total of 125 records, corresponding to the 6.3% of total patents, and an average number of 6.9 patents per year. During this time, the rate of patenting was steady, with few changes. The second trend is from 2001 to 2019, with 1873 new filed patents, representing 93% of the total number of documents. Fig. 3 also shows that the highest increase in the number of patents registered, indicated by the steepest slope, occurred in the period from 2001 to 2007, with an average increment of 58.7 patents per year. Likewise, 2012 and 2018 stand out in patenting activity, with 157 and 170 registered patents, respectively, the highest numbers of registered patents over time.

The first patent retrieved from our dataset in DII dates from 1983. Before discussing this patent, we first briefly describe some relevant patents for a historical background before that year. In 1953, Freudenberg, Cramer, and Plieninger registered the patent entitled "Methods for preparation inclusion compounds of physiologically active compounds" [23]. This document discloses how CDs' ICs increase the stability of biologically active compounds and the precipitation method to obtain them [8,24]. By 1976, the apogee of CDs was just beginning with the Japanese approval of βCD/dinoprostone complexes for the induction of labor in childbirth, through the oxytocin-like effects formulated as a sublingual tablet [25]. As the investigations progressed, it was understood that αCD had a stabilizing effect on the parenteral use of some prostaglandins, allowing for the development of Alprostadil Alphadex™, approved for the treatment of Buerger's disease in 1979 and, later, for the treatment of male erectile dysfunction. After that, the interest on CDs for the development of pharmaceutical technologies was notable and since then, several formulations containing CDs, in diverse physical forms for its administration by different routes, have been approved in many countries [2–5,26].

As we mentioned before, the first patent of our dataset dates from 1983 and belongs to Teijin Limited. This document deals with the role of CDs as adjuvants for the stabilization of vitamin D_3 and its preparation process [27,28].

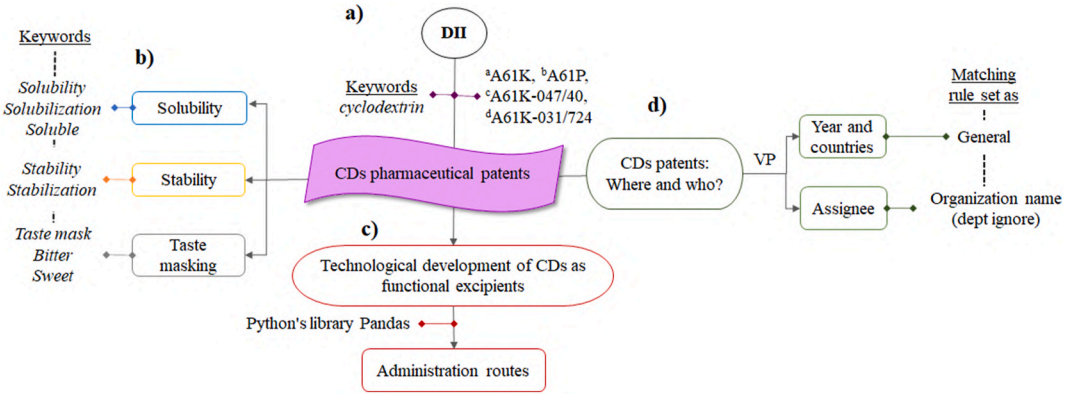

Fig. 2. Workflow showing a) general search to retrieve CD patents from DII; b) specific search to obtain CD patents disclosing solubility, stability, and taste-masking applications; c) text mining strategy to arrange the temporal evolution of patents according to the CD applications according to administration routes; d) procedure to analyze the CD patent dataset based on geographical region and assignee.
[a]A61K: Preparations for medical, dental, or toilet purposes
[b]A61P: Specific therapeutic activity of chemical compounds or medical preparations
[c]A61K-047/40: Cyclodextrins and derivatives thereof (medicinal preparations characterized by the non-active ingredients)
[d]A61K-031/724: Cyclodextrins (medicinal preparations containing organic active ingredients).

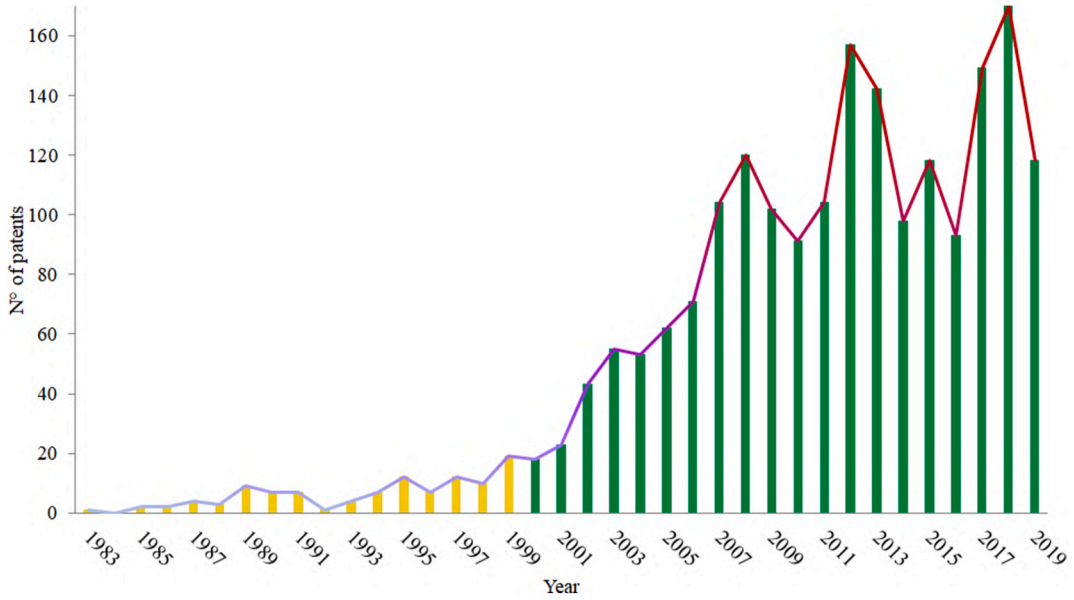

Fig. 3. Evolution of pharmaceutical CDs patents over time.

It is worth defining a couple of concepts related to patents. On the one hand, the term "priority art" refers to all the knowledge needed to develop the invention. In this case, all the priority art is linked to other patents or scientific papers that have demonstrated how CD complexation modifies the physicochemical properties of a given host, in particular, solubility and stability. It also refers to the relevance of the biological and physicochemical characterization of CD derivatives and their complexes [29–31]. Hence, this patent (No. US 4729895, Teijin Limited) and its corresponding priority art are directly related to the primary application of CDs, which is the solubility enhancement of a guest molecule as a result of the formation of an IC.

On the other hand, patent citations are the count of citations of the document in subsequent patents and, therefore, indicative of its impact on the development of new technology. In our search, the most cited patent, accounting for 413 citations, was registered by Kansas University in 1994. This document reports the successful functionalization of α, β, and γ CDs with sulfoalkyl substituents, for purposes of improving the physicochemical features of native CDs, their complexation capacity, and the decrease of their toxicity profile. This patent also mentions how CD derivatives can increase the solubility of drugs and, as a consequence, implement different administration routes such as oral, intranasal, parenteral, and rectal for ICs [32].

As we already mentioned, it was after the year 2000 when a breakthrough in CD patenting activity was observed. In fact, the most cited patent in the period between 2000 and 2019 corresponds to an innovation registered by CyDex Inc. in 2000, with a total of 193 citations. This patent describes sulfoalkyl ether CD-based controlled release solid pharmaceutical formulations, in which the CD derivatives were used, in combination with other components, to modify the bioavailability and/or rate of bioabsorption of therapeutic agents [33]. We consider this document to be a relevant innovation for several reasons. First, it introduces the terms "controlled release", "sustained release", "delayed release", and "targeted release", which are very popular in current CDs scientific papers but were revolutionary at that time, when CDs were pigeonholed as solubilizers/stabilizers. Second, it was based on modified rather than native CDs (sulfoalkyl ether moiety). Although the solubility enhancement could be implicit, the main goal of this invention was to control the delivery of drugs through CD-based solid platforms. All the priority art of this patent was published after 1989 and suggests a different driving force in the research and development activity related to CDs: the design of novel materials to control drug release and optimize the drugs' bioavailability by chemically modified CD derivatives, and the combination of different types of molecules and/or building blocks [34–36].

Thus, the milestone of CD patenting behavior is parallel to the emergence of intensive research activity in the drug delivery field, which in the last two decades has focused mainly on the design of versatile structures for carrying drugs and releasing them in a controlled manner. To date, this breakthrough has also integrated other disciplines into the field of CDs, such as supramolecular chemistry, materials sciences, and nanotechnology [37].

Despite the novelty projected for CDs in advanced drug delivery, their use in modifying the aqueous solubility of poorly soluble drugs has been—and continues to be—of great importance in the pharmaceutical industry. For instance, the use of CDs to solubilize an antineoplastic compound assigned to Pfizer Inc [38]. Fig. 4 summarizes the representative patents over time described above.

In 2004, Szejtli published a comprehensive review of CDs status in both, industrial and academic research, in which he forecasted that the use of CDs would expand in the coming years, due to more efficient forms of production. Also, he concluded that CDs in the pharmaceutical field would show slow but steady development [4]. Sixteen years later, we can say that the first two hypotheses were right. Contrary to what was thought, the interest in CDs has not grown slowly but, rather, has been rapidly increasing and is still engaging pharmaceutical and drug delivery research, with a boom stage starting in the early 2000s and continuing to the present day.

3.2. Solubility, stability, and taste-masking

CDs are primarily used for enhancing the aqueous solubility of poorly soluble drugs; improving the stability and masking unpleasant taste/odor of a formulation. Accordingly, we analyzed the CDs dataset to retrieve those patents devoted to each one of the mentioned attributes to then inspect their behavior over time.

3.2.1. Solubility

Aqueous solubility determines many aspects of drug discovery and development processes, including formulation, administration routes, and pharmacokinetics [39]. A poorly soluble drug cannot be formulated into a solution for parenteral or other administration routes (nasal, ocular, and otic). In addition, its bioavailability is limited if it is

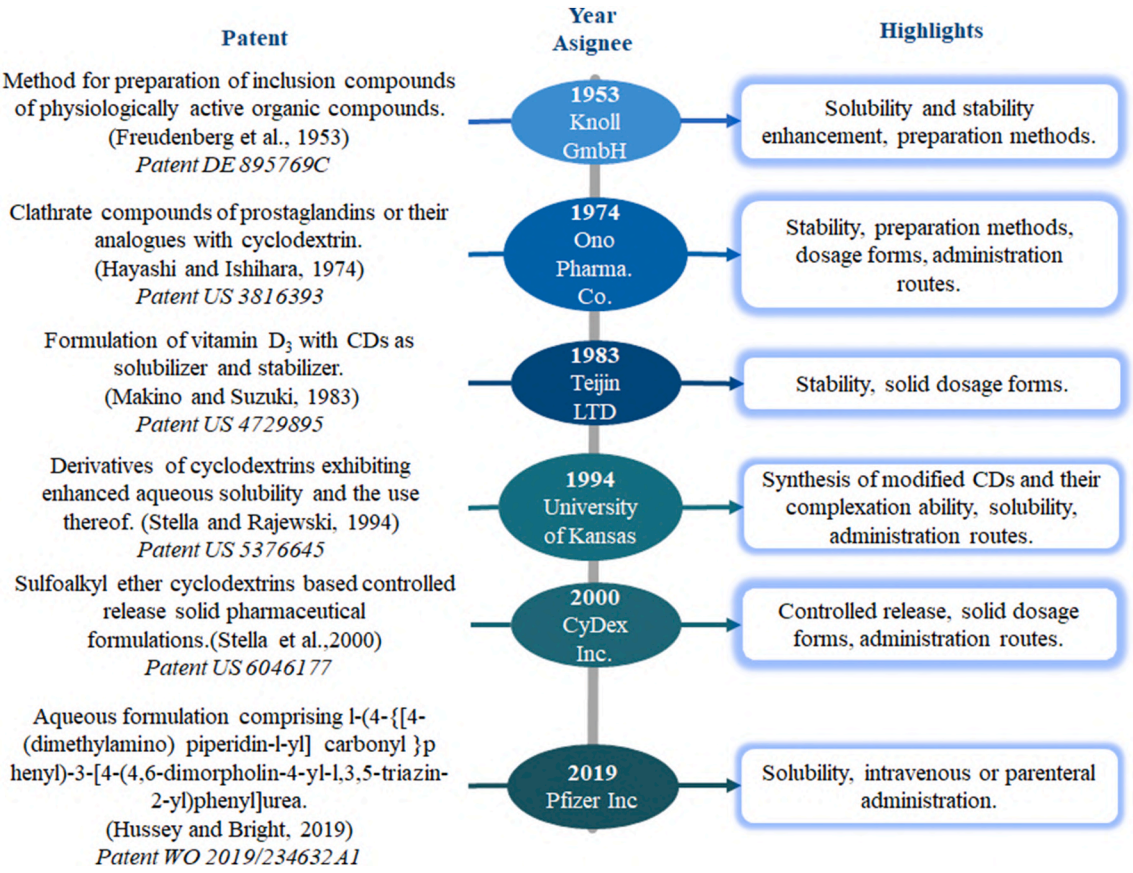

Fig. 4. Milestone patents of CDs with pharmaceutical applications over time.

administered orally.

CDs modify the apparent solubility of drugs through the formation of CD/drug ICs. In some cases, the solubility increase arises from non-inclusion aggregates, in which the CDs display the ability to form and stabilize supersaturated drug solutions [7]. Indeed, the supremacy of CDs is given by this attribute and the evolution of patents associated with solubility enhancement have substantially influenced the global trend of CDs pharmaceutical patents over time (Fig. 5).

Between the mid-80s and just before 1998, patenting activity was steady, reaching a peak in 1994, with 24 patents registered. After 2001, an inflection point marks the beginning of a very active period of patenting that is still observed to date; and 2013 outstands with 58 filed patents, the highest record in terms of solubility.

The first patent of our dataset is from 1983 and is related to water-soluble CD polymers substituted by ionic groups that, in addition to their abilities to complex with diverse guest molecules, they form salts

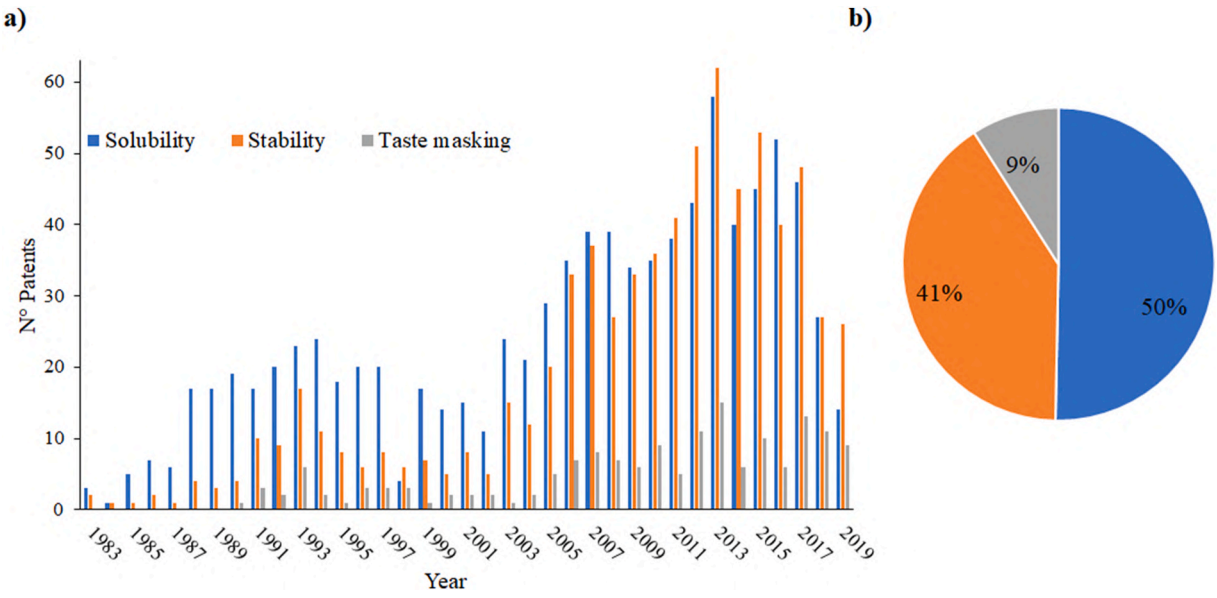

Fig. 5. a) Patenting trends of CDs and their uses for solubility, stability, and organoleptic properties enhancement; b) distribution of patents according to CD use.

thus broadening their applications [40]. The most cited patent regarding solubility enhancement corresponds to Stella & Rajewski, 1994, the most cited patent of the whole dataset (described in Section 3.1), just followed by a patent whose invention corresponds to Pitha, 1985, with 385 citations. The latter is another landmark in CDs history as it describes the preparation of alkylated CDs including HPβCD, one of the most important CD-derivatives, since its use has been approved for any administration route. The patent is also associated with the preparation of drug/alkylated-CD mixtures, emphasizing their amorphous state and high aqueous solubility [41].

Although Fig. 3 points out that 2018 was the year with the highest number of patents, Fig. 5 shows that, in this year, little activity was detected regarding solubility. After a while, the solubility enhancement of a poorly soluble drug was not a novelty anymore. Therefore, new effects, of course, associated or based on improved solubility, have had to be found. This may explain why the number of related patents started to decline.

Nonetheless, this does not mean that a simple IC to modify the solubility of a drug is not important. On the contrary, high-throughput screening strategies continuously propose new candidates, of which a large majority have low solubility. Therefore, CDs remain a valuable strategy for overcoming the challenges associated with these compounds. The same would happen with the repositioning of drugs, in which a change in their solubility, could be a trigger for their use in the treatment of a disease different from that for which they were originally created.

Similarly, CDs may enable formulations for the most convenient routes of administration, or reformulations for a relaunch of the product. For example, remdesivir, the drug that could be used to treat the SARS-CoV-2 infection, is poorly soluble in water—a limitation that has been overcome by the formation of an IC with SBEβCD for IV administration [42,43]. Other examples of patents using CDs for parenteral formulations are discussed in Section 3.3.1.

3.2.2. Stability

The effect of CDs on the chemical and physical stability of drugs has been well documented. In the solid state some CDs like MβCD can retard or suppress the degradation of some drugs. In addition, CDs can prevent thermal-sensitive drugs from degrading into oily products or, in turn, protect oily and volatile therapeutic molecules. Moreover, CDs can be used as a stabilizer agent for the whole formulation [10].

From 2002, an increase in the interest in the use of CDs as a stabilizing agent is seen, and 2010 is the year in which the number of patents of CDs as stabilizers, slightly exceeds the number of those for solubility. Today, the number of patents related to solubility and stability is comparable (Fig. 5). To note, a single patent can claim the use of both solubility and stability. This may be the case for patents that protect a vast number of drugs or formulations. Although less frequent, this could also happen for patents concerning a drug in which its hydrophobic part is also the sensitive part.

The first patent in this regard is related to the stabilization, conferred by CDs, of a solid formulation of vitamin D_3 [27,28]. An invention granted in 1985 by Janssen Pharmaceutica N.V. is on the preparation of HPβCD. The patent also describes the use of this derivative in pharmaceutical compositions to overcome the instability or low solubility of a variety of drugs, namely, non-steroid anti-rheumatic agents, steroids, benzodiazepines, imidazoles, and others. HPβCD is the most important CD-based solubilizer used on any type of administration, including the parenteral route, so far, which explains why this patent accounts for a significant number of citations (79 citations) and is the most cited patent concerning stability from our dataset [44]. Strikingly, it was few months later when the similar patent comprising pharmaceutical formulations using the alkylated CD-derivatives, discussed in Section 3.2.1, was filed [41]. The use of CDs as stabilizers to make a product last longer or to optimize the conditions of manufacturing, packing, and storage are examples of other CD applications [45].

When designing a formulation employing CDs as stabilizers, it must be considered that the formation of an IC can make some drugs more stable but some others more labile. Furthermore, it has been observed that drugs that are stabilized in aqueous solution by a CD can be destabilized by the same CD in a solid dosage form [10,46,47]. Therefore, the use of CDs to improve the stability of a given drug or formulation must be thoroughly studied and the formulation carefully designed.

3.2.3. Taste-masking

Many active pharmaceutical ingredients have undesirable taste and/or odor, which can lead to low patient compliance, thereby compromising the treatment efficiency, especially for geriatric and pediatric populations [48]. As the oral administration is the most accepted route, masking the unpleasant taste of drugs to an acceptable degree of palatability is important during formulation. Masking techniques can be integrated into three levels: 1) formulation level, through sweeteners and flavors; 2) particle level, by creating a physical barrier between the bitter component and the taste receptors; and 3) molecular level, through the complexation of the drug with CDs or ion-exchange resins [48,49].

In general, the global number of patents concerning taste-masking is considerably lower in comparison to solubility and stability applications and has slowly gained interest over time (Fig. 5).

The most cited patent (151 citations) describes a formulation of a nicotine lozenge for smoking cessation, to release nicotine in the buccal mucosa for reaching a maximum systemic level faster than the nicotine transdermal patch. Besides other components, the formulation involves an IC between βCD and an essential oil flavoring [50]. Another patent with a significant number of citations (35) is a technological innovation reporting βCD/ibuprofen complexes with an enhanced taste profile and bioavailability in comparison to sodium ibuprofen [51].

A patent published in 2002, entitled “Oral pharmaceutical compositions containing cyclodextrins as taste masking agent”, claims that CDs can mask the unpleasant taste of drugs without the preparation of an IC between the CD and the drug, which was thought to be essential. Besides the scientific contribution to the field, this was considered a breakthrough in terms of manufacturing processes, regarding simplicity and costs [52]. Later, in 2005 it was argued that the preparation of the CD/drug IC might not be necessary if the drug dose is small and the CD is in excess. If so, the CD will dissolve quickly in the saliva, giving rise to a saturated CD solution in which the bitter component instantly forms a complex with the CD [53]. CDs have also been useful as a taste-masking agent for chewable, fast-disintegrating, buccal, and sublingual tablets [54].

Taste-masking is also needed in nasal and pulmonary administration routes. Several potential drugs for inhalation therapy have an unpleasant taste, which, again, may result in incomplete therapy due to low patient compliance. For these formulations, bitter molecule encapsulation is the best option because other types of methodologies, such as coating, are not feasible. Some examples in this regard are reviewed in Section 3.3.4.

The use of CDs for taste-masking is still emerging and represents a great area of opportunity. Besides the improvement of organoleptic properties, CDs can simultaneously modify solubility and impart stability to the formulation, making them exceptional multifunctional excipients.

3.3. Administration routes

According to the previous sections, it is clear that CDs can be present in a variety of dosage forms intended for practically all administration routes. Hence, we were interested on knowing how the presence of CDs has evolved in formulations for different administration routes over time (Fig. 6).

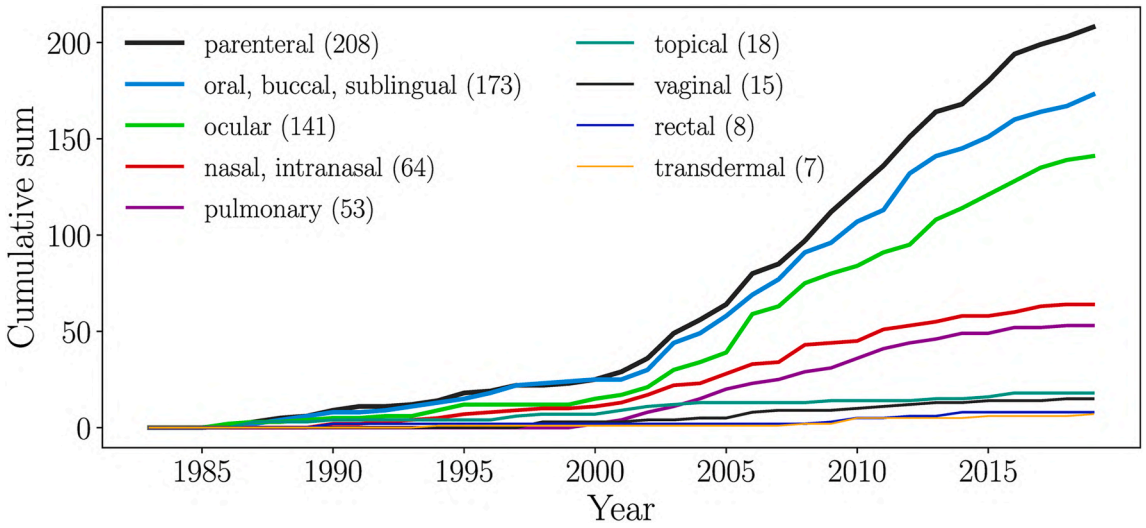

Fig. 6. Technological development of CDs in a variety of administration routes.

3.3.1. *Parenteral administration*

Certainly, the major strength of CDs is their ability to increase the apparent solubility of a drug through the formation of an IC. Therefore, their most attractive and robust application has been for preparing aqueous for parenteral administrations, clearly confirmed by the 208 patents observed in Fig. 6.

Although only αCD, HPβCD, and SBEβCD are approved for parenteral administration, their success is remarkable as there are numerous commercially available products for this aim. Some examples for IV administration are αCD/alprostadil (Caverject ™), HPβCD/itraconazole (Sporanox ™), SBEβCD/voriconazole (Vfend ™), and HPγCD/Tc-99 teoboroxime (Cardiotec ™). In terms of IM formulations are SBEβCD/aripiprazole (Abilify ™) and SBEβCD/ziprasidone mesylate (Geodon ™) [26,55–59]. As we have mentioned, the development of formulations for parenteral administration remains very active. Some examples of recent patents include: the parenteral formulation of clopidogrel through its complexation with sulfoalkyl ether CDs, patented by CyDex Inc. in 2019 [60]; the development of CD-based formulations for lansoprazole [61]; and sartans drug family [62].

This trend is expected to continue growing in the future as the formulation of new drugs, reformulations, and drug repurposing still strongly consider CDs technologies as an excellent tool for formulating low-water-soluble drugs, [42,63,64]. This scenario is possible only if research and development of pharmaceutical technology, as well as studies on pharmacokinetic and toxicological profiles of the ICs, are continuously conducted, as they have been so far. Because not all CDs or CD derivatives can be parenterally administered, the design and synthesis of new CD derivatives are highly desirable. Besides being biocompatible, a derivative must be water-soluble and present good complexation abilities. Furthermore, its production process should be robust and scalable to produce volumes that can fulfill the pharmaceutical industry's demands.

3.3.2. *Oral administration*

Oral route is the most accepted way to administer medications and, in turn, solid dosage forms, are the most common formulations intended for this aim. Despite its popularity, the oral route is challenging or sometimes not possible for several drugs, due to their low solubility/permeability, instability, degradation in the GI tract, extensive metabolism, and unpleasant organoleptic properties. CDs have demonstrated great potential to overcome these limitations directly or indirectly and even to modify a drug release profile.

Hydrophilic CDs can improve the oral absorption of the BCS Class II drugs (low solubility, high permeability), as CDs augment their solubility without altering their permeability to biological membranes. In the case of BCS Class IV drugs (low solubility, low permeability), CDs may increase their solubility and improve their availability at the mucosal surface to enhance their absorption. Lipophilic CDs such as MβCD are ideal to increase permeability through membranes, although their use for oral delivery is hampered by their toxicity. CDs can also be beneficial for BCS Class I drugs (high permeability, high solubility), not for modifying their bioavailability but for reducing gastrointestinal irritation, as in the case of some NSAIDs. The CDs effect on Class III drugs is negligible.

Although oral administration addresses liquid and solid forms, the success of CDs is reflected majorly in the latter, with several oral tablets already marketed: αCD/cefotiam-hexetil HCl (Pansporin T ™), βCD/omeprazole (Omebeta ™), βCD/piroxicam (Brexin ™), and βCD/tiaprofenic acid (Surgamyl ™). Although less common than tablets, capsules are also present included in the list of marketed CDs oral formulations, like Ulgut ™, a product based on a βCD/benexate IC [2,4,65]. In this context, our analysis will be focused on solid forms including conventional, sublingual and buccal tablets, and from here, with oral administration, we will only refer to these pharmaceutical forms.

Patents for CD-based oral formulations account for 173 files which makes them second in importance after parenteral formulations. The increasing number of patents (Fig. 6), especially from the early 2000, clearly indicates that they have been, and still are, a very attractive resource for oral pharmaceutical technologies. An example of a patent published in 1999 discloses the use of CDs in oral tablets for preventing sodium pravastatin degradation and isomerization by humidity or temperature before oral administration [66]. An example of a patent issued in 2019 discloses a CD-based oral tablet to enhance the bioavailability of meloxicam [67].

For a successful development of CD-based conventional tablets, some aspects must be carefully considered, for instance, whether CDs are used as ICs or as a physical mixture; their interaction with other components of the formulation; and the type of drug, its dose, and the size of the dosage form. In addition, the technologies to process them play a fundamental role in determining an outstanding performance [68]. Also, care must be taken in the amount of CD used in the formulation, as an excess of CDs could hinder the absorption of the drug through the GI tract [68,69]. Nonetheless, the fascinating recent research devoted to oral CD-based pharmaceutical technologies will certainly maintain the increasing trend observed herein [70–75].

Buccal formulations aim to deliver drugs through the buccal mucosa, which possesses a large surface area for absorption, to achieve a local or systemic effect. On the other hand, sublingual tablets, in which the drug

is placed beneath the tongue, seek a more rapid systemic absorption, in comparison to the conventional oral route, and avoids intestinal and hepatic first-pass metabolism of the drug. In this regard, CDs can enhance drug dissolution in the saliva, improve the organoleptic properties, or work at the absorption and bioavailability levels [76]. In fact, there are some buccal and sublingual medications containing CDs on the market: βCD/PGE2 (Prostarmon E ™), βCD/nitroglycerin (Nitropen™), and βCD/nicotine (Nicorette™), also formulated as a chewing gum (Nicogum™) [65,69].

Compelling research shows the promising potential of CDs for developing sublingual dosage forms [77–79]. Therefore, an important role of innovations in this matter is expected. The following are two examples of patents for sublingual formulations: 1) the use of CDs to provide faster dissolution times for reaching high levels of apomorphine in plasma to treat female sexual dysfunction [80]; 2) the use of CDs for the transformation of therapeutic oils into water-soluble dry powders for sublingual administration [81].

The combination with polymers has enabled the development of mucoadhesive buccal films, which appear to be emerging as a trending research area [82,83]. In this sense, very innovative approaches are being investigated and patented, like a CD-based hydrogel, which disintegrates at the human body temperature, to increase the bioavailability of aurantiin, with a good taste and suitable for children or particular patients [84].

CDs are an excellent resource for developing oral formulations and patents in this matter are expected to continue increasing in the next years. The progress in mucoadhesive materials is paving the way to design buccal mucoadhesive devices to provide convenient therapies to pediatric and geriatric patients, thus generating a very attractive research opportunity area.

3.3.3. Ocular administration

Ophthalmic preparations must allow the drug to permeate the structure of the corneal epithelium without irritating the ocular surface; otherwise, it will be rapidly cleared from the precorneal area a few minutes after administration, with an incomplete absorption. Suspensions, drops, gels, ointments, and solid inserts have been used to deliver drugs to the eye. Aqueous eye drops are the most common because they are the ones with the least adverse effects, especially irritation and blurred vision, which may influence the medication adherence. In eye drop formulations, the drug must be dissolved in a small aqueous volume, but at the same time, must preserve a moderately lipophilic character to penetrate the corneal epithelium and stroma into the aqueous humor.

CDs offer numerous advantages that can facilitate the development of convenient ocular formulations [69,85–87]. CDs enhance drug solubility, without interfering in its ability to permeate the lipophilic barriers, stabilize the formulation, and decrease irritation to the ocular surface. CDs do not cross the corneal epithelium; however, if they are complexing a lipophilic drug, they can keep it in the aqueous solution and afford a higher availability at the surface of the corneal barrier. There are currently two marketed ophthalmic drops employing CDs: the antibiotic Clorocil ™ containing MβCD/chloramphenicol, and the anti-inflammatory Voltaren Ophthalmic ™ comprising the HPγCD/diclofenac sodium IC [2,5]. Based on the number of patents, the use of CDs in ocular medications is one of the most important, just below parenteral and oral solid forms. Moreover, the interest on CDs has increased from the year 2000 and is still appealing, as evidenced by the rapid increase in the number of patents in the last 20 years. An example of a recent patent is the nano- and micro-suspensions containing αCD and γCD, where αCD forms an IC with cyclosporin A, while γCD promotes the formation of CD/cyclosporin A ICs aggregates. The formulation is intended to treat inflammatory ocular surface disorders and to enhance tear formation [88]. As we have discussed, the research on bioadhesive materials is driving the development of innovative technologies. Proof of this is a patented composition called nanoglue, comprising CDs, one or more bioadhesive polymers, one or more dendrimers, and (optionally) one or more therapeutic, prophylactic, or diagnostic agents. After external stimuli, like UV irradiation, the nanoglue forms a hydrogel at the target tissue that seals corneal wounds [89].

Recent research on ocular formulations containing CDs include: sustained-delivery eye drops [90,91]; in situ gelling systems [92,93]; mucoadhesive hydrogels [94,95]; CD/drug-loaded contact lenses [96,97]; and micro and nanosystems [86,98,99]. Also, CD-based formulations have shown potential to treat eye posterior segment diseases, such as diabetic retinopathy and age-related macular degeneration, which are commonly treated by intravitreal drug injections [100]. Certainly, the outcomes of such compelling investigations will be reflected in a higher patenting growth in the following years.

3.3.4. Nasal, intranasal, and pulmonary administration

The obvious and best way to treat nose and paranasal sinuses ailments is through nasal delivery medications. For a successful nasal delivery, drugs must dissolve in a very small volume of water, as the volume of the aqueous diffusion layer is small. Permeation enhancers and mucoadhesive components are highly desirable for nasal and intranasal formulations as they will promote the delivery of drugs before their clearance [101].

The promising role of CDs in formulations for nasal administration is associated to the modification of the absorption rate of the drugs at the site of delivery due to an increase of drug solubility and changes in nasal mucosa permeability [102,103]. For example, a patent disclosing a dry powder formulation of a group of indazoles, designed to inhibit the Janus dependent kinase for blocking the interplay of multiple inflammatory cells, in which CDs act as both solubilizers and bioadhesive components for the nasal mucosa [104]. Suitable formulations of corticosteroids are needed for rhinitis, sinusitis, asthma, and nasal polyps, among others. Several innovations have responded to this necessity through the implementation of CDs (especially sulfoalkyl ether derivatives) to enhance drugs solubility and permeability in nasal medications, while improving their organoleptic properties [105,106].

Intranasal delivery has gained great interest due to their potential to deliver drugs systemically, while avoiding phase I and II metabolism. Hence, is an attractive route for administering peptide drugs and hormones. Moreover, this route has been explored for brain delivery [107]. Recently, a new product called Baqsimi ™, used for the treatment of diabetes mellitus, has been approved by the FDA and EMA. It contains βCD as an inactive ingredient that improves the stability, solubility, and bioavailability of glucagon [108–110]. Another commercial product administrated nasally is RMβCD/17β-estradiol (Aerodiol ®) [2]. Thus, intranasal technologies using CDs have arisen over time. One example is a powder formulation containing glucagon or a glucagon analog for nasal administration, useful in the treatment of hypoglycemia, in which βCD performs as a filler and as a mucoadhesive agent to the nasal mucosal surface to promote the absorption of the active agent [111]. Another interesting patent is the intranasal formulation for the parathyroid hormone, in which βCD enables an aqueous formulation while preventing drug aggregation [112].

Patents of nasal and intranasal preparations employing CDs have evolved slowly over time. Although they have gained strength in the last 20 years, they can still be considered emerging. However, recent investigations [113–115] will generate new opportunities for innovations and a slow but steady increase in patents may be coming in the next years.

Although the pulmonary route has been mainly proposed for localized treatments, the large lung surface area and abundant blood supply make this route an alternative for systemic drug delivery. The efficacy of this route relies on the adequate aerosolization properties of the dosage form, as well as the drug permeability through the lung, its solubility in small aqueous volumes, and its suitable organoleptic properties. Both solid and dissolved CD/drug ICs have been formulated as dry powders and nebulizers, improving the aerosolization properties of formulations

and enhancing the drug dissolution in the lung fluids [116] and recent research continues showing the promising potential of using CDs for pulmonary medications [117–119].

Based on technological information, we found, for example, a preparation of a group of fluoroquinolones suitable for aerosolization for the treatment of pulmonary bacterial infections. In this formulation, CDs are complexing the therapeutic molecules to improve their solubility and stability [120]. Another example includes the CD complexation with compounds to treat inflammatory and fibrotic disorders at the protein kinase level, in which the CD is used as a solubilizer [121].

Innovations on pulmonary formulations containing CDs have progressed slower than nasal formulations (Fig. 6). Nonetheless, is notable that the interest in this regard has strengthened throughout the last decade, which will probably increase the number of patents in the short term.

3.3.5. Other administration routes

The number of patents regarding topical, transdermal, vaginal, and rectal routes is significantly lower than the number of patents for the administration routes already discussed and has remained unchanged over time (Fig. 6). The following section briefly discusses the roles of CDs for each of them.

3.3.5.1. Topical and transdermal. Topical delivery refers to medications that minimally penetrate the skin layer, creating a local effect. A meticulous selection of the vehicle is necessary for the CDs to display suitable performance. For example, hydrophilic CDs can increase the in vitro release rate of corticosteroids from water-based ointments but delay the drug release in oily-based vehicles. Moreover, some components of the ointments can displace the drug from the CD/drug IC [122]. These demanding requirements, however, have achieved fruitful results with Glymesason ™, an ointment containing dexamethasone and βCD. Our study revealed that only 18 patents disclose dermal formulations employing CDs. Some examples of them include a bio-adhesive film--forming pharmaceutical composition created for application directly to the skin or to a substrate to treat skin disorders, in which CDs perform principally as solubility enhancers [123]. Another invention uses the SBEβCD/silymarin IC for a composition useful in reducing facial redness in rosacea-prone skin, preventing skin aging, inhibiting oxidative stress in epidermal and dermal cells, and increasing collagen production. CD is used to enhance the solubility and availability of the active compound in the topical formulation [124]. Although the patenting behavior has remained without significant changes over time, the outcomes of recent research could change this trend as investigations range from ointments [125] to wearable biomimetic films for wound healing [126], including supramolecular gels [127] and nanosystems [128].

The transdermal route requires a formulation capable of penetrating the skin to exert its effect in deeper tissues or in systemic circulation. Transdermal formulations require penetration enhancers to enable the drug to cross the stratum corneum and reach systemic circulation. In this respect, CDs increase drug availability at the barriers surface, differently to penetration enhancers, which induce physicochemical changes within the barrier. However, the combination of both CDs and penetration enhancers results in additive effects. Thus, CDs can support the adequate performance of a transdermal preparation [129]. Only 7 patents were retrieved from the dataset, however, this behavior may change in the future due to the increasing interest in delivering drugs to systemic circulation with all the advantages that the transdermal route offers. Proof of this is the fascinating research for transdermal delivery using CDs: CD-based hydrogels [130]; CD/drug ICs loaded into microneedles [131] or patches [132]; and ICs with ionic CDs for iontophoretic transdermal delivery [133].

3.3.5.2. Vaginal and rectal administration. In vaginal formulations, drug absorption, distribution, and residence time may vary. The most common vaginal formulations are semisolid and fast-dissolving solid dosage forms, notwithstanding, bioadhesive systems have become highly desirable for local or systemic vaginal effects. Those drugs administered by this route include hormones, antibiotics, and antimycotics. However, other diseases, like those related to human papillomavirus, herpes simplex virus, and HIV, along with the unfortunate increase in the prevalence of cervix carcinoma, have recently driven the interest to develop vaginal formulations [134]. Several compelling investigations have shown that CDs are useful, as solubilizers, in the development of these type of formulations such as mucoadhesive gels, creams, and films for antifungal and antiviral activities [135–137]; gels for contraception purpose [138]; vaginal discs for the controlled delivery of antiretroviral drugs [139]; and mucoadhesive nanosystems for cervical cancer treatment [140]. Also studied are the mucoadhesive properties of CD derivatives in which CDs *perse* comprise the delivery systems [141].

From the 15 patents retrieved from the dataset we selected a recent invention for systemic effect: a vaginal formulation, in which CDs are used for solubility and stability enhancement containing MAGL inhibitors to treat systemic MAGL-mediated disorders such as pain, inflammatory disorders, traumatic brain injury, depression, anxiety, and Alzheimer's disease, among others [142].

The patenting pattern has remained without change, nevertheless, it is highly desirable to change the trend for the coming years. Likely the advances in the development of functional biomaterials will make an outstanding contribution to these technologies.

Rectal administration is an advantageous alternative to the oral route for children and for patients with difficulty for swallowing or those with intense nausea and vomiting. The constraints associated with this route are the limited surface area for drug absorption and the small volume of the rectal fluids in which the drug must be dissolved [143]. CDs and their derivatives have also been employed to optimize drug rectal delivery. CDs can improve drug stability in the suppository base and decrease the rectal irritation caused by drugs. Also, CDs can modify the release rate of drugs from the vehicles and promote their permeation through the rectal epithelium, with the subsequent optimization of the drug pharmacokinetic profile. If the formulation comprises a CD/lipophilic drug IC in an oleaginous vehicle, the IC will be well dispersed in it. Therefore, the drug dissolution at the interface of the oily base and the rectal fluids will improve. At the same time, the reverse diffusion of the drug into the vehicle is hindered [69,122,144].

As with ointments, the success of a formulation depends on the vehicle (aqueous or oleaginous), the physicochemical features of the CD in use, the drug, the CD/drug IC, and their interactions with the other components of the preparation. Despite these challenges, there are some rectal suppositories currently marketed: βCD/piroxicam (Cicladol ™ and Brexin ™), βCD/meloxicam (Mobitil ™), and HPβCD/cisapride (Prepulsid ™) [5]. According to our search, the number of patents concerning suppositories is relatively low (Fig. 6), nonetheless herein we discuss two recent examples of interesting technologies: 1) a novel rectal composition for the treatment of pediatric cancer in which CDs works as solubilizer [145]; 2) a rectal composition containing rifaximin, hydrocortisone, and CD, in which the latter is employed as a mucosal permeation enhancer improving the local retention and bioavailability of the drug for the treatment of anal diseases like anal fissure, ulcers, or hemorrhoidal diseases [146].

The number of academic publications is also low. A general search in the Scopus database for the last ten years (search criteria: cyclodextrin rectal delivery) revealed that only a few articles per year were published—or even no articles, as in the case of 2015. Fortunately, after that, compelling research has been done. For example, the study of HPβCD/budesonide ICs in the form of thermoreversible gels for ulcerative colitis [147]; or HPβCD/5-fluorouracil IC encapsulated in a thermoreversible gelling film for colorectal cancer [148]. Despite its low popularity, this administration route may still be hiding its potential to deliver drugs locally or systemically, and the use of mucoadhesive and

thermoresponsive materials whose development could be supported by CDs may provide interesting progress to the field.

3.4. CD patents: Where and who?

We aimed to identify those regions with high patenting activity around the world, as these may correspond to the regions with high market potential. This analysis was carried out using the dataset of 1998 patents. Fig. 7a shows the top ten countries that hold most of the CD pharmaceutical patents. Since 2011, China has become the nation with the highest patent filing activity in practically all kinds of technological fields [149]. CDs pharmaceutical innovations are no exception. According to our analysis, 1356 patents were filed in this country, just followed by the geographical region represented by WIPO, with 710 records. These numbers position China as the global technological leader in the field of CDs for pharmaceutical applications, as the number of patents registered here is 47% higher than that registered in the WIPO countries. Japan and the U.S. also stand out with 688 and 656 patents, correspondingly.

Besides the regions with the highest market potential, we aimed to provide information about the assignees—this is, the entities that have the right to exploit the patent. In accordance with what we have mentioned, Fig. 7b highlights that 7 out of the top 20 assignees are located in China, including both industry (five pharma companies) and academic institutions (two universities). Japan and Brazil (positions 3 and 8, respectively, in the top-10 countries) also appear in the top-20 assignees with patenting activity in both universities and pharma companies. Certainly, the holistic technological knowledge coming from industry and academia is highly relevant for the technological development of a region.

China, Japan, the U.S.A., and Brazil, each belonging to the top-10 ranking regions, are also present among the top-20 ranking of assignees. U.S.A has only 2 assignees in the top-20 list, Pfizer Inc. and CyDex Pharmaceutical Inc. Both companies have shown to have an active CDs patent portfolio (some of their patents have been discussed throughout this work). In particular, CyDex Pharmaceutical Inc. has played an important role in the development of CDs technologies, and owns one of the most influential patents in the area: Patent No.US 6046177 [33], which today is still a breakthrough in the evolution of CDs innovations in the pharmaceutical field.

There are several channels for spreading knowledge and technology across boundaries. Among them, FDI has been widely studied. FDI refers to an investment made by a firm or individual in one country into a business located in another country. This implies that patents that protect the same invention can be filed in different locations from where they were created, thereby generating different economic phenomena between developed and undeveloped countries [150,151]. FDI could be the reason why some countries in the top-10 ranking regions do not have an assignee backing up their position, as could be the case for Australia, the Korean Republic, Mexico, and Spain.

For the WIPO and the EPO regions, the dynamic is different because they encompass different cooperation treatments. On the one hand, the Patent Cooperation Treaty enables patents to be registered in the 193 countries that are part of the WIPO through only one procedure. On the other hand, EPO grants European patents in 44 countries and also facilitates the registration of a patent in different EPO countries in a single grant procedure. This explains why these two entities appear in the second and fifth positions of the top-20 ranking for geographical regions. Hence, it is expected that WIPO and EPO will remain at the top positions in terms of regions in which a certain technology is protected.

4. Conclusions

We analyzed the evolution of CD-based pharmaceutical technologies, using patent data as the technical source, through a text-mining approach based on the patents semantic content. In our dataset, the first-filed patent dated from the early '80s. During that decade, slow growth in CD patents was observed. However, the early 2000s saw very fast growth in the use of CDs for pharmaceutical applications.

The abilities of CDs to enhance the solubility and stability of drugs have determined their technological progress. Nonetheless, their abilities to modify organoleptic properties are emerging and represent a great area of opportunity. CDs are used in formulations for practically any route of administration. Although patents are majorly associated with the parenteral aqueous solutions, oral and ocular formulations are significantly growing, while nasal and pulmonary formulations seem to be promising. Of great importance was to revise patents associated with formulations for topical, transdermal, vaginal, and rectal routes. The interest on patenting these technologies seems to be neglected, however they may be hiding a great potential and represent opportunity research areas. Certainly, the better understanding of CDs, along with the progress in materials science, supramolecular chemistry, and nanotechnology, will drive a change in their patenting trend. Bottom line, the interest in CDs is still increasing and this trend is expected to continue in the coming years.

Patent monitoring allows the identification of relevant technologies and trends to prioritize research, development, and investment. Thus, knowledge mined from patents can be applied to foster technological innovations based on CDs or any other platform.

a)

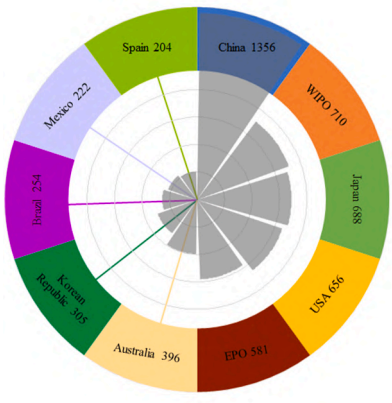

b)

Assignee	N° Patents
1. Tianjin Tianshi Pharmaceutical Co.	26
2. CyDex Pharmaceuticals Inc.	25
3. Nanjing Normal University	21
4. Ono Pharmaceutical Co.	20
5. Nanjing University	20
6. Novartis AG	17
7. Taisho Pharmaceutical Co.	17
8. Pfizer Inc.	16
9. Federal University of Sergipe	15
10. CSPC Pharmaceutical Group Limited	14
11. Hainan Weikang Pharmaceutical Qianshan Co	13
12. Jiangsu Aosaikang Pharmaceutical Co	13
13. Bayer Schering Pharma	12
14. French National Centre for Scientific Research	12
15.Tianjin Hankang Pharmaceutical Biotechnology Co	12
16. Kumamoto University	12
17.Minas Gerais Federal University	11
18. Kunming Pharmaceutical Corporation	10
19. Chengdu Qiankun Veterinary Pharmaceuticals Co	10
20. The Institute of Chemical Sciences of Kazakhstan	10

Fig. 7. a) Top-10 ranking countries for CDs patents on pharmaceutical applications. b) Top-20 ranking CDs patents assignees (colors correspond to the country the assignees belong). (For interpretation of the references to color in this figure legend, the reader is referred to the Web version of this article.)

Author statement

Juliana Rincón-López: Investigation, Methodology, Visualization, Writing - original draft, Yara Cecilia Almanza-Arjona: Conceptualization, Visualization, Writing - review & editing, Alejandro P. Riascos: Conceptualization, Methodology, Software, Visualization, Data curation, Writing - original draft, Writing - review & editing, Yareli Rojas-Aguirre: Conceptualization, Investigation, Writing - original draft, Writing - review & editing, Visualization, Supervision, Project administration, Funding acquisition,

Declaration of competing interest

The authors declare that they have no known competing financial interests or personal relationships that could have appeared to influence the work reported in this paper.

Acknowledgements

Y. R-A. acknowledges the financial support to Materials Research Institute, UNAM (Project 1306) and PAPIIT-UNAM IA200919. J. R-L. thanks to CONACyT for the MSc. scholarship CVU-1032640.

References

[1] H. Dodziuk, Molecules with holes – cyclodextrins, in: Cyclodextrins and Their Complexes, Wiley-VCH Verlag GmbH & Co. KGaA, 2006, pp. 1–30, https://doi.org/10.1002/3527608982.ch1.
[2] S.S. Jambhekar, P. Breen, Cyclodextrins in pharmaceutical formulations I: structure and physicochemical properties, formation of complexes, and types of complex, Drug Discov. Today 21 (2016) 356–362, https://doi.org/10.1016/J.DRUDIS.2015.11.017.
[3] M.E. Davis, M.E. Brewster, Cyclodextrin-based pharmaceutics: past, present and future, Nat. Rev. Drug Discov. 3 (2004) 1023–1035, https://doi.org/10.1038/nrd1576.
[4] J. Szejtli, Past, present, and future of cyclodextrin research, Pure Appl. Chem. 76 (2004) 1825–1845, https://doi.org/10.1351/pac200476101825.
[5] É. Fenyvesi, Approved pharmaceutical products containing cyclodextrins. https://cyclolab.hu/userfiles/cdn_2013_feb.pdf, 2013. (Accessed 11 May 2020).
[6] M.E. Brewster, T. Loftsson, Cyclodextrins as pharmaceutical solubilizers, Adv. Drug Deliv. Rev. 59 (2007) 645–666, https://doi.org/10.1016/j.addr.2007.05.012.
[7] T. Loftsson, Drug solubilization by complexation, Int. J. Pharm. 531 (2017) 276–280, https://doi.org/10.1016/j.ijpharm.2017.08.087.
[8] T. Loftsson, D. Duchêne, Cyclodextrins and their pharmaceutical applications, Int. J. Pharm. 329 (2007) 1–11, https://doi.org/10.1016/j.ijpharm.2006.10.044.
[9] T. Loftsson, M.E. Brewster, Pharmaceutical applications of cyclodextrins. 1, Drug Solubilization and Stabilization 85 (1996) 1017–1025, https://doi.org/10.1021/js950534b.
[10] K. Uekama, F. Hirayama, H. Arima, Pharmaceutical applications of cyclodextrins and their derivatives, Cyclodextrins and their Complexes (2006) 381–422, https://doi.org/10.1002/3527608982.ch14.
[11] A. Bergeaud, Y. Potiron, J. Raimbault, Classifying patents based on their semantic content, PloS One 12 (2017) 1–22, https://doi.org/10.1371/journal.pone.0176310.
[12] B. Yoon, Y. Park, A text-mining-based patent network: analytical tool for high-technology trend, J. High Technol. Manag. Res. 15 (2004) 37–50, https://doi.org/10.1016/j.hitech.2003.09.003.
[13] C. Liu, Q. Zhou, Y. Li, L.V. Garner, S.P. Watkins, L.J. Carter, J. Smoot, A.C. Gregg, A.D. Daniels, S. Jervey, D. Albaiu, Research and development on therapeutic agents and vaccines for COVID-19 and related human coronavirus diseases, ACS Cent. Sci. 6 (2020) 315–331, https://doi.org/10.1021/acscentsci.0c00272.
[14] J. Szejtli, Introduction and general overview of cyclodextrin chemistry, Chem. Rev. 98 (1998) 1743–1753, https://doi.org/10.1021/cr970022c.
[15] A.C. Deorsola, C.G. Mothé, L.G. de Oliviera, A.B. Deorsola, Technological monitoring of cyclodextrin - world panorama, World Patent Inf. 39 (2014) 41–49, https://doi.org/10.1016/j.wpi.2014.06.004.
[16] T. Coimbra Diniz, T.C. Costa Pinto, P. dos Passos Menezes, J. Cabral Silva, R.B. de Andrade Teles, R.C. Cavalcanti Ximenes, A. Gibara Guimarães, M. Russo Serafini, A. Antunes de Souza Araújo, L.J. Quintans Júnior, J.R. Guedes da Silva Almeida, Cyclodextrins improving the physicochemical and pharmacological properties of antidepressant drugs: a patent review, Expert Opin. Ther. Pat 28 (2018) 81–92, https://doi.org/10.1080/13543776.2017.1384816.
[17] G. de Oliveira Makson, A.G. Guimarães, A. Araújo Adriano, S. Quintans Jullyana, M.R. Santos, L.J. Quintans-Júnior, Cyclodextrins: improving the therapeutic response of analgesic drugs: a patent review, Expert Opin. Ther. Pat. 25 (2015) 897–907, https://doi.org/10.1517/13543776.2015.1045412.
[18] T.F. Kellici, G. Liapakis, A.G. Tzakos, T. Mavromoustakos, Pharmaceutical compositions for antihypertensive treatments: a patent review, Expert Opin. Ther. Pat. 25 (2015) 1305–1317, https://doi.org/10.1517/13543776.2015.1086337.
[19] WIPO, IPC publication. https://www.wipo.int/classifications/ipc/ipcpub/?notion=scheme&version=20200101&symbol=A61&menulang=en&lang=en&viewmode=f&fipcpc=no&showdeleted=yes&indexes=no&headings=yes&notes=yes&direction=o2n&initial=A&cwid=none&tree=no&searchmode=smart, 2020. (Accessed 25 May 2020).
[20] WIPO, WIPO guide to using patent information. https://www.wipo.int/edocs/pubdocs/en/wipo_pub_l434_3.pdf, 2015. (Accessed 25 May 2020).
[21] W. McKinney, Data structures for statistical computing in Python, Proc. 9th Python Sci. Conf. 1697900 (2010) 51–56, in: http://conference.scipy.org/proceedings/scipy2010/mckinney.html.
[22] Search Technology Inc, The VantagePoint Academic (trial version). https://www.thevantagepoint.com/, 2020. (Accessed 25 May 2020).
[23] K. Freudenberg, F. Cramer, H. Plieninger, Verfahren zur Herstellung von Einschlusverbindungen physiologisch wirksamer organischer Verbindun- gen (A method for the preparation of inclusion compounds of physiologically active organic compounds), Patent DE 895769C, 1953.
[24] G. Crini, Review: a history of cyclodextrins, Chem. Rev. 114 (2014) 10940–10975, https://doi.org/10.1021/cr500081p.
[25] M. Hayashi, A. Ishihara, Clathrate compounds of prostaglandins or their analogues with cyclodextrin, Patent US 3816393 (1974).
[26] T. Loftsson, M.E. Brewster, Pharmaceutical applications of cyclodextrins: basic science and product development, J. Pharm. Pharmacol. 62 (2010) 1607–1621, https://doi.org/10.1111/j.2042-7158.2010.01030.x.
[27] Y. Makino, Y. Suzuki, Composition for solid pharmaceutical preparations of active vitamins D3 and process for preparation thereof, Patent US 4729895 (1988).
[28] Y. Makino, Y. Suzuki, Composition for Solid Pharmaceutical Preparations of Active Vitamins D3, Patent EP 0116755B1, 1983.
[29] A. Bavley, W.A. Lazier, A.E. Timreck, Fat-soluble vitamin-containing products and process thereof, Patent US 2691619 (1954).
[30] J. Solms, Inclusion resins of cyclodextrin and methods of use, Patent US 3420788 (1969).
[31] H.P. Jones, Inclusion complex of β-cyclodextrin and digoxin, Patent US 4555504 (1982).
[32] V.J. Stella, R. Rajewski, Derivatives of cyclodextrins exhibiting enhanced aqueous solubility and the use thereof, Patent US 5376645 (1994).
[33] V.J. Stella, R.A. Rajewski, V.M. Rao, J.W. Mcginity, G.L. Mosher, Sulfoalkyl ether cyclodextrin based controlled release solid pharmaceutical formulations, Patent US 6046177 (2000).
[34] G. Motta, Process for preparing controlled release pharmaceutical forms and the forms and thus obtained, Patent US 5662935 (1997).
[35] S. Kim, Cyclodextrin liposomes encapsulating pharmacologic compounds and methods for their use, Patent US 5759573 (1998).
[36] G. Elger, S.T. Leslie, S.T.A. Malkowska, R.B. Miller, P.J. Neale, Controlled release pharmaceutical composition, Patent US 4834985 (1989).
[37] S. Simoes, A. Rey-Rico, A. Concheiro, C. Alvarez-Lorenzo, Supramolecular cyclodextrin-based drug nanocarriers, Chem. Commun. (2015) 6275–6289, https://doi.org/10.1039/c4cc10388b.
[38] J.J. Hussey, A.G. Bright, Aqueous Formulation Comprising L-(4-{ [4-(dimethylamino)piperidin-L-Yl] Carbonyl }p Henyl)-3-[4-(4,6-Dimorpholin-4-Yl-L,3,5-Triazin-2-Yl)phenyl]urea, Patent WO 2019/234632A1, 2019.
[39] L. Di, P.V. Fish, T. Mano, Bridging solubility between drug discovery and development, Drug Discov. Today 17 (2012) 486–495, https://doi.org/10.1016/j.drudis.2011.11.007.
[40] J. Szejtli, É. Fenyvesi, B. Zsadon, M. Szilasi, L. Décsei, Water soluble cyclodextrin polymers substituted by ionic groups and process for the preparation thereof, Patent US 4535152 (1983).
[41] J. Pitha, Pharmaceutical Preparations Containing Cyclodextrin Derivatives, Patent US4727064, 1988.
[42] E. de Wit, F. Feldmann, J. Cronin, R. Jordan, A. Okumura, T. Thomas, D. Scott, T. Cihlar, H. Feldmann, Prophylactic and therapeutic remdesivir (GS-5734) treatment in the rhesus macaque model of MERS-CoV infection, Proc. Natl. Acad. Sci. U. S. A 117 (2020) 6771–6776, https://doi.org/10.1073/pnas.1922083117.
[43] EMA, Summary on compassionate use. https://www.ema.europa.eu/en/documents/other/summary-compassionate-use-remdesivir-gilead_en.pdf, 2020. (Accessed 7 May 2020).
[44] W.W. Muller, U. Brauns, Pharmaceutical Compositions Containing Drugs Which Are Instable or Sparingly Soluble in Water and Methods for Their Preparation, Patent WO 85/02767, 1985.
[45] T. Backensfeld, W. Heil, R. Lipp, Composition of Estrogen-Cyclodextrin Complexes, Patent US 7569557B2, 2009.
[46] Y. Hamada, N. Nambu, T. Nagai, Interactions of α- and β-Cyclodextrin with several non-steroidal antiinflammatory drugs in aqueous solution, Chem. Pharm. Bull. (1974) 2091, https://doi.org/10.1248/cpb.23.1205.
[47] A. Popielec, T. Loftsson, Effects of cyclodextrins on the chemical stability of drugs, Int. J. Pharm. 531 (2017) 532–542, https://doi.org/10.1016/j.ijpharm.2017.06.009.
[48] H. Sohi, Y. Sultana, R.K. Khar, Taste masking technologies in oral pharmaceuticals, Recent Developments and Approaches 30 (2004) 429–448, https://doi.org/10.1081/DDC-120037477.
[49] X. Zheng, F. Wu, Y. Hong, L. Shen, X. Lin, Y. Feng, Developments in taste-masking techniques for traditional Chinese medicines, Pharmaceutics 10 (2018) 1–22, https://doi.org/10.3390/pharmaceutics10030157.

[50] G.C. Santus, Improved Nicotine Lozenge and Therapeutic Method for Smoking Cessation, Patent WO 1995003050A2, 1994.
[51] C. Hunter, Y. David, Pharmaceutical Composition, Patent US 5019563, 1991.
[52] F. Stroppolo, F. Ciccarello, R. Milani, L. Bellorini, Oral Pharmaceutical Compositions Containing Cyclodextrins as Taste Masking Agent, Patent WO 2002041920A1, 2002.
[53] J. Szejtli, L. Szente, Elimination of bitter, disgusting tastes of drugs and foods by cyclodextrins. https://doi.org/10.1016/j.ejpb.2005.05.006, 2005, 61, 115-125.
[54] S.K. Chay, A. V Keating, C. James, A.E. Aliev, S. Haider, D.Q.M. Craig, Evaluation of the Taste-Masking Effects of (2- Hydroxypropyl)-B-Cyclodextrin on Ranitidine Hydrochloride; a Combined Biosensor, Spectroscopic and Molecular Modelling Assessment, 2018, pp. 3564–3573, https://doi.org/10.1039/c7ra11015d.
[55] M.E. Brewster, J.W. Simpkins, M.S. Hora, W.C. Stern, N. Bodor, The potential use of cyclodextrins in parenteral formulations, J. Parenter. Sci. Technol. 43 (1989) 231–240.
[56] J. Pitha, A. Gerloczy, A. Olivi, Parenteral hydroxypropyl cyclodextrins: intravenous and intracerebral administration of lipophiles, J. Pharmacol. Sci. 83 (1994) 833–837, https://doi.org/10.1002/jps.2600830615.
[57] T.O. Carpenter, A. Gerloczy, J. Pitha, Safety of parenteral hydroxypropyl β-cyclodextrin, J. Pharmacol. Sci. 84 (1995) 222–225, https://doi.org/10.1002/jps.2600840220.
[58] S.V. Kurkov, T. Loftsson, Cyclodextrins, Int. J. Pharm. 453 (2013) 167–180, https://doi.org/10.1016/j.ijpharm.2012.06.055.
[59] P. Jansook, N. Ogawa, T. Loftsson, Cyclodextrins: structure, physicochemical properties and pharmaceutical applications, Int. J. Pharm. 535 (2018) 272–284, https://doi.org/10.1016/j.ijpharm.2017.11.018.
[60] G.L. Mosher, R.L. Wedel, K.T. Johnson, S.G. Machatha, J.A. Cowee, D.J. Cushing, Formulations Containing Clopidogrel and Sulfoalkyl Ether Cyclodextrin and Methods of Use, Patent US 10512697B2, 2019.
[61] P. Zhou, Y. Zhang, Q. Wu, Lansoprazole Freeze-Dried Preparation for Injection and Preparation Method Thereof, Patent CN 110538155A, 2019.
[62] J. Zhang, L. Wu, Y. He, C. Wang, G. Zhang, T. Guo, W. Zhang, L. Zhang, A Kind of Cyclodextrin-Metal Organic Framework Composition Improving Drug Solubility, Patent CN 110314241-A, 2019.
[63] J.B. Gérard Yaméogo, R. Mazet, D. Wouessidjewe, L. Choisnard, D. Godin-Ribuot, J.L. Putaux, R. Semdé, A. Gèze, Pharmacokinetic study of intravenously administered artemisinin-loaded surface-decorated amphiphilic γ-cyclodextrin nanoparticles, Mater. Sci. Eng. C 106 (2020) 110281, https://doi.org/10.1016/j.msec.2019.110281.
[64] K. Pillai, J. Akhter, D.L. Morris, Super aqueous solubility of albendazole in β-cyclodextrin for parenteral application in cancer therapy, J. Canc. 8 (2017) 913–923, https://doi.org/10.7150/jca.17301.
[65] T. Loftsson, M.E. Brewster, M. Másson, Role of cyclodextrins in improving oral drug delivery, Am. J. Drug Deliv. 2 (2004) 261–275, https://doi.org/10.2165/00137696-200402040-00006.
[66] M.S. Chang, W.S. Lim, S.W. Suh, J.K. Cha, J.M. Lee, T.S. Kang, A Drug Composition Containing Sodium Pravastatin, Patent WO 1999049896A1, 1999.
[67] H. Tabuteau, Pharmaceutical Compositions Comprising Meloxicam, Patent AU 2016218992B2, 2019.
[68] T. Loftsson, M.D. Moya-ortega, C. Alvarez-lorenzo, A. Concheiro, Pharmacokinetics of Cyclodextrins and Drugs after Oral and Parenteral Administration of Drug/cyclodextrin Complexes, 2015, pp. 1–12, https://doi.org/10.1111/jphp.12427.
[69] K. Uekama, F. Hirayama, T. Irie, Cyclodextrin drug carrier systems, Chem. Rev. 98 (1998) 2045–2076, https://doi.org/10.1021/cr970025p.
[70] W.X. De Paula, Â.M.L. Denadai, A.N.G. Braga, V.P. Shastri, S.V.B. Pinheiro, F. Frezard, R.A.S. Santos, R.D. Sinisterra, A long-lasting oral preformulation of the angiotensin II AT1 receptor antagonist losartan, Drug Dev. Ind. Pharm. 44 (2018) 1498–1505, https://doi.org/10.1080/03639045.2018.1467923.
[71] M. Hesler, D.H. Schwarz, S. Dähnhardt-Pfeiffer, S. Wagner, H. von Briesen, G. Wenz, Y. Kohl, Synthesis and in vitro evaluation of cyclodextrin hyaluronic acid conjugates as a new candidate for intestinal drug carrier for steroid hormones, Eur. J. Pharmaceut. Sci. 143 (2020) 1–12, https://doi.org/10.1016/j.ejps.2019.105181.
[72] F.G. Corazza, J.V. Ernesto, F.A.N. Nambu, L.R. de Carvalho, V.R. Leite-Silva, G.H. C. Varca, L.A. Calixto, D.P. Vieira, N. Andréo-Filho, P.S. Lopes, Papain-cyclodextrin complexes as an intestinal permeation enhancer: permeability and in vitro safety evaluation, J. Drug Deliv. Sci. Technol. 55 (2020) 101413, https://doi.org/10.1016/j.jddst.2019.101413.
[73] X. Nie, B. Wang, R. Hu, W. Lu, J. Chen, S. Liu, D. Jin, C. Sun, S. Gao, Y. Guo, W. Fang, H. Hao, Development and evaluation of controlled and simultaneous release of compound Danshen based on a novel colon-specific osmotic pump capsule, AAPS PharmSciTech 21 (2020) 1–12, https://doi.org/10.1208/s12249-019-1603-9.
[74] Z. Chen, T. Wang, Q. Yan, Building a polysaccharide hydrogel capsule delivery system for control release of ibuprofen, J. Biomater. Sci. Polym. Ed. 29 (2018) 309–324, https://doi.org/10.1080/09205063.2017.1415583.
[75] C. Tiefensee Ribeiro, J. Gasparotto, L.L. Petiz, P.O. Brum, D.O. Peixoto, A. Kunzler, H.T. da Rosa Silva, R.C. Bortolin, R.F. Almeida, L.J. Quintans-Junior, A.A. Araújo, J.C.F. Moreira, D.P. Gelain, Oral administration of carvacrol/β-cyclodextrin complex protects against 6-hydroxydopamine-induced dopaminergic denervation, Neurochem. Int. 126 (2019) 27–35, https://doi.org/10.1016/j.neuint.2019.02.021.
[76] J. Pitha, E.J. Anaissie, K. Uekama, γ-Cyclodextrin: testosterone complex suitable for sublingual administration, J. Pharmacol. Sci. 76 (1987) 788–790, https://doi.org/10.1002/jps.2600761007.
[77] V. Londhe, R. Shirsat, Formulation and characterization of fast-dissolving sublingual film of iloperidone using box–behnken design for enhancement of oral bioavailability, AAPS PharmSciTech 19 (2018) 1392–1400, https://doi.org/10.1208/s12249-018-0954-y.
[78] R. Kaartama, E. Turunen, K. Toljamo, H. Kokki, M. Lehtonen, V.P. Ranta, J. Savolainen, K. Järvinen, P. Jarho, The effect of hydroxypropyl-beta-cyclodextrin and sucrose on the sublingual absorption of midazolam in rabbits, Eur. J. Pharm. Biopharm. 81 (2012) 178–183, https://doi.org/10.1016/j.ejpb.2012.01.014.
[79] J.L. Manasco, C. Tang, N.A. Burns, C.D. Saquing, S.A. Khan, Rapidly dissolving poly(vinyl alcohol)/cyclodextrin electrospun nanofibrous membranes, RSC Adv. 4 (2014) 13274–13279, https://doi.org/10.1039/c3ra43836h.
[80] J.P. Heaton, M. Adams, Method and Compositions for the Treatment or Amelioration of Female Sexual Dysfunction, Patent US 6756407B2, 2004.
[81] J. Althaus, S. Goldner, Transformation of Cannabinol and Terpene Oils into Water Soluble Dry Powders Form Sublingual Delivery, Patent WO 2019/140145A1, 2019.
[82] I. d'Angelo, A. Fraix, F. Ungaro, F. Quaglia, A. Miro, Poly(ethylene oxide)/hydroxypropyl-β-cyclodextrin films for oromucosal delivery of hydrophilic drugs, Int. J. Pharm. 531 (2017) 606–613, https://doi.org/10.1016/j.ijpharm.2017.06.029.
[83] E. Kontogiannidou, M. Ferrari, A.D. Deligianni, N. Bouropoulos, D.A. Andreadis, M. Sorrenti, L. Catenacci, K. Nazari, M.S. Arshad, M.W. Chang, Z. Ahmad, D. G. Fatouros, In vitro and ex vivo evaluation of tablets containing piroxicam-cyclodextrin complexes for buccal delivery, Pharmaceutics 11 (2019), https://doi.org/10.3390/pharmaceutics11080398.
[84] Z. Wu, H. Zhang, Thixotropic Hydrogel Drug Matrix Used for Preparing Naringin Thixotropic Hydrogel Preparation and Improving Oral Compliance of Drug, Comprises Tragacanth Gum, Gelatin, Sodium Alginate, Agar, Beta-Cyclodextrin and Water, Patent CN 110025568-A, 2019.
[85] T. Loftsson, T. Järvinen, Cyclodextrins in ophthalmic drug delivery, Adv. Drug Deliv. Rev. 36 (1999) 59–79, https://doi.org/10.1016/S0169-409X(98)00055-6.
[86] P. Jansook, P. Kulsirachote, R. Asasutjarit, T. Loftsson, Development of celecoxib eye drop solution and microsuspension: a comparative investigation of binary and ternary cyclodextrin complexes, Carbohydr. Polym. 225 (2019) 115209, https://doi.org/10.1016/j.carbpol.2019.115209.
[87] T. Loftsson, E. Stefánsson, Cyclodextrins in ocular drug delivery: theoretical basis with dexamethasone as a sample drug, J. Drug Deliv. Sci. Technol. 17 (2007) 3–9, https://doi.org/10.1016/S1773-2247(07)50001-8.
[88] T. Loftsson, Formation of Cyclosporin A/cyclodextrin Nanoparticles, Patent US 2016/0346347A1, 2016.
[89] K. Rangaramanujam, W. Stark, S.P. Kambhampati, U. Soiberman, S. Yiu, A.-E. A. Al-Towerki, Dendrimer-bioadhesive Polymer Hydrogel Nanoglue and Use Thereof, Patent AU 2017217397B2, 2019.
[90] W.C. Huang, F. Cheng, Y.J. Wang, C.C. Chen, T.L. Hu, S.C. Yin, C.P. Liu, N.C. Yu, K.K. Huang, M.N. Lin, A corneal-penetrating eye drop formulation for enhanced therapeutic efficacy of soft corticosteroids against anterior uveitis, J. Drug Deliv. Sci. Technol. 54 (2019) 101341, https://doi.org/10.1016/j.jddst.2019.101341.
[91] J.H. Ahn, H. Do Kim, S.M. Abuzar, J.Y. Lee, S.E. Jin, E.K. Kim, S.J. Hwang, Intracorneal melatonin delivery using 2-hydroxypropyl-β-cyclodextrin ophthalmic solution for granular corneal dystrophy type 2, Int. J. Pharm. 529 (2017) 608–616, https://doi.org/10.1016/j.ijpharm.2017.07.016.
[92] P. Li, S. Wang, H. Chen, S. Zhang, S. Yu, Y. Li, M. Cui, W. Pan, X. Yang, A novel ion-activated in situ gelling ophthalmic delivery system based on κ-carrageenan for acyclovir, Drug Dev. Ind. Pharm. 44 (2018) 829–836, https://doi.org/10.1080/03639045.2017.1414232.
[93] H. Elmotasem, G.E.A. Awad, A stepwise optimization strategy to formulate in situ gelling formulations comprising fluconazole-hydroxypropyl-beta-cyclodextrin complex loaded niosomal vesicles and Eudragit nanoparticles for enhanced antifungal activity and prolonged ocular delivery, Asian J. Pharm. Sci. (2020), https://doi.org/10.1016/j.ajps.2019.09.003.
[94] M.A. Grimaudo, S. Nicoli, P. Santi, A. Concheiro, C. Alvarez-Lorenzo, Cyclosporine-loaded cross-linked inserts of sodium hyaluronan and hydroxypropyl-β-cyclodextrin for ocular administration, Carbohydr. Polym. 201 (2018) 308–316, https://doi.org/10.1016/j.carbpol.2018.08.073.
[95] A. Nanda, R.N. Sahoo, A. Pramanik, R. Mohapatra, S.K. Pradhan, A. Thirumurugan, D. Das, S. Mallick, Drug-in-mucoadhesive type film for ocular anti-inflammatory potential of amlodipine: effect of sulphobutyl-ether-beta-cyclodextrin on permeation and molecular docking characterization, Colloids Surf. B Biointerfaces 172 (2018) 555–564, https://doi.org/10.1016/j.colsurfb.2018.09.011.
[96] R. Li, X. Guan, X. Lin, P. Guan, X. Zhang, Z. Rao, J. Zhao, L. Du, J. Rong, J. Zhao, Poly(2-hydroxyethyl methacrylate)/β-cyclodextrin-hyaluronan contact lens with tear protein adsorption resistance and sustained drug delivery for ophthalmic diseases, Acta Biomater. (2020) 1–14, https://doi.org/10.1016/j.actbio.2020.04.002.
[97] M.G. Hewitt, P.W.J. Morrison, H.M. Boostrom, S.R. Morgan, M. Fallon, P. N. Lewis, D. Whitaker, A. Brancale, C. Varricchio, A.J. Quantock, M.J. Burton, C. M. Heard, In vitro topical delivery of chlorhexidine to the cornea: enhancement using drug-loaded contact lenses and β-cyclodextrin complexation, and the importance of simulating tear irrigation, Mol. Pharm. 17 (2020) 1428–1441, https://doi.org/10.1021/acs.molpharmaceut.0c00140.
[98] B. Lorenzo-Veiga, P. Diaz-Rodriguez, C. Alvarez-Lorenzo, T. Loftsson, H. H. Sigurdsson, In vitro and ex vivo evaluation of Nepafenac-based cyclodextrin microparticles for treatment of eye inflammation, Nanomaterials 10 (2020), https://doi.org/10.3390/nano10040709.

[99] F. Wang, X. Bao, A. Fang, H. Li, Y. Zhou, Y. Liu, C. Jiang, J. Wu, X. Song, Nanoliposome-encapsulated brinzolamide-hydropropyl-β-cyclodextrin inclusion complex: a potential therapeutic ocular drug-delivery system, Front. Pharmacol. 9 (2018) 1–9, https://doi.org/10.3389/fphar.2018.00091.
[100] T. Loftsson, E. Stefánsson, Cyclodextrins and topical drug delivery to the anterior and posterior segments of the eye, Int. J. Pharm. 531 (2017) 413–423, https://doi.org/10.1016/j.ijpharm.2017.04.010.
[101] P.G. Djupesland, Nasal drug delivery devices: characteristics and performance in a clinical perspective-a review, Drug Deliv. Transl. Res. 3 (2013) 42–62, https://doi.org/10.1007/s13346-012-0108-9.
[102] A. De Ascentiis, R. Bettini, G. Caponetti, P.L. Catellani, M.T. Peracchia, P. Santi, P. Colombo, Delivery of nasal powders of beta-cyclodextrin by insufflation, Pharm. Res. (N. Y.) 13 (1996) 734–738, https://doi.org/10.1023/a:1016099516757.
[103] J.C. Verhoef, E. Marttin, S.G. Romeijn, F.W. Merkus, P.H. van der Kuy, W. A. Hermens, N.G. Schipper, Cyclodextrins in nasal drug delivery, Adv. Drug Deliv. Rev. 36 (1999) 41–57, https://doi.org/10.1016/s0169-409x(98)00054-4.
[104] J. Coe Wadsworth, C.M. Dehnhardt, P. Jones, S.W. Korturn, F.M. Wakenhut, G. A. Whitlock, Indazoles, Patent US 8895544B2, 2013.
[105] J.D. Pipkin, R.O. Zimmerer, J.M. Siebert, Nasal and Ophthalmic Delivery of Aqueous Corticosteroid Solutions, Patent US 2009/0312724 A1, 2009.
[106] T.J. Webb, E. Primelles-Perez, Budesonide Cyclodextrin Formulation, Patent WO 2015/109201A1, 2015.
[107] L. Kozlovskaya, M. Abou-Kaoud, D. Stepensky, Quantitative analysis of drug delivery to the brain via nasal route, J. Contr. Release 189 (2014) 133–140, https://doi.org/10.1016/j.jconrel.2014.06.053.
[108] Cyclodextrin News, May 14, 2020), https://cyclodextrinnews.com/2020/02/14/nasal-delivery-with-beta-cyclodextrin-is-approved-a-short-story-of-baqsimi/, 2020.
[109] Eli Lilly, Company, Lilly Acquires Phase III Intranasal Glucagon from Locemia Solutions, Eli Lilly and Company, 2015. May 21, 2020, https://investor.lilly.com/news-releases/news-release-details/lilly-acquires-phase-iii-intranasal-glucagon-locemia-solutions.
[110] F.E. Reno, P. Normand, K. McInally, S. Silo, P. Stotland, M. Triest, D. Carballo, C. Piché, A novel nasal powder formulation of glucagon: toxicology studies in animal models, BMC Pharmacol. Toxicol. 16 (2015), https://doi.org/10.1186/s40360-015-0026-9.
[111] S. Mantripragada, C.A. Piche, J.J.F. Van Betsbrugge, Nasal Powder Formulation for Treatment of Hypoglycemia, Patent US 20190282666A1, 2019.
[112] S.C. Quay, H.R. Constantino, M.S. Kleppe, C.-Y. Li, Composition and Methods for Enhanced Mucosal Delivery of Parathyroid Hormone, Patent US 7435720B2, 2008.
[113] A. Belgamwar, S. Khan, P. Yeole, Intranasal chitosan-g-HPβCD nanoparticles of efavirenz for the CNS targeting, Artif. Cells, Nanomedicine Biotechnol. 46 (2018) 374–386, https://doi.org/10.1080/21691401.2017.1313266.
[114] W. Chen, R. Li, S. Zhu, J. Ma, L. Pang, B. Ma, L. Du, Y. Jin, Nasal timosaponin BII dually sensitive in situ hydrogels for the prevention of Alzheimer's disease induced by lipopolysaccharides, Int. J. Pharm. 578 (2020) 119115, https://doi.org/10.1016/j.ijpharm.2020.119115.
[115] P. Yang, Y. Li, W. Li, H. Zhang, J. Gao, J. Sun, X. Yin, A. Zheng, Preparation and evaluation of carfentanil nasal spray employing cyclodextrin inclusion technology, Drug Dev. Ind. Pharm. 44 (2018) 953–960, https://doi.org/10.1080/03639045.2018.1425426.
[116] G. Dufour, W. Bigazzi, N. Wong, F. Boschini, P. De Tullio, G. Piel, D. Cataldo, B. Evrard, Interest of cyclodextrins in spray-dried microparticles formulation for sustained pulmonary delivery of budesonide, Int. J. Pharm. 495 (2015) 869–878, https://doi.org/10.1016/j.ijpharm.2015.09.052.
[117] M. Guan, R. Shi, Y. Zheng, X. Zeng, W. Fan, Y. Wang, W. Su, Characterization, in vitro and in vivo evaluation of naringenin-hydroxypropyl-ß-cyclodextrin inclusion for pulmonary delivery, Molecules 25 (2020) 1–14, https://doi.org/10.3390/molecules25030554.
[118] N. Mohtar, K.M.G. Taylor, K. Sheikh, S. Somavarapu, Design and development of dry powder sulfobutylether-β-cyclodextrin complex for pulmonary delivery of fisetin, Eur. J. Pharm. Biopharm. 113 (2017) 1–10, https://doi.org/10.1016/j.ejpb.2016.11.036.
[119] Z. Zhao, X. Zhang, Y. Cui, Y. Huang, Z. Huang, G. Wang, R. Liang, X. Pan, L. Tao, C. Wu, Hydroxypropyl-β-cyclodextrin as anti-hygroscopicity agent inamorphous lactose carriers for dry powder inhalers, Powder Technol. 358 (2019) 29–38, https://doi.org/10.1016/j.powtec.2018.09.098.
[120] M.W. Surber, K.A. Bostian, M.N. Dudley, O. Rodny, D.C. Griffith, Aerosolized Fluoroquinolones and Uses Thereof, Patent US 20190381057A1, 2019.
[121] K. Kossen, S.D. Seiwert, D. Ruhrmund, L. Beigelman, L.F.M. Raveglia, S. Vallese, I. Bianchi, T. Hu, Compounds and Methods for Treating Inflammatory and Fibrotic Disorders, Patent US 8969347B2, 2015.
[122] H. Matsuda, H. Arima, Cyclodextrins in transdermal and rectal delivery, Adv. Drug Deliv. Rev. 36 (1999) 81–99, https://doi.org/10.1016/S0169-409X(98)00056-8.
[123] V.T. Bhalani, A.K. Paul, A.K. Sarkar, Topical Film Delivery System, Patent US 10080763B2, 2018.
[124] J.D. Pipkin, R. Rajewski, B. Mainous, Compositions Containing Silymarin and Sulfoalkyl Ether Cyclodextrin and Methods of Using the Same, Patent WO 2016/149685A1, 2016.
[125] T. Chen Chen, S.C. Yu, C.M. Hsu, F.J. Tsai, Y. Tsai, A water-based topical Chinese traditional medicine (Zicao) for wound healing developed using 2-hydroxypropyl-β-cyclodextrin, Colloids Surf. B Biointerfaces 165 (2018) 67–73, https://doi.org/10.1016/j.colsurfb.2018.02.013.
[126] D. Zhang, G. Cai, S. Mukherjee, Y. Sun, C. Wang, B. Mai, K. Liu, C. Yang, Y. Chen, Elastic, persistently moisture-retentive, and wearable biomimetic film inspired by fetal scarless repair for promoting skin wound healing, ACS Appl. Mater. Interfaces 12 (2020) 5542–5556, https://doi.org/10.1021/acsami.9b20185.
[127] A. Klaewklod, V. Tantishaiyakul, N. Hirun, T. Sangfai, L. Li, Characterization of supramolecular gels based on β-cyclodextrin and polyethyleneglycol and their potential use for topical drug delivery, Mater. Sci. Eng. C 50 (2015) 242–250, https://doi.org/10.1016/j.msec.2015.02.018.
[128] E. Vega, M.A. Egea, M.L. Garduño-Ramírez, M.L. García, E. Sánchez, M. Espina, A. C. Calpena, Flurbiprofen PLGA-PEG nanospheres: role of hydroxy-β-cyclodextrin on ex vivo human skin permeation and in vivo topical anti-inflammatory efficacy, Colloids Surf. B Biointerfaces 110 (2013) 339–346, https://doi.org/10.1016/j.colsurfb.2013.04.045.
[129] T. Loftsson, M. Masson, Cyclodextrins in topical drug formulations: theory and practice, Int. J. Pharm. 225 (2001) 15–30, https://doi.org/10.1016/S0378-5173(01)00761-X.
[130] F. Zhou, Z. Song, Y. Wen, H. Xu, L. Zhu, R. Feng, Transdermal delivery of curcumin-loaded supramolecular hydrogels for dermatitis treatment, J. Mater. Sci. Mater. Med. 30 (2019), https://doi.org/10.1007/s10856-018-6215-5.
[131] Z. Chen, B. Han, L. Liao, X. Hu, Q. Hu, Y. Gao, Y. Qiu, Enhanced transdermal delivery of polydatin via a combination of inclusion complexes and dissolving microneedles for treatment of acute gout arthritis, J. Drug Deliv. Sci. Technol. 55 (2020) 101487, https://doi.org/10.1016/j.jddst.2019.101487.
[132] R. Obaidat, N. Al-Shar'i, B. Tashtoush, T. Athamneh, Enhancement of levodopa stability when complexed with β-cyclodextrin in transdermal patches, Pharmaceut. Dev. Technol. 23 (2018) 986–997, https://doi.org/10.1080/10837450.2016.1245319.
[133] A. Juluri, S. Narasimha Murthy, Transdermal iontophoretic delivery of a liquid lipophilic drug by complexation with an anionic cyclodextrin, J. Contr. Release 189 (2014) 11–18, https://doi.org/10.1016/j.jconrel.2014.06.014.
[134] A. Hussain, F. Ahsan, The vagina as a route for systemic drug delivery, J. Contr. Release 103 (2005) 301–313, https://doi.org/10.1016/j.jconrel.2004.11.034.
[135] E. Bilensoy, M.A. Rouf, I. Vural, M. Şen, A.A. Hincal, Mucoadhesive, thermosensitive, prolonged-release vaginal gel for clotrimazole: β-cyclodextrin complex, AAPS PharmSciTech 7 (2006) 1–7, https://doi.org/10.1208/pt070238.
[136] M. Francois, E. Snoeckx, P. Putteman, F. Wouters, E. De Proost, U. Delaet, J. Peeters, M.E. Brewster, A mucoadhesive, cyclodextrin-based vaginal cream formulation of itraconazole, AAPS J. 5 (2003) 1–5, https://doi.org/10.1208/ps050105.
[137] C. Grammen, G. Van Den Mooter, B. Appeltans, J. Michiels, T. Crucitti, K.K. Ariën, K. Augustyns, P. Augustijns, J. Brouwers, Development and characterization of a solid dispersion film for the vaginal application of the anti-HIV microbicide UAMC01398, Int. J. Pharm. 475 (2014) 238–244, https://doi.org/10.1016/j.ijpharm.2014.08.054.
[138] C. Gaurav, R. Goutam, K.N. Rohan, K.T. Sweta, C.S. Abhay, G.K. Amit, (Copper-curcumin) β-cyclodextrin vaginal gel: delivering a novel metal-herbal approach for the development of topical contraception prophylaxis, Eur. J. Pharmaceut. Sci. 65 (2014) 183–191, https://doi.org/10.1016/j.ejps.2014.09.019.
[139] F. Notario-Pérez, A. Martín-Illana, R. Cazorla-Luna, R. Ruiz-Caro, A. Tamayo, J. Rubio, M.D. Veiga, Mucoadhesive vaginal discs based on cyclodextrin and surfactants for the controlled release of antiretroviral drugs to prevent the sexual transmission of HIV, Pharmaceutics 12 (2020), https://doi.org/10.3390/pharmaceutics12040321.
[140] Q. Qian, L. Shi, X. Gao, Y. Ma, J. Yang, Z. Zhang, J. Qian, X. Zhu, A paclitaxel-based mucoadhesive nanogel with multivalent interactions for cervical cancer therapy, Small 15 (2019) 1–11, https://doi.org/10.1002/smll.201903208.
[141] M. Ijaz, J.A. Griessinger, A. Mahmood, F. Laffleur, A. Bernkop-Schnürch, Thiolated cyclodextrin: development of a mucoadhesive vaginal delivery system for acyclovir, J. Pharmacol. Sci. 105 (2016) 1714–1720, https://doi.org/10.1016/j.xphs.2016.03.009.
[142] C.R. Butler, L.A. MCallister, E.M. Beck, M.A. Brodney, A.M. Gilbert, C.J. Helal, J. I. Montgomery, S.V. O'Neil, B.N. Rogers, P.R. Verhoest, D. Webb, 1,1,1-trifluoro-3-hydroxypropan-2-yl Carbamate Derivatives and 1,1,1-Trifluoro-4-Hydroxybutan-2-Yl Carbamate Derivatives as Magl Inhibitors, Patent US 2019/0382359A1, 2019.
[143] T.J. Purohit, S.M. Hanning, Z. Wu, Advances in rectal drug delivery systems, Pharmaceut. Dev. Technol. 23 (2018) 942–952, https://doi.org/10.1080/10837450.2018.1484766.
[144] H. Arima, T. Kondo, T. Irie, K. Uekama, Enhanced rectal absorption and reduced local irritation of the anti-inflammatory drug ethyl 4-biphenylylacetate in rats by complexation with water-soluble β-cyclodextrin derivatives and formulation as oleaginous suppository, J. Pharmacol. Sci. 81 (1992) 1119–1125, https://doi.org/10.1002/jps.2600811116.
[145] M. Cox, N. Nanda, Methods of Treating Pediatric Cancers, Patent US 2018/0133222A1, 2018.
[146] A. Safdi, D. Taylor, Rifaximin Anti-rectal Dysfunction Preparation, Patent US 8987292B2, 2015.
[147] C.M. Lázaro, C.C. de Oliveira, A. Gambero, T. Rocha, C.M.S. Cereda, D.R. de Araújo, G.R. Tofoli, Evaluation of budesonide–hydroxypropyl-β-cyclodextrin inclusion complex in thermoreversible gels for ulcerative colitis, Dig. Dis. Sci. (2020), https://doi.org/10.1007/s10620-020-06075-y.
[148] L.L. Wang, W.S. Zheng, S.H. Chen, Y.X. Han, J.D. Jiang, Development of rectal delivered thermo-reversible gelling film encapsulating a 5-fluorouracil hydroxypropyl-β-cyclodextrin complex, Carbohydr. Polym. 137 (2016) 9–18, https://doi.org/10.1016/j.carbpol.2015.10.042.

[149] H. Kroll, Exploring pathways of regional technological development in China through patent analysis, World Patent Inf. 46 (2016) 74–86, https://doi.org/10.1016/j.wpi.2016.06.003.
[150] V. Raghupathi, W. Raghupathi, Innovation at country-level: association between economic development and patents, J. Innov. Entrep. 6 (2017), https://doi.org/10.1186/s13731-017-0065-0.
[151] B. Xu, E.P. CHiang, Trade, patents and international technology diffusion, J. Int. Trade Econ. Dev. An Int. Comp. Rev. (2005) 37–41, https://doi.org/10.1080/0963819042000333270.

pharmaceutics

MDPI

Article

When Cyclodextrins Met Data Science: Unveiling Their Pharmaceutical Applications through Network Science and Text-Mining

Juliana Rincón-López [1], Yara C. Almanza-Arjona [2], Alejandro P. Riascos [3,*] and Yareli Rojas-Aguirre [1,*]

[1] Instituto de Investigaciones en Materiales, Universidad Nacional Autónoma de México, Ciudad Universitaria, Mexico City 04510, Mexico; juliana.rincon@comunidad.unam.mx
[2] Instituto de Ciencias Aplicadas y Tecnología, Universidad Nacional Autónoma de México, Ciudad Universitaria, Mexico City 04510, Mexico; yara.almanza@icat.unam.mx
[3] Instituto de Física, Universidad Nacional Autónoma de México, Ciudad Universitaria, Mexico City 04510, Mexico
* Correspondence: aperezr@fisica.unam.mx (A.P.R.); yareli.rojas@materiales.unam.mx (Y.R.-A.); Tel.: +52-555-622-5000 (A.P.R.); +52-555-622-6666 (ext. 45675) (Y.R.-A.)

Abstract: We present a data-driven approach to unveil the pharmaceutical technologies of cyclodextrins (CDs) by analyzing a dataset of CD pharmaceutical patents. First, we implemented network science techniques to represent CD patents as a single structure and provide a framework for unsupervised detection of keywords in the patent dataset. Guided by those keywords, we further mined the dataset to examine the patenting trends according to CD-based dosage forms. CD patents formed complex networks, evidencing the supremacy of CDs for solubility enhancement and how this has triggered cutting-edge applications based on or beyond the solubility improvement. The networks exposed the significance of CDs to formulate aqueous solutions, tablets, and powders. Additionally, they highlighted the role of CDs in formulations of anti-inflammatory drugs, cancer therapies, and antiviral strategies. Text-mining showed that the trends in CDs for aqueous solutions, tablets, and powders are going upward. Gels seem to be promising, while patches and fibers are emerging. Cyclodextrins' potential in suspensions and emulsions is yet to be recognized and can become an opportunity area. This is the first unsupervised/supervised data-mining approach aimed at depicting a landscape of CDs to identify trending and emerging technologies and uncover opportunity areas in CD pharmaceutical research.

Keywords: cyclodextrin; patents; network science; text-mining; dosage forms

check for updates

Citation: Rincón-López, J.; Almanza-Arjona, Y.C.; Riascos, A.P.; Rojas-Aguirre, Y. When Cyclodextrins Met Data Science: Unveiling Their Pharmaceutical Applications through Network Science and Text-Mining. *Pharmaceutics* **2021**, *13*, 1297. https://doi.org/10.3390/pharmaceutics13081297

Academic Editors: Ferenc Fenyvesi and Judit Váradi

Received: 19 July 2021
Accepted: 16 August 2021
Published: 19 August 2021

Publisher's Note: MDPI stays neutral with regard to jurisdictional claims in published maps and institutional affiliations.

Copyright: © 2021 by the authors. Licensee MDPI, Basel, Switzerland. This article is an open access article distributed under the terms and conditions of the Creative Commons Attribution (CC BY) license (https://creativecommons.org/licenses/by/4.0/).

1. Introduction

Cyclodextrins (CDs) are outstanding materials in the pharmaceutical field, where they have mainly performed as molecular containers of hydrophobic drugs for olubility enhancement. Likewise, through the apparent modification of guest molecules' physicochemical properties, CDs can improve the stability and organoleptic properties of a pharmaceutical formulation, compelling their use in developing dosage forms for their administration for practically any route [1,2]. Furthermore, CD derivatives are becoming relevant in developing drug-loaded bioadhesive materials [3,4], and CD-based cancer nanomedicines have reached or are currently in clinical trials [5].

More than 40 formulations containing native or modified CDs are currently marketed for diverse therapeutic purposes (Table S1, Supplementary Material). Furthermore, their use is expanding, as evidenced by at least six formulation approvals in the last five years (Table 1), which include Baqsimi® (Eli Lilly and Company, Indianapolis, IN, USA) for the nasal delivery of glucagon and Trappsol®Cyclo™ (Cyclo Therapeutics, Inc., Gainesville, FL, USA), for the treatment of Niemann–Pick disease type C, in which the active pharmaceutical ingredient (API) is the CD itself [6,7]. Two recent breakthroughs are Veklury®

(Gilead Sciences, Inc., Foster City, CA, USA) (SBEβCD/remdesivir) to treat hospitalized patients with severe COVID-19 and the Janssen COVID-19 vaccine containing HPβCD, which were FDA-approved for emergency use in 2020 and 2021, respectively [8,9].

Table 1. CD-based formulation approvals in the last five years [6–11].

	Trade Name	Type of CD	API	Dosage Form/Administration Route	Company
2021	* Janssen COVID-19 Vaccine	HPβCD	Ad26.COV2-S	Suspension for I.M. administration	Janssen Biotech, Inc. (Horsham, PA, USA), a Janssen Pharmaceutical Company of Johnson & Johnson
2020	* Veklury	SBEβCD	Remdesivir	Lyophilized powder for I.V. solution	Gilead Sciences, Inc. (Foster City, CA, USA)
	** Trappsol Cyclo	HPβCD	Cyclodextrin	I.V. solution	Cyclo Therapeutics, Inc. (Gainesville, FL, USA)
2019	Zulresso	SBEβCD	Brexanolone	I.V. solution	Sage Therapeutics, Inc. (Cambridge, MA, USA)
	Baqsimi	βCD	Glucagon	Nasal powder	Eli Lilly and Company (Indianapolis, IN, USA)
2017	Voriconazole	HPβCD	Voriconazole	Lyophilized powder for I.V. solution	Xellia Pharmaceuticals ApS (Copenhagen, Denmark)

* Emergency use authorization by the FDA; ** FDA fast track process.

Technological interest in CDs within the pharmaceutical field is continuously growing, and monitoring CD-based pharmaceutical technologies is fundamental to identifying emerging technologies and uncovering promising opportunity areas, which ultimately may support decision-making in CD pharmaceutical research.

Technological information, a substantial component of research and development, is commonly found in patents; hence, the analysis of patent documents may provide indicators for novel developments, inform about emerging technological areas, and support the identification of opportunities for technological forecasting [12].

As some technologies and innovations in a patent are not usually published in scientific literature, important information can remain hidden from researchers [13]. Therefore, articles rarely cite patents, although patents often cite articles. Thus, understanding the interplay between scientific literature and patents is a practical approach to prioritize investigations and investment and forecast the success of specific research in academia [12,14,15]. Moreover, it can foster innovations quickly, particularly when the innovation cycle becomes more complex and shorter and when the market demands rapid responses [16]. Such is the case of the efforts to develop therapies to treat or prevent SARS-CoV-2 infection [15,17].

The content, length, and structure of patents are different from that of scientific articles. Additionally, patents display an intricated writing style, characterized by complex and long sentences that could shield important information. This particular communication method can make the analysis of patents a challenging task [18].

Network science studies emergent patterns in a system, considering their parts and interactions [19]. In general terms, a network consists of nodes (vertices) that describe the elements of the system and edges (links) that represent relationships between the elements. Network science is a fundamental paradigm in the description of complex systems, and it has gained enormous importance in the understanding of social networks, citation networks, bioinformatics, and even the functional organization of a living cell [19–22].

Although little has been done in the analysis of patent data through network science, there is evidence that it is a valuable tool that provides a mathematical framework to analyze patents at different levels, from single documents to complete text databases, and may allow the obtaining of a patent landscape in which patents can be analyzed as a whole while detecting the relationships among them. Community detection algorithms in a network of patents allow the identification of sets of nodes densely connected internally but with reduced connectivity between communities; this particular organization serves as a clustering method for the unsupervised classification of patents with similar content.

General clustering techniques constitute an essential data mining component and are fundamental in unsupervised machine learning tasks [23,24]. Thus, community detection in the patent landscape may unveil low-patented technological areas, emerging trends, and even academic or industry partners to collaborate with in future research [12,15,25].

We recently reviewed the evolution of CD pharmaceutical technologies in terms of administration routes by analyzing a dataset of 1998 pharmaceutical CD patents retrieved from the Derwent Innovation Index database [1]. The review was achieved by text-mining techniques that enabled knowledge extraction from patent texts according to their semantic content. This review is the first of its type for CD pharmaceutical applications. Nonetheless, that work required specific sets of keywords, necessarily provided by experts in the field. Motivated by the fascinating unsupervised data-driven approaches to extract knowledge from data, herein, we present a research work divided into two stages. In the first stage, we mine the same dataset, but, this time, by implementing network science tools to establish a coarse-grained unsupervised technological representation that automatically retrieves knowledge in the form of keywords describing groups of patents without prior expertise in this field, thus reducing possible bias in the interpretation of results. In this way, we represented all the CD patent information as a network, where each node represents a patent and connections describe their similarity (Figure 1).

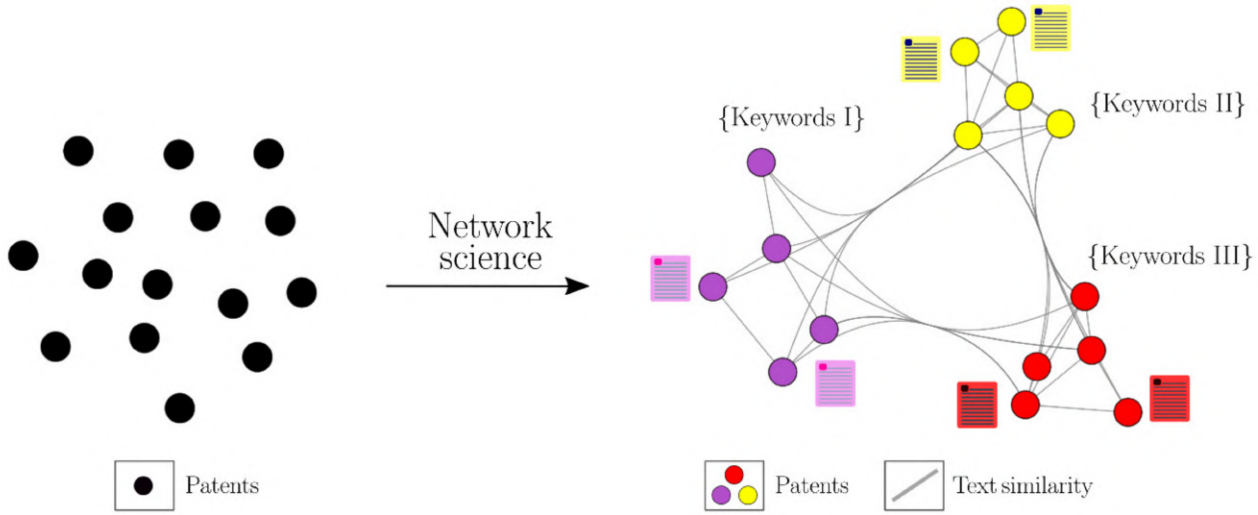

Figure 1. CD patent analysis and keyword identification through network science.

In the second stage, the keywords provided by the networks guide a further text-mining of the patent dataset, the discussion of which was based on the obtained networks and supported by our previous review. The whole analysis was based on the patent's semantic content in the "*Novelty*" and "*Use*" sections of the document.

The increasing availability of data in different scientific fields conceives significant opportunities to leverage the data to guide research [26–33]. Thus, data-driven approaches based on methods similar to those presented herein [18,34,35], along with recent discoveries in machine learning, natural language processing, and text-mining, can pave the way for scientific discoveries and innovation in the pharmaceutical field for both academia and industry.

2. Methods

2.1. Analysis of CD Pharmaceutical Patents by Network Science

We followed the flowchart shown in Figure 2 to mine the CD pharmaceutical patents according to their semantic content. The description of each one of the steps is given below.

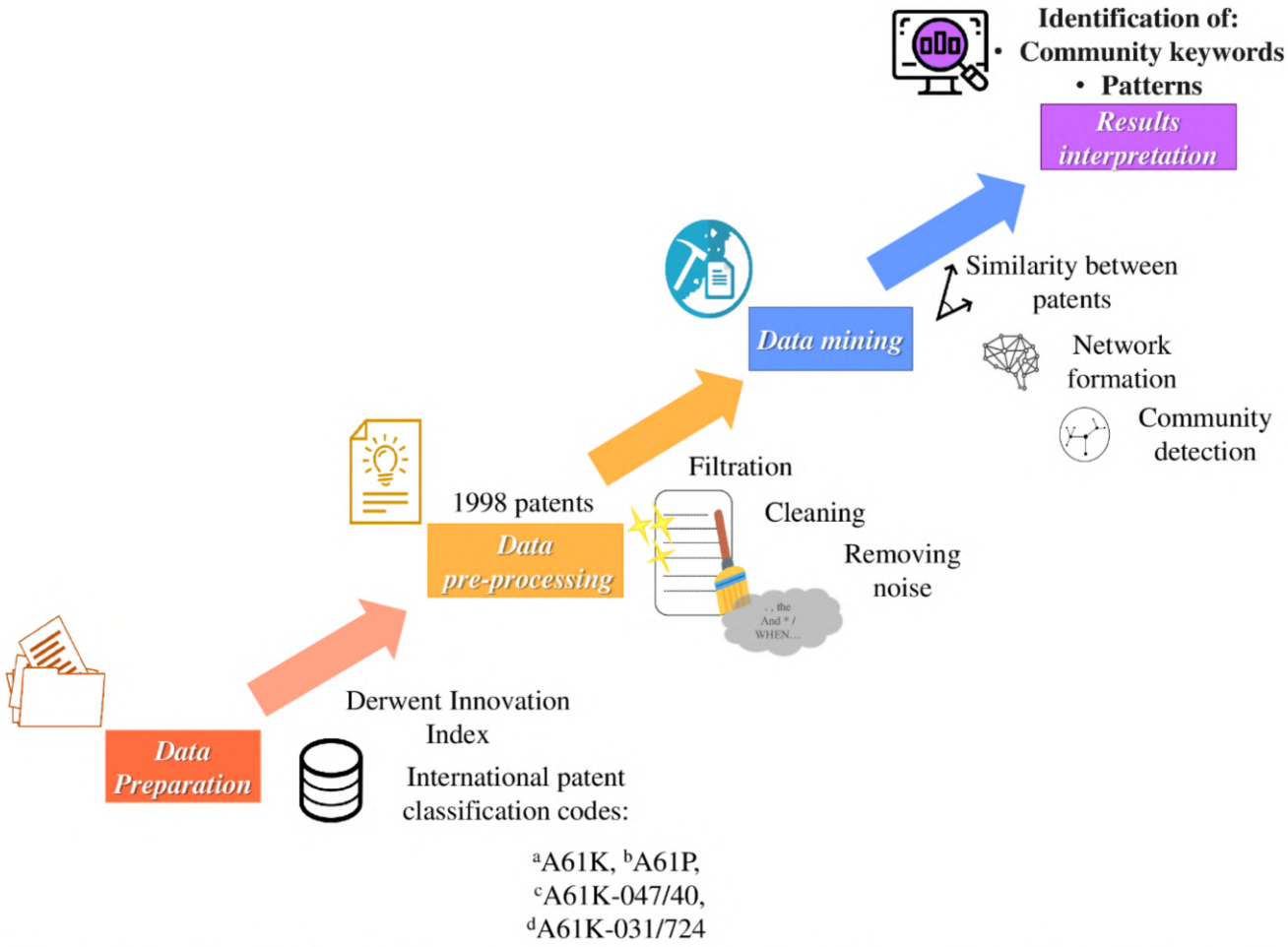

Figure 2. Data mining flowchart. [a]A61K: preparations for medical, dental, or toilet purposes; [b]A61P: specific therapeutic activity of chemical compounds or medical preparations; [c]A61K-047/40: cyclodextrins and derivatives thereof (medicinal preparations characterized by the non-active ingredients); [d]A61K-031/724: cyclodextrins (medicinal preparations containing active organic ingredients). A61Q, referring to "specific use of cosmetics or similar toilet preparations", was excluded from our search.

2.1.1. Data Preparation

We employed the 1998 patent dataset, whose retrieval was previously reported [1]. Briefly, all patents containing the truncated keyword *cyclodextrin* were collected from the Derwent Innovation Index (DII) database (Clarivate, 2020; access through the National Autonomous University of Mexico, Mexico City, Mexico) until 2019. We used specific International Patent Classification codes to delimit the search (Figure 2).

2.1.2. Pre-Processing

We developed a classification method that extracted the information in the fields of "*Novelty*" and "*Use*" in each patent based on the following pre-processing operations:

- Punctuation and symbols. We removed punctuation and special characters, such as numbers and math symbols, and lowered all words.
- Stop words. We removed commonly used stop words (such as "the", "in", and "is") that are unnecessary in patent classification.
- Text lemmatization. In this stage, families of words derived from a unique root were replaced by a unique base or dictionary form known as the lemma.
- Common words. Because we were interested in specific CD applications, we removed those words commonly found in the text that did not provide a particular context. In this category, we included different types of words such as adjectives, verbs, and

adverbs, for example, “consists”, “contain”, “effect”, “enables”, “excellent”, “exhibit", “good”, “main”, “method”, among others.

These pre-processing operations were implemented in Python using the Natural Language ToolKit [36] and pandas [37] libraries.

2.1.3. Data Mining

We created a ranking of words based on their frequency and position in each text from the list of words obtained in the pre-processing stage. After that, we chose the first M-classified words, meaning that M words describe each patent with their frequencies. Using all the pre-processed dataset words, we defined a d-dimensional Euclidean space of keywords in which a patent with M non-null entries, with its respective frequencies of words, is represented as a vector. After that, we defined a measure to quantify the similarity between two patents.

We used the cosine similarity that provides a measure proportional to the angle between patents i and j; we defined the similarity coefficient $c_{ij} = \frac{2}{\pi} arccos\left[\frac{\hat{v}_i \cdot \hat{v}_j}{|\hat{v}_i||\hat{v}_j|}\right]$, where $\hat{v}_i$ denotes the vector describing the patent i, $\hat{v}_i \cdot \hat{v}_j$ is the dot product between vectors, and $|\hat{v}_i| = \sqrt{\hat{v}_i \cdot \hat{v}_i}$ is the norm. Specifically, we have the value $c_{ij} = 0$, if the list of selected words representing two patents coincides; this is the case when a patent is compared to itself. When all the words examined in patents i and j are different, we have $c_{ij} = 1$.

Afterward, we statistically analyzed the c_{ij} similarity coefficients to define a threshold value H, which determines whether two patents are connected or not. Thus, by using the similarity coefficients and H values, we generated a network of patents in which a link (connection) between two different patents i and j is established if $0 < c_{ij} \leq H$, that is, a network described by a matrix A (denoted as A_{ij}), with element 1 if two nodes (patents) are connected and element 0 otherwise; therefore, $A_{ij} = 1$ if $0 \leq c_{ij} \leq H$ and $A_{ij} = 0$ for $c_{ij} > H$ for our network. By definition, the matrix considers the diagonal entries $A_{ii} = 0$ to avoid loops or connections of a node to itself.

Once the structure was defined, we applied different Python library tools [38] for its analysis. We centered our analysis on the largest connected component (LCC), which detects the largest set of connected nodes within the network; this subnetwork does not include individual or small patent clusters. On the other hand, we studied network degrees, defined as $k_i = \sum_{l=1}^{N} A_{il}$ (N being the size of the LCC), that provided the number of connections of the patent i. The statistical analysis of those degrees allowed us to define the network type [21].

Finally, we applied the Louvain algorithm [39] to detect communities in the network; these are groups of patents in which connections between nodes are denser than connections among the rest of the network [19]. In other words, we detected groups of patents with similar semantic content.

The analyses were conducted in Python, and the codes are available from the authors upon request.

2.1.4. Interpretation

Community detection allowed us to further expose the relative frequency of words in each one of the groups. Then, by analyzing the ten most common words found for each group, we identified predominant patterns in the organization of words within the CD patent landscape.

2.2. Text Mining

The resulting network showed the presence of keywords associated with dosage forms in most of the communities. Therefore, we carried out further mining of the 1998 patent dataset, guided by words corresponding to pharmaceutical dosage forms, aiming to determine the number of patents related to each of them and observe how they have evolved. We employed our previously reported techniques to identify specific words

in each patent [1]. The words used in the queries for dosage forms were based on U.S. Pharmacopeia definitions [40].

3. Results and Discussion

3.1. Data Mining by Network Science

The pre-processing stage resulted in a subset of data containing those terms providing the context to detect groups of patents containing similar keywords. Considering $M = 5$ keywords, we found 2807 and 2223 words describing the patents in *Novelty* and *Use*. These words also defined the dimension of the Euclidean space for both fields. At this stage, the patents were represented as points distributed in that space, in which the distance between them (cosine similarity) can be measured, something that would not be possible by just comparing the texts and reading them.

We computed the cosine similarity coefficients $c = c_{ij}$ between all patents i, j in these spaces, storing the information in an $N \times N$ matrix, with $N = 1998$ (patents in the dataset). Afterward, through a statistical analysis of all c values, we determined the probability density $\rho(c)$ for the words in the *Novelty* and *Use* fields (Figure 3a). In both cases, the curves showed a relative maximum around $c = 0.85$, and a high fraction of the similarity values were in the interval of $0.6 < c < 1$.

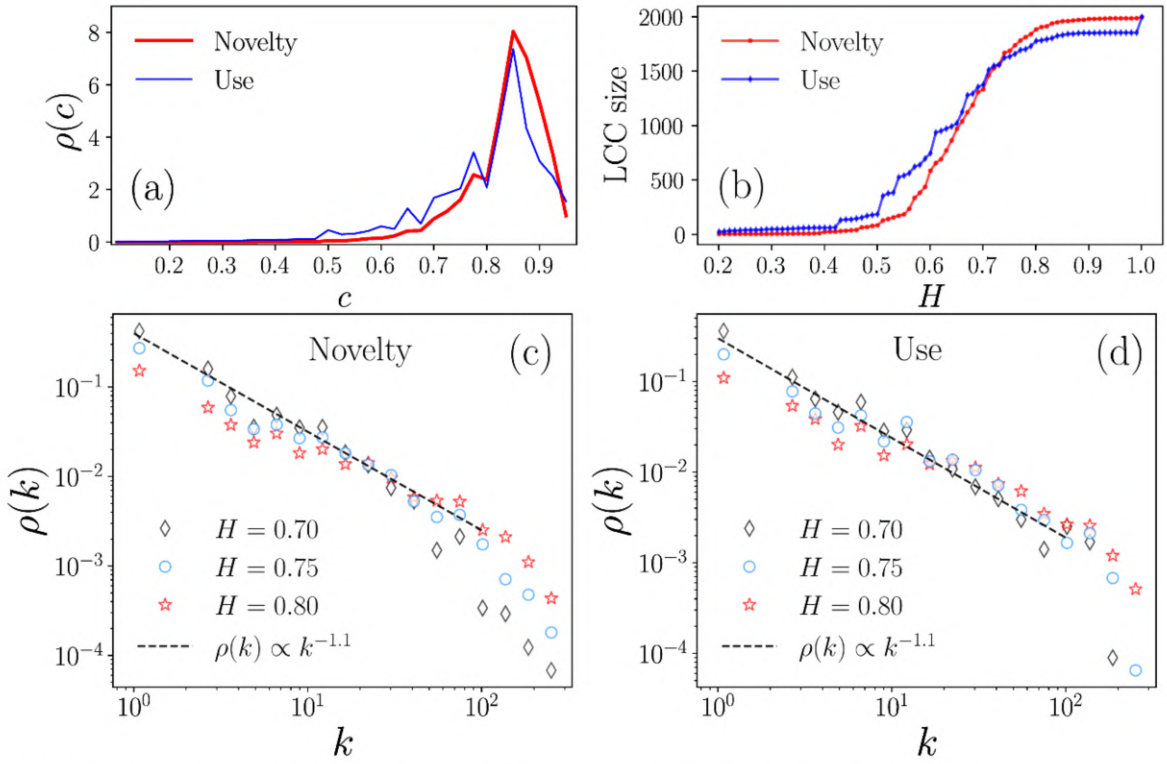

Figure 3. Characterization of similarity networks from the semantic content analysis in the *Novelty* and *Use* sections of CD patents. (**a**) Statistical analysis of similarity values c in the interval $0.1 \leq c \leq 0.95$; (**b**) LCC size generated with threshold values H; probability density of the k degrees for the networks generated for $H = 0.7,\ 0.75,\ 0.8$ within the (**c**) *Novelty* and (**d**) *Use* fields.

Similarity coefficients provided the necessary information to build a network of patents: a multidimensional representation for global data analysis, in which each node is a patent, and links or connections are defined in terms of the threshold value H between two patents. We identified a range of c to establish the parameters for constructing the patent network. Then, we explored different threshold H values to determine if two $i,\ j$ patents are connected if $0 < c_{ij} \leq H$, considering that for small H values, only highly similar patents are joined, while when H is close to 1, nested structures with minor restrictions

are produced, and a higher number of patents are connected. On the other hand, $H = 1$ depicts a fully connected network in which a link would connect all patents.

The effect of H on the network was determined based on the LCC that indicates the number of nodes of the largest connected network, obtained through a given threshold value H. As seen in Figure 3b, $H < 0.5$ generates LCCs that include only a few patents, whereas values of $H \geq 0.7$ produce connected networks that include a high fraction of the 1998 patents.

In that way, we analyzed the structure of networks with threshold values $H = 0.7,\ 0.75,\ 0.8$. For each one of them, we calculated the degree k, which denotes the number of connections of a patent. The subsequent statistical analysis [21] informed us that the probability density of the degree $\rho(k)$ follows an inverse power-law $\rho(k) \propto k^{-\gamma}$, a behavior observed for our dataset patents with $1 \leq k \leq 100$ connections (Figure 3c,d illustrates the case $\rho(k) \propto k^{-1.1}$, with dashed lines as a guide). In network science, structures with a power-law distribution $\rho(k) \propto k^{-\gamma}$ are called scale-free and describe a hierarchical structure in which their nodes, arranged in small groups, organize hierarchically in increasingly larger groups through links connecting the whole network, namely, a complex network [19,41]. Therefore, our findings revealed that the CD pharmaceutical patents, when analyzed through semantic content similarity in terms of their *Novelty* and *Use* fields, are organized in complex networks. This fascinating behavior has been observed in different systems, such as biological, social, and communications [19,41].

3.1.1. Community Detection in CD Patents' Complex Networks

Once we generated the networks with different H values, we aimed to detect communities by applying the Louvain algorithm. Community detection endorses identifying local patterns and guides the understanding of community interaction in a complex structure. In this work, the communities represent groups of patents with similar semantic content, which arose from considering all the information contained in the network, something not immediately visible if comparing the patent texts in a standard table or chart.

For the case of the *Novelty* field, the network was generated with a threshold value $H = 0.75$. With this choice, the LCC is constituted by $N = 1623$ nodes, organized in nine communities (shown in different colors in Figure 4a). In this representation, we see how communities are formed by subsets of nodes that are intensely connected to each other. To exemplify the communities' topology, we selected Communities 1 and 7, depicted in Figure 4b, accompanied by their respective histograms, showing the relative frequency of the 10 most common words found for each community.

A similar analysis was carried out for those words analyzed in the *Use* field. In this case, through exploring different configurations, we selected the threshold value of $H = 0.8$ to define the similarity structure with an LCC of $N = 1779$. This larger H value makes the similarity of patents less restrictive than in the *Novelty* network. Here, the Louvain algorithm detected 11 clusters (Figure 5a). Figure 5b depicts Community 1 and Community 4 as examples to observe their topology. The relative frequency of their 10 most common words is also included.

3.1.2. Analysis of Community Keywords

Comparing the semantic content for all pairs of patents of our dataset, achieved by implementing the approaches described above, was the primary motivation of this work. In this way, network science provided a natural conceptual framework for a multiscale description of the patents' similarity. On a large scale, we found a complex network encompassing the semantic similarity of patents as a whole. At the intermediate scale, it was possible to visualize patents clustering into groups containing information that, at the finest scale, formally partitioned the dataset in order to identify patterns through the analysis of those keywords that describe the semantic content of the patents in each community. Table 2 shows the five most common words and their respective relative frequencies, associated with each community, for the *Novelty* and *Use* networks.

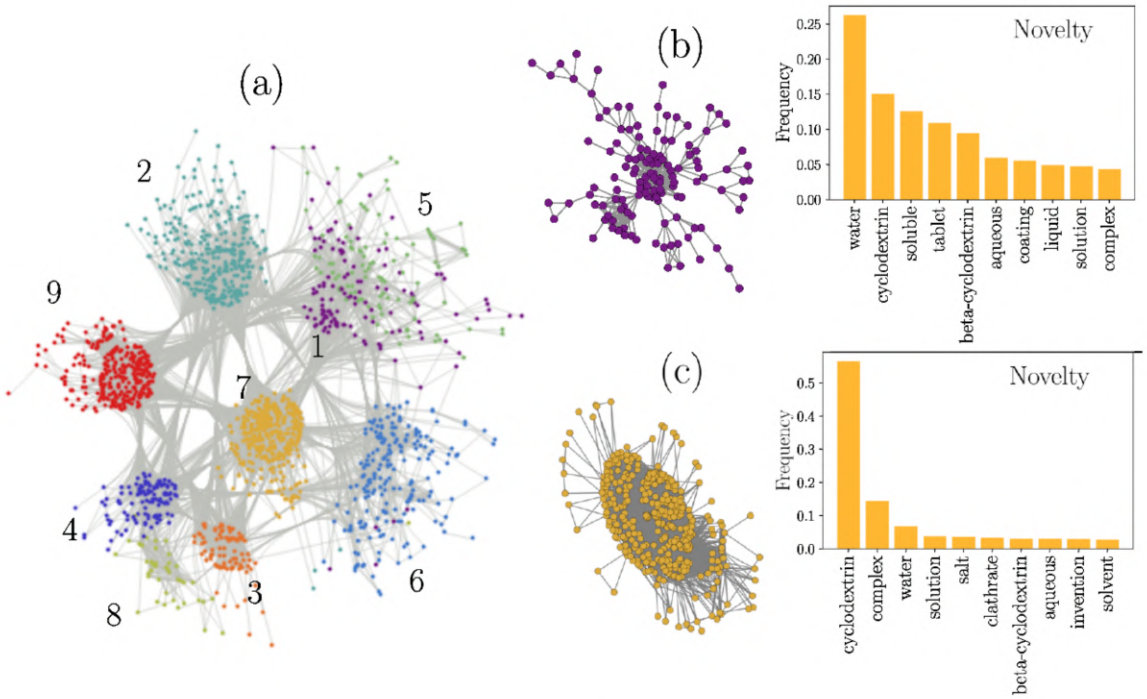

Figure 4. Graphical representation of the complex network formed from CD patents for the *Novelty* field. (**a**). Communities 1 (**b**) and 7 (**c**), with their histograms representing the relative frequency of the 10 most common words found for each community.

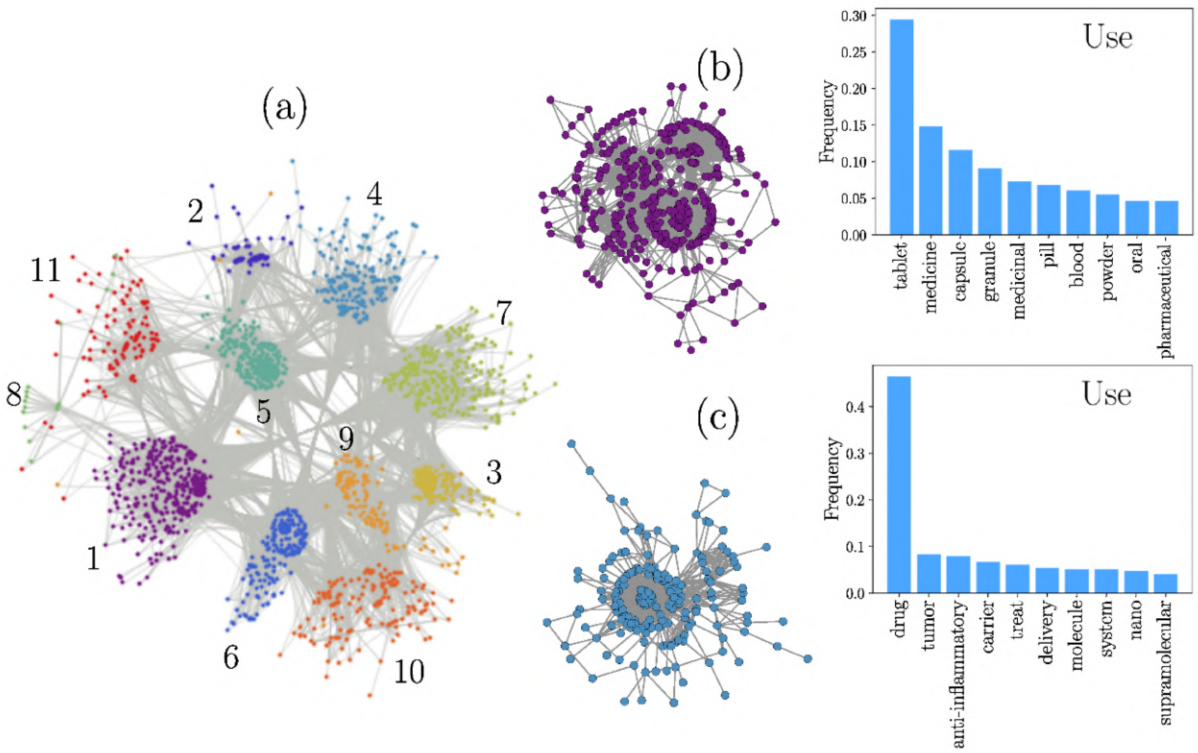

Figure 5. Graphical representation of the complex network formed from CD patents for the *Use* field (**a**); Communities (**b**) 1 and (**c**) 4, with the histograms representing the relative frequency of their 10 most common words.

Table 2. Top 5 words found in network communities for (**a**) *Novelty* and (**b**) *Use*. C refers to community, W to word, and F to frequency.

	C	Size	W I	F	W II	F	W III	F	W IV	F	W V	F
(a) *Novelty*	1	129	water	0.35	cyclodextrin	0.2	soluble	0.17	tablet	0.15	beta-cyclodextrin	0.13
	2	294	cyclodextrin	0.28	salt	0.25	pharmaceutical	0.21	component	0.14	active	0.11
	3	88	acid	0.63	cyclodextrin	0.14	beta-cyclodextrin	0.08	salt	0.08	solution	0.07
	4	112	solution	0.53	water	0.12	beta-cyclodextrin	0.12	aqueous	0.12	cyclodextrin	0.11
	5	102	sodium	0.33	cellulose	0.21	hydroxypropyl	0.16	beta-cyclodextrin	0.16	starch	0.15
	6	197	material	0.3	powder	0.28	beta-cyclodextrin	0.15	cyclodextrin	0.14	radix	0.14
	7	357	cyclodextrin	0.66	complex	0.17	water	0.08	solution	0.04	salt	0.04
	8	42	oil	0.41	mixture	0.18	volatile	0.17	beta-cyclodextrin	0.15	water	0.09
	9	302	beta-cyclodextrin	0.53	hydroxypropyl	0.23	acid	0.1	hydrochloride	0.07	cyclodextrin	0.07
	C	**Size**	**W I**	**F**	**W II**	**F**	**W III**	**F**	**W IV**	**F**	**W V**	**F**
(b) *Use*	1	342	tablet	0.41	medicine	0.2	capsule	0.16	granule	0.13	medicinal	0.1
	2	59	sustained	0.58	hydrochloride	0.25	antibacterial	0.06	patient	0.05	drug	0.05
	3	136	cancer	0.64	cell	0.13	disease	0.08	breast	0.08	lung	0.07
	4	175	drug	0.62	tumor	0.11	anti-inflammatory	0.11	carrier	0.09	treat	0.08
	5	238	disease	0.55	disorder	0.23	syndrome	0.11	inflammatory	0.06	chronic	0.05
	6	183	pharmaceutical	0.57	drink	0.14	animal	0.11	cosmetic	0.09	drug	0.09
	7	256	pain	0.39	complex	0.22	bone	0.14	cyclodextrin	0.13	oral	0.12
	8	16	particle	0.58	peptide	0.19	active	0.08	ingredient	0.08	heat	0.08
	9	124	injection	0.42	powder	0.24	freeze	0.14	dried	0.14	soluble	0.05
	10	151	treatment	0.32	infection	0.31	virus	0.18	disease	0.13	medicament	0.07
	11	99	eye	0.28	nasal	0.28	allergic	0.18	drop	0.14	macular	0.12

3.1.3. Novelty

The words ranking revealed that CD pharmaceutical patents' *Novelty* relies primarily on incrementing drug solubility to formulate aqueous solutions. This is evident when observing Community 7, the largest in the network. Within the words comprising this community, we found *complex*, *water*, and *solution*, which refers to CDs' use to increase the water solubility of a drug by forming inclusion complexes, facilitating their formulation as aqueous solutions. This cluster confirms the supremacy of CDs as solubilizers in the pharmaceutical field.

The same is true for Community 4 and Community 1. The latter contains the word *tablet*, pointing out CDs' importance in these dosage forms [42]. Community 6, also significant in size, includes the word *powder*, which might refer to a final dosage form (solutes for reconstitution) or to intermediates that are further processed to produce other formulations. A broader discussion about CD patents for tablets, powders, and other dosage forms is presented in Section 3.2.

Community 8 shows the words *oil* and *volatile*, bringing to light the role that CDs have played in facilitating the incorporation of these compounds into suitable formulations, either as amorphous powders or by overcoming the low water solubility and instability associated with them [43,44].

To summarize, it is observed that the *Novelty* of pharmaceutical patents of CDs consists of the aqueous solubility enhancement of drugs for their proper formulation as aqueous solutions. Additionally, the importance of tablets and powders was revealed.

3.1.4. Use

In this network, the patents are grouped according to their pharmaceutical forms, which might be expected since the ultimate goal of using CDs is to develop optimal dosage forms by improving drug solubility, stability, and permeability, among other properties. Nonetheless, target diseases and drug families also made the patents form communities.

3.1.5. Dosage Forms

Community 1, the largest of the network, is mainly associated with tablets, in agreement with Community 1 for *Novelty*, confirming the relevance of CDs or CD/drug ICs in those dosage forms.

Community 11, although small, confirms that CDs are advantageous in formulations to treat eye disorders. The use of CDs to develop eye drops and other ophthalmic ailments, including CD-based macular degeneration therapies, has gained significant importance over time [45], with an increasing number of patents observed in the last ten years [1]. The following are two examples of recent patents in the field: (1) A formulation of an aqueous

ophthalmic solution of brinzolamide to treat ocular hypertension and open-angle glaucoma using HPβCD as a solubilizer agent [46]; (2) a formulation of at least two of the following active agents—a corticosteroid, a non-steroidal anti-inflammatory drug (NSAID), and an antibiotic—to treat a variety of eye conditions. By forming CD/NSAID and CD/antibiotic ICs, soluble and stable formulations were obtained [47]. Fascinating research in the field indeed announces that this upward trend will continue [48–52].

Community 11 also contains the word *nasal*. CDs' abilities to enhance drug solubility, permeability and optimize organoleptic properties make them attractive components for nasal formulations. Proof of this is a recent patent describing an intranasal epinephrine formulation to treat medical emergency hypersensitivity reactions, such as anaphylaxis, in an out-of-hospital setting, in which CDs work as absorption enhancers of the drug [53]. Another striking example, in which the CD is the active ingredient, is an aqueous solution containing 2,6-di-O-methyl-βCD (DIMEB), which, after nasal administration, is effective in treating prion disease. This patent showed how the intranasal administration of 0.032 mg/day of DIMEB significantly increased the survival of C57BL mice suffering from the disease [54]. Hence, the increasing significance in nasal delivery and compelling investigations on nasal mucoadhesive CD-based materials could soon make these technologies gain more strength [55,56].

3.1.6. CDs in Cancer

Communities 3 and 4 highlight the interest in using CDs for cancer therapies. Several anticancer drugs are characterized by low solubility, poor intestinal permeability, and low bioavailability, hampering the development of suitable formulations for parenteral or enteral administration. CDs have been widely investigated to overcome these drawbacks, either as CD/chemotherapeutic non-covalent ICs or through CD-covalent conjugates as chemotherapeutic delivery platforms [57]. Some CD-based anticancer treatments are currently under clinical evaluation [5]. Several patents concerning CDs and cancer therapies were found within our dataset. We chronologically describe some examples below.

A patent filed in the late 1980s disclosed the solubility enhancement of 1,1-cyclobutanedicarboxylatediammineplatinum (II) (a cis-platinum derivative compound) through the complexation with αCD to allow the preparation of solutions for parenteral or oral administration [58].

The interest in patenting CD/chemotherapeutic ICs continued during the 1990s. For instance, the CD/toremifene IC enabled the formulation of topical preparations to treat cancers localized in the skin or a short distance from the skin, such as metastatic lesions of breast cancer [59]. In another case, the complex DMβCD/taxol increases the apparent taxol solubility to facilitate its absorption when administered either through the IV or oral route to cancer patients [60].

SuperGen, Inc. (now Astex Pharmaceuticals, Inc., Pleasanton, CA, USA) presented an exciting application of CDs, beyond drug solubility enhancement, addressing the reduction of vascular irritation and extravasation when a combination of CDs and antineoplastic drugs were administered intravenously [61].

In recent years, the exhaustive investigation of CD-based chemotherapies in the nanomedicine field has brought about several promising approaches. One of them is CRLX101, a CD-based nanoparticle consisting of camptothecin conjugated to a copolymer of βCD and polyethylene glycol that achieves the sustained release of the drug with high systemic concentration. This nanosystem is now in Phase I/II clinical trials for small cell lung cancer, with a completion date estimated at 2027 [62–64]. The success of CRLX101 prompted similar CD-based polymeric nanotechnologies, also patented by Cerulean Pharma Inc., for example, the CD–camptothecin conjugate combined with bevacizumab for advanced renal carcinoma [65,66] and linear CD polymers, covalently bound to a therapeutic agent such as etoposide or tubulysin, for the treatment of breast, lung, colon, and ovarian cancer. For the latter example, efficacy studies in implanted HT-29 colorectal

carcinoma xenografts, treated with the CD polymer tubulysin, resulted in substantial antitumor activity during a 90-day study, without significant toxicity [67].

In 2019, Yale University patented spatiotemporally tuned particles (STPs) for spatial and temporal delivery of two or more agents to the same targeted cell. The STPs comprise a polymeric core containing one drug and a functional surface that could be a CD for further complexation with another drug, the first to be released. In vivo studies on female C57BL6/J mice administered with SPTs and tamoxifen demonstrated a superior immune tolerance compared to simple co-encapsulated nanoparticles [68]. Undoubtedly, CDs have accompanied the search and development of cancer therapies, in which they have been used as solubilizers, and, more recently, in the development of platforms for the controlled release of anticancer drugs. These efforts are expected to bear fruit in the short term.

3.1.7. CDs in Antiviral Therapies

The case of Community 10 reflects the appealing role that CDs have played in developing antiviral therapies. Several antivirals are far ideal due to their low aqueous solubility, low permeability, and short half-life. CDs can form ICs with some of these drugs, overcoming the limitations mentioned above [69,70]. Such is the case of remdesivir, the first recommended drug to treat COVID-19, a low water-soluble compound formulated as an IC with SBEβCD for IV administration [71]. CDs have also been explored in conjugates [72] and nano delivery systems [73]. CDs also exhibit an antiviral profile by themselves [74,75]. Moreover, HPβCD has debuted in the field of vaccines, with its use in the Janssen COVID-19 biologic [8,76]. The following are some examples of patents employing CDs in the development of antiviral therapies.

A patent registered in the early 1990s disclosed a preparation for intranasal administration to treat the common cold caused by rhinoviruses of ICs formed from CDs and diverse antiviral compounds. The preparation enabled continuous and controlled drug delivery for sustained periods [77]. An invention filed in 2003 described pharmaceutical compositions of antiviral proteins (i.e., cyanovirins) for the treatment or prevention of infections caused by retroviruses, in particular HIV-1 or HIV-2, in which CDs perform as absorption enhancers [78]. In another case, βCD was used to block viruses' ability to infect the cells by disrupting the host's lipid raft structure through cholesterol extraction to treat or prevent AIDS, genital herpes, or human papillomaviruses [79]. Another innovation describes the use of 3,3′-di-indolymethane to treat respiratory syncytial virus infection and how CDs enable a diversity of formulations: aerosols, dry particles for oral use, and emulsions for IV and parenteral administration. The formulations resulted in a significant reduction in viral counts in the lung tissues of RSV-infected Balb/c mice [80]. A recent patent claims a CD derivative as a broad spectrum virucidal. The CD is functionalized with sulfonic acid groups to mimic the negatively charged surface of cell receptors, commonly used by the viruses for attachment (i.e., heparan sulfate proteoglycans), thus preventing virus entry into cells [81]. Certainly, CDs' versatility in the development of antiviral therapies makes them an appealing tool that is gaining attention in the fight against viral infections, including SARS-CoV-2 [70,82,83].

3.1.8. CDs and Anti-Inflammatory Drugs

Optimization of formulations containing anti-inflammatory drugs has succeeded with several commercial products (Table S1). This could explain Community 5, one of the largest within the network generated under the "*Use*" context. The same is true for Community 7, pointing out CDs to formulate analgesics through the word *pain*. As expected, numerous patents have been published on this topic over the last decades. For example, in 1992, Chiesi Farmaceutici, S.p.A. filed a patent related to preparing βCD/piroxicam ICs and their different dosage forms. When formulated as tablets, they resulted in a higher dissolution rate than piroxicam alone, improving pharmacokinetics and gastric tolerability. Additionally, the ICs were advantageous to the preparation of pharmaceutical compositions for rectal and topical administration [84]. βCD/piroxicam oral tablets are still marketed in

Europe by the same laboratory under the trade name of Cycladol® (Chiesi Farmaceutici S.p.A., Parma, Italy).

In another example, a CD/ibuprofen clathrate to be taken as a hot drink was patented in 1993 [85]. Other recent patents describe CD/NSAID aqueous solutions or liquid throat sprays [86,87]. Interestingly, Albuquerque et al. published a patent related to the preparation of CD conjugates with anti-inflammatory drugs, displaying anti-tumoral properties, exemplifying Community 4, which contains both words [88]. Comprehensive reviews about patents of CDs and anti-inflammatory drugs and analgesics have been presented before [89,90].

In summary, the analysis of both *Novelty* and *Use* complex networks reaffirmed how CDs have supported the preparation of aqueous solutions by enhancing drug solubility and exposed the relevance of CDs in tablets and powders. Additionally, it pointed out the important role that CDs have played in the formulation of anti-inflammatory drugs, the optimization of cancer therapies, and the development of antiviral strategies.

It is well known that a complex network is the consequence of a growth process (the increment in the number of nodes over time) with preferential attachment, meaning that a new node tends to link to the more connected nodes ("the richest get richer") [41]. That means that for the CDs resulting in complex networks, a discovery or innovation may trigger new ones; new patents with similar content emerge and, eventually, generate a community. In other words, solubility enhancement was initially the ultimate goal of CD ICs. Later, novel effects based on improved solubility gave rise to cutting-edge consolidated and emergent applications.

3.2. Analysis of Patenting Trends by Text-Mining

The resulting networks indicate that most of the patents are related to solubility enhancement for the subsequent development of suitable dosage forms (i.e., solutions, powders, and tablets) for determined purposes, which could be somehow expected. However, knowing the patenting patterns over time will enrich the understanding of the CDs' complex networks (see above, Section 3.1) and may give an insight into the possible technological opportunities in the field of CDs. Accordingly, we carried out further mining of the 1998 patent dataset, now guided by words corresponding to pharmaceutical dosage forms, aiming to inform the number of patents related to each of them and how they have evolved. We emphasized our analysis on solutions, powders, and tablets. However, we were motivated to mine other dosage forms to get a broader overview of the technological trends of CDs.

Figure 6 shows that CDs are present in a diversity of dosage forms and most of the patents are related to aqueous solutions, tablets, and powders. The latter is in accordance with what network analysis pointed out (Section 3.1.5).

3.2.1. Solutions

Most of the patents in our dataset refer to aqueous solutions, with 413 retrieved records (Figure 6). These outcomes support the observations arisen from Figure 4, showing that the network's largest community is formed from patents related to aqueous solutions, certainly resulting from CD/drug-soluble ICs. This result is not surprising, as CDs have been primarily studied for their ability to form water-soluble ICs with poorly soluble compounds to yield aqueous solutions for parenteral, enteral, or local administration [91–93]. We highlight the case of ophthalmic and nasal solutions, described in the analysis of Community 11 (Section 3.1.5), which appeared as an emerging trend, as discussed in our previous work, which also mentions examples of patents issued for CD-based aqueous solutions for parenteral, nasal, and ocular administration [1].

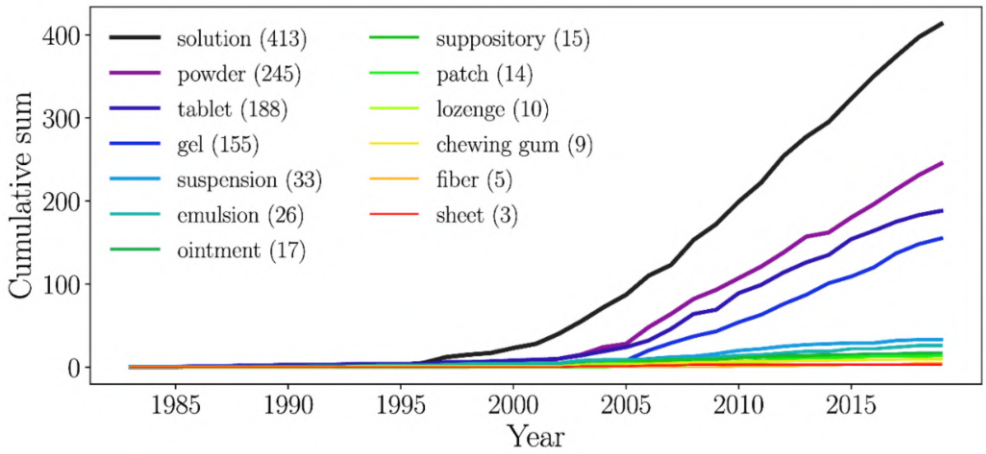

Figure 6. Patenting trends according to CD-based dosage forms.

Since the early 2000s, the number of issued patents in this area has grown significantly, and this trend remains the same up to this day, reflecting that the use of CDs for solubility enhancement is not old-fashioned. On the contrary, the modification of apparent solubility through CDs, although not a novelty, is still a very valid approach in pharmaceutics, including drug-repurposing and the development of innovative therapies, whose performance depends on the suitable solubility of one or more of their components.

3.2.2. Powders

Figure 6 shows that powders and tablets emerged jointly in the early 2000s, and, after 2005, both had substantial growth. However, it is notable that the number of patents for powders is higher since these patents may refer to powders as the final form (for example, for nasal or pulmonary administration) or to intermediates that are further reconstituted for parenteral administration or processed to produce other physical forms (i.e., tablets or hard gelatin capsules). These results are in accordance with Table 2, which shows the contribution of the word *powder* on defining communities in both *Novelty* and *Use* networks.

An example of a powder technology as a final dosage form is a patent filed in 2019 by Pfizer Inc. (New York, NY, USA), comprising a tetrahydroquinazoline derivative, a KRAS inhibitor (one of the most hard-to-hit cancer-related proteins), in the form of dry powder for inhalation or intranasal administration; the formulation uses a CD as a solubilizer, stabilizer, taste-masking, and bioadhesive agent [94]. In another case, the βCD/ethinyl estradiol IC is patented as an amorphous powder for further processing into tablets, lozenges, or pellets. The complexation with βCD resulted in enhanced API solubility and stability and improved batch-to-batch reproducibility [95].

The patenting rate in CD-based powders is increasing, and thorough investigation into the role of CDs in the mucoadhesion, rheological and mechanical properties of powders may boost the development of CD-based powder technologies for innovative therapies, an already attractive emerging area.

3.2.3. Tablets

Tablets are the most common dosage forms for oral administration. They are advantageous because of their high-precision dosing; chemical, physical, and microbiological stability; and affordable manufacturing processes. The latter generally comprises the compression of mixtures containing the active ingredient and one or more excipients. CDs play an essential role as multifunctional excipients for these dosage forms. CDs can work as direct compression fillers, binders, and disintegrating components of the mixture; they can stabilize the formulation and improve its organoleptic properties. Moreover, they can increase the dissolution rate, improving the oral bioavailability of the Biopharmaceutics Classification System Class II and IV drugs and modifying the API's release profile. They

can be used for uncoated and coated, orally disintegrating, effervescent, modified release, osmotic pump, chewable, mucoadhesive-buccal, and sublingual tablets [42].

All these recognized attributes give CDs a significant presence in the formulation of these dosage forms, as evidenced by the number of commercial tablets containing CDs (Table S1) and the significant increase in the number of patents since 2005 (Figure 6). Examples of patented technologies include a tablet containing an active compound to treat acute myeloid leukemia. In this formulation, HPβCD enables the required moldability, stability, ease of disintegration, and solubility, resulting in a composition of rapid dispersibility, dissolution, and bioavailability [96]. A βCD/progesterone IC, formulated as a rapidly disintegrating tablet for sublingual administration, demonstrating greater drug bioavailability, is another example of a recent patent [97]. Likewise, a newfangled innovative work claims that the use of insoluble and water-soluble fractions of a CD polymer conjugate generates a multifunctional excipient—with distinctive compression, drug dispersion, solubilization, and disintegration—for tablet formulations containing insoluble active ingredients [98].

Patents for tablets account for 188 files and are in the third place of importance after aqueous solutions and powders, also reflected in the communities formed through this word within the networks discussed before. Indeed, research around the multifunctional performance of CDs for oral, buccal, and sublingual tablets [99,100] would strengthen these technologies in the short term.

3.2.4. Gels

Motivated by the course observed for patents related to the word *gel*, we included a brief discussion of it in this section, despite that *gel* was not in the 10 top-ranked words. Gels accounted for 155 records in the dataset. In 2010, their growth began to differ markedly, and numerous patents, reporting CDs to develop hydrogels for pharmaceutical applications, have been granted since then.

In hydrogels, CDs can be covalently attached to give rise to supramolecular architectures with tunable drug release profiles. If CD cavities are available, they can host drug molecules while simultaneously preventing their release upon media dilution. Moreover, promising potential for delivering the drugs in a sequential manner or in response to a stimulus has been observed [101]. We briefly describe some examples of patents related to CD-based gels: a thermosensitive gel formed by polyethylene glycol, αCD, and polycaprolactone to deliver a neurolytic agent to treat certain cardiopulmonary conditions has been patented [102]; a thermoreversible system that gels upon contact with the body to sustain drug release, in which CDs act as temperature modulating agents (studies in guinea pigs, female sheep, rabbits, and Sprague–Dawley rats showed that the gel sustained the release of the active agent for periods of 5 to 7 days) [103]; an implant substance comprising an injectable tissue adhesive hydrogel, including γCD, used as a skin glue to promote tissue regeneration [104]; an aqueous system for local administration of antifungal or antipsoriatic drugs (i.e., hydrocortisone, triamcinolone acetonide, econazole) for treating nail diseases; it consists of a thermosensitive hydrogel, liquid at room temperature, that gels once applied on the nail's surface, forming a thin film; a methylated derivative of βCD is used as a solubilizing agent, enabling high concentrations of hydrophobic active agents) [105].

The convergence of nanotechnology and pharmaceutical and materials sciences is reflected in nanosystems like the one patented by Fahmy et al. in 2017, which comprises a lipidic nanoshell surrounding a CD-based hydrogel containing a drug to treat the symptoms of inflammatory or autoimmune diseases [106].

Photo-responsive βCD supramolecular hydrogels for delivering drugs on demand [107], injectable αCD hydrogels for plasmid delivery [108], chitosan–βCD hydrogels for wound dressing [109], and gelatin–βCD self-healing gels for cell delivery [110] show how recent research is expanding the scope of fascinating CD-based hydrogel technologies. Hence, CD-based gels are an emerging technology, and a significant increase in research, patents, and innovations in this direction is expected in the years to come.

3.2.5. Other Dosage Forms

Figure 6 shows that the use of CDs for other dosage forms, namely, suspensions, emulsions, ointments, suppositories, patches, lozenges, chewing gums, fibers, and sheets, has been explored. The patenting rate has remained unchanged over time; nevertheless, CDs' performance proves their versatility and potential as functional excipients for those formulations.

3.2.6. Suspensions

In the case of suspensions, those for ophthalmic administration stand out, where it has been shown that CDs improve physical and chemical stability, can act as permeability enhancers, and decrease eye irritation [49,111,112]. For instance, there is a patent that describes an aqueous ophthalmic suspension comprising solid CD/drug (i.e., dexamethasone) particles, ranging from 10 nm to 1 mm in size, suspended in the aqueous phase to treat conditions of the posterior segment of the eye (impossible to reach with conventional eye drops), such as the vitreous and optic nerve. In vivo studies in female albino rabbits showed how the ocular suspension enhances drug delivery into the posterior segment of the eye [113].

CDs have also been helpful as suspending agents, thus enabling the development of suspensions intended for being administered by other routes. Such is the case of an invention registered in 2019 that presents the composition, methods, and systems for nasal or pulmonary delivery of a biologically active compound for the treatment of inflammatory or obstructive pulmonary disease through a metered-dose inhaler, where CDs control the solubility of the system and also act as suspending agents [114]. More investigation about CDs' role in suspensions, their interaction with the rest of the formulation components, and their performance as suspending agents can expand their potential in these dosage forms.

3.2.7. Emulsions

Emulsions can be prepared using CDs instead of surfactants [115] and are very useful in Pickering pharmaceutical emulsion stabilization [116]. In 2012, Laza-Knoerr et al. patented emulsions with remarkable stability, containing CD-based polymers and lipophilic compounds, the methods to obtain them, and their uses. Emulsion stabilization is given by host–guest interactions between the CD polymers and the lipophilic active ingredients without using organic solvents, surfactants, co-surfactants, or other additives, thus showing great potential for pharmaceutical applications [117]. Although CDs appear as an attractive tool to formulate surfactant-free emulsions, their application in these pharmaceutical technologies remains unrevealed.

3.2.8. Chewing Gums

Medicated chewing gums represent a very particular dosage form useful for local (dental health or buccal therapies) or systemic drug delivery. For the latter, it overcomes the limitations associated with gastrointestinal drug degradation and first-pass metabolism. The drug release depends on its aqueous solubility: water-soluble drugs are fully and rapidly released, whereas poor-soluble substances are slowly and incompletely delivered [118]. CDs have been successfully used as solubilizers and taste-masking agents for these technologies [119]. There is an invention describing compressed chewing gums containing peptides of 5 to 11 amino acids (i.e., antimicrobial peptides) for their buccal administration. In these compositions, CD derivatives are used as absorption enhancers and bulk sweeteners [120]. Despite the challenges related to the formulation of medicated chewing gums, they represent a suitable alternative for drug administration for children, geriatrics, and patients with severe sore throat conditions. More investigation is required to expand the potential of these dosage forms. Lozenges, along with other formulations for oral and buccal administration, were discussed in our previous work [1].

3.2.9. Patches and Fibers

The transdermal patch has become an important pharmaceutical technology in the last decade due to its many advantages, such as the sustained delivery of drugs across the skin into systemic circulation while bypassing first-pass metabolism, avoidance of gastric drug degradation, and low dosage requirements. However, direct loading of low-soluble drugs into patches for their transdermal delivery is still challenging [121]. CDs have been demonstrated to overcome drug solubility limitations and improve stability when loaded into patches [122–124]. The same is true for buccal patches, in which the solubilizing and stabilizing abilities of CDs, combined with their mucoadhesive properties, clearly evidences the great potential of CDs for this aim [125]. CDs have also had a suitable performance in the fabrication of drug-loaded transdermal fibers [126] and even as wearable epidermal biosensors [127] and coated implants [128]. As expected, fascinating recent innovations have arisen in this field. One of them is a CD-collagen-based matrix composition used as a therapeutic eye patch for corneal repair. In this technology, CDs increased collagen thermal stability and reduced collagen fibrogenesis [129]. In 2015, an invention registered by Caltech described a layered polymeric monofilament fiber drug delivery device, suitable for implantation in a patient, to control the delivery of antibiotics or antimicrobial drugs to treat periodontitis and ocular diseases, among others. The device comprises at least two side-by-side layers exposed to the environment, and the drug release is tuned by controlling the characteristics of the individual fibers, such as chemical composition and structural design. Incorporating CDs through covalent or non-covalent interactions to the backbone polymer yields a structure (crosslinked through host–guest interactions) that enables the gradual release of the therapeutic agent over a determined period of time. Some of the performed in vitro studies showed that, in the implant, the two fibers sustained the release of levofloxacin over 10–15 days, while a third fiber released 90% of levofloxacin on the first day. In in vivo studies, in which the levofloxacin-loaded device was implanted in the eyes of New Zealand white rabbits, showed levels of levofloxacin, detected in tears, that were expected to have antimicrobial effects for 6 days [130].

Undoubtedly, CDs' ability to modify the aqueous solubility of a guest molecule has positioned CDs in the pharmaceutical field and triggered novel new effects based or associated with it, making CDs applicable to the development of a variety of dosage forms. The progress in materials science, supramolecular chemistry, and nanotechnology may lead to striking innovations and, therefore, an increment in patenting of those dosage forms that have not received much attention but in which CDs could play a vital role. Patches and fibers must be underscored as they are backed up by recent fascinating research. The same is true for the suppositories discussed in our previous work [1]. The potential of CDs in suspensions and emulsions has yet to be recognized. Although the utility of CDs for chewing gums is undeniable, an in-depth investigation is needed for these alternative pharmaceutical forms.

4. Conclusions

Data science tools automatically enabled the immediate visualization of CD pharmaceutical technologies. CD patents formed complex networks that evidenced how solubility enhancement employing CDs has triggered cutting-edge applications for a variety of pharmaceutical purposes.

Most CD pharmaceutical patents were associated with the development of aqueous solutions for parenteral or local administration. Significant technological progress is observed for tablets, while gels seem to be very promising. Patches and fibers using CDs are emerging, and fascinating recent research backing them up may elicit an increment in their patenting trend in the short term. The potential of CDs in suspensions and emulsions has yet to be recognized, and a better understanding of CDs in these dosage forms will make these technologies a great opportunity area. Optimization of cancer therapies through CDs has been widely explored, while antiviral approaches could reach the same maturity level in the short term.

The interest in CDs is still increasing, and, based on our analysis, this trend will continue in the coming years due to their versatility and fascinating ability to improve pharmaceutical formulations in the design of innovative therapies.

Through the approach presented herein, which can also be implemented to analyze scientific papers, we aim to contribute to the intercourse between scientific and technological literature that, in turn, in an integrated manner, can foster innovations for both academia and industry for CDs and other materials with potential in the pharmaceutical and drug delivery fields.

Supplementary Materials: The following are available online at https://www.mdpi.com/article/10.3390/pharmaceutics13081297/s1, Table S1: Commercially available CD-based formulations. References [6–11,42,90,131–133] are cited in the supplementary materials.

Author Contributions: Conceptualization, Y.R.-A., A.P.R. and Y.C.A.-A.; Data curation, A.P.R.; Formal analysis, Y.R.-A.; Funding acquisition, Y.R.-A.; Investigation, Y.R.-A. and J.R.-L.; Methodology, A.P.R. and J.R.-L.; Project administration, Y.R.-A.; Software, A.P.R.; Visualization, A.P.R. and J.R.-L.; Writing—original draft, Y.R.-A., A.P.R., J.R.-L. and Y.C.A.-A.; Writing—review and editing, Y.R.-A., A.P.R. and Y.C.A.-A. All authors have read and agreed to the published version of the manuscript.

Funding: This research was funded by the Materials Research Institute UNAM (Project 1306) and the National Autonomous University of Mexico (Project PAPIIT-UNAM IA200821).

Institutional Review Board Statement: Not applicable.

Informed Consent Statement: Not applicable.

Data Availability Statement: The codes are available from the authors upon request.

Acknowledgments: R.-L.J. thanks CONACyT for the MSc. scholarship (CVU-1032640).

Conflicts of Interest: The authors declare no conflict of interest.

References

1. Rincón-López, J.; Almanza-Arjona, Y.C.; Riascos, A.P.; Rojas-Aguirre, Y. Technological evolution of cyclodextrins in the pharmaceutical field. *J. Drug Deliv. Sci. Technol.* **2020**, *61*, 102156. [CrossRef] [PubMed]
2. Jambhekar, S.S.; Breen, P. Cyclodextrins in pharmaceutical formulations i: Structure and physicochemical properties, formation of complexes, and types of complex. *Drug Discov. Today* **2016**, *21*, 356–362. [CrossRef]
3. Varan, C.; Şen, M.; Sandler, N.; Aktaş, Y.; Bilensoy, E. Mechanical characterization and Ex Vivo Evaluation of anticancer and antiviral drug printed bioadhesive film for the treatment of cervical cancer. *Eur. J. Pharm. Sci.* **2019**, *130*, 114–123. [CrossRef]
4. Feng, Q.; Wei, K.; Lin, S.; Xu, Z.; Sun, Y.; Shi, P.; Li, G.; Bian, L. Mechanically resilient, injectable, and bioadhesive supramolecular gelatin hydrogels crosslinked by weak host-guest interactions assist cell infiltration and in situ tissue regeneration. *Biomaterials* **2016**, *101*, 217–228. [CrossRef]
5. Tian, B.; Hua, S.; Liu, J. Cyclodextrin-based delivery systems for chemotherapeutic anticancer drugs: A review. *Carbohydr. Polym.* **2020**, *232*, 115805. [CrossRef]
6. FDA. FDA-Approved Drugs: Baqsimi. Available online: https://www.accessdata.fda.gov/scripts/cder/daf/index.cfm?event=overview.process&ApplNo=210134 (accessed on 12 July 2021).
7. Sohajda, T. Cyclo Therapeutics Announces Design of Pivotal Phase 3 Study Evaluating Trappsol®CycloTM in Niemann-Pick Type C1. Available online: https://cyclodextrinnews.com/2021/04/29/cyclo-therapeutics-announces-design-of-pivotal-phase-3-study-evaluating-trappsol-cyclo-in-niemann-pick-type-c1/ (accessed on 7 July 2021).
8. FDA. Janssen COVID-19 Vaccine | FDA Emergency Use Authorization. Available online: https://www.fda.gov/emergency-preparedness-and-response/coronavirus-disease-2019-covid-19/janssen-covid-19-vaccine#additional (accessed on 6 July 2021).
9. FDA. COVID-19 Update: FDA Broadens Emergency Use Authorization for Veklury (Remdesivir) to Include All Hospitalized Patients for Treatment of COVID-19. Available online: https://www.fda.gov/news-events/press-announcements/covid-19-update-fda-broadens-emergency-use-authorization-veklury-remdesivir-include-all-hospitalized (accessed on 6 July 2021).
10. FDA. Drug Approval Package: Zulresso. Available online: https://www.accessdata.fda.gov/drugsatfda_docs/nda/2019/211371Orig1s000TOC.cfm (accessed on 12 July 2021).
11. FDA. Drug Approval Package: Voriconazole for Injection. Available online: https://www.accessdata.fda.gov/drugsatfda_docs/nda/2017/208562Orig1s000TOC.cfm (accessed on 12 July 2021).
12. Rodriguez-Esteban, R.; Bundschus, M. Text mining patents for biomedical knowledge. *Drug Discov. Today* **2016**, *21*, 997–1002. [CrossRef] [PubMed]
13. Asche, G. 80% of technical information found only in patents—Is there proof of this? *World Pat. Inf.* **2017**, *48*, 16–28. [CrossRef]

14. Agarwal, P.; Searls, D.B. Can literature analysis identify innovation drivers in drug discovery? *Nat. Rev. Drug Discov.* **2009**, *8*, 865–878. [CrossRef]
15. Boyack, K.W.; Smith, C.; Klavans, R. A detailed open access model of the pubmed literature. *Sci. Data* **2020**, *7*, 1–16. [CrossRef]
16. Bergeaud, A.; Potiron, Y.; Raimbault, J. Classifying patents based on their semantic content. *PLoS ONE* **2017**, *12*, 176310. [CrossRef] [PubMed]
17. Liu, C.; Zhou, Q.; Li, Y.; Garner, L.V.; Watkins, S.P.; Carter, L.J.; Smoot, J.; Gregg, A.C.; Daniels, A.D.; Jervey, S.; et al. Research and development on therapeutic agents and vaccines for COVID-19 and related human coronavirus diseases. *ACS Cent. Sci.* **2020**, *6*, 315–331. [CrossRef]
18. Sarica, S.; Luo, J.; Wood, K.L. TechNet: Technology semantic network based on patent data. *Expert Syst. Appl.* **2020**, *142*, 112995. [CrossRef]
19. Newman, M. *Networks: An Introduction*, 1st ed.; Oxford University Press: Oxford, UK, 2010; ISBN 9780199206650.
20. Vogt, M.; Stumpfe, D.; Maggiora, G.M.; Bajorath, J. Lessons Learned from the design of chemical space networks and opportunities for new applications. *J. Comput. Aided. Mol. Des.* **2016**, *30*, 191–208. [CrossRef]
21. Barabási, A.; Oltvai, Z.N. Network biology: Understanding the cell's functional organization. *Nat. Rev. Genet.* **2004**, *5*, 101–113. [CrossRef] [PubMed]
22. Recanatini, M.; Cabrelle, C. Drug research meets network science: Where are we? *J. Med. Chem.* **2020**, *63*, 8653–8666. [CrossRef]
23. Müller, A.C.; Guido, S. *Introduction to Machine Learning with Python*, 1st ed.; O´REILLY: Murrieta, CA, USA, 2017; ISBN 9781449369415.
24. Gan, G.; Ma, C.; Wu, J. *Data Clustering: Theory, Algorithms, and Applications*, 2nd ed.; ASA-SIAM Series on Statistics and Applied Probability; ASA-SIAM: Philadelphia, PA, USA, 2007; ISBN 9780898716238.
25. Pereira, C.G.; Picanco-Castro, V.; Covas, D.T.; Porto, G.S. Patent mining and landscaping of emerging recombinant factor viii through network analysis. *Nat. Biotechnol.* **2018**, *36*, 585–590. [CrossRef] [PubMed]
26. Kononova, O.; He, T.; Huo, H.; Trewartha, A.; Olivetti, E.A.; Ceder, G. Opportunities and challenges of text mining in materials research. *iScience* **2021**, *24*, 1–20. [CrossRef] [PubMed]
27. McCoy, K.; Gudapati, S.; He, L.; Horlander, E.; Kartchner, D.; Kulkarni, S.; Mehra, N.; Prakash, J.; Thenot, H.; Vanga, S.V.; et al. Biomedical text link prediction for drug discovery: A case study with covid. *Pharmaceutics* **2021**, *13*, 794. [CrossRef]
28. Barnard, A.S.; Opletal, G. Predicting structure/property relationships in multi-dimensional nanoparticle data using t-distributed stochastic neighbour embedding and machine learning. *Nanoscale* **2019**, *11*, 23165–23172. [CrossRef] [PubMed]
29. Sizochenko, N.; Syzochenko, M.; Fjodorova, N.; Rasulev, B.; Leszczynski, J. Evaluating genotoxicity of metal oxide nanoparticles: Application of advanced supervised and unsupervised machine learning techniques. *Ecotoxicol. Environ. Saf.* **2019**, *185*, 109733. [CrossRef]
30. Peng, T.; Wei, C.; Yu, F.; Xu, J.; Zhou, Q.; Shi, T.; Hu, X. Predicting nanotoxicity by an integrated machine learning and metabolomics approach. *Environ. Pollut.* **2020**, *267*, 115434. [CrossRef] [PubMed]
31. Brown, K.A.; Brittman, S.; Maccaferri, N.; Jariwala, D.; Celano, U. Machine learning in nanoscience: Big data at small scales. *Nano Lett.* **2020**, *20*, 2–10. [CrossRef] [PubMed]
32. Severson, K.A.; Attia, P.M.; Jin, N.; Perkins, N.; Jiang, B.; Yang, Z.; Chen, M.H.; Aykol, M.; Herring, P.K.; Fraggedakis, D.; et al. Data-Driven prediction of battery cycle life before capacity degradation. *Nat. Energy* **2019**, *4*, 383–391. [CrossRef]
33. Tshitoyan, V.; Dagdelen, J.; Weston, L.; Dunn, A.; Rong, Z.; Kononova, O.; Persson, K.A.; Ceder, G.; Jain, A. Unsupervised word embeddings capture latent knowledge from materials science literature. *Nature* **2019**, *571*, 95–98. [CrossRef]
34. Lee, C.; Kwon, O.; Kim, M.; Kwon, D. Early identification of emerging technologies: A machine learning approach using multiple patent indicators. *Technol. Forecast. Soc. Chang.* **2018**, *127*, 291–303. [CrossRef]
35. Hu, J.; Li, S.; Yao, Y.; Yu, L.; Yang, G.; Hu, J. Patent keyword extraction algorithm based on distributed representation for patent classification. *Entropy* **2018**, *20*, 104. [CrossRef]
36. Bird, S.; Klein, E.; Loper, E. *Natural Language Processing with Python*, 1st ed.; O´REILLY: Murrieta, CA, USA, 2009; ISBN 9780596516499.
37. McKinney, W. Data structures for statistical computing in python. In Proceedings of the 9th Python in Science Conference (SciPy 2010), Austin, TX, USA, 28 June–3 July 2010; Volume 1697900, pp. 51–56.
38. Hagberg, A.A.; Schult, D.A.; Swart, P.J. Exploring network structure, dynamics, and function using networkx. In Proceedings of the 97th Python in Science Conference, Pasadena, CA, USA, 19–24 August 2008; pp. 11–15.
39. Blondel, V.D.; Guillaume, J.-L.; Lambiotte, R.; Lefebvre, E. Fast unfolding of communities in large networks. *J. Stat. Mech. Theory Exp.* **2008**, *2008*, P10008. [CrossRef]
40. USP. Nomenclature guidelines. *Br. J. Pharmacol.* **2016**, *148*, 121–122. [CrossRef]
41. Barabási, A.-L. *Network Science*, 1st ed.; Cambridge University Press: Cambridge, UK, 2016; ISBN 1107076269.
42. Conceição, J.; Adeoye, O.; Cabral-marques, H.M.; Manuel, J.; Lobo, S. Cyclodextrins as excipients in tablet formulations. *Drug Discov. Today* **2018**, *23*, 1274–1284. [CrossRef]
43. Cabral-Marques, H.M. A review on cyclodextrin encapsulation of essential oils and volatiles. *Flavour Fragance J.* **2010**, *25*, 313–326. [CrossRef]

44. De Oliveira-Filho, R.D.; e Silva, A.R.A.; de Azevedo Moreira, R.; Nogueira, N.A.P. Biological activities and pharmacological applications of cyclodextrins complexed with essential oils and their volatile components: A systematic review. *Curr. Pharm. Des.* **2018**, *24*, 3951–3963. [CrossRef] [PubMed]
45. Loftsson, T.; Stefánsson, E. Cyclodextrins and topical drug delivery to the anterior and posterior segments of the eye. *Int. J. Pharm.* **2017**, *531*, 413–423. [CrossRef]
46. Saraganachari, A.; Narayanaswame, A.; Reddy, S.; Shivakumar, P. Ophthalmic Compositions of Brinzolamide. Patent WO 2019/207380A1, 31 October 2019.
47. El-Shabrawi, Y. Methods and Compositions for the Treatment of Ophthalmic Conditions. U.S. Patent 2019/0070198A1, 7 March 2019.
48. Grimaudo, M.A.; Nicoli, S.; Santi, P.; Concheiro, A.; Alvarez-Lorenzo, C. Cyclosporine-Loaded cross-linked inserts of sodium hyaluronan and hydroxypropyl-β-cyclodextrin for ocular administration. *Carbohydr. Polym.* **2018**, *201*, 308–316. [CrossRef]
49. Jansook, P.; Kulsirachote, P.; Asasutjarit, R.; Loftsson, T. Development of celecoxib eye drop solution and microsuspension: A comparative investigation of binary and ternary cyclodextrin complexes. *Carbohydr. Polym.* **2019**, *225*, 115209. [CrossRef]
50. Ahn, J.H.; Kim, H.-D.; Abuzar, S.M.; Lee, J.Y.; Jin, S.E.; Kim, E.K.; Hwang, S.J. Intracorneal melatonin delivery using 2-Hydroxypropyl-β-cyclodextrin ophthalmic solution for granular corneal dystrophy type. *Int. J. Pharm.* **2017**, *529*, 608–616. [CrossRef]
51. Li, R.; Guan, X.; Lin, X.; Guan, P.; Zhang, X.; Rao, Z.; Zhao, J.; Du, L.; Rong, J.; Zhao, J. Poly(2-Hydroxyethyl Methacrylate)/β-cyclodextrin-hyaluronan contact lens with tear protein adsorption resistance and sustained drug delivery for ophthalmic diseases. *Acta Biomater.* **2020**, *110*, 1–14. [CrossRef] [PubMed]
52. Johannsdottir, S.; Jansook, P.; Stefansson, E.; Myrdal, I.; Loftsson, T. Topical drug delivery to the posterior segment of the eye: Dexamethasone concentrations in various eye tissues after topical administration for up to 15 days to rabbits. *J. Drug Deliv. Sci. Technol.* **2018**, *45*, 449–454. [CrossRef]
53. Lowenthal, R.; Maggio, E.T.; Bell, R.G.; Shah, P. Intranasal Epinephrine Formulations and Methods for the Treatment of Disease. Patent WO 2019157099A1, 15 August 2019.
54. Sedel, F.; Haik, S.; Bizat, N. Method for Treating Prion Disease. Patent EP 3603649A1, 31 July 2018.
55. Rassu, G.; Fancello, S.; Roldo, M.; Malanga, M.; Szente, L.; Migheli, R.; Gavini, E.; Giunchedi, P. Investigation of cytotoxicity and cell uptake of cationic beta-cyclodextrins as valid tools in nasal delivery. *Pharmaceutics* **2020**, *12*, 658. [CrossRef]
56. Liu, S.; Ho, P.C. Intranasal administration of brain-targeted HP-β-CD/chitosan nanoparticles for delivery of scutellarin, a compound with protective effect in cerebral ischaemia. *J. Pharm. Pharmacol.* **2017**, *69*, 1495–1501. [CrossRef]
57. Tian, B.; Liu, Y.; Liu, J. Cyclodextrin as a magic switch in covalent and non-covalent anticancer drug release systems. *Carbohydr. Polym.* **2020**, *242*, 116401. [CrossRef]
58. Stoddart, J.F.; Alston, D.R. Solubilized Platinum Compound. U.S. Patent 4696918, 29 September 1987.
59. DeGregorio, M.W.; Kurkela, K.O.A. Topical Administration of Toremifene and Its Metabolites. U.S. Patent 5605700, 25 February 1997.
60. Hamada, H.; Saito, K.; Mikuni, K.; Kuwahara, N.; Takahshi, H. Cyclodextrin Inclusion Complex of Taxol and Method for Its Production and Its Use. U.S. Patent 5,684,169, 4 November 1997.
61. Rubinfeld, J. Pharmaceutical Formulation. U.S. Patent 5,602,112, 11 February 1997.
62. ClinicalTrials. Trial of CRLX101 in People with Relapsed/Refractory Small Cell Lung Cancer. Available online: https://clinicaltrials.gov/ct2/show/study/NCT02769962 (accessed on 19 December 2020).
63. Weiss, G.J.; Chao, J.; Neidhart, J.D.; Ramanathan, R.K.; Bassett, D.; Neidhart, J.A.; Choi, C.H.J.; Chow, W.; Chung, V.; Forman, S.J.; et al. First-in-human phase 1/2a trial of CRLX101, a cyclodextrin-containing polymer-camptothecin nanopharmaceutical in patients with advanced solid tumor malignancies. *Investig. New Drugs* **2013**, *31*, 986–1000. [CrossRef]
64. Cheng, J.; Davis, M.E.; Khin, K.T. Cyclodextrin-Based Polymers for Delivering the Therapeutic Agents Covalently Bound Thereto. Patent EP 1534340, 4 September 2011.
65. Ryan, J. Treatment of Cancer. U.S. Patent 2016/0058875A1, 3 March 2016.
66. Voss, M.H.; Hussain, A.; Vogelzang, N.; Lee, J.L.; Keam, B.; Rha, S.Y.; Vaishampayan, U.; Harris, W.B.; Richey, S.; Randall, J.M.; et al. A randomized phase ii trial of CRLX101 in combination with bevacizumab versus standard of care in patients with advanced renal cell carcinoma. *Ann. Oncol.* **2017**, *28*, 2754–2760. [CrossRef]
67. Davis, M.E.; Hwang, J.; Ke, T.; Lim, C.; Schluep, T. Polymeric Drug Conjugates with Tether Groups for Controlled Drug Delivery. U.S. Patent 2018/0008719A1, 11 January 2018.
68. Fahmy, T.M.; Kong, P.; Bickerton, S.; Mchugh, M.D.; Lee, J.S. Particles for Spatiotemporal Release of Agents. Patent WO 2019/217552A1, 14 November 2019.
69. Nair, A.B.; Attimarad, M.; Al-dhubiab, B.E.; Wadhwa, J.; Harsha, S.; Ahmed, M. Enhanced oral bioavailability of acyclovir by inclusion complex using hydroxypropyl-β—Cyclodextrin. *Drug Deliv.* **2014**, *21*, 7544. [CrossRef]
70. Garrido, P.F.; Calvelo, M.; Blanco-González, A.; Veleiro, U.; Suárez, F.; Conde, D.; Cabezón, A.; Piñeiro, Á.; Garcia-Fandino, R. The lord of the nanorings: Cyclodextrins and the battle against SARS-CoV. *Int. J. Pharm.* **2020**, *588*, 119689. [CrossRef]
71. De Wit, E.; Feldmann, F.; Cronin, J.; Jordan, R.; Okumura, A.; Thomas, T.; Scott, D.; Cihlar, T.; Feldmann, H. Prophylactic and therapeutic remdesivir (GS-5734) treatment in the rhesus macaque model of MERS-CoV infection. *Proc. Natl. Acad. Sci. USA* **2020**, *117*, 6771–6776. [CrossRef]

72. Pedotti, S.; Pistarà, V.; Cannavà, C.; Carbone, C.; Cilurzo, F.; Corsaro, A.; Puglisi, G.; Anna, C. Synthesis and physico-chemical characterization of a ß-cyclodextrin conjugate for sustained release of acyclovir. *Carbohydr. Polym.* **2015**, *131*, 159–167. [CrossRef] [PubMed]
73. Lembo, D.; Trotta, F.; Cavalli, R. Cyclodextrin-based nanosponges as vehicles for antiviral drugs: Challenges and perspectives. *Nanomedicine* **2018**, *13*, 477–480. [CrossRef]
74. Braga, S.S. Cyclodextrins: Emerging medicines of the new millennium. *Biomolecules* **2019**, *9*, 801. [CrossRef]
75. Jones, S.T.; Cagno, V.; Janeček, M.; Ortiz, D.; Gasilova, N.; Piret, J.; Gasbarri, M.; Constant, D.A.; Han, Y.; Vuković, L.; et al. Modified cyclodextrins as broad-spectrum antivirals. *Sci. Adv.* **2020**, *2*, eaax9318. [CrossRef] [PubMed]
76. Puskás, I. Cyclodextrin News: HPβCD Is a Unique Component in Janssen's COVID-19 Vaccine Candidate. Available online: https://cyclodextrinnews.com/2021/02/25/hpbcd-is-a-unique-component-in-janssens-covid-19-vaccine-candidate/ (accessed on 6 July 2021).
77. Mesens, J.L.; Andries, K.J.L. Antiviral Pharmaceutical Compositions Containing Cyclodextrins. U.S. Patent 4,956,351, 11 September 1990.
78. Boyd, M.R. Conjugates of Antiviral Proteins or Peptides and Virus Or Viral Envelope Glycoproteins. U.S. Patent 6586392B2, 1 July 2003.
79. Hildreth, J.E. β-Cyclodextrin Compositions, and Use to Prevent Transmission of Sexually Transmitted Disease. U.S. Patent 7589080B2, 15 September 2009.
80. Zeligs, M.A. Use of Diindolymethane-Related Indoles for the Treatment and Prevention of Respiratory Syncytial Virus Associated Conditions. U.S. Patent 7989486B2, 2 August 2011.
81. Jones, S.; Stellacci, F. Virucidal Compounds and Uses Thereof. U.S. Patent 2019/0275073, 12 September 2019.
82. Braga, S.S.; Barbosa, J.S.; Santos, N.E.; El-Saleh, F.; Paz, F.A.A. Cyclodextrins in antiviral therapeutics and vaccines. *Pharmaceutics* **2021**, *13*, 409. [CrossRef] [PubMed]
83. Jicsinszky, L.; Martina, K.; Cravotto, G. Cyclodextrins in the antiviral therapy. *J. Drug Deliv. Sci. Technol.* **2021**, *64*, 102589. [CrossRef]
84. Carli, F.; Chiesi, P. Process for Preparing Piroxicam/Cyclodextrin Complexes, the Products Obtained and Their Pharmaceutical Compositions. U.S. Patent 5,164,380, 17 November 1992.
85. Grattan, T.J. Use of Ibuprofen-Beta-Cyclodextrin Complex for Oral Consumption. Patent EP 0633787B1, 2 April 1993.
86. Beech, E.; Rodwell, A.; Squires, M. Pharmaceutical Formulation Comprising NSAID and Cyclodextrin. U.S. Patent 9138482B2, 22 September 2015.
87. Beech, E.; Rodwell, A.; Squires, M. Pharmaceutical Formulation Comprising NSAID and Cyclodextrin. U.S. Patent 2016/0008478A1, 14 June 2016.
88. Albuquerque Rocha Gonsalves, A.M.; Serra, A.C.; Fernandes Soares Vieira, A.C.; de Albuquerque Carvalho, R.; Ramalho Figueras, A.R. Process to Produce a Diclofenac Cyclodextrin Conjugate. Patent EP 2422818A2, 29 February 2012.
89. de Oliveira Makson, G.; Guimarães, A.G.; Araújo Adriano, A.; Quintans Jullyana, S.; Santos, M.R.; Quintans-Júnior, L.J. Cyclodextrins: Improving the therapeutic response of analgesic drugs: A patent review. *Expert Opin. Ther. Pat.* **2015**, *25*, 897–907. [CrossRef]
90. Fenyvesi, É.; Puskás, I.; Szente, L. Applications of steroid drugs entrapped in cyclodextrins. *Environ. Chem. Lett.* **2019**, *17*, 375–391. [CrossRef]
91. Loftsson, T. Cyclodextrins in parenteral formulations. *J. Pharm. Sci.* **2020**, *110*, 654–664. [CrossRef] [PubMed]
92. Cirri, M.; Maestrelli, F.; Mennini, N.; Di, L.; Mannelli, C.; Micheli, L.; Ghelardini, C.; Mura, P. Development of a stable oral pediatric solution of hydrochlorothiazide by the combined use of cyclodextrins and hydrophilic polymers. *Int. J. Pharm.* **2020**, *587*, 119692. [CrossRef] [PubMed]
93. Cal, K.; Centkowska, K. Use of cyclodextrins in topical formulations: Practical aspects. *Eur. J. Pharm. Biopharm.* **2008**, *68*, 467–478. [CrossRef]
94. Planken, S.; Cheng, H.; Collins, M.R.; Spangler, J.E.; Brooun, A.; Maderna, A.; Palmer, C.; Linton, M.A.; Nagata, A.; Chen, P. Tetrahydroquinazoline Derivatives Useful as Anticancer Agents. U.S. Patent 2019/0248767A1, 15 August 2019.
95. Ribeiro, A.M.; Moya-Ortega, M.D. Ethinyl Estradiol-Beta-Cyclodextrin Complex and Process for Preparing Thereof. Patent EP 3666260A1, 13 December 2018.
96. Oba, S.; Toyota, H.; Ikeuchi, S. Tablet Containing Composite with Cyclodextrin. Patent WO 2014/055397 A1, 10 April 2014.
97. Bellorini, L.; Nocelli, L.; Zoppetti, G. Pharmaceutical Composition for the Sublingual Administration of Progesterone, and Method for Its Preparation. U.S. Patent 2015/0265631A1, 24 September 2015.
98. Martel, B.; Blanchemain, N.; Flament, M.-P.; Willart, J.-F.; Tabary, N.; Garcia Fernandez, M.J. Use of Soluble and Insoluble Fractions of a cyclodextrin Polymer and of Mixtures Thereof as an Excipient in a Tablet. Patent WO 2017/046506A1, 23 March 2017.
99. Abouhussein, D.M.N.; Nabarawi, M.A.; Shalaby, S.H.; El-Bary, A.A. Sertraline-Cyclodextrin complex orodispersible sublingual tablet: Optimization, stability, and pharmacokinetics. *J. Pharm. Innov.* **2019**, *16*, 136–151. [CrossRef]
100. Mura, P.; Cirri, M.; Mennini, N.; Casella, G.; Maestrelli, F. Polymeric mucoadhesive tablets for topical or systemic buccal delivery of clonazepam: Effect of cyclodextrin complexation. *Carbohydr. Polym.* **2016**, *152*, 755–763. [CrossRef] [PubMed]
101. Concheiro, A.; Alvarez-Lorenzo, C. Chemically cross-linked and grafted cyclodextrin hydrogels: From nanostructures to drug-eluting medical devices. *Adv. Drug Deliv. Rev.* **2013**, *65*, 1188–1203. [CrossRef]

102. Bright, C. Systems and Methods for Cardiac Plexus Neuromodulation. U.S. Patent 2019/0216899A1, 18 July 2019.
103. Ye, Q.; Dellamary, L.A.; Piu, F. Modulation of Gel Temperature of Poloxamer-Containing Formulations. U.S. Patent 2018/0125781A1, 10 May 2018.
104. Park, K.D.; Park, K.M.; Lee, Y.K.; Hoang, T.T.T.; Le, T.P. Injectable Tissue Adhesive Hydrogel Including Gamma-Cyclodextrin and Biomedical Use Thereof. U.S. Patent 2017/0281781A1, 5 October 2017.
105. Otero Espinar, F.J.; Nogueiras Nieto, L.; Anguiano Igea, F. Aqueous Pharmaceutical System for the Administration of Drug to the Nails. U.S. Patent 2013/0115181A1, 9 May 2013.
106. Fahmy, T.M.; Look, M.; Craft, J. Methods of Treating Inflammatory and Autoimmune Disease and Disorders Using Nanolipogels. U.S. Patent 9603800B2, 28 March 2017.
107. Zhao, W.; Li, Y.; Zhang, X.; Zhang, R.; Hu, Y.; Boyer, C.; Xu, F.J. Photo-Responsive supramolecular hyaluronic acid hydrogels for accelerated wound healing. *J. Control. Release* **2020**, *323*, 24–35. [CrossRef] [PubMed]
108. Lin, Q.; Yang, Y.; Hu, Q.; Guo, Z.; Liu, T.; Xu, J.; Wu, J.; Kirk, T.B.; Ma, D.; Xue, W. Injectable supramolecular hydrogel formed from α-cyclodextrin and PEGylated arginine-functionalized poly(L-Lysine) dendron for sustained MMP-9 ShRNA plasmid delivery. *Acta Biomater.* **2017**, *49*, 456–471. [CrossRef] [PubMed]
109. Flores, C.; Lopez, M.; Tabary, N.; Neut, C.; Chai, F.; Betbeder, D.; Herkt, C.; Cazaux, F.; Gaucher, V.; Martel, B.; et al. Preparation and characterization of novel chitosan and β-cyclodextrin polymer sponges for wound dressing applications. *Carbohydr. Polym.* **2017**, *173*, 535–546. [CrossRef] [PubMed]
110. Sisso, A.M.; Boit, M.O.; DeForest, C.A. Self-Healing injectable gelatin hydrogels for localized therapeutic cell delivery. *J. Biomed. Mater. Res. Part. A* **2020**, *108*, 1112–1121. [CrossRef] [PubMed]
111. Jansook, P.; Maw, P.D.; Soe, H.M.S.H.; Chuangchunsong, R.; Saiborisuth, K.; Payonitikarn, N.; Autthateinchai, R.; Pruksakorn, P. Development of amphotericin B nanosuspensions for fungal keratitis therapy: Effect of self-assembled γ-cyclodextrin. *J. Pharm. Investig.* **2020**, *50*, 513–525. [CrossRef]
112. Muankaew, C.; Jansook, P.; Sigurcrossed D Signsson, H.H.; Loftsson, T. Cyclodextrin-Based telmisartan ophthalmic suspension: Formulation development for water-insoluble drugs. *Int. J. Pharm.* **2016**, *507*, 21–31. [CrossRef] [PubMed]
113. Loftsson, T.; Stefansson, E. Cyclodextrin Nanotechnology for Ophthalmic Drug Delivery. U.S. Patent 8999953B2, 7 April 2015.
114. Vehring, R.; Hartman, M.S.; Smith, A.E.; Joshi, V.B.; Dwivedi, S.K. Compositions for Pulmonary Delivery of Long-Acting Muscarinic Antagonists or Long-Acting B2 Adrenergic Receptor Agonist and Associated Methods and Systems. U.S. Patent 2019/0307676A1, 10 October 2019.
115. Duchêne, D.; Bochot, A.; Yu, S.C.; Pépin, C.; Seiller, M. Cyclodextrins and emulsions. *Int. J. Pharm.* **2003**, *266*, 85–90. [CrossRef]
116. Leclercq, L.; Nardello-Rataj, V. Pickering emulsions based on cyclodextrins: A smart solution for antifungal azole derivatives topical delivery. *Eur. J. Pharm. Sci.* **2016**, *82*, 126–137. [CrossRef] [PubMed]
117. Laza-Knoerr, A.-L.; Gref, R.; Amiel, C.; Couvreur, P. Method for Forming Cyclodextrin Polymer and lipophilic Compound Emulsions, Resulting Emulsions, and Compositions Including Said Emulsions. U.S. Patent 2012/0304577A1, 3 May 2012.
118. Romer Rassing, M. Chewing gum as a drug delivery system. *Adv. Drug Deliv. Rev.* **1994**, *13*, 89–121. [CrossRef]
119. Al Hagbani, T.; Altomare, C.; Kamal, M.M.; Nazzal, S. Mechanical characterization and dissolution of chewing gum tablets (CGTs) containing co-compressed health in gum® and curcumin/cyclodextrin inclusion complex. *AAPS PharmSciTech* **2018**, *19*, 3742–3750. [CrossRef]
120. Andersen, C.; Isager, P.P. Compressed chewing Gum Comprising Peptide. Patent WO 2009/080023A1, 2 July 2009.
121. Alkilani, A.Z.; McCrudden, M.T.C.; Donnelly, R.F. Transdermal drug delivery: Innovative pharmaceutical developments based on disruption of the barrier properties of the stratum corneum. *Pharmaceutics* **2015**, *7*, 438–470. [CrossRef]
122. Xiao, S.; Yan, Y.; Zhao, J.; Zhang, Y.; Feng, N. Increased microneedle-mediated transdermal delivery of tetramethyl. *Int. J. Pharm.* **2020**, *575*, 118962. [CrossRef]
123. Obaidat, R.; Al-Shar'i, N.; Tashtoush, B.; Athamneh, T. Enhancement of levodopa stability when complexed with β-cyclodextrin in transdermal patches. *Pharm. Dev. Technol.* **2018**, *23*, 986–997. [CrossRef]
124. Zhou, X.; Luo, Z.; Baidya, A.; Kim, H.-j.; Wang, C.; Jiang, X.; Qu, M.; Zhu, J.; Ren, L.; Vajhadin, F.; et al. Biodegradable β-cyclodextrin conjugated gelatin methacryloyl microneedle for delivery of water-insoluble drug. *Adv. Healthc. Mater.* **2020**, *9*, 1–12. [CrossRef] [PubMed]
125. Jug, M.; Kosalec, I.; Maestrelli, F.; Mura, P. Development of low methoxy amidated pectin-based mucoadhesive patches for buccal delivery of triclosan: Effect of cyclodextrin complexation. *Carbohydr. Polym.* **2012**, *90*, 1794–1803. [CrossRef] [PubMed]
126. Tonglairoum, P.; Ngawhirunpat, T.; Rojanarata, T.; Panomsuk, S.; Kaomongkolgit, R.; Opanasopit, P. Fabrication of mucoadhesive chitosan coated polyvinylpyrrolidone/cyclodextrin/clotrimazole sandwich patches for oral candidiasis. *Carbohydr. Polym.* **2015**, *132*, 173–179. [CrossRef] [PubMed]
127. Kim, K.O.; Kim, G.J.; Kim, J.H. A cellulose/β-cyclodextrin nanofiber patch as a wearable epidermal glucose sensor. *RSC Adv.* **2019**, *9*, 22790–22794. [CrossRef]
128. Zhang, M.; Zhang, J.; Chen, J.; Zeng, Y.; Zhu, Z.; Wan, Y. Fabrication of curcumin-modified TiO2 nanoarrays via cyclodextrin based polymer functional coatings for osteosarcoma therapy. *Adv. Healthc. Mater.* **2019**, *8*, 1–12. [CrossRef]
129. Elisseeff, J.; Guo, Q.; Majumdar, S. Compositions Comprising Cyclodextrin Incorporated Collagen Matrices for Use in Biomedical Applications. Patent WO 2015/164733A1, 29 October 2015.

130. Mack, B.C.; Davis, M.E.; Wright, K.W. Layered Drug Delivery Polymer Monofilament Fibers. U.S. Patent 8974814B2, 10 March 2015.
131. Szejtli, J. Past, Present, and Future of Cyclodextrin Research. *Pure Appl. Chem.* **2004**, *76*, 1825–1845. [CrossRef]
132. Loftsson, T.; Brewster, M.E. Pharmaceutical Applications of Cyclodextrins: Basic Science and Product Development. *J. Pharm. Pharmacol.* **2010**, *62*, 1607–1621. [CrossRef]
133. FDA Pazeo (Olopatadine Hydrochloride) Ophthalmic Solution FDA Approval. Available online: https://www.accessdata.fda.gov/drugsatfda_docs/nda/2015/206276Orig1s000TOC.cfm (accessed on 12 July 2021).

Journal of Drug Delivery Science and Technology xxx (xxxx) xxx

Contents lists available at ScienceDirect

Journal of Drug Delivery Science and Technology

journal homepage: www.elsevier.com/locate/jddst

Research paper

Experimental and theoretical studies of pegylated-β-cyclodextrin: A step forward to understand its tunable self-aggregation abilities

Juliana Rincón-López [a], Norma J. Ramírez-Rodríguez [a], Alberto S. Luviano [b], Miguel Costas [b], José L. López-Cervantes [c], Arturo A. García-Figueroa [c], Héctor Domínguez [d], Rubén Mendoza-Cruz [d], Patricia Guadarrama [a], Salvador López-Morales [d], Yareli Rojas-Aguirre [a,*]

[a] Laboratorio de Materiales Supramoleculares (SupraMatLab), Instituto de Investigaciones en Materiales, Universidad Nacional Autónoma de México, Circuito Exterior S/N, Ciudad Universitaria, 04510, Mexico City, Mexico
[b] Laboratorio de Biofisicoquímica, Departamento de Fisicoquímica, Facultad de Química, Universidad Nacional Autónoma de México, Mexico City, 04510, Mexico
[c] Laboratorio de Superficies, Departamento de Fisicoquímica, Facultad de Química, Universidad Nacional Autónoma de México, Mexico City, 04510, Mexico
[d] Instituto de Investigaciones en Materiales, Universidad Nacional Autónoma de México, Circuito Exterior S/N, Ciudad Universitaria, 04510, Mexico City, Mexico

ARTICLE INFO

Keywords:
Cyclodextrin
Self-aggregation
Nanostructure
Density
Surface tension
Computational modeling

ABSTRACT

In this work we studied the self-aggregation abilities of βCDPEG5, a star-shaped pegylated derivative comprising seven PEG chains selectively conjugated to the primary face of βCD via triazole linkers. The critical aggregation concentration, determined by density measurements, yielded a value of 0.5 mM. Dynamic light scattering (DLS) showed that βCDPEG5 forms nanoaggregates of a hydrodynamic diameter (Dh) of ~150 nm in water at 25 °C. βCDPEG5 significantly decreased the surface tension of water, thus confirming the aggregation phenomenon. Transmission electron microscopy upheld the presence of the nanoaggregates and revealed their quasi-spherical shape. Nanostructures of 9 nm coexisting with the nanoaggregates were also observed in DLS and correspond to βCDPEG5 dimers. Computational studies analyzed dimers as the initial stage in the βCDPEG5 nanoaggregation process.

Both βCDPEG5 nanoaggregates and dimers displayed their same Dh pattern in acidic, neutral, and basic conditions; likewise, when modifying the ionic strength of the medium. Interestingly, the nanoaggregates and dimers varied depending on the experimental conditions, being the former predominant when increasing pH and ionic strength, a behavior attributed to the triazole linkers, which seem to respond smartly to changes in the environment. At 37 °C, only βCDPEG5 nanoaggregates were present with a Dh mean value similar to that at 25 °C. The scattering behavior of nanoaggregates and dimers was studied for 55 days. We found that Dh of both species remains unchanged; nevertheless, at the end of the analysis, the nanoaggregates population was predominant.

These overall results demonstrate that βCDPEG5 is an amphiphilic non-ionic system with a remarkable ability to aggregate in water and form defined nanostructures. Moreover, depending on the βCDPEG5 concentration, pH, ionic strength, and temperature, the dimeric or nanoaggregated state can be tuned, being this an attractive feature to load and control the release of a drug.

1. Introduction

β-cyclodextrin (βCD) is a truncated cone-shaped macrocycle well-known for hosting low polar molecules within its hydrophobic cavity to form host-guest inclusion complexes (ICs). The host-guest complexation is an exploited attribute in the pharmaceutical field, allowing the enhancement of the aqueous solubility of hydrophobic drugs and formulations' stability and organoleptic properties [1,2].

The random or selective functionalization of the βCD primary or secondary –OH groups has yielded numerous βCD derivatives. If βCD is derivatized with alkyl chains or hydrophobic moieties, amphiphilic βCDs (a-βCDs) are obtained. The relevance of a-βCDs relies on enhanced

* Corresponding author.
E-mail address: yareli.rojas@materiales.unam.mx (Y. Rojas-Aguirre).

https://doi.org/10.1016/j.jddst.2021.102975
Received 17 June 2021; Received in revised form 5 November 2021; Accepted 9 November 2021
Available online 13 November 2021

interaction with hydrophobic drugs on one hand; on the other, they can self-assemble and form nanoparticles spontaneously without requiring a surfactant. Some of these nanoparticles have shown outstanding performance as drug delivery systems as they can contain higher loads of drugs in comparison to βCD, either through non-covalent associations within the aliphatic chains or by covalent attachment to the nanostructure [3–7]. For instance, CRLX101, a linear βCD-polyethylene glycol copolymer conjugated to camptothecin, that self-assemblies into polymeric nanoparticles and is currently in Phase 2 studies for small-cell lung and ovarian cancer [8,9].

Polyethylene glycol (PEG) is the most investigated synthetic polymer in the nanomedicine field. PEG can improve the solubility, colloidal stability, and pharmacokinetic profile of biomacromolecules and nanomaterials; it also can be used as a bridge to attach drugs or targeting ligands to a nanocarrier [10,11]. PEG is considered hydrophilic; however, when its MW increases (above 4700/5000), it behaves more like an amphiphile in solution due to the hydrophobicity conferred by the $–CH_2$ groups and the hydrophilic character given by the interaction of –O with water molecules by H-bonding [12]. Thus, PEG can interact through hydrophobic or electrostatic interactions and even coordinate bonds with diverse substrates (i.e., water, proteins, surfaces) [10], which in turn, will depend on PEG MW and grafting density [10,12,13]. In terms of grafting density, when it is low, PEG adopts a mushroom conformation. When the grafting density increases, the polymer acquires a brush arrangement with long and thin chains extending in the space. PEG brush conformation has been reported for Y-shaped, multiblock, and star-shaped polymers. If a suitable solvent surrounds the PEG brush, repulsive forces may predominate, and coagulation of colloids is prevented, thus providing stability to the system. Further increase in the brush grafting density induces attractive interactions, mainly Van der Waals and depletion effects, making the PEG brush low responsive to the environment [10,14,15]. Therefore, through a careful pegylation design, the responsiveness of the pegylated material to the surroundings can be tuned and must be considered for the rational design of successful pegylated drug delivery systems.

In a scenario of molecular platforms design, PEG can be incorporated into βCD via host-guest interactions or by covalent attachment to the βCDs primary or secondary face [16–21]. The primary purposes of βCDs pegylation have been obtaining soluble and stable βCD-based nanomaterials with diverse functionalities for their use in the drug and gene delivery fields [22,23].

We previously reported the synthesis of βCDPEG5 (Fig. 1), a star-shaped βCD pegylated derivative with seven PEG 5 kDa (PEG5) chains selectively conjugated via triazole linkers to the βCD primary face by click chemistry. MALDI-TOF confirmed the star-shaped structure and the presence of βCDPEG5 dimers [19]. Although βCDPEG5 does not bear hydrophobic substituents as such, we hypothesized that PEG MW and the arrangement of the seven PEG5 chains in the βCD primary face give βCDPEG5 the ability to self-aggregate in water.

In this work, to assess the self-aggregation abilities of βCDPEG5, we investigated the critical aggregation concentration (CAC) of βCDPEG5 by density measurements. Then, we analyzed the βCDPEG5 aggregates

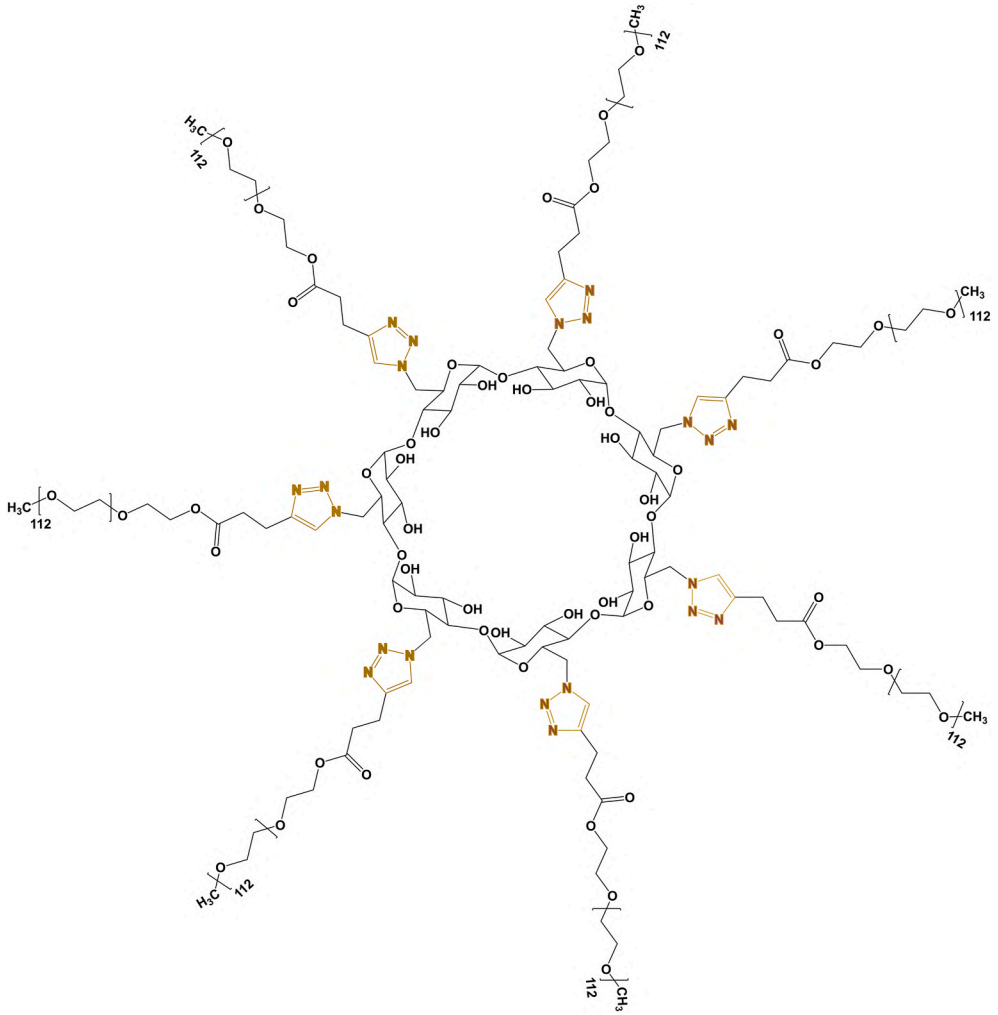

Fig. 1. Chemical structure of βCDPEG5.

and their hydrodynamic diameter through dynamic light scattering (DLS). Surface tension measurements corroborated the aggregation phenomenon of βCDPEG5. The aggregates' shape and size were upheld by transmission electron microscopy. Finally, computational studies supported the analysis of the aggregation process.

Although the elucidation of the aggregation mechanisms of native, modified, and a-βCDs is still challenging, through this work, we aim to provide information towards understanding the aggregation behavior of pegylated βCDs, which is fundamental for its further use in a pharmaceutical formulation or as a functional drug delivery platform.

The study of the aggregation phenomena for native and modified CDs is of great importance as CDs aggregates can impact the solubility and stability of some pharmaceutical formulations. In other cases, the aggregation can be exploited to prompt innovative CD-based pharmaceutical technologies [24,25]. Moreover, the size, shape, and physicochemical forces holding together the CDs aggregates will determine the drug loading capacity, the drug release process, and the interactions with biological interfaces [26].

When designing a drug delivery nanosystem, research generally centers on characterizing the size, drug loading, and biological evaluations mostly performed only on cells related to specific applications for which the nanoparticle was designed. Hence, unknown physicochemical and biological features for the novel nanomaterial may hamper its progress in biological and clinical evaluations [27]. Therefore, in-depth investigations of nanomaterials at their early stages of development are necessary even without being loaded with a drug. Under this context, we expect that the findings presented herein contribute to the future development of assembled soft materials based on the widely used βCD or PEG for drug delivery applications.

2. Materials and methods

2.1. Materials

β-cyclodextrin 98% (βCD), poly-(ethylene glycol)-methyl ether average *Mn* 5 kDa (PEG5), sodium acetate ACS reagent ≥99% w/w, and sodium chloride (NaCl) ACS reagent ≥99% w/w were purchased from Sigma-Aldrich. Phosphate-buffered saline tablets (0.01 M phosphate, 0.0027 M KCl, and 0.137 mM NaCl for a 200 mL solution) were acquired from Thermo Fisher Scientific. Sodium dodecyl sulfate ≥99.0% (GC) dust-free pellets, was purchased from Sigma-Aldrich. βCDPEG5 material was obtained as previously reported [19]. All dissolutions were prepared with deionized water provided by the Institute of Materials Research (IIM) UNAM.

2.2. Aggregation of βCDPEG5

2.2.1. Determination of the critical aggregation concentration

We determined the CAC through density measurements performed on an Anton Paar DMA 4500 densimeter at 25 ± 0.2 °C using an oscillating U-tube method for βCDPEG5 samples in the range of 0.005–1.100 mM. Before each measurement, ethanol and deionized water were used to clean the equipment. For every three assessments of βCDPEG5 at different concentrations, we did one measurement with deionized water to ensure repeatability. The density uncertainty was 0.00003 g/cm^3 at a confidence level of 95%. Density data were smoothed using the UnivariateSpline function of degree 4 and 1.1 nodes from the SciPy package in Python. The first, second, and third derivatives of density values as a function of βCDPEG5 concentration were obtained from the quotient of the discrete differences of density and concentration from the NumPy package in Python. The CAC value was determined under the criterion of the third derivative [28,29]. As a reference point, we measured the surfactant sodium dodecyl sulfate in the range of 0.849–5.278 mM. The density data were treated otherwise the same as for βCDPEG5 to compute the surfactant's CAC.

2.2.2. Dynamic light scattering

The detection of the βCDPEG5 nanoaggregates and their corresponding size, expressed as the hydrodynamic diameter (Dh), was carried out through DLS using a Nanotrack Wave instrument (Microtrac Inc., Philadelphia, PA, USA) equipped with a 180° scattering angle and a 780 nm laser wavelength. This technique is based on the Brownian motion of the particles whose Dh is computed by applying the Stokes-Einstein equation $D_h = k_B T/3\pi\eta D$, where k_B is the Boltzman constant, T is the absolute temperature, η is the solvent viscosity, and D is the diffusion coefficient. The particle size displayed as the volume distribution function was directly provided by the Microtrac 'Flex' instrument software ver. 11.0.0.4 [30].

For DLS measurements, we prepared 0.5 mM aqueous samples of βCDPEG5. A physical mixture (PM), prepared by mixing βCD and PEG5 in water at their equivalent 0.5 mM concentration relative to βCDPEG5, was also measured. Aqueous solutions of native βCD and free PEG5, both at 0.5 mM, were included for DLS analysis. To explore the scattering behavior of βCDPEG5 above its CAC, we assessed βCDPEG5 at 5 and 10 mM. All samples were filtered through a 0.45 μm PET filter (Chromafil® Xtra) and allowed to stand for 30 min before analysis. The βCD sample was sonicated for 1 min (Ultrasonic LC 20H) before filtration. The samples were measured once with six runs per measurement and a detection period of 60 s per run (n = 6). For the case of βCDPEG5 0.5 mM, three independent samples were prepared and measured under the abovementioned conditions (n = 18). All these samples were analyzed at 25 °C ± 0.5 °C.

2.2.3. Surface tension measurements

The surface tension change, produced by the βCDPEG5 in the range of 0.0001–1.2 mM, PEG5, βCD and the PM at the equivalent concentrations relative to βCDPEG5, at the air/water interface, was measured by the pendant drop technique using an image drop profile tensiometer (OCA20, DataPhysics, Germany). A high-resolution camera (max 123 fps) was used to capture the drop profiles and analyze them solving the Young-Laplace equation. The drops were kept at a constant temperature using a home-designed thermostatized cell constructed with optical glass by Helma, Germany [31]. The measurements were performed at 25 °C ± 0.1 °C, controlled by a thermobath (Haake K20, Thermo Scientific), and at least three replicates were performed at each concentration. The βCDPEG5 drops were allowed to equilibrate for at least 6 h.

2.2.4. Transmission electron microscopy

The morphology and size of the βCDPEG5 nanoaggregates were determined by transmission electron microscopy (TEM) to correlate with the DLS analysis. The measurements were carried out at Laboratorio Universitario de Microscopía Electrónica (LUME-UNAM) in a JEOL ARM200F microscope, operated at 200 kV, reducing the electron dose, and using a small objective aperture to compensate the low-contrast expected from the sample. A small amount of the dried sample was dispersed in distilled water using a vortex; then, a sample drop was placed onto a Cu carbon-coated grid and let to dry completely before characterization.

2.2.5. Computer simulations methodology

To obtain more information on the βCDPEG5 aggregation, some computer simulations were conducted. However, since the real βCDPEG5 nanoaggregates are too big to do an all-atom simulation, only the dimer was simulated, and the results were extrapolated to compare them with the present experiments. The βCDPEG5 molecule was constructed, as in Fig. 1, using an all-atom model with GROMOS 54A7 force field generated from the Automated Force Field Topology Builder (ATB, http://compbio.biosci.uq.edu.au/atb) [32], the βCD + triazole core was explicitly modeled, however, instead of $(CH_2–CH_2–O-)_{112}$ chains, $(CH_2–CH_2–O-)_{28}$ chains were simulated, i.e., a quarter of the entire chain, this is, a smaller system, to facilitate the computational methods and analysis. The initial βCDPEG5 molecule was minimized and ran for 1

ns in the NVT ensemble; then, the dimer was built up by replicating the monomer and placing both molecules facing their OH groups. The final system was solvated with 50000 water molecules using the SPCE model [33]. All simulations were carried out using GROMACS-21 software [34] with periodic boundary conditions in all directions in the NPT ensemble. Temperature and pressure were set to T = 298.15 K and P = 1 bar using the V-scale thermostat, with a relaxation time of τ_T = 0.2 ps, and Parinello-Rahman barostat, with a relaxation time of τ_P = 2.0 ps, respectively. Electrostatic interactions were handled with the particle mesh Ewald method [35], and the short-range interactions were cut off at 2.0 nm. Bond lengths were constrained using the Lincs algorithm [36]. Then, simulations were carried out up to 80 ns, with a timestep of dt = 0.002 ps, using the last 10 ns for data analysis.

2.3. Influence of temperature, pH, and ionic strength on βCDPEG5 nanoaggregates

An aqueous sample of βCDPEG5 0.5 mM was introduced to the DLS instrument and heated at 37 °C (rate 1°C/min) before measurements to determine the influence of temperature in the nanoaggregates.

βCDPEG5 0.5 mM samples were prepared in acetate buffer pH 3.8, PBS pH 7.4, and in PBS adjusted with NaOH to pH 8.0 to determine the effect of pH on the nanoaggregates behavior. To study the influence of ionic strength, we prepared samples of βCDPEG5 0.5 mM in 0.9% and 7.5% NaCl solutions. In all cases, samples were treated as described in Section 2.2.2. and then analyzed in the DLS instrument at 25 °C ± 0.5 °C.

2.4. Behavior of βCDPEG5 nanoaggregates' over time

DLS measurements for βCDPEG5 0.5 mM were performed in water at 25 °C, every day from day 2–5, every five days from day 5–35, and the last analysis was carried out at day 55. The sample was measured once with six runs per measurement as described above (n = 6 per day).

2.5. Statistics

To determine the statistical differences among the Dh of the βCDPEG5 nanoaggregates obtained under the experimental conditions described above, we computed a one-way ANOVA with a Dunnett *post hoc* correction for multiple comparisons using the software Graph Pad Prism Version 7.0 for Windows (Graph Pad Software, San Diego, California, www.graphpad.com). The alpha value was set at 0.05, and a p-value <0.05 was considered the criteria for significance. In this way, we report the average Dh values as mean ± SD with n = 6 for all measurements otherwise specified.

3. Results

3.1. Investigation of the βCDPEG5 self-aggregation

3.1.1. Determination of the CAC of βCDPEG5

The CAC refers to the minimum concentration at which molecules self-assemble to form aggregates. In the drug delivery field, it is desirable that amphiphilic copolymers self-assemble at low CAC values, which improves the aggregates' structural stability under diluted conditions. Moreover, if the aggregates are designed to be further loaded with low polar drugs, a small CAC leads to enhanced aggregates' solubilization properties [37–40].

Aggregation is assumed as a dehydration process in which the number of free water molecules, previously bounded to the non-aggregated monomers, increase, being this a change monitorable by density measurements. Hence, densimetric analyses are among the several methods to determine aggregation and CAC [41,42]. As far as we know, this is the first time that density measurements have been employed to investigate the CAC of CDs aggregates.

Fig. 2A shows the density change as a function of different concentrations (from 0.05 to 1.1 mM) of βCDPEG5 aqueous samples. The first, second, and third derivatives were calculated, and the CAC was identified when the third derivative was equal to zero (Fig. 2B): 0.496 mM.

We included in these experiments the analysis of the widely known surfactant sodium dodecyl sulfate (SDS) as a reference point to compare with βCDPEG5. Striking and unexpectedly, the changes in the density medium induced by βCDPEG5 were significantly higher than in SDS. Likewise, the CAC value of βCDPEG5 was much smaller than SDS, which was 2.730 mM (Fig. S1).

Recently, Loftsson et al. published a compelling work reporting the CAC values, determined by permeation through semi-permeable cellophane membranes, of native CDs and 2-hydroxypropyl-β-CD, ranging from 7 to 84 mM [26]. Within this context stands out the βCDPEG5 low CAC, which seems to be very promising for the development of delivery systems of poorly soluble drugs. It has been stated that density measurements are not reliable to obtain CAC values for non-ionic surfactants at low concentrations since density, in those cases, is practically the same that pure water [42]. Notably, in our case, the densimetric analysis revealed that neutral βCDPEG5 molecules self-aggregate at relatively low concentrations and modify the density media to a more significant extent than even SDS.

3.1.2. Dynamic light scattering analysis

The light scattering data of the 0.5 mM sample revealed the presence of βCDPEG5 nanoaggregates with a Dh1 mean value of 156.5 nm ± 20 (n = 18); a second population showed a Dh2 mean value of 9.0 ± 0.1 nm (Fig. 3A, Table S1). Based on the findings of our previous work, in which MALDI-TOF of βCDPEG5 exhibited the presence of dimers [19], we assigned the 9.0 nm population to two associated βCDPEG5 molecules.

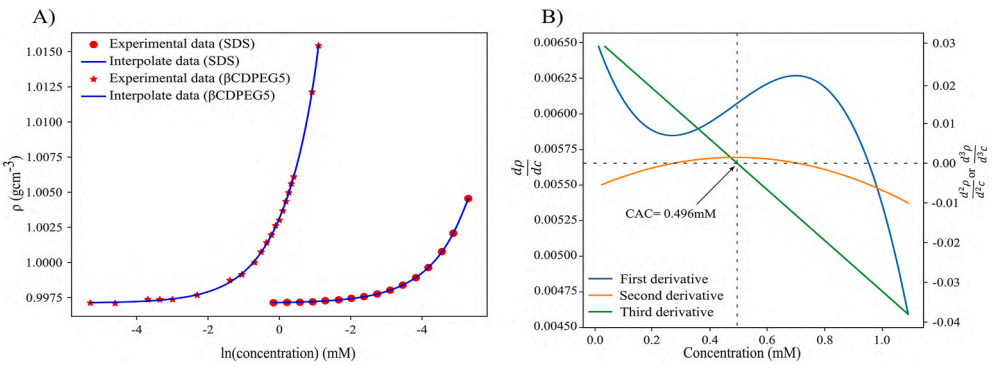

Fig. 2. A) Density as a function of the logarithm of the concentration of aqueous samples of βCDPEG5 and SDS. B) First, second and third derivatives of density as a function of concentration for βCDPEG5.

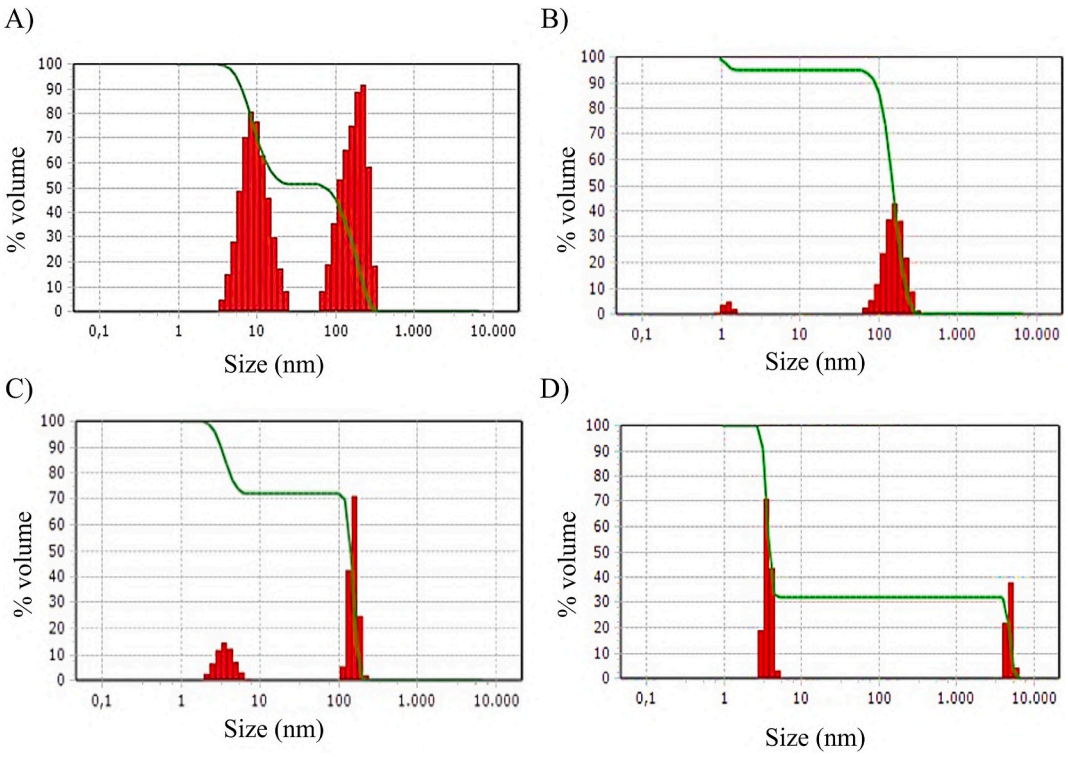

Fig. 3. Particle size distribution of A) βCDPEG5; B) βCD; C) PEG5; D) βCD and PEG5 PM.

The DLS volume distribution function, estimating the relative amount of multimodal samples, showed that both populations coexist to a comparable extent with 55.1% and 44.9% for the nanoaggregates and dimers, respectively.

We carried out a DLS analysis for βCD/PEG5 PM to determine whether the aggregation of βCDPEG5 occurs only when PEG5 chains are covalently attached to βCD. We also analyzed the separate components βCD and PEG5.

When measuring βCD, it was possible to detect aggregates of a Dh mean value of 148.4 nm coexisting with 1.2 nm-sized βCD monomers (Fig. 3B, Table S2). Our outcomes agree with previous works analyzing βCD aggregation through DLS that have reported βCD aggregates in the range of 120–300 nm at different concentrations and the presence of βCD monomers of 1–2 nm size [43–46]. The scattering results of PEG5 revealed two populations: one with an average Dh of 148.8 nm and another of 3.6 nm (Fig. 3C, Table S3). These observations are in accordance with previous works that have described clusters and aggregates of PEG of various MW in water. The aggregation of PEG molecules, though still controversial, has been attributed to water-polymer interaction through the attractive H- bonding between the polymer chain and water molecules; and the repulsive hydrophobic forces between $–CH_2$ and water [47–51]. DLS results for the PM displayed the population of 3.6 nm (observed for free PEG5) (Fig. 3D, Table S4) and another population of larger entities in the range of 930–5080 nm. These large particles may arise from the formation of ICs between PEG chains and βCD that further interact with other ICs, with free PEG or with βCD, occurring immediately after the sample filtration. This huddle of interactions might result in unstable clusters with fluctuating size and variable volume distribution.

The scattering around 150 and 9 nm, observed for βCDPEG5 0.5 mM, was absent in the PM, indicating that the aggregation pattern observed for βCDPEG5 only occurs when PEG5 chains are anchored to the βCD primary face. Without being covalently attached, βCD and PEG5 may interact through different mechanisms, including the formation of ICs between βCD and PEG5, a phenomenon that has already been observed [20,21].

Aiming to explore the aggregation of βCDPEG5 at concentrations above the CAC, and taking into account the concentration interval previously reported for βCDs aggregation (1–10 mM) [5,44,52,53], we carried out DLS measurements at 10 and 5 mM. The scattering data showed that there is a tendency to form larger aggregates as the sample concentration increases. At 10 mM, large aggregates with Dh values fluctuating between 4289 and 5140 nm were observed (Table S5). At 5 mM, the sample displayed aggregates with Dh values in the range of 1082 and 2329 nm (Table S6). Additionally, a second population with variable Dh values was detected in four out of the six lectures. We postulate that transient and unstable non-spherical microclusters [26] are present for both 10 and 5 mM samples that form after filtration and during the 30 min timeframe before the scattering measurements.

3.1.3. *Surface tension measurements*

We carried out surface tension measurements to confirm the aggregation of βCDPEG5. Fig. 4A shows the temporal evolution of the surface tension of βCDPEG5, PEG5, βCD, and PM. Results pointed out that βCD sample performed like pure water, a behavior that has also been observed for αCD [31,44,54]. The PEG5 sample exhibited a constant surface tension behavior. This constant value was obtained immediately after the drop was placed, as it was the case for the PM; for the latter, it appears that each molecule acts on the interface as if they were separated. Since βCD did not produce any change, we attribute the surface tension behavior to PEG5 chains, even if they form ICs with βCD. In contrast, βCDPEG5, at concentrations equal or higher than CAC, slowly adsorbs on the liquid/air interface.

Fig. 4B shows the equilibrium surface tension for βCDPEG5, PEG5, and the PM. PEG5 and the PM exhibited a constant equilibrium surface tension through the evaluated concentration range, consistent with previously reported values for PEG (MW 6 kDa) [55]. PEG molecules in water form coils [50,51]. Therefore, the adsorption of PEG5 chains, and their consequent unfolding at the surface explain the change in the surface tension.

Then, irrespective of the concentration, and even if there exist ICs, the surface tension for the PM is equal to that for PEG5. In contrast,

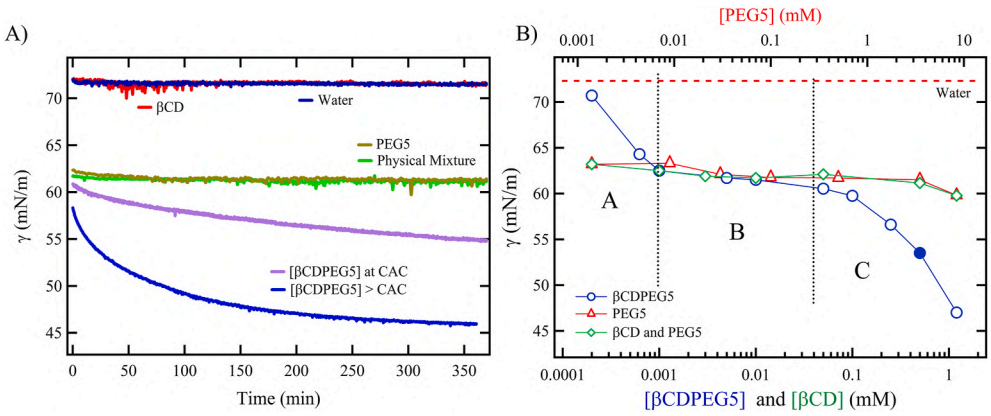

Fig. 4. A) Dynamic surface tension for water, βCDPEG5, βCD, PEG5, and physical mixture of βCD and PEG5; βCDPEG5>CAC refers to 1.2 mM. B) Equilibrium surface tension for βCDPEG5, PEG5 and a physical mixture of βCD and PEG5; the fill blue dot points out the CAC. (For interpretation of the references to colour in this figure legend, the reader is referred to the Web version of this article.)

βCDPEG5 induced different changes in the surface tension. Knowing that every experiment has approximately the same available drop area and that the changes in the surface are a direct consequence of the bulk, we identified three different regions in the surface tension-concentration curve of βCDPEG5. In region A, comprising the range of 0.0001–0.001 mM, βCDPEG5 slightly changed the water surface tension, inferring that βCDPEG5 molecules remain mainly in the bulk as individual entities. From 0.001 to 0.05 mM (region B in Fig. 4B), βCDPEG5 behaved similarly to PEG5 and the PM, suggesting that, at these concentrations, the formation of dimers is induced. The dimers that reached the surface unfold with enough available area to reduce the surface tension just like the PEG5 chains do. This behavior indicates that PEG5 conformation in the βCDPEG5 dimers may assume coil conformation, thus resembling that of free PEG5. At region C (0.005–1.2 mM), the CAC is exceeded, and nanoaggregates are formed in the bulk. These aggregates eventually migrate to the surface and drastically reduce the surface tension. The surface tension decrement suggests that the conformation of the PEG5 chains in the βCDPEG5 nanoaggregate differs from that in dimers, possibly towards helical arrangement, and therefore, their interaction with water molecules is also different. The bottom line, the change in surface tension is an indirect consequence of the existence of βCDPEG5 nanosized aggregates in the bulk and their presence on the surface.

3.1.4. Transmission electron microscopy

We performed TEM imaging to correlate the nanoaggregates size estimation obtained by DLS for the 0.5 mM sample. Fig. 5, corresponding to a βCDPEG5 sample dispersed in distilled water, revealed the presence of nanoaggregates conformed into a quasi-spherical morphology with an average diameter of 120 nm, estimated by measuring several nanoaggregates. To note, DLS measures the hydrodynamic diameter, which could be slightly larger than the diameter observed by TEM; therefore, this result is in close agreement with the estimated average obtained by DLS analysis.

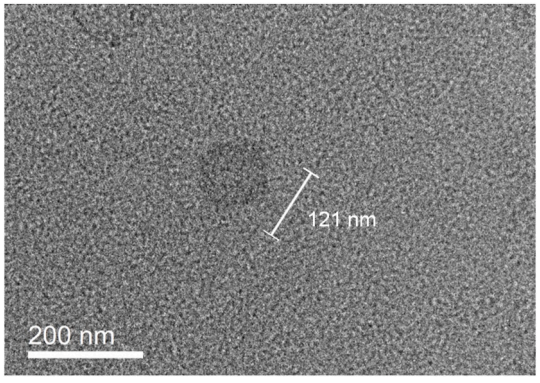

Fig. 5. TEM micrograph of βCDPEG5 at 0.5 mM sample in water showing βCDPEG5 quasi-spherical nanoaggregates.

3.1.5. Computational data

Due to the complexity of simulating the βCDPEG5 aggregate, these computational studies analyzed the interaction between two βCDPEG5 molecules as a first stage in the process of the βCDPEG5 aggregates ~150 nm in size formation. Fig. 6 shows the water density profiles and the βCDPEG5 dimer, along with the last configuration of βCDPEG5, obtained by computer simulations. It is noted that the water profile is reduced in the region of the βCDPEG5 dimer, suggesting a reduction of water molecules inside the structure, which is in accordance with the density measurements (Section 3.1.1.). As it can be observed, the βCD rims are arranged in such a way that they are surrounded by the PEG

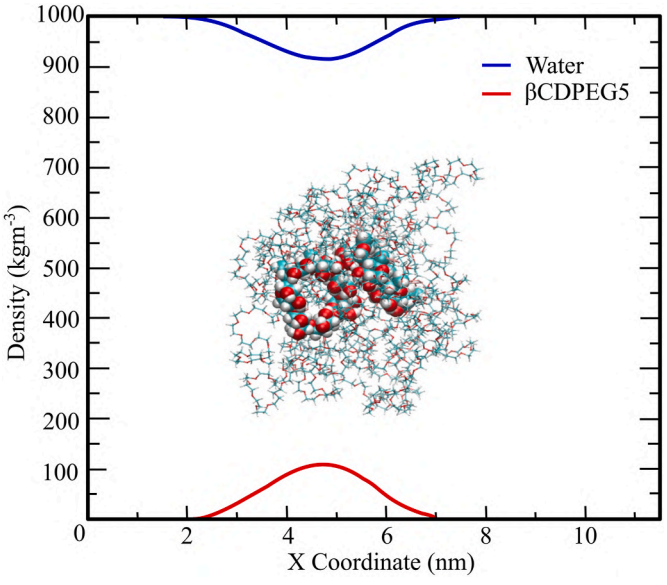

Fig. 6. Density profile in X-direction of the βCDPEG5/water system. The bottom red line is the βCDPEG5 dimer profile and the top blue line is the water profile. In the middle, the last configuration of the dimer is shown. The blue balls represent the carbon atoms, the red ones the oxygens and the white ones the hydrogens. The thin sticks are the PEG chains. (For interpretation of the references to colour in this figure legend, the reader is referred to the Web version of this article.)

chains, thus supporting the PEG5 coil conformation discussed above. From the simulations, it was possible to calculate the radius and the eccentricity of the βCDPEG5 dimer. The radius value was 2.18 nm, whereas, for the eccentricity (measured with the moments of inertia), the value was 0.0338. Since the eccentricity should be zero for a sphere, the value obtained in our case pinpoints a quasi-spherical shape for βCDPEG5 dimers. As suggested by the density profiles, the βCD rings are nearly in the middle of the structure. Subsequently, we calculated the separation between the two monomers by measuring the distance between the βCD rims, and a value of 1.26 nm was found. It is also worth mentioning that the picture obtained from the simulations does not show a complete alignment of the monomers facing each other their –OH groups; instead, they appear to form an angle between the planes containing the βCD rims. With all these calculated data, the picture of the complete βCDPEG5 dimer can be seen as a structure of 4.36 nm size in total, composed of a βCD core of about 2.52 nm diameter, surrounded by 1.84 nm of wide PEG5 chains. Since the simulations were conducted with almost a quarter size of the actual PEG5 chains, it is possible to estimate the dimer's actual size by multiplying four times the calculated PEG5 size and adding the core diameter, which results in about 9.88 nm that is in close agreement with DLS dimers analysis (Section 3.1.2.) The number of hydrogen bonds between PEG5 chains and water was also calculated, founding a total number of 230 bonds. If there are $(CH_2–CH_2–O-)_{28}$ groups and 14 chains, then the average number of bonds per PEG repeating unit is about 0.59.

Based on all the outcomes presented above, we could consider βCDPEG5 as an A-B diblock amphiphilic structure with remarkable abilities to self-aggregate in water as a function of its concentration (Fig. 7A). A-block comprises βCD, with its wide rim available to approach another βCDPEG5, which eventually could interact through intermolecular H-bonds between their secondary face –OH groups, giving rise to the βCDPEG5-βCDPEG5 dimers (Fig. 7B).

The seven PEG5 chains constitute the B-block, dominating the amphiphilicity of βCDPEG5 and promoting the self-association of βCDPEG5 molecules and dimers into nanoaggregates when the concentration of βCDPEG5 increases. The βCDPEG5 nanoaggregates would be held together by attractive forces between PEG5 blocks and between PEG5 blocks and water molecules, that in turn, would induce a more stretched state of those PEG chains enveloping the nanoaggregate (Fig. 7C).

These features make βCDPEG5 a very versatile and attractive candidate for encapsulating and carrying therapeutic agents. Below the CAC, the most likely form of encapsulation of a hydrophobic drug would be through host-guest complexation between the drug and the cavity of βCDPEG5. The complex formation would be driven by the displacement, by the drug, of water molecules residing in the βCD cavity. This extensively accepted complexation mechanism [56–58] ensures the non polar-non polar interactions inside the hydrophobic cavity, with the concomitant increase of entropy as several water molecules drift to the aqueous medium. In this way, the apparent solubility of the guest drug would be enhanced, and the IC's net solubility is expected to be high due to the PEG chains.

At the CAC and above it, the drug encapsulation would be the combination of two mechanisms. First, the formation of ICs between the drug and the cavities of βCDPEG5 in the nanoaggregate; second, its entrapment, guided by hydrophobic interactions, in both the amphiphilic PEG chains in the βCDPEG5 core and in those chains surrounding the nanoaggregate (Fig. 7) [59]. Both mechanisms would cooperate to increase the drug's solubility in the nanoaggregate significantly.

βCDPEG5 could also perform as a nanocarrier for hydrophilic drugs. In this case, the drug-nanoaggregate interactions would be, preferentially, in the outer PEG chains of the nanoaggregate, through polar-polar interactions favored by the negative partial charge of the oxygen atoms of the PEG chains [60].

3.2. *Influence of temperature, pH, ionic strength on βCDPEG5 nanoaggregates*

The aggregates formed from native and modified CDs are metastable and dynamic in aqueous solutions. Therefore, the aggregation phenomenon and the aggregates' size may depend on several factors such as the hydrophobic/hydrophilic balance on the βCD, the solvent medium, and temperature [5,26,43–46,52,53,61]. Accordingly, we assessed the βCDPEG5 aggregation under different conditions.

3.2.1. *Effect of temperature*

We investigated the effect of a temperature increase (37 °C) on the βCDPEG5 nanoaggregation. Nanoaggregates with a Dh mean value of 152.4 ± 3.3 nm were detected (Fig. 8A and C, Table S7), similarly to that recorded at 25 °C. Hence, a temperature of 37 °C did not affect the aggregation phenomenon. Strikingly, βCDPEG5 dimers were absent.

There is evidence that the solvation of unstretched PEG is given by the double coordination of water, through –H bonds, to two neighboring oxygen PEG atoms forming water bridges [62]. This would be the case for βCDPEG5 dimers, in which PEG5 are coiled-shaped, as suggested by results on surface tension (Section 3.1.3.) and computational studies, which, besides, provided the average number of bonds per PEG repeating unit and water (Section 3.1.5.). On the other hand, if PEG chains are unfolded, a single water molecule forms one –H bond with one oxygen atom. The solvation mode for coiled PEG has a high entropy cost and thus becomes unfavorable at high temperatures. In contrast, for stretched PEG, the entropy gain of released water compensates the conformational entropy penalty of PEG stretching and, therefore, the free energy of stretched PEG chains does not depend on temperature [62]. This statement could explain why PEG5 solvation in βCDPEG5 dimers becomes unfavorable at higher temperatures, and thus, their

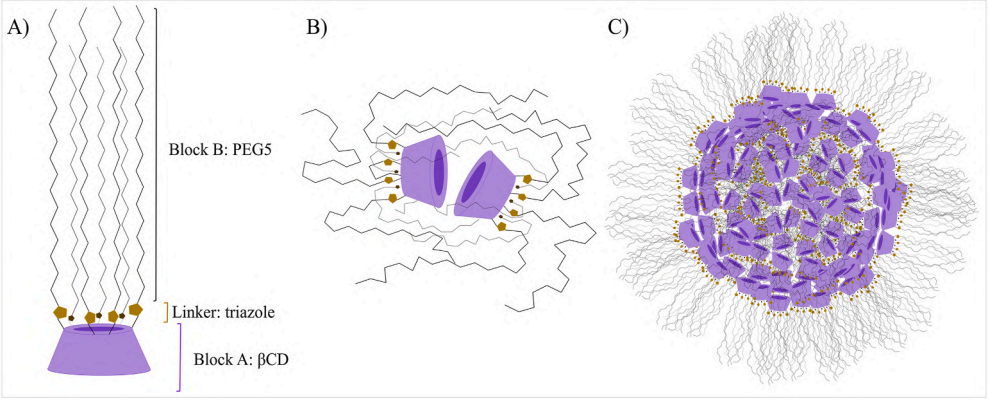

Fig. 7. Schematic representation of A) βCDPEG5; B) βCDPEG5 dimer; and C) βCDPEG5 nanoaggregate.

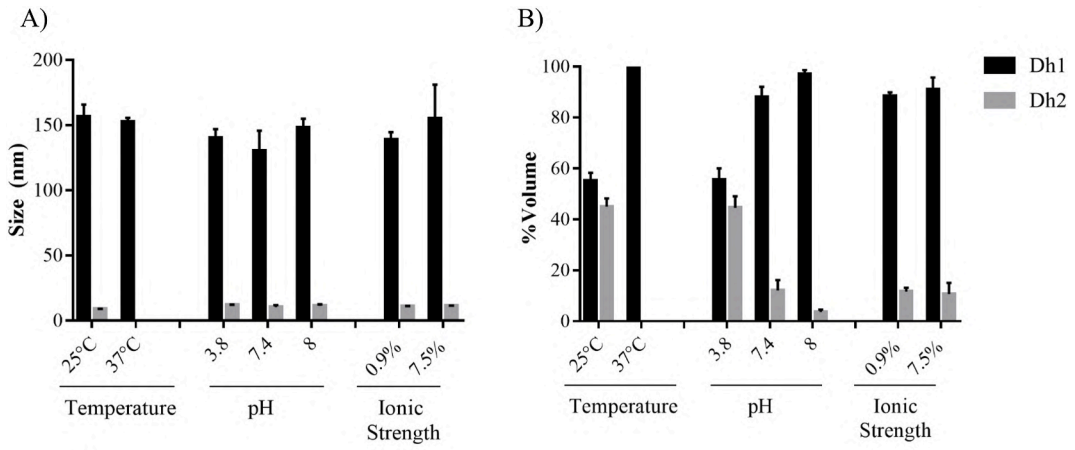

C)

Effect	Dh1 (nm)	%Vol1	Dh2 (nm)	%Vol2
Temperature				
37°C	152.4±3.3	--	--	--
pH				
3.8	140.4±6.5	55.5±4.5	11.9±0.3	44.6±4.1
7.4	130.5±15.3	87.9±4.1	10.4±1.5	12.1±4.1
8.	148.3±6.7	97.0±1.7	11.4±1.1	3.6±0.9
Ionic strength				
0.9%	139.0±5.2	88.4±1.5	10.9±0.3	11.7±1.5
7.5%	155.1±25.9	89.3±4.4	11.2±0.3	10.7±4.4

Fig. 8. Effect of temperature, pH, and ionic strength on nanoaggregates and dimers A) Dh and B) volume distribution; error bars correspond to SD with an n = 6. C) values represented in A) and B) are included in a table format to facilitate their reading.

tendency to form aggregate increases, likewise, the unchanged behavior of βCDPEG5 aggregates at 37 °C.

3.2.2. *Effect of pH and ionic strength*

Bimodal populations with Dh1 and Dh2 values similar to those for water at 25 °C were detected for acidic, neutral, and basic pH (Fig. 8A and C, Table S8). The same was true for isotonic and hypertonic conditions (Fig. 8A and C, Table S9). We carried out a one-way ANOVA to compare all Dh1 results against the Dh1 value in water at 25 °C. Because of the minimal variation among Dh2±SD data, we only analyzed Dh1 values. The statistical analysis showed that pH 7.4 and an isotonic NaCl solution induced a moderate decrease of 16.6% and 11.2% respectively in the nanoaggregates' Dh1 mean value, whereas, under the other evaluated factors, the Dh1 remained unchanged.

Unlike Dh values, the volume distribution was significantly influenced by pH and ionic strength (Fig. 8B and C). When analyzing the effect of pH, we found that the volume distribution of the dimers decreases when the pH value increases. At an acidic pH, the volume distribution of both populations is comparable. At a neutral pH, 12.1% of dimers were present in the sample, revealing a 3.7-fold decrease in this population compared to acidic pH. At pH 8.0, only 3.6% accounted for dimers. In this case, an increment in 0.6 pH units produced a 3.4-fold decrease for the dimer's population. This behavior could be explained by the triazole groups formed during the click reaction to bind PEG5 chains to the primary face of βCD. The triazole groups are strong bases with a pK_b of 1.2, which protonate on acidic conditions and, due to electrostatic repulsions, would be prompting βCDPEG5 towards a dimeric state. Even though these triazoles are in a relatively lower proportion in the di-block structure, they would actuate as "intelligent linkers" due to their response to pH, which generates an effect unachievable by the βCD and PEG5 blocks.

The volume distribution of the dimers in isotonic and hypertonic solutions was comparable. Interestingly, the volume distribution of these samples resembled that at pH 7.4. It is worth mentioning that we employed phosphate buffer tablets to prepare the pH 7.4 solution, which contains, besides the phosphate salts, NaCl and KCl. When we imposed ionic strength by adding NaCl and KCl, the nanoaggregates were significantly increased. This behavior illustrates the delicate competition of interactions on the βCDPEG5 system: as the ions appear, they compete with the PEG5 chains for water molecules. As expected, the solvation of the ions is more favored, and the interactions PEG5-PEG5 chains are enhanced, resulting in higher aggregation abilities and tighter nanoaggregates, which explains the slight Dh1 decrease in the presence of salts.

In summary, we have shown that nanoaggregates and dimers are present under different pH and ionic strength conditions. At 37 °C, only the nanoaggregates were present with a Dh1 mean value comparable to the rest of the experiments. The volume distribution function pointed out that changes in the aqueous media alter the delicate molecular forces that favor either nanoaggregates or dimers. As Dh1 values did not increase, βCDPEG5 dimers would be forming the ~150 nanoaggregates instead of incorporating them into the already existing nanostructures, which could be explained based on a steric hindrance imposed by the PEG5 envelope in the βCDPEG5 nanoaggregates. Thus, by regulating the βCDPEG5 concentration, temperature, and the solvent medium, the dimeric or aggregated state can be tuned. This offers a great advantage to control the design of a βCDPEG5-based delivery system, depending on the drug and the desired final form of the carrier, either as IC or nanoparticle.

3.3. *Behavior of βCDPEG5 over time*

We analyzed βCDPEG5 0.5 mM for 55 days to investigate their ability to preserve their aggregation pattern over time. There was a global decreasing trend for Dh1 mean values in which a reduction of 27.5% in the nanoaggregate size was observed after 55 days (Fig. 9A). Dh2 mean values of dimers remained unchanged over time. The volume distribution had significant variations (Fig. 9B). The proportion of both dimers

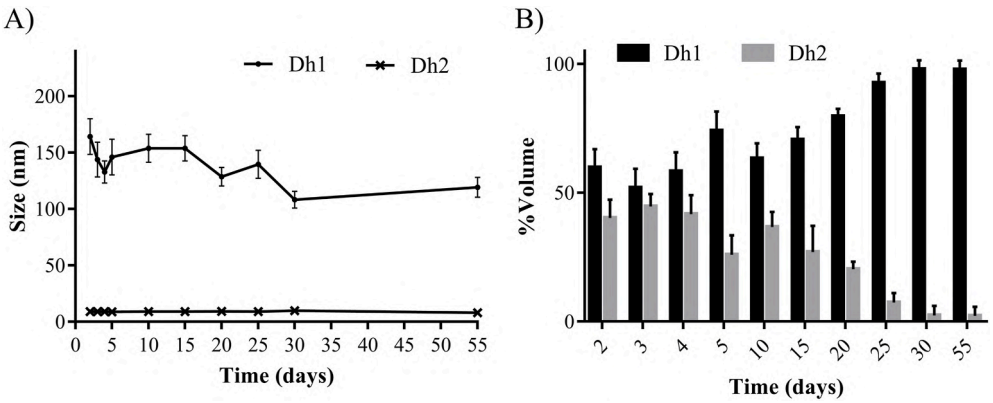

Fig. 9. Effect of time on A) aggregation size and B) volume distribution of the βCDPEG5 nanoaggregates. Error bars correspond to SD with an n = 6.

and nanoaggregates moderately fluctuated during the first five days. Then, the volume distribution of the dimers gradually decreased, reaching 6.7%, while nanoaggregates represented 97.8% at the end of the experiment. Fig. S2 and Table S10 show the particle size distribution histograms and DLS results per day, respectively.

These results suggest that individual βCDPEG5 can initially self-associate to form dimers that further interact to form those ~150 nm nanoaggregates, whose size slightly decreased over time. This type of aggregation of CDs has already been described [26]. As we have mentioned, the nanoaggregates could be displaying an arrangement induced by PEG5 that generates short-range repulsive hydration, thus preventing the interaction with other entities, either βCDPEG5 molecules or βCDPEG5 nanoaggregates. Different is the case of βCDPEG5 dimers, which tend to interact with others to form those observed stable nanoaggregates.

4. Conclusions

In this work, we have shown through several techniques that βCDPEG5 molecules have the ability to self-aggregate and form quasi-spherical nanoaggregates ~150 nm in size, at a CAC of 0.5 mM. DLS revealed the presence of dimers of 9.0 nm in size in coexistence with the nanoaggregates. βCDPEG5 dimers are probably the first stage in the βCDPEG5 nanoaggregation process. Nanoaggregates and dimers displayed the same Dh1 and Dh2 pattern in acidic, neutral, and basic conditions; likewise, when modifying the ionic strength of the medium. Interestingly, the number of nanoaggregates and dimers varied depending on the experimental conditions. In water at 25 °C, nanoaggregates and dimers were present at a comparable extent. However, an increase in pH and ionic strength made the nanoaggregates prevail over the dimers. At 37 °C, only βCDPEG5 nanoaggregates were present with a Dh mean value similar to that at 25 °C. After 55 days, nanoaggregates were predominant. These overall results show that the selective anchoring of the seven PEG5 chains and their arrangement in the restricted space of the primary face of βCD make βCDPEG5 an amphiphilic non-ionic system with a remarkable ability to self-aggregate in water and form defined nanostructures.

Moreover, depending on the βCDPEG5 concentration, pH, ionic strength, and temperature, the dimeric or aggregated state can be tuned, being this a crucial feature to control drug's loading and release. The influence of guest molecules (i.e., drugs) on the nanoaggregation process and the study of the delivery of a drug cargo from the nanoaggregates is yet to be studied and is part of our future work. We expect the results presented herein to pave the way for the rational development of a-βCDs and other biocompatible amphiphiles and soft-matter structures for drug delivery purposes.

Author statement

Yareli Rojas-Aguirre: Conceptualization, Investigation, Visualization, Writing - Original Draft, Writing - Review & Editing, Supervision, Project administration, Funding acquisition. Juliana Rincón-López: Investigation, Formal Analysis, Visualization, Writing - Original Draft, Writing - Review & Editing. Norma Jassel Ramírez-Rodríguez: Investigation, Formal Analysis, Visualization. Alberto S. Luviano: Methodology, Formal Analysis, Visualization, Writing - Original Draft Miguel Costas: Methodology, Formal Analysis, Visualization, Writing - Original Draft José Luis López-Cervantes: Methodology, Formal Analysis, Visualization, Writing - Original Draft Arturo A. García Figueroa: Methodology, Formal Analysis, Visualization, Writing - Original Héctor Domínguez: Methodology, Formal Analysis, Visualization, Writing - Original Patricia Guadarrama: Conceptualization, Writing - Original Draft, Writing - Review & Editing Rubén Mendoza-Cruz: Methodology, Writing - Original Draft, Writing - Review & Editing Salvador López-Morales: Methodology, Supervision.

Declaration of competing interest

The authors declare that they have no known competing financial interests or personal relationships that could have appeared to influence the work reported in this paper.

Acknowledgments

Y. R-A. Acknowledges the financial support to Materials Research Institute, UNAM (Project 1306), and PAPIIT-UNAM IA200919. J. R-L. thanks to CONACyT for the MSc. scholarship CVU-1032640. A.S-L. thanks to DGAPA, UNAM for the postdoctoral fellowship. H.D. thanks to LANCAD-UNAM-DGTIC-238 for supercomputer facilities and CONACyT-A1-S- 29587. P.G. acknowledges the financial support from Materials Research Institute, UNAM (Project 1316). Also, the authors thank L. Bazán-Díaz and J. Romero-Ibarra for their technical support in electron microscopy analysis.

Appendix A. Supplementary data

Supplementary data to this article can be found online at https://doi.org/10.1016/j.jddst.2021.102975.

References

[1] W. Sliwa, T. Girek, Cyclodextrins: Properties and Applications, First, Wiley-VCH Verlag GmbH & Co. KGaA, 2017, https://doi.org/10.1002/9783527695294.
[2] J. Rincón-López, Y.C. Almanza-Arjona, A.P. Riascos, Y. Rojas-Aguirre, Technological evolution of cyclodextrins in the pharmaceutical field, J. Drug Deliv. Sci. Technol. (2020) 102156, https://doi.org/10.1016/j.jddst.2020.102156.

[3] L. Zerkoune, A. Angelova, S. Lesieur, Nano-assemblies of modified cyclodextrins and their complexes with guest molecules: incorporation in nanostructured membranes and amphiphile nanoarchitectonics design, Nanomaterials 4 (2014) 741–765, https://doi.org/10.3390/nano4030741.
[4] G. Varan, C. Varan, N. Erdoğar, A.A. Hıncal, E. Bilensoy, Amphiphilic cyclodextrin nanoparticles, Int. J. Pharm. 531 (2017) 457–469, https://doi.org/10.1016/j.ijpharm.2017.06.010.
[5] Z. Fülöp, S.V. Kurkov, T.T. Nielsen, K.L. Larsen, T. Loftsson, Self-assembly of cyclodextrins: formation of cyclodextrin polymer based nanoparticles, J. Drug Deliv. Sci. Technol. 22 (2012) 215–221, https://doi.org/10.1016/S1773-2247(12)50032-8.
[6] E. Bilensoy, A.A. Hincal, Recent advances and future directions in amphiphilic cyclodextrin nanoparticles, Expet Opin. Drug Deliv. 6 (2009) 1161–1173, https://doi.org/10.1517/17425240903222218.
[7] L. Jiang, Y. Yan, J. Huang, Versatility of cyclodextrins in self-assembly systems of amphiphiles, Adv. Colloid Interface Sci. 169 (2011) 13–25, https://doi.org/10.1016/j.cis.2011.07.002.
[8] A.C. Anselmo, S. Mitragotri, Nanoparticles in the clinic: an update, Bioeng. Transl. Med. 4 (2019) 1–16, https://doi.org/10.1002/btm2.10143.
[9] G.J. Weiss, J. Chao, J.D. Neidhart, R.K. Ramanathan, D. Bassett, J.A. Neidhart, C.H. J. Choi, W. Chow, V. Chung, S.J. Forman, E. Garmey, J. Hwang, D.L. Kalinoski, M. Koczywas, J. Longmate, R.J. Melton, R. Morgan, J. Oliver, J.J. Peterkin, J. L. Ryan, T. Schluep, T.W. Synold, P. Twardowski, M.E. Davis, Y. Yen, First-in-human phase 1/2a trial of CRLX101, a cyclodextrin-containing polymer-camptothecin nanopharmaceutical in patients with advanced solid tumor malignancies, Invest. N. Drugs 31 (2013) 986–1000, https://doi.org/10.1007/s10637-012-9921-8.
[10] A.A. D'souza, R. Shegokar, Polyethylene glycol (PEG): a versatile polymer for pharmaceutical applications, Expet Opin. Drug Deliv. 13 (2016) 1257–1275, https://doi.org/10.1080/17425247.2016.1182485.
[11] K. Knop, R. Hoogenboom, D. Fischer, U.S. Schubert, Poly(ethylene glycol) in drug delivery: pros and cons as well as potential alternatives, Angew. Chem. Int. Ed. 49 (2010) 6288–6308, https://doi.org/10.1002/anie.200902672.
[12] J. Wu, C. Zhao, W. Lin, R. Hu, Q. Wang, H. Chen, L. Li, S. Chen, J. Zheng, Binding characteristics between polyethylene glycol (PEG) and proteins in aqueous solution, J. Mater. Chem. B. 2 (2014) 2983–2992, https://doi.org/10.1039/c4tb00253a.
[13] L. Bekale, D. Agudelo, H.A. Tajmir-Riahi, The role of polymer size and hydrophobic end-group in PEG-protein interaction, Colloids Surf. B Biointerfaces 130 (2015) 141–148, https://doi.org/10.1016/j.colsurfb.2015.03.045.
[14] J.V. Jokerst, T. Lobovkina, R.N. Zare, S.S. Gambhir, Nanoparticle PEGylation for imaging and therapy, Nanomedicine 6 (2011) 715–728, https://doi.org/10.2217/nnm.11.19.
[15] W.J. Brittain, S. Minko, A structural definition of polymer brushes, J. Polym. Sci. Part A Polym. Chem. 45 (2007) 3505–3512, https://doi.org/10.1002/pola.22180.
[16] A.M. O'Mahony, J. Ogier, S. Desgranges, J.F. Cryan, R. Darcy, C.M. O'Driscoll, A click chemistry route to 2-functionalised PEGylated and cationic β-cyclodextrins: Co-formulation opportunities for siRNA delivery, Org. Biomol. Chem. 10 (2012) 4954–4960, https://doi.org/10.1039/c2ob25490e.
[17] B.M.D.C. Godinho, J.R. Ogier, A. Quinlan, R. Darcy, B.T. Griffin, J.F. Cryan, M.O. D. Caitriona, PEGylated cyclodextrins as novel siRNA nanosystems: correlations between polyethylene glycol length and nanoparticle stability, Int. J. Pharm. 473 (2014) 105–112, https://doi.org/10.1016/j.ijpharm.2014.06.054.
[18] B. Kost, M. Brzezinski, M. Socka, M. Basko, T. Biela, Biocompatible polymers combined with cyclodextrins: fascinating materials for drug delivery applications, Molecules 25 (2020) 3404, https://doi.org/10.3390/molecules25153404.
[19] Y. Rojas-Aguirre, M.A. Torres-Mena, L.J. López-Méndez, S.L. Alcaraz-Estrada, P. Guadarrama, J.M. Urucha-Ortíz, PEGylated β-cyclodextrins: click synthesis and in vitro biological insights, Carbohydr. Polym. 223 (2019) 115113, https://doi.org/10.1016/j.carbpol.2019.115113.
[20] A. Abdulrahman, A new perspective for possible formulation and characterization of beta- cyclodextrin/poly(ethylene glycol) crystalline inclusion complexes, J. Clin. Trials (2018) 4172, https://doi.org/10.4172/2167-0870-c3-029.
[21] K.A. Udachin, L.D. Wilson, J.A. Ripmeester, Solid polyrotaxanes of polyethylene glycol and cyclodextrins: the single crystal x-ray structure of PEG-β-cyclodextrin, J. Am. Chem. Soc. 122 (2000) 12375–12376, https://doi.org/10.1021/ja002189k.
[22] J.D. Heidel, T. Schluep, Cyclodextrin-containing polymers: versatile platforms of drug delivery materials, J. Drug Deliv. 2012 (2012) 1–17, https://doi.org/10.1155/2012/262731.
[23] M.E. Davis, The first targeted delivery of siRNA in humans via a self-assembling, cyclodextrin polymer-based nanoparticle: from concept to clinic, Mol. Pharm. 6 (2009) 659–668, https://doi.org/10.1021/mp900015y.
[24] T. Loftsson, E. Stefánsson, Cyclodextrins and topical drug delivery to the anterior and posterior segments of the eye, Int. J. Pharm. 531 (2017) 413–423, https://doi.org/10.1016/j.ijpharm.2017.04.010.
[25] T. Loftsson, E. Stefánsson, Cyclodextrin Nanotechnology for Ophthalmic Drug Delivery, US patent 8633172B2, 2014.
[26] T. Loftsson, P. Saokham, A.R. Sá Couto, Self-association of cyclodextrins and cyclodextrin complexes in aqueous solutions, Int. J. Pharm. 560 (2019) 228–234, https://doi.org/10.1016/j.ijpharm.2019.02.004.
[27] B. Pelaz, C. Alexiou, R.A. Alvarez-Puebla, F. Alves, A.M. Andrews, S. Ashraf, L. P. Balogh, L. Ballerini, A. Bestetti, C. Brendel, S. Bosi, M. Carril, W.C.W. Chan, C. Chen, X. Chen, X. Chen, Z. Cheng, D. Cui, J. Du, C. Dullin, A. Escudero, N. Feliu, M. Gao, M. George, Y. Gogotsi, A. Grünweller, Z. Gu, N.J. Halas, N. Hampp, R. K. Hartmann, M.C. Hersam, P. Hunziker, J. Jian, X. Jiang, P. Jungebluth, P. Kadhiresan, K. Kataoka, A. Khademhosseini, J. Kopeček, N.A. Kotov, H.F. Krug, D.S. Lee, C.M. Lehr, K.W. Leong, X.J. Liang, M.L. Lim, L.M. Liz-Marzán, X. Ma, P. Macchiarini, H. Meng, H. Möhwald, P. Mulvaney, A.E. Nel, S. Nie, P. Nordlander, T. Okano, J. Oliveira, T.H. Park, R.M. Penner, M. Prato, V. Puntes, V.M. Rotello, A. Samarakoon, R.E. Schaak, Y. Shen, S. Sjöqvist, A.G. Skirtach, M. G. Soliman, M.M. Stevens, H.W. Sung, B.Z. Tang, R. Tietze, B.N. Udugama, J. Scott VanEpps, T. Weil, P.S. Weiss, I. Willner, Y. Wu, L. Yang, Z. Yue, Q. Zhang, Q. Zhang, X.E. Zhang, Y. Zhao, X. Zhou, W.J. Parak, Diverse applications of nanomedicine, ACS Nano 11 (2017) 2313–2381, https://doi.org/10.1021/acsnano.6b06040.
[28] Y. Moroi, Critical micelle concentration, in: Micelles Theor. Appl. Asp., first ed., Springer US, New York, 1992, pp. 47–55.
[29] J.N. Phillips, The energetics of micelle formation, Trans. Faraday Soc. 51 (1955) 561–569, https://doi.org/10.1039/tf9555100561.
[30] Microtrac, Dynamic Light Scattering: DLS Particle Analyzer. https://www.microtrac.com/products/particle-size-shape-analysis/dynamic-light-scattering/, 2021. (Accessed 13 September 2021) accessed.
[31] A.S. Luviano, J. Hernández-Pascacio, D. Ondo, R.A. Campbell, Á. Piñeiro, J. Campos-Terán, M. Costas, Highly viscoelastic films at the water/air interface: α-Cyclodextrin with anionic surfactants, J. Colloid Interface Sci. 565 (2020) 601–613, https://doi.org/10.1016/j.jcis.2019.12.012.
[32] A.K. Malde, L. Zuo, M. Breeze, M. Stroet, D. Poger, P.C. Nair, C. Oostenbrink, A. E. Mark, An automated force field Topology builder (ATB) and repository: version 1.0, J. Chem. Theor. Comput. 7 (2011) 4026–4037, https://doi.org/10.1021/ct200196m.
[33] H.J.C. Berendsen, J.R. Grigera, T.P. Straatsma, The missing term in effective pair potentials, J. Phys. Chem. 91 (1987) 6269–6271, https://doi.org/10.1021/j100308a038.
[34] B. Hess, C. Kutzner, D. van der Spoel, E. Lindahl, GROMACS 4: algorithms for highly efficient, load-balanced, and scalable molecular simulation, J. Chem. Theor. Comput. 4 (2008) 435–447, https://doi.org/10.1021/ct700301q.
[35] U. Essmann, L. Perera, M.L. Berkowitz, T. Darden, H. Lee, L.G. Pedersen, A smooth particle mesh Ewald method, J. Chem. Phys. 103 (1995) 8577–8593, https://doi.org/10.1063/1.470117.
[36] B. Hess, H. Bekker, H.J.C. Berendsen, J.G.E.M. Fraaije, LINCS: a linear constraint solver for molecular simulations, J. Comput. Chem. 18 (1997) 1463–1472, https://doi.org/10.1002/(SICI)1096-987X(199709)18:12<1463::AID-JCC4>3.0.CO;2-H.
[37] Y. Lu, E. Zhang, J. Yang, Z. Cao, Strategies to improve micelle stability for drug delivery, Nano Res. 11 (2018) 4985–4998, https://doi.org/10.1007/s12274-018-2152-3.
[38] S.S. Kulthe, Y.M. Choudhari, N.N. Inamdar, V. Mourya, Polymeric micelles: authoritative aspects for drug delivery, Des. Monomers Polym. 15 (2012) 465–521, https://doi.org/10.1080/1385772X.2012.688328.
[39] K. Szutkowski, Z. Kołodziejska, Z. Pietralik, I. Zhukov, A. Skrzypczak, K. Materna, M. Kozak, Clear distinction between CAC and CMC revealed by high-resolution NMR diffusometry for a series of bis-imidazolium gemini surfactants in aqueous solutions, RSC Adv. 8 (2018) 38470–38482, https://doi.org/10.1039/c8ra07081d.
[40] F. Aydin, X. Chu, G. Uppaladadium, D. Devore, R. Goyal, N.S. Murthy, Z. Zhang, J. Kohn, M. Dutt, Self-Assembly and critical aggregation concentration measurements of ABA triblock copolymers with varying B block types: model development, prediction, and validation, J. Phys. Chem. B 120 (2016) 3666–3676, https://doi.org/10.1021/acs.jpcb.5b12594.
[41] Z. Zhang, H. Wang, W. Shen, Densities, conductivities, and aggregation numbers of aqueous solutions of quaternary ammonium surfactants with hydroxyethyl substituents in the headgroups, J. Chem. Eng. Data 58 (2013) 2326–2338, https://doi.org/10.1021/je400463n.
[42] D.R. Perinelli, M. Cespi, N. Lorusso, G.F. Palmieri, G. Bonacucina, P. Blasi, Surfactant self-assembling and critical micelle concentration: one approach fits all? Langmuir 36 (2020) 5745–5753, https://doi.org/10.1021/acs.langmuir.0c00420.
[43] F.B. De Sousa, A.C. Lima, Â.M.L. Denadai, C.P.A. Anconi, W.B. De Almeida, W.T. G. Novato, H.F. Dos Santos, C.L. Drum, R. Langer, R.D. Sinisterra, Superstructure based on β-CD self-assembly induced by a small guest molecule, Phys. Chem. Chem. Phys. 14 (2012) 1934–1944, https://doi.org/10.1039/c2cp22768a.
[44] A.R. Sá Couto, A. Ryzhakov, T. Loftsson, Self-Assembly of α-cyclodextrin and β-cyclodextrin: identification and development of analytical techniques, J. Pharm. Sci. 107 (2018) 2208–2215, https://doi.org/10.1016/j.xphs.2018.03.028.
[45] M. Bonini, S. Rossi, G. Karlsson, M. Almgren, P. Lo Nostro, P. Baglioni, Self-assembly of β-cyclodextrin in water. Part 1: cryo-TEM and dynamic and static light scattering, Langmuir 22 (2006) 1478–1484, https://doi.org/10.1021/la052878f.
[46] G. González-Gaitano, P. Rodríguez, J.R. Isasi, M. Fuentes, G. Tardajos, The aggregation of cyclodextrins as studied by photon correlation spectroscopy, J. Inclusion Phenom. Macrocycl. Chem. 44 (2002) 101–105, https://doi.org/10.1023/A:1023065823358.
[47] K.L. Linegar, A.E. Adeniran, A.F. Kostko, M.A. Anisimov, Hydrodynamic radius of polyethylene glycol in solution obtained by dynamic light scattering, Colloid J. 72 (2010) 279–281, https://doi.org/10.1134/S1061933X10020195.
[48] D.L. Ho, B. Hammouda, S.R. Kline, Clustering of poly(ethylene oxide) in water revisited, J. Polym. Sci., Part B: Polym. Phys. 41 (2003) 135–138, https://doi.org/10.1002/polb.10340.
[49] J. Dey, R. Ghosh, R. Das Mahapatra, Self-Assembly of unconventional low-molecular-mass amphiphiles containing a PEG chain, Langmuir 35 (2019) 848–861, https://doi.org/10.1021/acs.langmuir.8b00779.
[50] M.L. Alessi, A.I. Norman, S.E. Knowlton, D.L. Ho, S.C. Greer, Helical and coil conformations of poly(ethylene glycol) in isobutyric acid and water, Macromolecules 38 (2005) 9333–9340, https://doi.org/10.1021/ma051339e.

[51] A.C.B. Rego, J.F. de Melo, A.O.W. Neto, J.L.C. Fonseca, Coil interpenetration, segment aggregation and adsorption of PEG at water/air interface, J. Surfactants Deterg. 20 (2017) 977–983, https://doi.org/10.1007/s11743-017-1959-3.
[52] M. Messner, S.V. Kurkov, P. Jansook, T. Loftsson, Self-assembled cyclodextrin aggregates and nanoparticles, Int. J. Pharm. 387 (2010) 199–208, https://doi.org/10.1016/j.ijpharm.2009.11.035.
[53] Y. He, P. Fu, X. Shen, H. Gao, Cyclodextrin-based aggregates and characterization by microscopy, Micron 39 (2008) 495–516, https://doi.org/10.1016/j.micron.2007.06.017.
[54] J. Hernandez-Pascacio, Á. Piñeiro, J.M. Ruso, N. Hassan, R.A. Campbell, J. Campos-Terán, M. Costas, Complex behavior of aqueous α-cyclodextrin solutions. Interfacial morphologies resulting from bulk aggregation, Langmuir 32 (2016) 6682–6690, https://doi.org/10.1021/acs.langmuir.6b01646.
[55] R. Singh, S. Chauhan, K. Sharma, Surface tension, viscosity, and refractive index of sodium dodecyl sulfate (SDS) in aqueous solution containing poly(ethylene glycol) (PEG), poly(vinyl pyrrolidone) (PVP), and their blends, J. Chem. Eng. Data 62 (2017) 1955–1964, https://doi.org/10.1021/acs.jced.6b00978.
[56] J. Szejtli, Introduction and general overview of cyclodextrin chemistry, Chem. Rev. 98 (1998) 1743–1753, https://doi.org/10.1021/cr970022c.
[57] S. Barman, D. Ekka, S. Saha, M.N. Roy, NMR, surface tension and conductance study to investigate host-guest inclusion complexes of three sequential ionic liquids with β-cyclodextrin in aqueous media, Chem. Phys. Lett. 658 (2016) 43–50, https://doi.org/10.1016/j.cplett.2016.06.017.
[58] S. Saha, A. Roy, K. Roy, M.N. Roy, Study to explore the mechanism to form inclusion complexes of β-cyclodextrin with vitamin molecules, Sci. Rep. 6 (2016) 1–12, https://doi.org/10.1038/srep35764.
[59] A. Hirano, K. Shiraki, T. Arakawa, Polyethylene glycol behaves like weak organic solvent, Biopolymers 97 (2012) 117–122, https://doi.org/10.1002/bip.21708.
[60] B. Ensing, A. Tiwari, M. Tros, J. Hunger, S.R. Domingos, C. Pérez, G. Smits, M. Bonn, D. Bonn, S. Woutersen, On the origin of the extremely different solubilities of polyethers in water, Nat. Commun. 10 (2019) 1–8, https://doi.org/10.1038/s41467-019-10783-z.
[61] P. Jansook, N. Ogawa, T. Loftsson, Cyclodextrins: structure, physicochemical properties and pharmaceutical applications, Int. J. Pharm. 535 (2018) 272–284, https://doi.org/10.1016/j.ijpharm.2017.11.018.
[62] S. Liese, M. Gensler, S. Krysiak, R. Schwarzl, A. Achazi, B. Paulus, T. Hugel, J. P. Rabe, R.R. Netz, Hydration effects turn a highly stretched polymer from an entropic into an energetic spring, ACS Nano 11 (2017) 702–712, https://doi.org/10.1021/acsnano.6b07071.